PERFORMANCE AND ANALYSIS OF MIRROR GAS TURBINE AT VARIABLE SPECIFIC HEAT

A THESIS/ DISSERTATION SUBMITTED TO THE " DELHI UNIVERSITY (DELHI COLLEGE OF ENGINEERING)", DELHI IN PARTIAL FULFILMENT OF THE REQUIREMENT

FOR

THE AWARD OF DEGREE OF

MASTER OF ENGINEERING

IN

MECHANICAL ENGINEERING
(THERMAL ENGINEERING)

SUBMITTED BY

RAJAT KUMAR SAHU

14/ME/98

UNDER THE GUIDANCE OF

PROF. B. B. ARORA

DEPARTMENT OF MECHANICAL ENGINEERING
DELHI COLLEGE OF ENGINEERING
DELHI

CERTIFICATE

This is to certify that this dissertation titled " **Performance and analysis of mirror gas turbine at variable specific heat** " is being submitted by **Rajat Kumar Sahu (14/ME/98)** in partial fulfillment of the requirement for the award of the degree of Master of Engineering (Thermal Engineering) and this work has been done by him under my supervision and guidance.

The results contained in this work are original and has not been submitted to any other University or Institute for the award of any degree or diploma.

Prof. B. B. Arora
Department of Mechanical Engineering
Delhi College of Engineering, Delhi

ACKNOWLEDGEMENT

''Vision Is The Art Of Seeing Invisible"

Projects are never a failure. However, the results can be in favour or against. But in one way or another they help to explore, the Invisible. Probably, the thrill, the awe, and the high lurks inside the unknown, motivates an individual towards research.

Sometimes words are a poor substitute in expressing one's feeling, but eventually they are the only means for expressing oneself. I express my sense of sincerity & deep gratitude to my guide **Prof. B.B.Arora,** Mechanical Engineering Department, Delhi College of Engineering, Delhi, for his nurtured vision & invaluable guidance, which he poured constantly and drove me towards that invisible. His valiant efforts, dedicated support & multifunctional approach smoothened the whole process.

1 am extremely thankful to **Prof. Majhi** (H.O.D mechanical) and other faculty members for their generous advice for the completion of this project.

I am also thankful to my fellow students of Master of Engineering, for their whole-hearted support, encouragement and cooperation, which boosted me to sail through an extensive river of uncertainties & difficulties.

I am extremely thankful to **Mr. G. Bimal Nambiar, Mr. Durai and Mr. Somnath Prusty** for their help and valuable suggestions in completing this project a success.

At home I am thankful to my wife **Susandhya Rani,** son **Vipul** and parents for bearing with me throughout my Master of Engineering course.

RAJAT KUMAR SAHU
M.E. (Thermal engineering)
14/ME (Thermal) /1998
Delhi College of Engineering

ABSTRACT

There have been many developments on the thermodynamic analysis of various combined or cogeneration cycle schemes, with more advance heat recovery capabilities. One of such novel cycles is the mirror cycle. The mirror gas turbine is a conceptual combination of Brayton and inverted Brayton cycles with a heat sink by intercooling. And options chosen for further development seem to aim at more marketable system in recent years. The split-shaft engine can offer better flexibility of operation for the needs of combined or cogeneration system. In this work, performance analysis of the mirror gas turbine associated with split-shaft engine is obtained. The obtained results provide significant guidance to the performance evaluation and improvement of the mirror gas turbine.

Heat energy of exhaust gas of gas turbine is extremely large and therefore can be retrieved by cogeneration system in modern industrial gas turbines [6]. However, there may be a possibility for reutilization of exhaust gas directly if the inverted Brayton cycle is adequately used in bottoming cycle. This new conceptual combination of Brayton and inverted Brayton cycles is dubbed as a **"Mirror Gas Turbine" [**3] This Mirror Gas Turbine Cycle has been evaluated and analyzed for different method to improve performance of gas turbine such as intercooling in stages of compression and reheating in stages of expansion in turbine.

Computer programs have been generated for analysis of mirror gas turbine cycle at variable specific heat of air. In analysis different parameters such as specific output, thermal efficiency, power ratio, and specific fuel consumption have been studied for optimum performance of Mirror Gas Turbine Cycle. It is revealed that number of intercooler in stages of compression of bottoming cycle should be optimized to two and reheating is not beneficial in respect of thermal efficiency.

A Comparison has been made with the parameters at different pressure ratio and different specific heat. The Mirror Gas Turbine may be applied to many fields in the recuperation, combined Brayton/Rankine cycle with great promise. In other words, the Mirror Gas Turbine, that is a set of positive and negative gas turbines, may be competitive with the combined gas and steam turbine. It is tentatively concluded that technical difficulties of using a high pressure and temperature steam turbine with a boiler, condenser, and pump will be removed by successful use of the Mirror Gas Turbine in the Future.

GLOSSARY

t1 - Compressor inlet Temperature in topping cycle.

t2 - Compressor exit Temperature in topping cycle.

t3 - Turbine inlet Temperature in topping cycle.

t4 - Turbine exhaust Temperature from topping cycle.

t5 - Turbine exhaust Temperature from topping cycle

t6 - Compressor inlet Temperature in bottoming cycle.

t7 - Compressor exit Temperature in bottoming cycle.

n - Number of intercooling stages.

wttot - Net work of topping cycle.

etop - Thermal efficiency of topping cycle.

wbot - Net work of bottoming cycle.

ebot - Thermal efficiency of bottoming cycle.

wtot - Net work of mirror gas turbine cycle.

etot - Thermal efficiency of mirror gas turbine cycle.

sfc - specific fuel consumption of mirror gas turbine cycle.

ratio - power ratio of topping &bottoming cycle in mirror gas turbine cycle.

ma - Mass of air in mirror gas turbine cycle.

rp1 - Pressure ratio of topping cycle.

TIT - turbine inlet temperature.

mf - mass of fuel.

ecc - Efficiency of combustion chamber.

cpa - Specific heat of Air.

cpg - specific heat of gas.

ec - Efficiency of compressor.

et - Efficiency of turbine.

γ - Isentropic index of air.

HRSG - heat recovery steam generator.

CONTENTS

Certificate

Acknowledgement

Abstract

CHAPTER 1: INTRODUCTION AND LITERATURE REVIEW **1-11**

1.1 Introduction 1

1..2 Brayton Cycle 2

1.2.1 The Gas To Gas Recuperation Cycle 3

1.2.2 Combined Bray ton And Rankine Cycle 4

1.2.3 The Brayton - Kalina cycle 4

1.2.4 The Brayton - Brayton cycle 4

1.2.5 The Brayton - Diesel cycle 4

1.2.6 The Brayton –Stirling cycle 5

1.3 Inverted Brayton Cycle 5

1.3.1. Inter Cooling Of Compression Process 6

1.4 Mirror Gas Turbine Cycle 7

1.4.1. Features Of Mirror Gas Turbine 9

1.5 Literature Review **10-11**

CHAPTER 2: ANALYSIS OF MIRROR GAS TURBINE CYCLE **12-16**

2.1 Cycle Analysis 12

2.1.1 Topping Cycle 13

2.1.2 Bottoming Cycle 14

2.2 Selection Of Pressure Ratio 14

CHAPTER 3: RESULTS AND DISCUSSION **17-186**

3.1 Results & Discussion-1 (Mirror Gas Turbine or Without Intercooler & Without Reheat) 17

Results of computer program for analysis of Mirror gas turbine cycle 19-72

Graphs showing variation of parameters of mirror gas turbine cycle Vs pressure ratio at γ=1.1 73-79

Graphs showing variation of parameters of mirror gas turbine cycle Vs pressure ratio at γ=1.2 80-86

Graphs showing variation of parameters of mirror gas turbine cycle Vs pressure ratio at γ=1.3 87-93

Graphs showing variation of parameters of mirror gas turbine cycle Vs pressure ratio at γ=1.4 94-100

Graphs showing variation of parameters of mirror gas turbine cycle Vs pressure ratio at γ=1.5 101-107

Graphs showing variation of parameters of mirror gas turbine cycle Vs pressure ratio at γ=1.6 108-114

Graphs showing variation of parameters of mirror gas turbine cycle Vs pressure ratio at γ=1.66 115-121

Graphs showing variation of parameters of mirror gas turbine cycle Vs pressure ratio at different specific heat 122-128

Graphs showing variation of parameters of mirror gas turbine cycle Vs pressure ratio with and without intercooler 129-152

3.2 Discussion of results 153-186

CHAPTER-4: CONCLUSION **187**

ANNEXURE **188-191**

REFERENCES **192-193**

CHAPTER - 1

INTRODUCTION AND LITERATURE REVIEW

1.1 Introduction

Out of the various means of producing mechanical power the turbine is in many respects the most satisfactory .The absence of reciprocating and rubbing members means the balancing problems are few, that the lubricating oil consumption is exceptionally low, and the reliability can be high.

The advantages of turbine were first realized using water as the working fluid, and hydroelectric power is still a significant contributor to world's energy resources. Around the turn of the twentieth century the steam turbine began its career and, quite apart from its wide use as a marine power plant it has become the most important prime mover for electricity generation. But disadvantages of steam turbine is that production of high pressure high temperature steam involves the installation of bulky and expensive steam generating equipment [l].

It was realized that instead of water being heated indirectly to generate steam if product of combustion are directly expanded in turbine than compact power plant was feasible. Thus the concept of gas turbine came into picture. In its initial years of development gas turbines is only used for aviation and peaks load power production as its thermal efficiency was very low and it was not economical to use gas turbine for long running hours. As a result of this innovative modifications were made in conventional power plant to improve thermal efficiency and specific work output.

On the basis of process of combustion, gas turbine is classified as follows

- Constant Pressure Combustion Type: -Cycle working on this principle is called Joule or Brayton cycle.
- Constant volume combustion type: - Cycle working on this principle is called Atkinson cycle.

The combustion at constant volume although more efficient was more intermittent in nature and pose practical difficulties and thus constant pressure combustion was accepted as having great potential in future.

1.2. The Brayton cycle

The thermodynamic cycle upon which all gas turbines operate-is called the Brayton cycle. Figure 1.1 shows the classical pressure versus volume (P-V) and temperature versus entropy (T-S) diagrams for this cycle. The numbers on this diagram correspond to the numbers also used in Figure 1.1. Path 1 to 2 represents the compression occurring in the compressor, path 2 to 3 represents the constant pressure addition of heat in the combustion chamber, and path 3 to 4 represents the expansion occurring in the turbine. The path from 4 back to 1 on the Brayton cycle diagrams indicates a constant pressure cooling process. In the open cycle gas turbine, this cooling is done by the atmosphere, which provides fresh, cool air at point 1 on a continuous basis in exchange for the hot "gases exhausted to the atmosphere at point 4 [4].

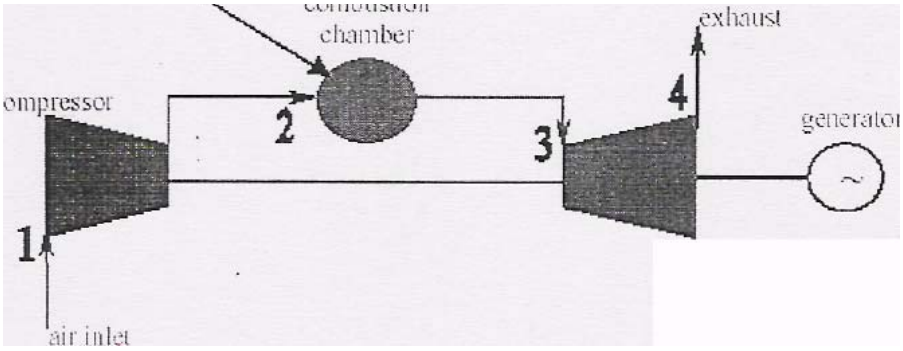

Figure1.1 : The simple-cycle gas turbine

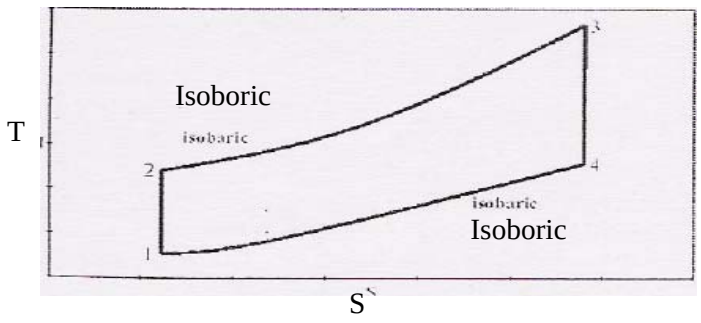

The exhaust temperature of gas turbine is very high i.e. 8OOK to 900K.Hence heat of exhaust of simple gas turbine has to be recovered. As a result emphasis has been given on the various advance cycles on heat recovery from the gas turbine exhaust.

Various cycle have been implemented for exhaust gas heat recovery as follows

1.2.1. The gas to gas recuperation cycle

The exhaust heat of simple gas turbine can be recovered when gas-to-gas recuperation is employed and this has been used in conjunction with industrial gas turbines for more than 50 years. This arrangement is illustrated in Figure 3.1. The use of recuperation is limited, however, by the compressor outlet temperature due to metallurgical problems of the heat exchanger temperature. Complete heat exchange between hot gas and cold gas may be considered as one of the most difficult techniques. Particularly the materials of an exchanger must be changed into a super alloy or ceramics from a conventional aluminum alloy if the working gas temperature becomes high [7]. Thermal properties of such high-cost materials are not necessarily of good quality for efficient heat transfer and not easy for fabrication. The recuperated gas turbines are expected to obtain efficiencies from 39% to 43%, which are higher compared to 25% to 40% for other simple-cycle gas turbines of same capacity [6].

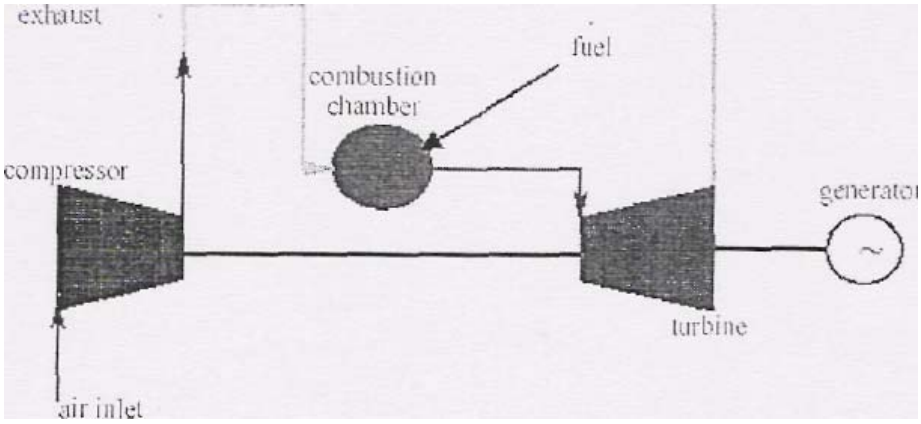

Figure 1.2: Gas to gas recuperation

1.2.2.Combined Brayton And Rankine Cycle

Conventional method of recuperation has disadvantages in the regime of high component efficiency of 0.90. Therefore, large gas turbines with a very high-pressure ratio, in which it is no longer possible to employ the recuperation due to enough high temperature at the compressor exit, have been usually operated as a combined cycle of Brayton and Rankine cycles. The exhaust heat energy in the Brayton cycle has been recovered by steam turbines at a high pressure of 180-200 times the atmospheric pressure in the Rankine cycle. But combined cycle has technical difficulties of using a high pressure and temperature steam turbine with a boiler, condenser and pump

1.2.3.The Brayton - Kalina cycle

The Kalina cycle is a novel bottoming cycle, which uses zeotropic mixture of ammonia and water as the working fluid [6]. Its characteristics arc such that its temperature tracks the turbine exhaust temperature in the waste heat boiler. However, the thermodynamic advantages of this small boiler temperature difference compared to a steam cycle would be lost at the condensing stage, assuming the condenser cooling medium temperature would be the same in both cases. The novelty of the Kalina cycle lies in the solution to this problem

1.2.4. The Brayton - Brayton cycle

Two Brayton cycles can be combined by an air-gas heat exchanger. The exhaust of the primary gas turbine is sent to a heat exchanger, which, in turn, heats the air in the secondary gas turbine cycle [2]. Air is expanded in the turbine to generate additional power. In comparison to the conventional combined cycle, this scheme does not require bulky steam equipment (boiler, steam turbine, condenser), or a water-processing unit, and allows unmanned operation.

1.2.5.The Brayton - Diesel cycle

Preheating of the inlet air of a Diesel engine can sufficiently improve its

performance. The gas turbine exhaust can be applied in order to increase the temperature of the air, which is extracted from the compressor and fed into the Diesel engine.

1.2.6. The Brayton - Stirling cycle

In a combination of a gas turbine and a Stirling engine, the heater of the latter can be placed either in the combustion chamber of the turbine, or after the turbine in the exhaust flow.

Thus it is revealed from above discussion that various cycle have been implemented for exhaust gas heat recovery. On the other hand, there may be a possibility for reutilization of exhaust gas directly as a shaft horsepower working with a gas substance if the inverted Brayton cycle can be adequately used as bottoming cycle.

1.3.Inverted Brayton Cycle:

Gas turbines operate on the Brayton cycle, which begins with compression, heat addition and terminate in expansion. In the inverted Brayton, the processes are reversed in which expansion first occurs and then heat of the working gas is extracted by a heat exchanger and sucked by a fan or compressor. The working principle of this cycle has been explained fully by Wilson [9]. However, nobody has paid attention because the thermal efficiency of cycle is very low. No hardware of test rig has been constructed. On the contrary, many efforts have been concentrated only on the Brayton cycle, mainly in improving the performance of turbo machinery and combustors for the past decades in the real world. Users of gas turbines have spread in many sectors other than aircraft, which include land industries, marine, vehicles, and electric power generation.

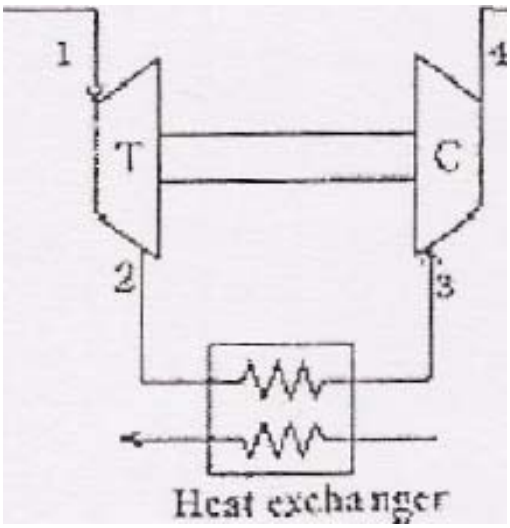

Figl.3.Inverted Brayton Cycle

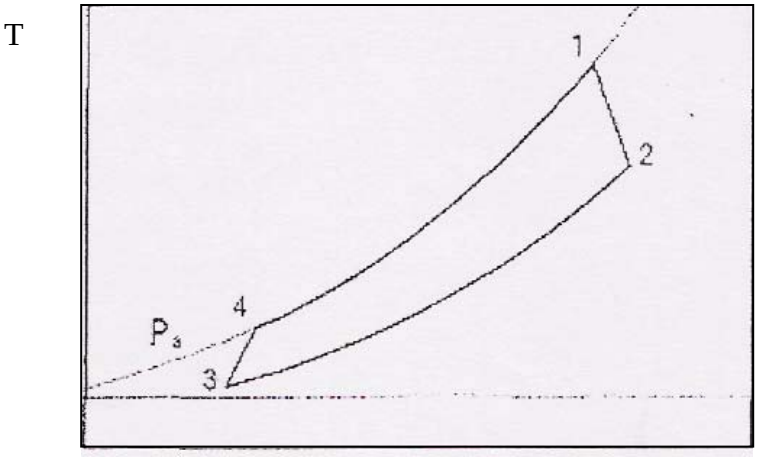

Figl.4. Temperature and entropy diagram of inverted Brayton Cycle

1.3.1. Inter Cooling of Compression Process

The technique of cooling at intermediate processes of compression has sometimes been employed to raise the overall thermal efficiency of gas turbines. However, lowering

of air temperature in entering a combustor requires a much larger fuel flow rate than that before cooling. Particularly in case of a high turbine inlet temperature and high values of adiabatic efficiency of turbo machinery with large pressure ratio. Therefore, the intercooling sometimes gives no benefit.

On the contrary, there is no burning in the inverted Brayton so that the thermal efficiency becomes always' higher as the strength of a heat sink by the intercooling is much more increased [3]. It can be fairly said that the intercooling is surely an effective way to improve the thermal efficiency only in the inverted Brayton machine. Figure is a calculation of indicating the effect of a number of cooling steps on thermal efficiency for three values of adiabatic efficiency of turbo machines at the turbine inlet temperature of 1200 K. It is revealed that three steps of intercooling may be most efficient from a viewpoint of engineering. The thermal efficiency of 30 percent would be possible at an inlet temperature of 1200 K with component efficiency of 0.9. which is an eight percent improvement in thermal efficiency from the uncooled cycle mentioned previously.

1.4. Mirror Gas Turbine Cycle

There is a possibility for reutilization of exhaust gas directly as a shaft horsepower working with a gas substance if intercooled inverted Bray ton cycle can be adequately used in bottoming cycle. It is method proposed by S.Fujji, K Kaneko and K.Otani [3]'to recover exhaust heat of simple gas turbine named as "Mirror Gas Turbine Cycle".

In this cycle first Compression, burning, and expansion, and then reversibly expansion, cooling down, and compression would continuously proceed. It can be said that the conventional gas turbine works as a topping cycle together with a bottoming cycle of an inverted Bray ton. A conceptual configuration of proposed application is shown in figure

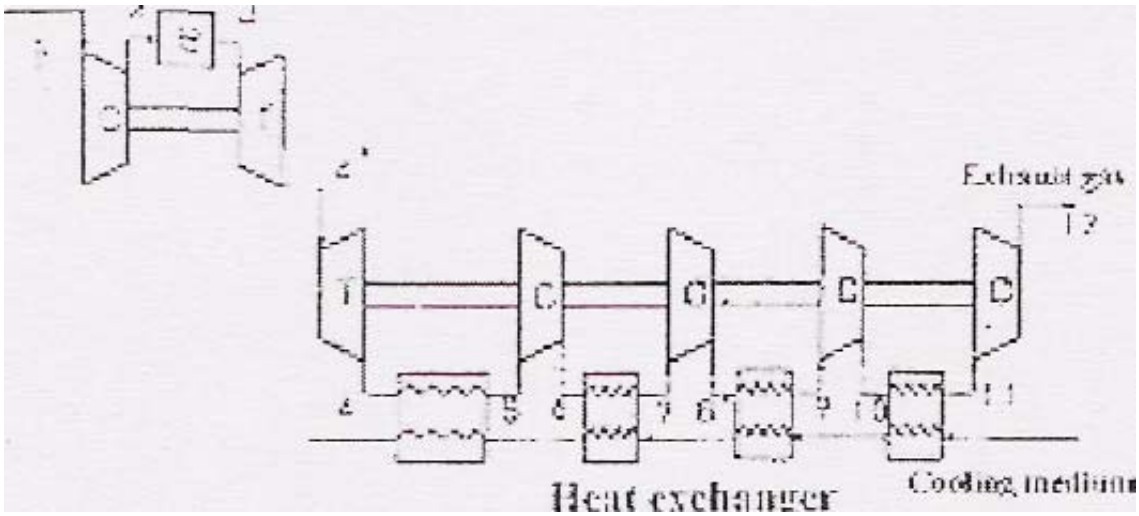
Exhaust gas
Heat exchanger
Cooling medium

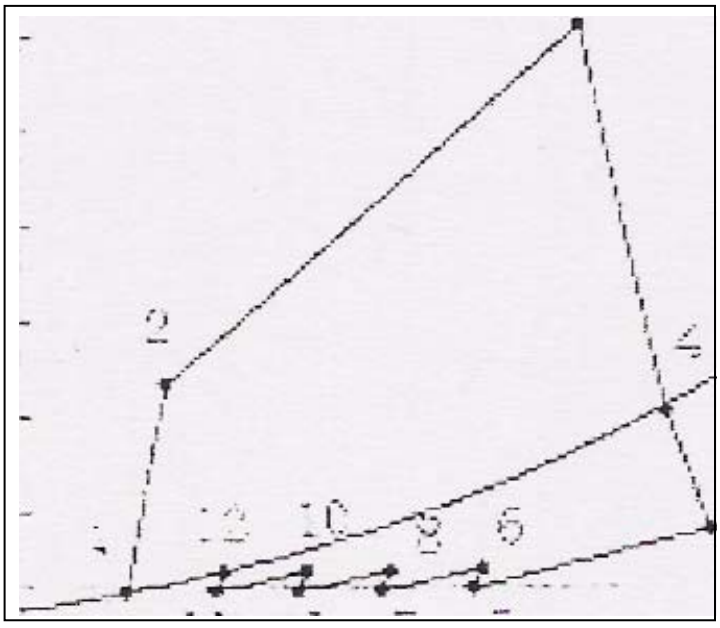
T
S
2
4
12
10
8
6

Thus mirror gas turbine is combination of Brayton cycle and inverted Brayton cycle. It can be imagined that this might be realized as a result of reflection by mirror virtually placed between both cycle. Hence the cycle is named as Mirror Gas Turbine.

1.4.1.Features Of Mirror Gas Turbine

* The main feature of a mirror cycle is that thermal efficiency may be raised up by an additional power generation from the bottoming cycle while the fuel flow rate is kept the same as that of a single gas turbine.

* Another feature is seen in the temperature/entropy diagram that the regime below atmospheric pressure but still above the surrounding temperature, which has never been taken into account in conventional gas turbines, will play an important role in energy utilization.

1.5. LITERATURE REVIEW

Wilson, D. G., 1985 [10], has proposed inverted Brayton cycle. In the inverted Brayton, the processes are reversed in which expansion first occurs and then heat of the working gas is extracted by a heat exchanger and sucked by a fan or compressor. The working principle of this cycle has been explained fully by Wilson. However, nobody has paid attention because the thermal efficiency of cycle is very low.

Tsujikawa. Y., Kaneko, K, and Fujii, S., 2001 [3], The first hardware test on inverted Brayton cycle was successfully made by use of tiny turbo machines to confirm the operation of inverted processes of expansion, cooling, and draft. It is calculated that drawbacks encountered in the inverted cycle may be improved by intercooling, showing a possibility of additionally raising up another eight percent in thermal efficiency. A new conceptual combination of Brayton and inverted Brayton cycles with intercooling, which is dubbed the mirror gas turbine has been proposed.

Tsujikawa. Y., Kaneko, K, and Fujii, S., 2000 [5|, has presented paper and considers another application of the mirror cycle for the gasification of LNG -liquid natural gas. Although it is only at the stage of a conceptual study, we have much better results of overall thermal efficiency in comparison with the conventional gasification terminals in Japan, which use seawater.

A study of energy recovery with a high temperature of 1200 K from a fuel cell is being conducted at the authors' institute by use of the inverted Brayton cycle

Najjar Y.S.H., 2000 [21, has taken review of some novel cycle, it has been found that In order to provide better heat recovery in the heat recovery steam generator, more than one pressure level is used. With a single pressure heat recovery steam generator typically about 30% of the total plant output is generated in the steam turbine. A dual pressure arrangement can increase the power output of the steam cycle by up to 10%, and an additional 3% can result by choosing a triple pressure cycle.

Heppenstall T., 1998 [07] concluded that a regenerator would provide a more efficient cycle than a recuperator. This is due to the very high thermal effectiveness of regenerators since values of around 95% are possible. However, maximum efficiency occurs at very low-pressure ratios, typically less than 5. Consequently, even if the theoretical performance could be achieved, relatively large turbines would be required

Korobitsyn M.A., 1998 [6], has published technical paper on Kalina cycle and concluded that Kalina cycle can produce 10% to 30% more power than a Rankine cycle. Because the exhaust pressure of the vapor turbine in the Kalina cycle is above atmospheric pressure, no vacuum is needed to be maintained in the condenser during operation. Another advantage is the smaller size of the whole unit. The footprint of the Kalina plant is about 60% of the size of a Rankine plant design.

Korobitsyn M.A., 1998 [6], studies feasibility of Brayton -Brayton cycle. These reported an increase of power by 18% to 30% depending on the number of intercoolers, and an efficiency growth of up to 10% points. Bray ton-Bray ton cycle is a combination of Brayton cycle in topping cycle and Brayton cycle in bottoming cycle.

Rao A.D., Yi V., Samuelsen G.S., 2003 [1], proposes Brayton fuel cell cycle and found that, the use of the fuel cells integrated with combustion chambers allows efficiency to approach 70%. The Brayton- fuel cell cycle is claimed to have the highest efficiency of any advance cycle, and can, therefore, be seen as a choice for the future power plants.

CHAPTER - 2

ANALYSIS OF MIRROR GAS TURBINE CYCLE

2.1 CYCLE ANALYSIS:

For this Mirror gas turbine cycle analysis, the following figure has been considered

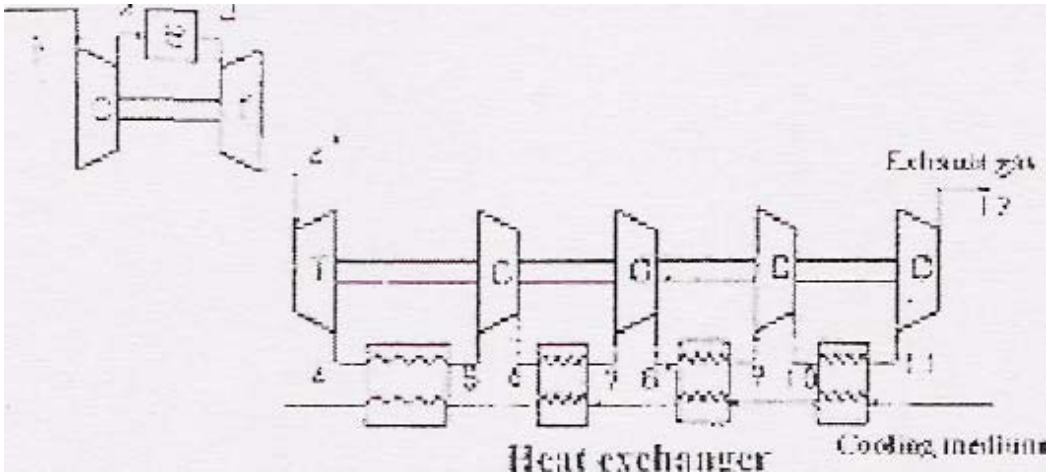

Figure 2.1 Mirror gas turbine cycle

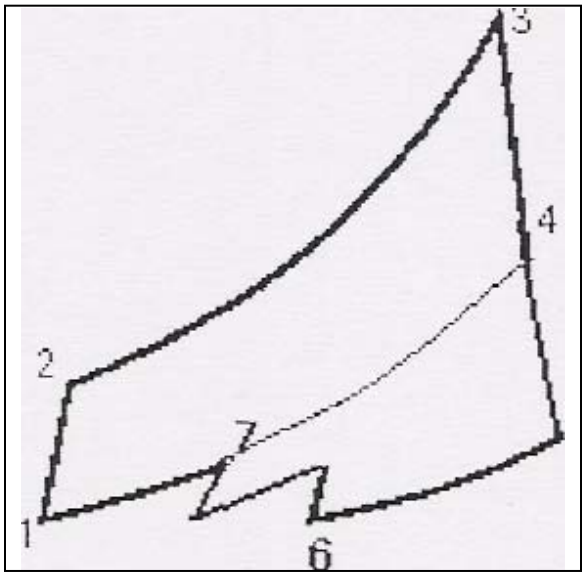

Figure 2.2 Temperautre and entropy diagram of Mirror gas turbine cycle

2.1.1 Simple Gas Turbine As Topping Cycle

It is assumed that, tl = 297 K

$$t2 = [l/ec*tl \{(rp1)^{a}-1\}+t1$$

Where, rpl = Pressure ratio of compressor of Topping Cycle

a = $(\gamma -1)/\gamma)$ for air.

ec = Isentropic efficiency of the compressor

And t3 is varied from 1 000 K to 1 800 K.

Now $$t4 = [t3-et*t3*\{l-(rp1)^{-g}]$$

Where, g = $(\gamma - 1) / \gamma$, for gas

et = Isentropic efficiency of turbine.

The work of compressor of Topping Cycle; wctop.

$$wctop - ma *cp_a * (t2 - tl)$$

Where, ma = Mass of air =lkg

cp_a = Specific heat of air.

The work of turbine of Topping Cycle; wttop.

$$wttop = mg * cp_g* (t3 - t4)$$

mg=mass of gas

cp_g= specific heat of gas

Heat input given to mirror gas turbinc,q

$$q=(I/ecc)*(mg*cpg*t3-ma*cpa*t2)$$

where ecc= combustion efficiency

The net work done of Topping Cycle; wttot.

$$wttot = wttop - wctop$$

The topping cycle efficiency is given by

$$etop=-wttot/q,$$

2.1.2 Inverted Brayton Cycle As Bottoming Cycle

Bottoming cycle in mirror gas turbine is inverted gas turbine,

Expansion from 4 to 5 in turbine,

$$t5 = [t4-et*l4*\{ l-(rp2)^{-g}]$$

The work of turbine of bottoming Cycle; wttop.

$$wtbot - mg * cp_g * (t4 -t5)$$

If n no of stages of intercooling is provided in compression then.

Temperature of gas after cooling in heat exchanger is assumed to be t6=t1-10

$$t7=[l/ec * t6(rp2)^{(g/(n+1)}-1] + t6$$

The work of compression of bottoming cycle;wctop

$$wcbot= (n+1)*mg*cp_g*(t7 -16)$$

Total work of bottoming cycle, wtot

$$wbtot = wtbot - wcbot.$$

Thc inverted brayton cycle efficiency is given by

$$ebot = wbtot / (mg*cpg*t4 -ma*cpa*tl)$$

Total work of mirror gas turbine, wtot

$$wtot = wttot+wbtot,$$

The mirror brayton cycle efficiency is given by

$$ebot = wtot/q$$

2.2 Selection Of Pressure Ratio

The mirror gas turbines have a set of two pressure ratios, which would give the maximum overall efficiency. The mirror gas turbine efficiency is written as

$$etot=(wttot+w btot)/q$$

That is, the efficiency is increased by additional power of the inverted Brayton,

wbtot with input fuel energy (q) kept as constant. In a mirror gas turbine, the maximization of gas turbine efficiency at the topping cycle does not necessarily give the maximum overall efficiency. As well as maximization of specific output of lopping cycle does not necessarily give maximum thermal efficiency of mirror gas turbine. The values of wttot and wbtot are 'a function of two pressure ratios of topping and bottoming cycles that interact with each other. We must find the maximum by computer optimization changing pressure ratios.

The optimum pressure ratio of an inverted Brayton, has One constraint in actual application. As the pressure ratio is increased, that diameters of proceeding turbo machines must be made large to prevent a rapid acceleration of axial velocity in flows. Therefore, The pressure ratio of bottoming cycle is limited to 4 in all the calculations made above [3].

$$rp2=4$$

The limit of 4 means that the diameter becomes 1.7 times greater than that of the topping cycle for no acceleration of axial flows through the turbine, taking into account the change in both gas density and temperature [3]. If the further enlargement of the diameter of the compressor and the turbine is not tolerable for large gas turbines, it is suggested that two bottoming cycle machines should be placed in parallel. For small mirror gas turbines, increase of diameter and hence of the Reynolds number will be beneficial to the component adiabatic efficiency. In our estimation drop of overall efficiency is approximately two to three percent by a deviation of the pressure ratio from the optimum for the large gas turbine with adiabatic efficiency of 0.9.

Hence for work optimization

$$wtot=mg*cpg*et*t3*[l-(4*rp1)^{(-g)}]$$

$$(1/ec)* \{ma*cpa*t1*[(rpl)^{a}-l]+mg*cpg*t6*\{(rp2\}^{g}-1]$$

therefore

d/drpl(wtot)=0,gives

optimised pressure ratio

$$(rpl)=\{(l/4^{g})*[(mg*cpg*6*g*ee*et)/(ma*cpa*t1*a)]^{(1/g+a)}$$

Mirror gas turbine having lopping cycle work on this optimized pressure ratio gives maximum work.

CHAPTER - 3

RESULTS AND DISCUSSION

3.1.1 RESULTS AND IMSCUSS1ON-1

A computer programme has been generated for the analysis of:

1) Specific Work Output Of Mirror Gas Turbine Cycle, **wtot.**

2) Thermal Efficiency Of Mirror Gas Turbine Cycle, **etot.**

3) Specific Work Output Of Topping Cycle, **wttot.**

4) Thermal Efficiency Of Topping Cycle, **etop.**

5) Specific Work Output Of Bottoming Cycle, **wbtot.**

6) Thermal Efficiency Of Bottoming Cycle, **ebof.**

7) Specific Fuel Consumption of Mirror Gas Turbine Cycle**, sf'c**.

8) Power ratio(wttot/wbtot) of Mirror gas Turbine**,ratio**

The following variables have been varied.

1) Turbine inlet Temperature of Topping Cycle, **t3**

2) Number of Fntercoolers, **n.**

3) Pressure Ratio of topping cycle, **rpl.**

Assumptions:

Mass of Air. ma= I Kg

Air Fuel Ratio=60

Efficiency of Combustion Chamber, **ecc**-- 0.96

Specific Heal of Air, **cpa=** 1.005 KJ/Kg K

Specific i feat of Gas, **cpg**= 1.14 KJ/Kg K

Efficiency of Compressor**, ec**= 0.90,

Efficiency of Turbine, **et**= 0.90

Iscntropic index of Air, γ=l .1,1.2,1.3,1.4,1.5,1.6,1.66.

Isentropic index of Gas, γ =-1.33

Ambient condition,tl= 297 K

The Results Starts From Next Page: -

****(For Programme Code, Refer To Annexure-1)**

RESULT OF COMPUTER PROGRAM FOR ANALYSIS OF MIRROR GAS TURBINE IS AS SHOWN

For γ=1.1(for n=0,1,2)

TIT	rp1	wtot	wttot	wbtot	etot	etop	ebot	sfc	ratio
1000	2	251.9261	143.24	108.69	0.288	0.164	0.156	0.238	1.318
1000	2	264.9393	143.24	121.703	0.303	0.164	0.175	0.226	1.177
1000	2	268.9505	143.24	125.714	0.308	0.164	0.181	0.223	1.139
1000	4	331.3749	259.03	72.343	0.39	0.305	0.13	0.181	3.581
1000	4	344.388	259.03	85.356	0.405	0.305	0.153	0.174	3.035
1000	4	348.3992	259.03	89.368	0.41	0.305	0.16	0.172	2.898
1000	6	369.4876	315.68	53.806	0.442	0.378	0.111	0.162	5.867
1000	6	382.5007	315.68	66.819	0.458	0.378	0.137	0.157	4.724
1000	6	386.5119	315.68	70.83	0.463	0.378	0.146	0.155	4.457
1000	8	393.1477	351.41	41.739	0.477	0.426	0.095	0.153	8.419
1000	8	406.1609	351.41	54.753	0.493	0.426	0.124	0.148	6.418
1000	8	410.1721	351.41	58.764	0.497	0.426	0.134	0.146	5.98
1000	10	409.6902	376.73	32.955	0.502	0.462	0.081	0.146	11.432
1000	10	422.7034	376.73	45.969	0.518	0.462	0.113	0.142	8.195
1000	10	426.7146	376.73	49.98	0.523	0.462	0.123	0.141	7.538
1000	12	422.0888	395.96	26.131	0.522	0.49	0.069	0.142	15.153
1000	12	435.1019	395.96	39.144	0.538	0.49	0.103	0.138	10.115
1000	12	439.1131	395.96	43.155	0.543	0.49	0.113	0.137	9.175
1000	14	431.8175	411.22	20.596	0.538	0.512	0.057	0.139	19.966
1000	14	444.8307	411.22	33.61	0.554	0.512	0.094	0.135	12.235
1000	14	448.8419	411.22	37.621	0.559	0.512	0.105	0.134	10.931
1000	16	439.7043	423.73	15.971	0.551	0.531	0.047	0.136	26.532
1000	16	452.7175	423.73	28.984	0.568	0.531	0.085	0.133	14.62
1000	16	456.7287	423.73	32.995	0.573	0.531	0.097	0.131	12.842

1000	18	446.2558	434.24	12.016	0.563	0.548	0.037	0.134	36.139
1000	18	459.2689	434.24	25.029	0.579	0.548	0.077	0.131	17.35
1000	18	463.2801	434.24	29.04	0.585	0.548	0.089	0.13	14.953
1000	20	451.8021	443.23	8.575	0.573	0.562	0.027	0.133	51.691
1000	20	464.8153	443.23	21.588	0.59	0.562	0.069	0.129	20.531
1000	20	468.8265	443.23	25.599	0.595	0.562	0.082	0.128	17.314
1000	22	456.5693	451.03	5.538	0.582	0.575	0.018	0.131	81.441
1000	22	469.5825	451.03	18.551	0.599	0.575	0.061	0.128	24.313
1000	22	473.5937	451.03	22.563	0.604	0.575	0.075	0.127	19.99
1000	24	460.7179	457.89	2.828	0.59	0.587	0.01	0.13	161.906
1000	24	473.7311	457.89	15.841	0.607	0.587	0.054	0.127	28.905
1000	24	477.7423	457.89	19.852	0.612	0.587	0.068	0.126	23.065
1000	26	464.3657	463.98	0.386	0.597	0.597	0.001	0.129	1201.11
1000	26	477.3789	463.98	13.399	0.614	0.597	0.047	0.126	34.627
1000	26	481.3901	463.98	17.411	0.619	0.597	0.062	0.125	26.649
1000	28	467.6013	469.43	-1.832	0.604	0.606	-0.007	0.128	-256.287
1000	28	480.6145	469.43	11.181	0.621	0.606	0.041	0.125	41.983
1000	28	484.6257	469.43	15.193	0.626	0.606	0.055	0.124	30.899
1000	30	470.4929	474.35	-3.86	0.61	0.615	-0.015	0.128	122.883
1000	30	483.506	474.35	9.153	0.627	0.615	0.034	0.124	51.825
1000	30	487.5172	474.35	13.164	0.632	0.615	0.049	0.123	36.034
1200	2	336.9681	176.2	160.771	0.302	0.158	0.18	0.178	1.096
1200	2	349.9813	176.2	173.784	0.314	0.158	0.194	0.171	1.014
1200	2	353.9925	176.2	177.795	0.317	0.158	0.199	0.169	0.991
1200	4	436.9009	319.75	117.155	0.4	0.293	0.161	0.137	2.729
1200	4	449.914	319.75	130.168	0.412	0.293	0.179	0.133	2.456
1200	4	453.9252	319.75	134.179	0.416	0.293	0.184	0.132	2.383
1200	6	485.4609	390.55	94.91	0.451	0.363	0.148	0.124	4.115
1200	6	498.474	390.55	107.923	0.463	0.363	0.168	0.12	3.619

1200	6	502.4852	390.55	111.934	0.467	0.363	0.174	0.119	3.489
1200	8	515.9214	435.49	80.43	0.484	0.409	0.137	0.116	5.415
1200	8	528.9346	435.49	93.443	0.496	0.409	0.159	0.113	4.66
1200	8	532.9458	435.49	97.455	0.5	0.409	0.166	0.113	4.469
1200	10	537.4143	467.52	69.889	0.508	0.442	0.128	0.112	6.689
1200	10	550.4275	467.52	82.903	0.521	0.442	0.151	0.109	5.639
1200	10	554.4387	467.52	86.914	0.524	0.442	0.159	0.108	5.379
1200	12	553.6591	491.96	61.7	0.527	0.468	0.12	0.108	7.973
1200	12	566.6723	491.96	74.713	0.54	0.468	0.145	0.106	6.585
1200	12	570.6835	491.96	78.724	0.543	0.468	0.152	0.105	6.249
1200	14	566.5068	511.45	55.059	0.543	0.49	0.112	0.106	9.289
1200	14	579.52	511.45	68.072	0.555	0.49	0.139	0.104	7.513
1200	14	583.5312	511.45	72.083	0.559	0.49	0.147	0.103	7.095
1200	16	577.0006	527.49	49.508	0.555	0.508	0.105	0.104	10.655
1200	16	590.0137	527.49	62.521	0.568	0.508	0.133	0.102	8.437
1200	16	594.0249	527.49	66.532	0.572	0.508	0.142	0.101	7.928
1200	18	585.7809	541.02	44.762	0.567	0.523	0.099	0.102	12.087
1200	18	598.7941	541.02	57.775	0.579	0.523	0.128	0.1	9.364
1200	18	602.8053	541.02	61.786	0.583	0.523	0.137	0.1	8.756
1200	20	593.2667	552.63	40.633	0.576	0.537	0.093	0.101	13.601
1200	20	606.2798	552.63	53.646	0.589	0.537	0.123	0.099	10.302
1200	20	610.291	552.63	57.657	0.593	0.537	0.132	0.098	9.585
1200	22	599.7451	562.76	36.989	0.585	0.549	0.088	0.1	15.214
1200	22	612.7582	562.76	50.002	0.597	0.549	0.118	0.098	11.255
1200	22	616.7695	562.76	54.013	0.601	0.549	0.128	0.097	10.419
1200	24	605.421	571.68	33.737	0.592	0.559	0.082	0.099	16.945
1200	24	618.4341	571.68	46.75	0.605	0.559	0.114	0.097	12.229
1200	24	622.4454	571.68	50.761	0.609	0.559	0.124	0.096	11.262
1200	26	610.4449	579.64	30.807	0.599	0.569	0.077	0.098	18.815
1200	26	623.4581	579.64	43.82	0.612	0.569	0.11	0.096	13.228

1200	26	627.4693	579.64	47.831	0.616	0.569	0.12	0.096	12.118
1200	28	614.9305	586.79	28.145	0.605	0.578	0.073	0.098	20.849
1200	28	627.9437	586.79	41.158	0.618	0.578	0.106	0.096	14.257
1200	28	631.9549	586.79	45.169	0.622	0.578	0.116	0.095	12.991
1200	30	618.9653	593.25	25.711	0.611	0.586	0.068	0.097	23.074
1200	30	631.9785	593.25	38.724	0.624	0.586	0.102	0.095	15.32
1200	30	635.9897	593.25	42.735	0.628	0.586	0.113	0.094	13.882
1400	2	422.0101	209.16	212.852	0.311	0.154	0.195	0.142	0.983
1400	2	435.0233	209.16	225.865	0.321	0.154	0.207	0.138	0.926
1400	2	439.0345	209.16	229.876	0.324	0.154	0.21	0.137	0.91
1400	4	542.4269	380.46	161.967	0.407	0.285	0.18	0.111	2.349
1400	4	555.44	380.46	174.98	0.417	0.285	0.195	0.108	2.174
1400	4	559.4512	380.46	178.991	0.42	0.285	0.199	0.107	2.126
1400	6	601.4342	465.42	136.014	0.456	0.353	0.17	0.1	3.422
1400	6	614.4474	465.42	149.027	0.466	0.353	0.186	0.098	3.123
1400	6	618.4586	465.42	153.038	0.469	0.353	0.191	0.097	3.041
1400	8	638.695	519.57	119.121	0.489	0.397	0.162	0.094	4.362
1400	8	651.7082	519.57	132.134	0.498	0.397	0.18	0.092	3.932
1400	8	655.7194	519.57	136.146	0.502	0.397	0.185	0.092	3.816
1400	10	665.1384	558.31	106.824	0.512	0.43	0.155	0.09	5.227
1400	10	678.1516	558.31	119.837	0.522	0.43	0.174	0.088	4.659
1400	10	682.1628	558.31	123.848	0.525	0.43	0.18	0.088	4.508
1400	12	685.2294	587.96	97.269	0.53	0.455	0.149	0.088	6.045
1400	12	698.2426	587.96	110.282	0.541	0.455	0.169	0.086	5.331
1400	12	702.2538	587.96	114.293	0.544	0.455	0.175	0.085	5.144
1400	14	701.196	611.67	89.521	0.545	0.476	0.144	0.086	6.833
1400	14	714.2092	611.67	102.534	0.556	0.476	0.165	0.084	5.966
1400	14	718.2204	611.67	106.546	0.559	0.476	0.171	0.084	5.741
1400	16	714.2968	631.25	83.045	0.558	0.493	0.139	0.084	7.601
1400	16	727.31	631.25	96.058	0.568	0.493	0.161	0.082	6.572

1400	16	731.3212	631.25	100.069	0.571	0.493	0.167	0.082	6.308
1400	18	725.3061	647.8	77.508	0.569	0.508	0.134	0.083	8.358
1400	18	738.3192	647.8	90.521	0.579	0.508	0.157	0.081	7.156
1400	18	742.3304	647.8	94.533	0.582	0.508	0.164	0.081	6.853
1400	20	734.7312	662.04	72.69	0.578	0.521	0.13	0.082	9.108
1400	20	747.7444	662.04	85.704	0.588	0.521	0.154	0.08	7.725
1400	20	751.7556	662.04	89.715	0.591	0.521	0.161	0.08	7.379
1400	22	742.9209	674.48	68.439	0.586	0.532	0.126	0.081	9.855
1400	22	755.934	674.48	81.453	0.597	0.532	0.15	0.079	8.281
1400	22	759.9452	674.48	85.464	0.6	0.532	0.158	0.079	7.892
1400	24	750.1241	685.48	64.645	0.594	0.542	0.123	0.08	10.604
1400	24	763.1372	685.48	77.659	0.604	0.542	0.147	0.079	8.827
1400	24	767.1484	685.48	81.67	0.607	0.542	0.155	0.078	8.393
1400	26	756.5242	695.3	61.227	0.6	0.552	0.119	0.079	11.356
1400	26	769.5373	695.3	74.24	0.611	0.552	0.144	0.078	9.366
1400	26	773.5485	695.3	78.251	0.614	0.552	0.152	0.078	8.885
1400	28	762.2598	704.14	58.122	0.606	0.56	0.116	0.079	12.115
1400	28	775.2729	704.14	71.135	0.617	0.56	0.142	0.077	9.899
1400	28	779.2841	704.14	75.146	0.62	0.56	0.15	0.077	9.37
1400	30	767.4378	712.16	55.282	0.612	0.568	0.112	0.078	12.882
1400	30	780.451	712.16	68.295	0.622	0.568	0.139	0.077	10.428
1400	30	784.4622	712.16	72.306	0.626	0.568	0.147	0.076	9.849
1600	2	507.0521	242.12	264.933	0.317	0.151	0.205	0.118	0.914
1600	2	520.0653	242.12	277.946	0.325	0.151	0.215	0.115	0.871
1600	2	524.0765	242.12	281.957	0.328	0.151	0.218	0.114	0.859
1600	4	647.9529	441.17	206.778	0.412	0.28	0.193	0.093	2.134
1600	4	660.9661	441.17	219.792	0.42	0.28	0.205	0.091	2.007
1600	4	664.9773	441.17	223.803	0.422	0.28	0.209	0.09	1.971
1600	6	717.4075	540.29	177.118	0.46	0.346	0.185	0.084	3.05
1600	6	730.4207	540.29	190.131	0.468	0.346	0.199	0.082	2.842

1600	6	734.4319	540.29	194.143	0.471	0.346	0.203	0.082	2.783
1600	8	761.4687	603.66	157.812	0.492	0.39	0.179	0.079	3.825
1600	8	774.4819	603.66	170.825	0.5	0.39	0.193	0.077	3.534
1600	8	778.4931	603.66	174.836	0.503	0.39	0.198	0.077	3.453
1600	10	792.8625	649.1	143.758	0.515	0.421	0.173	0.076	4.515
1600	10	805.8757	649.1	156.771	0.523	0.421	0.189	0.074	4.14
1600	10	809.8869	649.1	160.782	0.526	0.421	0.194	0.074	4.037
1600	12	816.7998	683.96	132.838	0.533	0.446	0.169	0.073	5.149
1600	12	829.8129	683.96	145.851	0.541	0.446	0.185	0.072	4.689
1600	12	833.8241	683.96	149.863	0.544	0.446	0.19	0.072	4.564
1600	14	835.8853	711.9	123.984	0.547	0.466	0.164	0.072	5.742
1600	14	848.8985	711.9	136.997	0.556	0.466	0.182	0.071	5.196
1600	14	852.9097	711.9	141.008	0.559	0.466	0.187	0.07	5.049
1600	16	851.593	735.01	116.582	0.56	0.483	0.161	0.07	6.305
1600	16	864.6062	735.01	129.595	0.568	0.483	0.179	0.069	5.672
1600	16	868.6174	735.01	133.607	0.571	0.483	0.184	0.069	5.501
1600	18	864.8312	754.58	110.254	0.57	0.497	0.157	0.069	6.844
1600	18	877.8444	754.58	123.268	0.579	0.497	0.176	0.068	6.121
1600	18	881.8556	754.58	127.279	0.581	0.497	0.181	0.068	5.929
1600	20	876.1957	771.45	104.748	0.579	0.51	0.154	0.068	7.365
1600	20	889.2089	771.45	117.762	0.588	0.51	0.173	0.067	6.551
1600	20	893.2201	771.45	121.773	0.591	0.51	0.179	0.067	6.335
1600	22	886.0966	786.21	99.89	0.587	0.521	0.151	0.068	7.871
1600	22	899.1098	786.21	112.903	0.596	0.521	0.171	0.067	6.964
1600	22	903.121	786.21	116.915	0.599	0.521	0.177	0.066	6.725
1600	24	894.8271	799.27	95.554	0.595	0.531	0.148	0.067	8.365
1600	24	907.8403	799.27	108.567	0.603	0.531	0.168	0.066	7.362
1600	24	911.8515	799.27	112.578	0.606	0.531	0.174	0.066	7.1
1600	26	902.6034	810.96	91.647	0.601	0.54	0.145	0.066	8.849
1600	26	915.6166	810.96	104.66	0.61	0.54	0.166	0.066	7.748

1600	26	919.6278	810.96	108.672	0.612	0.54	0.172	0.065	7.462
1600	28	909.589	821.49	88.098	0.607	0.548	0.143	0.066	9.325
1600	28	922.6022	821.49	101.112	0.616	0.548	0.164	0.065	8.125
1600	28	926.6134	821.49	105.123	0.618	0.548	0.17	0.065	7.815
1600	30	915.9103	831.06	84.853	0.612	0.556	0.14	0.066	9.794
1600	30	928.9234	831.06	97.866	0.621	0.556	0.162	0.065	8.492
1600	30	932.9346	831.06	101.877	0.624	0.556	0.168	0.064	8.157
1800	2	592.0941	275.08	317.014	0.322	0.15	0.213	0.101	0.868
1800	2	605.1073	275.08	330.027	0.329	0.15	0.221	0.099	0.834
1800	2	609.1185	275.08	334.038	0.331	0.15	0.224	0.099	0.823
1800	4	753.4789	501.89	251.59	0.415	0.276	0.203	0.08	1.995
1800	4	766.4921	501.89	264.603	0.422	0.276	0.213	0.078	1.897
1800	4	770.5033	501.89	268.614	0.424	0.276	0.216	0.078	1.868
1800	6	833.3808	615.16	218.222	0.463	0.342	0.196	0.072	2.819
1800	6	846.394	615.16	231.236	0.47	0.342	0.208	0.071	2.66
1800	6	850.4052	615.16	235.247	0.472	0.342	0.211	0.071	2.615
1800	8	884.2423	687.74	196.503	0.494	0.384	0.191	0.068	3.5
1800	8	897.2555	687.74	209.516	0.501	0.384	0.203	0.067	3.283
1800	8	901.2667	687.74	213.527	0.503	0.384	0.207	0.067	3.221
1800	10	920.5866	739.89	180.692	0.517	0.415	0.186	0.065	4.095
1800	10	933.5998	739.89	193.705	0.524	0.415	0.2	0.064	3.82
1800	10	937.611	739.89	197.716	0.526	0.415	0.204	0.064	3.742
1800	12	948.3701	779.96	168.407	0.534	0.44	0.182	0.063	4.631
1800	12	961.3833	779.96	181.421	0.542	0.44	0.196	0.062	4.299
1800	12	965.3945	779.96	185.432	0.544	0.44	0.201	0.062	4.206
1800	14	970.5746	812.13	158.446	0.549	0.459	0.179	0.062	5.126
1800	14	983.5877	812.13	171.459	0.556	0.459	0.194	0.061	4.737
1800	14	987.5989	812.13	175.47	0.558	0.459	0.198	0.061	4.628
1800	16	988.8893	838.77	150.119	0.561	0.476	0.176	0.061	5.587
1800	16	1001.9024	838.77	163.133	0.568	0.476	0.191	0.06	5.142

1800	16	1005.9136	838.77	167.144	0.571	0.476	0.196	0.06	5.018
1800	18	1004.3564	861.36	143.001	0.571	0.49	0.173	0.06	6.023
1800	18	1017.3695	861.36	156.014	0.579	0.49	0.189	0.059	5.521
1800	18	1021.3807	861.36	160.025	0.581	0.49	0.194	0.059	5.383
1800	20	1017.6603	880.85	136.806	0.58	0.502	0.17	0.059	6.439
1800	20	1030.6734	880.85	149.82	0.588	0.502	0.187	0.058	5.879
1800	20	1034.6846	880.85	153.831	0.59	0.502	0.192	0.058	5.726
1800	22	1029.2724	897.93	131.341	0.588	0.513	0.168	0.058	6.837
1800	22	1042.2856	897.93	144.354	0.596	0.513	0.185	0.058	6.22
1800	22	1046.2968	897.93	148.365	0.598	0.513	0.19	0.057	6.052
1800	24	1039.5302	913.07	126.463	0.595	0.523	0.166	0.058	7.22
1800	24	1052.5434	913.07	139.476	0.603	0.523	0.183	0.057	6.546
1800	24	1056.5546	913.07	143.487	0.605	0.523	0.188	0.057	6.363
1800	26	1048.6827	926.62	122.067	0.602	0.532	0.163	0.057	7.591
1800	26	1061.6958	926.62	135.081	0.609	0.532	0.181	0.057	6.86
1800	26	1065.707	926.62	139.092	0.611	0.532	0.186	0.056	6.662
1800	28	1056.9182	938.84	118.075	0.607	0.54	0.161	0.057	7.951
1800	28	1069.9314	938.84	131.088	0.615	0.54	0.179	0.056	7.162
1800	28	1073.9426	938.84	135.1	0.617	0.54	0.185	0.056	6.949
1800	30	1064.3827	949.96	114.424	0.613	0.547	0.159	0.056	8.302
1800	30	1077.3959	949.96	127.437	0.62	0.547	0.178	0.056	7.454
1800	30	1081.4071	949.96	131.448	0.623	0.547	0.183	0.055	7.227

For γ=1.2(for n=0,1,2)

TIT	rp1	wtot	wttot	wbtot	etot	etop	Ebot	sfc	ratio
1000	2	232.7942	124.1	108.69	0.273	0.145	0.156	0.258	1.142
1000	2	245.8074	124.1	121.703	0.288	0.145	0.175	0.244	1.02
1000	2	249.8186	124.1	125.714	0.293	0.145	0.181	0.24	0.987
1000	4	289.5189	217.18	72.343	0.359	0.269	0.13	0.207	3.002
1000	4	302.5321	217.18	85.356	0.375	0.269	0.153	0.198	2.544

1000	4	306.5433	217.18	89.368	0.38	0.269	0.16	0.196	2.43
1000	6	312.4681	258.66	53.806	0.403	0.333	0.111	0.192	4.807
1000	6	325.4812	258.66	66.819	0.42	0.333	0.137	0.184	3.871
1000	6	329.4924	258.66	70.83	0.425	0.333	0.146	0.182	3.652
1000	8	324.4539	282.71	41.739	0.431	0.375	0.095	0.185	6.773
1000	8	337.4671	282.71	54.753	0.448	0.375	0.124	0.178	5.163
1000	8	341.4783	282.71	58.764	0.454	0.375	0.134	0.176	4.811
1000	10	331.3859	298.43	32.955	0.451	0.406	0.081	0.181	9.056
1000	10	344.399	298.43	45.969	0.469	0.406	0.113	0.174	6.492
1000	10	348.4102	298.43	49.98	0.474	0.406	0.123	0.172	5.971
1000	12	335.5557	309.43	26.131	0.467	0.431	0.069	0.179	11.841
1000	12	348.5689	309.43	39.144	0.485	0.431	0.103	0.172	7.905
1000	12	352.5801	309.43	43.155	0.491	0.431	0.113	0.17	7.17
1000	14	338.0535	317.46	20.596	0.479	0.45	0.057	0.177	15.413
1000	14	351.0667	317.46	33.61	0.498	0.45	0.094	0.171	9.445
1000	14	355.0779	317.46	37.621	0.504	0.45	0.105	0.169	8.438
1000	16	339.4676	323.5	15.971	0.49	0.467	0.047	0.177	20.256
1000	16	352.4808	323.5	28.984	0.509	0.467	0.085	0.17	11.161
1000	16	356.492	323.5	32.995	0.514	0.467	0.097	0.168	9.804
1000	18	340.1447	328.13	12.016	0.499	0.481	0.037	0.176	27.308
1000	18	353.1578	328.13	25.029	0.518	0.481	0.077	0.17	13.11
1000	18	357.169	328.13	29.04	0.524	0.481	0.089	0.168	11.299
1000	20	340.302	331.73	8.575	0.506	0.494	0.027	0.176	38.687
1000	20	353.3151	331.73	21.588	0.526	0.494	0.069	0.17	15.366
1000	20	357.3263	331.73	25.599	0.532	0.494	0.082	0.168	12.959
1000	22	340.0827	334.54	5.538	0.513	0.505	0.018	0.176	60.407
1000	22	353.0959	334.54	18.551	0.533	0.505	0.061	0.17	18.033
1000	22	357.1071	334.54	22.563	0.539	0.505	0.075	0.168	14.827
1000	24	339.585	336.76	2.828	0.519	0.515	0.101	0.1771	19.074
1000	24	352.5982	336.76	15.841	0.539	0.515	0.054	0.17	21.258

1000	24	356.6094	336.76	19.852	0.545	0.515	0.068	0.168	16.963
1000	26	338.878	338.49	0.386	0.524	0.524	0.001	0.177	876.258
1000	26	351.8911	338.49	13.399	0.544	0.524	0.047	0.171	25.262
1000	26	355.9023	338.49	17.411	0.55	0.524	0.062	0.169	19.442
1000	28	338.0116	339.84	-1.832	0.529	0.532	-0.007	0.178	-185.537
1000	28	351.0248	339.84	11.181	0.549	0.532	0.041	0.171	30.393
1000	28	355.036	339.84	15.193	0.555	0.532	0.055	0.169	22.369
1000	30	337.0231	340.88	-3.86	0.533	0.539	-0.015	0.178	-88.307
1000	30	350.0363	340.88	9.153	0.554	0.539	0.034	0.171	37.243
1000	30	354.0475	340.88	13.164	0.56	0.539	0.049	0.169	25.895
1200	2	317.8362	157.07	160.771	0.29	0.143	0.18	0.189	0.977
1200	2	330.8494	157.07	173.784	0.302	0.143	0.194	0.181	0.904
1200	2	334.8606	157.07	177.795	0.306	0.143	0.199	0.179	0.883
1200	4	395.0449	277.89	117.155	0.377	0.265	0.161	0.152	2.372
1200	4	408.0581	277.89	130.168	0.389	0.265	0.179	0.147	2.135
1200	4	412.0693	277.89	134.179	0.393	0.265	0.184	0.146	2.071
1200	6	428.4414	333.53	94.91	0.421	0.328	0.148	0.14	3.514
1200	6	441.4545	333.53	107.923	0.434	0.328	0.168	0.136	3.09
1200	6	445.4657	333.53	111.934	0.438	0.328	0.174	0.135	2.98
1200	8	447.2275	366.8	80.43	0.45	0.369	0.137	0.134	4.56
1200	8	460.2407	366.8	93.443	0.463	0.369	0.159	0.13	3.925
1200	8	464.2519	366.8	97.455	0.467	0.369	0.166	0.129	3.764
1200	10	459.11	389.22	69.889	0.47	0.399	0.128	0.131	5.569
1200	10	472.1231	389.22	82.903	0.484	0.399	0.151	0.127	4.695
1200	10	476.1343	389.22	86.914	0.488	0.399	0.159	0.126	4.478
1200	12	467.126	405.43	61.7	0.487	0.422	0.12	0.128	6.571
1200	12	480.1392	405.43	74.713	0.5	0.422	0.145	0.125	5.426
1200	12	484.1504	405.43	78.724	0.504	0.422	0.152	0.124	5.15
1200	14	472.7428	417.68	55.059	0.499	0.441	0.112	0.127	7.586

1200	14	485.7559	417.68	68.072	0.513	0.441	0.139	0.124	6.136
1200	14	489.7671	417.68	72.083	0.517	0.441	0.147	0.123	5.794
1200	16	476.7639	427.26	49.508	0.51	0.457	0.105	0.126	8.63
1200	16	489.777	427.26	62.521	0.524	0.457	0.133	0.123	6.834
1200	16	493.7882	427.26	66.532	0.528	0.457	0.142	0.122	6.422
1200	18	479.6698	434.91	44.762	0.519	0.471	0.099	0.125	9.716
1200	18	492.683	434.91	57.775	0.534	0.471	0.128	0.122	7.528
1200	18	496.6942	434.91	61.786	0.538	0.471	0.137	0.121	7.039
1200	20	481.7665	441.13	40.633	0.527	0.483	0.093	0.125	10.857
1200	20	494.7797	441.13	53.646	0.542	0.483	0.123	0.121	8.223
1200	20	498.7909	441.13	57.657	0.546	0.483	0.132	0.12	7.651
1200	22	483.2585	446.27	36.989	0.534	0.493	0.088	0.124	12.065
1200	22	496.2717	446.27	50.002	0.549	0.493	0.118	0.121	8.925
1200	22	500.2829	446.27	54.013	0.553	0.493	0.128	0.12	8.262
1200	24	484.2881	450.55	33.737	0.541	0.503	0.082	0.124	13.355
1200	24	497.3013	450.55	46.75	0.555	0.503	0.114	0.121	9.637
1200	24	501.3125	450.55	50.761	0.56	0.503	0.124	0.12	8.876
1200	26	484.9572	454.15	30.807	0.546	0.511	0.077	0.124	14.742
1200	26	497.9704	454.15	43.82	0.561	0.511	0.11	0.12	10.364
1200	26	501.9816	454.15	47.831	0.565	0.511	0.12	0.12	9.495
1200	28	485.3409	457.2	28.145	0.551	0.519	0.073	0.124	16.244
1200	28	498.354	457.2	41.158	0.566	0.519	0.106	0.12	11.108
1200	28	502.3652	457.2	45.169	0.57	0.519	0.116	0.119	10.122
1200	30	485.4956	459.78	25.711	0.556	0.526	0.068	0.124	17.883
1200	30	498.5087	459.78	38.724	0.571	0.526	0.102	0.12	11.873
1200	30	502.5199	459.78	42.735	0.575	0.526	0.113	0.119	10.759
1400	2	402.8782	190.03	212.852	0.301	0.142	0.195	0.149	0.893
1400	2	415.8914	190.03	225.865	0.311	0.142	0.207	0.144	0.841
1400	2	419.9026	190.03	229.876	0.314	0.142	0.21	0.143	0.827
1400	4	500.5709	338.6	161.967	0.388	0.263	0.18	0.12	2.091

1400	4	513.5841	338.6	174.98	0.398	0.263	0.195	0.117	1.935
1400	4	517.5953	338.6	178.991	0.401	0.263	0.199	0.116	1.892
1400	6	544.4147	408.4	136.014	0.432	0.324	0.17	0.11	3.003
1400	6	557.4279	408.4	149.027	0.443	0.324	0.186	0.108	2.74
1400	6	561.4391	408.4	153.038	0.446	0.324	0.191	0.107	2.669
1400	8	570.0012	450.88	119.121	0.461	0.365	0.162	0.105	3.785
1400	8	583.0144	450.88	132.134	0.472	0.365	0.18	0.103	3.412
1400	8	587.0256	450.88	136.146	0.475	0.365	0.185	0.102	3.312
1400	10	586.8341	480.01	106.824	0.482	0.394	0.155	0.102	4.493
1400	10	599.8472	480.01	119.837	0.493	0.394	0.174	0.1	4.006
1400	10	603.8584	480.01	123.848	0.496	0.394	0.18	0.099	3.876
1400	12	598.6964	501.43	97.269	0.498	0.417	0.149	0.1	5.155
1400	12	611.7095	501.43	110.282	0.509	0.417	0.169	0.098	4.547
1400	12	615.7207	501.43	114.293	0.512	0.417	0.175	0.097	4.387
1400	14	607.432	517.91	89.521	0.511	0.436	0.144	0.099	5.785
1400	14	620.4452	517.91	102.534	0.522	0.436	0.165	0.097	5.051
1400	14	624.4564	517.91	106.546	0.526	0.436	0.171	0.096	4.861
1400	16	614.0601	531.02	83.045	0.522	0.452	0.139	0.098	6.394
1400	16	627.0733	531.02	96.058	0.533	0.452	0.161	0.096	5.528
1400	16	631.0845	531.02	100.069	0.537	0.452	0.167	0.095	5.306
1400	18	619.195	541.69	77.508	0.532	0.465	0.134	0.097	6.989
1400	18	632.2081	541.69	90.521	0.543	0.465	0.157	0.095	5.984
1400	18	636.2193	541.69	94.533	0.546	0.465	0.164	0.094	5.73
1400	20	623.231	550.54	72.69	0.54	0.477	0.13	0.096	7.574
1400	20	636.2442	550.54	85.704	0.551	0.477	0.154	0.094	6.424
1400	20	640.2554	550.54	89.715	0.554	0.477	0.161	0.094	6.137
1400	22	626.4343	557.99	68.439	0.547	0.487	0.126	0.096	8.153
1400	22	639.4475	557.99	81.453	0.558	0.487	0.15	0.094	6.851
1400	22	643.4587	557.99	85.464	0.562	0.487	0.158	0.093	6.529
1400	24	628.9912	564.35	64.645	0.553	0.496	0.123	0.095	8.73

1400	24	642.0043	564.35	77.659	0.564	0.496	0.147	0.093	7.267
1400	24	646.0155	564.35	81.67	0.568	0.496	0.155	0.093	6.91
1400	26	631.0364	569.81	61.227	0.559	0.504	0.119	0.095	9.307
1400	26	644.0496	569.81	74.24	0.57	0.504	0.144	0.093	7.675
1400	26	648.0608	569.81	78.251	0.574	0.504	0.152	0.093	7.282
1400	28	632.6701	574.55	58.122	0.564	0.512	0.116	0.095	9.885
1400	28	645.6833	574.55	71.135	0.575	0.512	0.142	0.093	8.077
1400	28	649.6945	574.55	75.146	0.579	0.512	0.15	0.092	7.646
1400	30	633.968	578.69	55.282	0.569	0.519	0.112	0.095	10.468
1400	30	646.9812	578.69	68.295	0.58	0.519	0.139	0.093	8.473
1400	30	650.9924	578.69	72.306	0.584	0.519	0.147	0.092	8.003
1600	2	487.9202	222.99	264.933	0.309	0.141	0.205	0.123	0.842
1600	2	500.9334	222.99	277.946	0.317	0.141	0.215	0.12	0.802
1600	2	504.9446	222.99	281.957	0.32	0.141	0.218	0.119	0.791
1600	4	606.0969	399.32	206.778	0.396	0.261	0.193	0.099	1.931
1600	4	619.1101	399.32	219.792	0.404	0.261	0.205	0.097	1.817
1600	4	623.1213	399.32	223.803	0.407	0.261	0.209	0.096	1.784
1600	6	660.388	483.27	177.118	0.44	0.322	0.185	0.091	2.729
1600	6	673.4012	483.27	190.131	0.449	0.322	0.199	0.089	2.542
1600	6	677.4124	483.27	194.143	0.452	0.322	0.203	0.089	2.489
1600	8	692.7748	534.96	157.812	0.469	0.362	0.179	0.087	3.39
1600	8	705.788	534.96	170.825	0.478	0.362	0.193	0.085	3.132
1600	8	709.7992	534.96	174.836	0.48	0.362	0.198	0.085	3.06
1600	10	714.5582	570.8	143.758	0.49	0.391	0.173	0.084	3.971
1600	10	727.5713	570.8	156.771	0.499	0.391	0.189	0.082	3.641
1600	10	731.5825	570.8	160.782	0.502	0.391	0.194	0.082	3.55
1600	12	730.2667	597.43	132.838	0.506	0.414	0.169	0.082	4.497
1600	12	743.2799	597.43	145.851	0.515	0.414	0.185	0.081	4.096
1600	12	747.2911	597.43	149.863	0.518	0.414	0.19	0.08	3.987
1600	14	742.1213	618.14	123.984	0.519	0.432	0.164	0.081	4.986

1600	14	755.1344	618.14	136.997	0.528	0.432	0.182	0.079	4.512
1600	14	759.1456	618.14	141.008	0.531	0.432	0.187	0.079	4.384
1600	16	751.3563	634.77	116.582	0.53	0.448	0.161	0.08	5.445
1600	16	764.3695	634.77	129.595	0.539	0.448	0.179	0.078	4.898
1600	16	768.3807	634.77	133.607	0.542	0.448	0.184	0.078	4.751
1600	18	758.7201	648.47	110.254	0.539	0.461	0.157	0.079	5.882
1600	18	771.7333	648.47	123.268	0.549	0.461	0.176	0.078	5.261
1600	18	775.7445	648.47	127.279	0.552	0.461	0.181	0.077	5.095
1600	20	764.6956	659.95	104.748	0.548	0.473	0.154	0.078	6.3
1600	20	777.7087	659.95	117.762	0.557	0.473	0.173	0.077	5.604
1600	20	781.7199	659.95	121.773	0.56	0.473	0.179	0.077	5.419
1600	22	769.6101	669.72	99.89	0.555	0.483	0.151	0.078	6.705
1600	22	782.6232	669.72	112.903	0.564	0.483	0.171	0.077	5.932
1600	22	786.6344	669.72	116.915	0.567	0.483	0.177	0.076	5.728
1600	24	773.6943	678.14	95.554	0.561	0.492	0.148	0.078	7.097
1600	24	786.7074	678.14	108.567	0.571	0.492	0.168	0.076	6.246
1600	24	790.7186	678.14	112.578	0.573	0.492	0.174	0.076	6.024
1600	26	777.1157	685.47	91.647	0.567	0.5	0.145	0.077	7.479
1600	26	790.1288	685.47	104.66	0.576	0.5	0.166	0.076	6.549
1600	26	794.14	685.47	108.672	0.579	0.5	0.172	0.076	6.308
1600	28	779.9993	691.9	88.098	0.572	0.507	0.143	0.077	7.854
1600	28	793.0125	691.9	101.112	0.582	0.507	0.164	0.076	6.843
1600	28	797.0237	691.9	105.123	0.585	0.507	0.17	0.075	6.582
1600	30	782.4405	697.59	84.853	0.577	0.514	0.14	0.077	8.221
1600	30	795.4537	697.59	97.866	0.586	0.514	0.162	0.075	7.128
1600	30	799.4649	697.59	101.877	0.589	0.514	0.168	0.075	6.847
1800	2	572.9622	255.95	317.014	0.315	0.141	0.213	0.105	0.807
1800	2	585.9754	255.95	330.027	0.322	0.141	0.221	0.102	0.776
1800	2	589.9866	255.95	334.038	0.324	0.141	0.224	0.102	0.766
1800	4	711.623	460.03	251.59	0.402	0.26	0.203	0.084	1.829

1800	4	724.6361	460.03	264.603	0.409	0.26	0.213	0.083	1.739
1800	4	728.6473	460.03	268.614	0.411	0.26	0.216	0.082	1.713
1800	6	776.3613	558.14	218.222	0.446	0.32	0.196	0.077	2.558
1800	6	789.3745	558.14	231.236	0.453	0.32	0.208	0.076	2.414
1800	6	793.3857	558.14	235.247	0.456	0.32	0.211	0.076	2.373
1800	8	815.5485	619.05	196.503	0.474	0.36	0.191	0.074	3.15
1800	8	828.5616	619.05	209.516	0.482	0.36	0.203	0.072	2.955
1800	8	832.5728	619.05	213.527	0.484	0.36	0.207	0.072	2.899
1800	10	842.2823	661.59	180.692	0.495	0.389	0.186	0.071	3.661
1800	10	855.2954	661.59	193.705	0.503	0.389	0.2	0.07	3.415
1800	10	859.3066	661.59	197.716	0.505	0.389	0.204	0.07	3.346
1800	12	861.837	693.43	168.407	0.512	0.412	0.182	0.07	4.118
1800	12	874.8502	693.43	181.421	0.519	0.412	0.196	0.069	3.822
1800	12	878.8614	693.43	185.432	0.522	0.412	0.201	0.068	3.74
1800	14	876.8105	718.36	158.446	0.525	0.43	0.179	0.068	4.534
1800	14	889.8237	718.36	171.459	0.533	0.43	0.194	0.067	4.19
1800	14	893.8349	718.36	175.47	0.535	0.43	0.198	0.067	4.094
1800	16	888.6526	738.53	150.119	0.536	0.445	0.176	0.068	4.92
1800	16	901.6657	738.53	163.133	0.544	0.445	0.191	0.067	4.527
1800	16	905.6769	738.53	167.144	0.546	0.445	0.196	0.066	4.419
1800	18	898.2453	755.24	143.001	0.545	0.458	0.173	0.067	5.281
1800	18	911.2584	755.24	156.014	0.553	0.458	0.189	0.066	4.841
1800	18	915.2696	755.24	160.025	0.555	0.458	0.194	0.066	4.72
1800	20	906.1601	769.35	136.806	0.553	0.47	0.17	0.066	5.624
1800	20	919.1733	769.35	149.82	0.561	0.47	0.187	0.065	5.135
1800	20	923.1845	769.35	153.831	0.564	0.47	0.192	0.065	5.001
1800	22	912.7859	781.45	131.341	0.56	0.48	0.168	0.066	5.95
1800	22	925.799	781.45	144.354	0.568	0.48	0.185	0.065	5.413
1800	22	929.8102	781.45	148.365	0.571	0.48	0.19	0.065	5.267
1800	24	918.3973	791.93	126.463	0.567	0.489	0.166	0.065	6.262

1800	24	931.4105	791.93	139.476	0.575	0.489	0.183	0.064	5.678
1800	24	935.4217	791.93	143.487	0.577	0.489	0.188	0.064	5.519
1800	26	923.1949	801.13	122.067	0.573	0.497	0.163	0.065	6.563
1800	26	936.2081	801.13	135.081	0.581	0.497	0.181	0.064	5.931
1800	26	940.2193	801.13	139.092	0.583	0.497	0.186	0.064	5.76
1800	28	927.3286	809.25	118.075	0.578	0.504	0.161	0.065	6.854
1800	28	940.3417	809.25	131.088	0.586	0.504	0.179	0.064	6.173
1800	28	944.3529	809.25	135.1	0.588	0.504	0.185	0.064	5.99
1800	30	930.913	816.49	114.424	0.583	0.511	0.159	0.064	7.136
1800	30	943.9261	816.49	127.437	0.591	0.511	0.178	0.064	6.407
1800	30	947.9373	816.49	131.448	0.593	0.511	0.183	0.063	6.211

For γ=1.3(for n=0,1,2)

TIT	rp1	wtot	wttot	wbtot	etot	etop	ebot	sfc	ratio
1000	2	215.9853	107.3	108.69	0.258	0.128	0.156	0.278	0.987
1000	2	228.9985	107.3	121.703	0.274	0.128	0.175	0.262	0.882
1000	2	233.0097	107.3	125.714	0.279	0.128	0.181	0.258	0.853
1000	4	250.9235	178.58	72.343	0.328	0.233	0.13	0.239	2.469
1000	4	263.9367	178.58	85.356	0.344	0.233	0.153	0.227	2.092
1000	4	267.9479	178.58	89.368	0.35	0.233	0.16	0.224	1.998
1000	6	258.3839	204.58	53.806	0.359	0.284	0.111	0.232	3.802
1000	6	271.397	204.58	66.819	0.377	0.284	0.137	0.221	3.062
1000	6	275.4082	204.58	70.83	0.383	0.284	0.146	0.218	2.888
1000	8	257.9782	216.24	41.739	0.377	0.316	0.095	0.233	5.181
1000	8	270.9913	216.24	54.753	0.396	0.316	0.124	0.221	3.949
1000	8	275.0025	216.24	58.764	0.402	0.316	0.134	0.218	3.68
1000	10	254.4242	221.47	32.955	0.389	0.339	0.081	0.236	6.72
1000	10	267.4374	221.47	45.969	0.409	0.339	0.113	0.224	4.818
1000	10	271.4486	221.47	49.98	0.415	0.339	0.123	0.221	4.431
1000	12	249.4211	223.29	26.131	0.397	0.355	0.069	0.241	8.545

1000	12	262.4342	223.29	39.144	0.417	0.355	0.103	0.229	5.704
1000	12	266.4454	223.29	43.155	0.424	0.355	0.113	0.225	5.174
1000	14	243.7154	223.12	20.596	0.402	0.368	0.057	0.246	10.833
1000	14	256.7286	223.12	33.61	0.423	0.368	0.094	0.234	6.639
1000	14	260.7398	223.12	37.621	0.43	0.368	0.105	0.23	5.931
1000	16	237.6769	221.71	15.971	0.405	0.378	0.047	0.252	13.882
1000	16	250.69	221.71	28.984	0.427	0.378	0.085	0.239	7.649
1000	16	254.7012	221.71	32.995	0.434	0.378	0.097	0.236	6.719
1000	18	231.5028	219.49	12.016	0.407	0.386	0.037	0.259	18.267
1000	18	244.5159	219.49	25.029	0.43	0.386	0.077	0.245	8.769
1000	18	248.5271	219.49	29.04	0.437	0.386	0.089	0.241	7.558
1000	20	225.3038	216.73	8.575	0.408	0.392	0.027	0.266	25.276
1000	20	238.3169	216.73	21.588	0.431	0.392	0.069	0.252	10.039
1000	20	242.3281	216.73	25.599	0.439	0.392	0.082	0.248	8.466
1000	22	219.1437	213.61	5.538	0.408	0.398	0.018	0.274	38.57
1000	22	232.1569	213.61	18.551	0.432	0.398	0.061	0.258	11.514
1000	22	236.1681	213.61	22.563	0.44	0.398	0.075	0.254	9.467
1000	24	213.0598	210.23	2.828	0.408	0.402	0.01	0.282	74.336
1000	24	226.073	210.23	15.841	0.433	0.402	0.054	0.265	13.271
1000	24	230.0842	210.23	19.852	0.44	0.402	0.068	0.261	10.59
1000	26	207.0735	206.69	0.386	0.407	0.406	0.001	0.29	35.054
1000	26	220.0867	206.69	13.399	0.432	0.406	0.047	0.273	15.425
1000	26	224.0979	206.69	17.411	0.44	0.406	0.062	0.268	11.871
1000	28	201.1967	203.03	-1.832	0.405	0.409	-0.007	0.298	-110.843
1000	28	214.2099	203.03	11.181	0.431	0.409	0.041	0.28	18.158
1000	28	218.2211	203.03	15.193	0.439	0.409	0.055	0.275	13.364
1000	30	195.4353	199.3	-3.86	0.403	0.411	-0.015	0.307	-51.628
1000	30	208.4484	199.3	9.153	0.43	0.411	0.034	0.288	21.774
1000	30	212.4596	199.3	13.164	0.438	0.411	0.049	0.282	15.139

1200	2	301.0273	140.26	160.771	0.279	0.13	0.18	0.199	0.872
1200	2	314.0405	140.26	173.784	0.291	0.13	0.194	0.191	0.807
1200	2	318.0517	140.26	177.795	0.295	0.13	0.199	0.189	0.789
1200	4	356.4495	239.29	117.155	0.354	0.237	0.161	0.168	2.043
1200	4	369.4627	239.29	130.168	0.367	0.237	0.179	0.162	1.838
1200	4	373.4739	239.29	134.179	0.371	0.237	0.184	0.161	1.783
1200	6	374.3572	279.45	94.91	0.39	0.291	0.148	0.16	2.944
1200	6	387.3704	279.45	107.923	0.403	0.291	0.168	0.155	2.589
1200	6	391.3816	279.45	111.934	0.407	0.291	0.174	0.153	2.497
1200	8	380.7518	300.32	80.43	0.412	0.325	0.137	0.158	3.734
1200	8	393.765	300.32	93.443	0.426	0.325	0.159	0.152	3.214
1200	8	397.7762	300.32	97.455	0.43	0.325	0.166	0.151	3.082
1200	10	382.1483	312.26	69.889	0.427	0.349	0.128	0.157	4.468
1200	10	395.1615	312.26	82.903	0.441	0.349	0.151	0.152	3.767
1200	10	399.1727	312.26	86.914	0.446	0.349	0.159	0.15	3.593
1200	12	380.9914	319.29	61.7	0.438	0.367	0.12	0.157	5.175
1200	12	394.0045	319.29	74.713	0.453	0.367	0.145	0.152	4.274
1200	12	398.0157	319.29	78.724	0.457	0.367	0.152	0.151	4.056
1200	14	378.4047	323.35	55.059	0.446	0.381	0.112	0.159	5.873
1200	14	391.4178	323.35	68.072	0.461	0.381	0.139	0.153	4.75
1200	14	395.429	323.35	72.083	0.466	0.381	0.147	0.152	4.486
1200	16	374.9731	325.47	49.508	0.453	0.393	0.105	0.16	6.574
1200	16	387.9863	325.47	62.521	0.468	0.393	0.133	0.155	5.206
1200	16	391.9975	325.47	66.532	0.473	0.393	0.142	0.153	4.892
1200	18	371.0279	326.27	44.762	0.458	0.403	0.099	0.162	7.289
1200	18	384.0411	326.27	57.775	0.474	0.403	0.128	0.156	5.647
1200	18	388.0523	326.27	61.786	0.479	0.403	0.137	0.155	5.281
1200	20	366.7683	326.14	40.633	0.462	0.411	0.093	0.164	8.026
1200	20	379.7815	326.14	53.646	0.478	0.411	0.123	0.158	6.079
1200	20	383.7927	326.14	57.657	0.484	0.411	0.132	0.156	5.656

1200	22	362.3195	325.33	36.989	0.465	0.418	0.088	0.166	8.795
1200	22	375.3327	325.33	50.002	0.482	0.418	0.118	0.16	6.506
1200	22	379.3439	325.33	54.013	0.487	0.418	0.128	0.158	6.023
1200	24	357.7629	324.03	33.737	0.468	0.424	0.082	0.168	9.605
1200	24	370.7761	324.03	46.75	0.485	0.424	0.114	0.162	6.931
1200	24	374.7873	324.03	50.761	0.49	0.424	0.124	0.16	6.383
1200	26	353.1528	322.35	30.807	0.47	0.429	0.077	0.17	10.464
1200	26	366.1659	322.35	43.82	0.488	0.429	0.11	0.164	7.356
1200	26	370.1771	322.35	47.831	0.493	0.429	0.12	0.162	6.739
1200	28	348.526	320.38	28.145	0.472	0.434	0.073	0.172	11.383
1200	28	361.5391	320.38	41.158	0.49	0.434	0.106	0.166	7.784
1200	28	365.5503	320.38	45.169	0.495	0.434	0.116	0.164	7.093
1200	30	343.9078	318.2	25.711	0.474	0.438	0.068	0.174	12.376
1200	30	356.9209	318.2	38.724	0.492	0.438	0.102	0.168	8.217
1200	30	360.9321	318.2	42.735	0.497	0.438	0.113	0.166	7.446
1400	2	386.0693	173.22	212.852	0.293	0.131	0.195	0.155	0.814
1400	2	399.0824	173.22	225.865	0.302	0.131	0.207	0.15	0.767
1400	2	403.0936	173.22	229.876	0.306	0.131	0.21	0.149	0.754
1400	4	461.9755	300.01	161.967	0.37	0.24	0.18	0.13	1.852
1400	4	474.9887	300.01	174.98	0.38	0.24	0.195	0.126	1.715
1400	4	478.9999	300.01	178.991	0.383	0.24	0.199	0.125	1.676
1400	6	490.3305	354.32	136.014	0.408	0.295	0.17	0.122	2.605
1400	6	503.3437	354.32	149.027	0.419	0.295	0.186	0.119	2.378
1400	6	507.3549	354.32	153.038	0.422	0.295	0.191	0.118	2.315
1400	8	503.5255	384.4	119.121	0.432	0.33	0.162	0.119	3.227
1400	8	516.5386	384.4	132.134	0.443	0.33	0.18	0.116	2.909
1400	8	520.5498	384.4	136.146	0.446	0.33	0.185	0.115	2.823
1400	10	509.8724	403.05	106.824	0.448	0.354	0.155	0.118	3.773
1400	10	522.8856	403.05	119.837	0.46	0.354	0.174	0.115	3.363
1400	10	526.8968	403.05	123.848	0.463	0.354	0.18	0.114	3.254

1400	12	512.5617	415.29	97.269	0.461	0.374	0.149	0.117	4.27
1400	12	525.5749	415.29	110.282	0.473	0.374	0.169	0.114	3.766
1400	12	529.5861	415.29	114.293	0.476	0.374	0.175	0.113	3.634
1400	14	513.0939	423.57	89.521	0.471	0.389	0.144	0.117	4.732
1400	14	526.1071	423.57	102.534	0.483	0.389	0.165	0.114	4.131
1400	14	530.1183	423.57	106.546	0.486	0.389	0.171	0.113	3.976
1400	16	512.2693	429.22	83.045	0.479	0.401	0.139	0.117	5.169
1400	16	525.2825	429.22	96.058	0.491	0.401	0.161	0.114	4.468
1400	16	529.2937	429.22	100.069	0.495	0.401	0.167	0.113	4.289
1400	18	510.5531	433.04	77.508	0.485	0.412	0.134	0.118	5.587
1400	18	523.5662	433.04	90.521	0.498	0.412	0.157	0.115	4.784
1400	18	527.5774	433.04	94.533	0.502	0.412	0.164	0.114	4.581
1400	20	508.2328	435.54	72.69	0.491	0.421	0.13	0.118	5.992
1400	20	521.246	435.54	85.704	0.504	0.421	0.154	0.115	5.082
1400	20	525.2572	435.54	89.715	0.507	0.421	0.161	0.114	4.855
1400	22	505.4953	437.06	68.439	0.496	0.429	0.126	0.119	6.386
1400	22	518.5084	437.06	81.453	0.508	0.429	0.15	0.116	5.366
1400	22	522.5196	437.06	85.464	0.512	0.429	0.158	0.115	5.114
1400	24	502.466	437.82	64.645	0.5	0.435	0.123	0.119	6.773
1400	24	515.4791	437.82	77.659	0.513	0.435	0.147	0.116	5.638
1400	24	519.4903	437.82	81.67	0.517	0.435	0.155	0.115	5.361
1400	26	499.232	438.01	61.227	0.503	0.441	0.119	0.12	7.154
1400	26	512.2452	438.01	74.24	0.516	0.441	0.144	0.117	5.9
1400	26	516.2564	438.01	78.251	0.52	0.441	0.152	0.116	5.597
1400	28	495.8552	437.73	58.122	0.506	0.447	0.116	0.121	7.531
1400	28	508.8684	437.73	71.135	0.519	0.447	0.142	0.118	6.154
1400	28	512.8796	437.73	75.146	0.524	0.447	0.15	0.117	5.825
1400	30	492.3802	437.1	55.282	0.509	0.452	0.112	0.122	7.907
1400	30	505.3934	437.1	68.295	0.522	0.452	0.139	0.119	6.4
1400	30	509.4046	437.1	72.306	0.526	0.452	0.147	0.118	6.045

1600	2	471.1113	206.18	264.933	0.302	0.132	0.205	0.127	0.778
1600	2	484.1244	206.18	277.946	0.31	0.132	0.215	0.124	0.742
1600	2	488.1356	206.18	281.957	0.313	0.132	0.218	0.123	0.731
1600	4	567.5015	360.72	206.778	0.381	0.242	0.193	0.106	1.744
1600	4	580.5147	360.72	219.792	0.389	0.242	0.205	0.103	1.641
1600	4	584.5259	360.72	223.803	0.392	0.242	0.209	0.103	1.612
1600	6	606.3038	429.19	177.118	0.42	0.297	0.185	0.099	2.423
1600	6	619.317	429.19	190.131	0.429	0.297	0.199	0.097	2.257
1600	6	623.3282	429.19	194.143	0.432	0.297	0.203	0.096	2.211
1600	8	626.2991	468.49	157.812	0.445	0.333	0.179	0.096	2.969
1600	8	639.3123	468.49	170.825	0.454	0.333	0.193	0.094	2.742
1600	8	643.3235	468.49	174.836	0.457	0.333	0.198	0.093	2.68
1600	10	637.5965	493.84	143.758	0.463	0.358	0.173	0.094	3.435
1600	10	650.6097	493.84	156.771	0.472	0.358	0.189	0.092	3.15
1600	10	654.6209	493.84	160.782	0.475	0.358	0.194	0.092	3.071
1600	12	644.132	511.29	132.838	0.476	0.378	0.169	0.093	3.849
1600	12	657.1452	511.29	145.851	0.486	0.378	0.185	0.091	3.506
1600	12	661.1564	511.29	149.863	0.489	0.378	0.19	0.091	3.412
1600	14	647.7832	523.8	123.984	0.487	0.393	0.164	0.093	4.225
1600	14	660.7963	523.8	136.997	0.496	0.393	0.182	0.091	3.823
1600	14	664.8075	523.8	141.008	0.499	0.393	0.187	0.09	3.715
1600	16	649.5656	532.98	116.582	0.495	0.406	0.161	0.092	4.572
1600	16	662.5787	532.98	129.595	0.505	0.406	0.179	0.091	4.113
1600	16	666.5899	532.98	133.607	0.508	0.406	0.184	0.09	3.989
1600	18	650.0782	539.82	110.254	0.503	0.417	0.157	0.092	4.896
1600	18	663.0914	539.82	123.268	0.513	0.417	0.176	0.09	4.379
1600	18	667.1026	539.82	127.279	0.516	0.417	0.181	0.09	4.241
1600	20	649.6974	544.95	104.748	0.509	0.427	0.154	0.092	5.202
1600	20	662.7105	544.95	117.762	0.519	0.427	0.173	0.091	4.628
1600	20	666.7217	544.95	121.773	0.522	0.427	0.179	0.09	4.475

1600	22	648.671	548.78	99.89	0.514	0.435	0.151	0.092	5.494
1600	22	661.6842	548.78	112.903	0.525	0.435	0.171	0.091	4.861
1600	22	665.6954	548.78	116.915	0.528	0.435	0.177	0.09	4.694
1600	24	647.1691	551.61	95.554	0.519	0.442	0.148	0.093	5.773
1600	24	660.1822	551.61	108.567	0.529	0.442	0.168	0.091	5.081
1600	24	664.1934	551.61	112.578	0.533	0.442	0.174	0.09	4.9
1600	26	645.3113	553.66	91.647	0.523	0.449	0.145	0.093	6.041
1600	26	658.3244	553.66	104.66	0.534	0.449	0.166	0.091	5.29
1600	26	662.3356	553.66	108.672	0.537	0.449	0.172	0.091	5.095
1600	28	643.1844	555.09	88.098	0.527	0.455	0.143	0.093	6.301
1600	28	656.1976	555.09	101.112	0.537	0.455	0.164	0.091	5.49
1600	28	660.2088	555.09	105.123	0.541	0.455	0.17	0.091	5.28
1600	30	640.8527	556	84.853	0.53	0.46	0.14	0.094	6.553
1600	30	653.8658	556	97.866	0.541	0.46	0.162	0.092	5.681
1600	30	657.877	556	101.877	0.544	0.46	0.168	0.091	5.458
1800	2	556.1533	239.14	317.014	0.309	0.133	0.213	0.108	0.754
1800	2	569.1664	239.14	330.027	0.316	0.133	0.221	0.105	0.725
1800	2	573.1776	239.14	334.038	0.318	0.133	0.224	0.105	0.716
1800	4	673.0276	421.44	251.59	0.389	0.243	0.203	0.089	1.675
1800	4	686.0407	421.44	264.603	0.396	0.243	0.213	0.087	1.593
1800	4	690.0519	421.44	268.614	0.398	0.243	0.216	0.087	1.569
1800	6	722.2772	504.05	218.222	0.429	0.299	0.196	0.083	2.31
1800	6	735.2903	504.05	231.236	0.436	0.299	0.208	0.082	2.18
1800	6	739.3015	504.05	235.247	0.439	0.299	0.211	0.081	2.143
1800	8	749.0728	552.57	196.503	0.454	0.335	0.191	0.08	2.812
1800	8	762.0859	552.57	209.516	0.462	0.335	0.203	0.079	2.637
1800	8	766.0971	552.57	213.527	0.464	0.335	0.207	0.078	2.588
1800	10	765.3206	584.63	180.692	0.472	0.361	0.186	0.078	3.236
1800	10	778.3338	584.63	193.705	0.48	0.361	0.2	0.077	3.018
1800	10	782.345	584.63	197.716	0.483	0.361	0.204	0.077	2.957

1800	12	775.7024	607.29	168.407	0.486	0.381	0.182	0.077	3.606
1800	12	788.7155	607.29	181.421	0.495	0.381	0.196	0.076	3.347
1800	12	792.7267	607.29	185.432	0.497	0.381	0.201	0.076	3.275
1800	14	782.4724	624.03	158.446	0.498	0.397	0.179	0.077	3.938
1800	14	795.4856	624.03	171.459	0.506	0.397	0.194	0.075	3.64
1800	14	799.4968	624.03	175.47	0.508	0.397	0.198	0.075	3.556
1800	16	786.8618	636.74	150.119	0.507	0.41	0.176	0.076	4.242
1800	16	799.875	636.74	163.133	0.515	0.41	0.191	0.075	3.903
1800	16	803.8862	636.74	167.144	0.518	0.41	0.196	0.075	3.81
1800	18	789.6034	646.6	143.001	0.515	0.421	0.173	0.076	4.522
1800	18	802.6165	646.6	156.014	0.523	0.421	0.189	0.075	4.145
1800	18	806.6277	646.6	160.025	0.526	0.421	0.194	0.074	4.041
1800	20	791.1619	654.36	136.806	0.521	0.431	0.17	0.076	4.783
1800	20	804.1751	654.36	149.82	0.53	0.431	0.187	0.075	4.368
1800	20	808.1863	654.36	153.831	0.532	0.431	0.192	0.074	4.254
1800	22	791.8468	660.51	131.341	0.527	0.44	0.168	0.076	5.029
1800	22	804.86	660.51	144.354	0.536	0.44	0.185	0.075	4.576
1800	22	808.8712	660.51	148.365	0.538	0.44	0.19	0.074	4.452
1800	24	791.8721	665.41	126.463	0.532	0.447	0.166	0.076	5.262
1800	24	804.8853	665.41	139.476	0.541	0.447	0.183	0.075	4.771
1800	24	808.8965	665.41	143.487	0.543	0.447	0.188	0.074	4.637
1800	26	791.3905	669.32	122.067	0.536	0.454	0.163	0.076	5.483
1800	26	804.4037	669.32	135.081	0.545	0.454	0.181	0.075	4.955
1800	26	808.4149	669.32	139.092	0.548	0.454	0.186	0.074	4.812
1800	28	790.5137	672.44	118.075	0.541	0.46	0.161	0.076	5.695
1800	28	803.5268	672.44	131.088	0.549	0.46	0.179	0.075	5.13
1800	28	807.538	672.44	135.1	0.552	0.46	0.185	0.074	4.977
1800	30	789.3252	674.9	114.424	0.544	0.465	0.159	0.076	5.898
1800	30	802.3383	674.9	127.437	0.553	0.465	0.178	0.075	5.296
1800	30	806.3495	674.9	131.448	0.556	0.465	0.183	0.074	5.134

For γ=1.4(for n=0,1,2)

TIT	rp1	wtot	wttot	wbtot	etot	etop	ebot	sfc	ratio
1000	2	200.8629	92.17	108.69	0.245	0.112	0.156	0.299	0.848
1000	2	213.8761	92.17	121.703	0.261	0.112	0.175	0.281	0.757
1000	2	217.8873	92.17	125.714	0.265	0.112	0.181	0.275	0.733
1000	4	214.7446	142.4	72.343	0.295	0.195	0.13	0.279	1.968
1000	4	227.7578	142.4	85.356	0.313	0.195	0.153	0.263	1.668
1000	4	231.769	142.4	89.368	0.318	0.195	0.16	0.259	1.593
1000	6	206.4541	152.65	53.806	0.31	0.229	0.111	0.291	2.837
1000	6	219.4672	152.65	66.819	0.33	0.229	0.137	0.273	2.285
1000	6	223.4784	152.65	70.83	0.336	0.229	0.146	0.268	2.155
1000	8	193.0544	151.32	41.739	0.313	0.246	0.095	0.311	3.625
1000	8	206.0675	151.32	54.753	0.334	0.246	0.124	0.291	2.764
1000	8	210.0787	151.32	58.764	0.341	0.246	0.134	0.286	2.575
1000	10	178.2604	145.31	32.955	0.31	0.253	0.081	0.337	4.409
1000	10	191.2736	145.31	45.969	0.333	0.253	0.113	0.314	3.161
1000	10	195.2848	145.31	49.98	0.34	0.253	0.123	0.307	2.907
1000	12	163.2552	137.12	26.131	0.303	0.254	0.069	0.368	5.248
1000	12	176.2683	137.12	39.144	0.327	0.254	0.103	0.34	3.503
1000	12	180.2795	137.12	43.155	0.334	0.254	0.113	0.333	3.177
1000	14	148.479	127.88	20.596	0.293	0.252	0.057	0.404	6.209
1000	14	161.4922	127.88	33.61	0.318	0.252	0.094	0.372	3.805
1000	14	165.5034	127.88	37.621	0.326	0.252	0.105	0.363	3.399
1000	16	134.1024	118.13	15.971	0.28	0.247	0.047	0.447	7.397
1000	16	147.1156	118.13	28.984	0.307	0.247	0.085	0.408	4.076
1000	16	151.1268	118.13	32.995	0.315	0.247	0.097	0.397	3.58
1000	18	120.1849	108.17	12.016	0.265	0.239	0.037	0.499	9.002
1000	18	133.198	108.17	25.029	0.294	0.239	0.077	0.45	4.322
1000	18	137.2092	108.17	29.04	0.303	0.239	0.089	0.437	3.725

1000	20	106.7371	98.16	8.575	0.249	0.229	0.027	0.562	11.448
1000	20	119.7502	98.16	21.588	0.279	0.229	0.069	0.501	4.547
1000	20	123.7614	98.16	25.599	0.289	0.229	0.082	0.485	3.835
1000	22	93.7476	88.21	5.538	0.231	0.217	0.018	0.64	15.928
1000	22	106.7608	88.21	18.551	0.263	0.217	0.061	0.562	4.755
1000	22	110.772	88.21	22.563	0.273	0.217	0.075	0.542	3.91
1000	24	81.1955	78.37	2.828	0.211	0.203	0.01	0.739	27.71
1000	24	94.2087	78.37	15.841	0.244	0.203	0.054	0.637	4.947
1000	24	98.2199	78.37	19.852	0.255	0.203	0.068	0.611	3.947
1000	26	69.0562	68.67	0.386	0.189	0.188	0.001	0.869	177.767
1000	26	82.0694	68.67	13.399	0.225	0.188	0.047	0.731	5.125
1000	26	86.0806	68.67	17.411	0.236	0.188	0.062	0.697	3.944
1000	28	57.3042	59.14	-1.832	0.165	0.171	-0.007	1.047	-32.285
1000	28	70.3174	59.14	11.181	0.203	0.171	0.041	0.853	5.289
1000	28	74.3286	59.14	15.193	0.214	0.171	0.055	0.807	3.892
1000	30	45.9149	49.78	-3.86	0.14	0.151	-0.015	1.307	-12.894
1000	30	58.9281	49.78	9.153	0.179	0.151	0.034	1.018	5.438
1000	30	62.9393	49.78	13.164	0.191	0.151	0.049	0.953	3.781
1200	2	285.9049	125.13	160.771	0.269	0.118	0.18	0.21	0.778
1200	2	298.9181	125.13	173.784	0.281	0.118	0.194	0.201	0.72
1200	2	302.9293	125.13	177.795	0.285	0.118	0.199	0.198	0.704
1200	4	320.2706	203.12	117.155	0.33	0.209	0.161	0.187	1.734
1200	4	333.2838	203.12	130.168	0.344	0.209	0.179	0.18	1.56
1200	4	337.295	203.12	134.179	0.348	0.209	0.184	0.178	1.514
1200	6	322.4274	227.52	94.91	0.356	0.251	0.148	0.186	2.397
1200	6	335.4405	227.52	107.923	0.37	0.251	0.168	0.179	2.108
1200	6	339.4517	227.52	111.934	0.374	0.251	0.174	0.177	2.033
1200	8	315.828	235.4	80.43	0.368	0.275	0.137	0.19	2.927
1200	8	328.8412	235.4	93.443	0.383	0.275	0.159	0.182	2.519
1200	8	332.8524	235.4	97.455	0.388	0.275	0.166	0.18	2.415

1200	10	305.9845	236.1	69.889	0.375	0.289	0.128	0.196	3.378
1200	10	318.9977	236.1	82.903	0.391	0.289	0.151	0.188	2.848
1200	10	323.0089	236.1	86.914	0.396	0.289	0.159	0.186	2.716
1200	12	294.8255	233.13	61.7	0.378	0.299	0.12	0.204	3.778
1200	12	307.8387	233.13	74.713	0.394	0.299	0.145	0.195	3.12
1200	12	311.8499	233.13	78.724	0.399	0.299	0.152	0.192	2.961
1200	14	283.1683	228.11	55.059	0.378	0.305	0.112	0.212	4.143
1200	14	296.1814	228.11	68.072	0.395	0.305	0.139	0.203	3.351
1200	14	300.1926	228.11	72.083	0.401	0.305	0.147	0.2	3.165
1200	16	271.3986	221.89	49.508	0.377	0.308	0.105	0.221	4.482
1200	16	284.4118	221.89	62.521	0.395	0.308	0.133	0.211	3.549
1200	16	288.423	221.89	66.532	0.4	0.308	0.142	0.208	3.335
1200	18	259.71	214.95	44.762	0.374	0.31	0.099	0.231	4.802
1200	18	272.7232	214.95	57.775	0.393	0.31	0.128	0.22	3.72
1200	18	276.7344	214.95	61.786	0.399	0.31	0.137	0.217	3.479
1200	20	248.2016	207.57	40.633	0.37	0.31	0.093	0.242	5.108
1200	20	261.2147	207.57	53.646	0.39	0.31	0.123	0.23	3.869
1200	20	265.226	207.57	57.657	0.396	0.31	0.132	0.226	3.6
1200	22	236.9234	199.93	36.989	0.366	0.309	0.088	0.253	5.405
1200	22	249.9365	199.93	50.002	0.386	0.309	0.118	0.24	3.999
1200	22	253.9477	199.93	54.013	0.392	0.309	0.128	0.236	3.702
1200	24	225.8986	192.16	33.737	0.36	0.307	0.082	0.266	5.696
1200	24	238.9118	192.16	46.75	0.381	0.307	0.114	0.251	4.11
1200	24	242.923	192.16	50.761	0.388	0.307	0.124	0.247	3.786
1200	26	215.1354	184.33	30.807	0.354	0.304	0.077	0.279	5.983
1200	26	228.1486	184.33	43.82	0.376	0.304	0.11	0.263	4.207
1200	26	232.1598	184.33	47.831	0.382	0.304	0.12	0.258	3.854
1200	28	204.6335	176.49	28.145	0.348	0.3	0.073	0.293	6.271
1200	28	217.6466	176.49	41.158	0.37	0.3	0.106	0.276	4.288
1200	28	221.6578	176.49	45.169	0.377	0.3	0.116	0.271	3.907

1200	30	194.3874	168.68	25.711	0.341	0.296	0.068	0.309	6.561
1200	30	207.4006	168.68	38.724	0.364	0.296	0.102	0.289	4.356
1200	30	211.4118	168.68	42.735	0.371	0.296	0.113	0.284	3.947
1400	2	370.9469	158.1	212.852	0.285	0.121	0.195	0.162	0.743
1400	2	383.9601	158.1	225.865	0.295	0.121	0.207	0.156	0.7
1400	2	387.9713	158.1	229.876	0.298	0.121	0.21	0.155	0.688
1400	4	425.7966	263.83	161.967	0.351	0.218	0.18	0.141	1.629
1400	4	438.8098	263.83	174.98	0.362	0.218	0.195	0.137	1.508
1400	4	442.821	263.83	178.991	0.366	0.218	0.199	0.135	1.474
1400	6	438.4007	302.39	136.014	0.382	0.263	0.17	0.137	2.223
1400	6	451.4139	302.39	149.027	0.393	0.263	0.186	0.133	2.029
1400	6	455.4251	302.39	153.038	0.397	0.263	0.191	0.132	1.976
1400	8	438.6017	319.48	119.121	0.399	0.291	0.162	0.137	2.682
1400	8	451.6148	319.48	132.134	0.411	0.291	0.18	0.133	2.418
1400	8	455.626	319.48	136.146	0.415	0.291	0.185	0.132	2.347
1400	10	433.7086	326.89	106.824	0.41	0.309	0.155	0.138	3.06
1400	10	446.7218	326.89	119.837	0.422	0.309	0.174	0.134	2.728
1400	10	450.733	326.89	123.848	0.426	0.309	0.18	0.133	2.639
1400	12	426.3958	329.13	97.269	0.417	0.322	0.149	0.141	3.384
1400	12	439.409	329.13	110.282	0.43	0.322	0.169	0.137	2.984
1400	12	443.4202	329.13	114.293	0.434	0.322	0.175	0.135	2.88
1400	14	417.8575	328.34	89.521	0.422	0.331	0.144	0.144	3.668
1400	14	430.8707	328.34	102.534	0.435	0.331	0.165	0.139	3.202
1400	14	434.8819	328.34	106.546	0.439	0.331	0.171	0.138	3.082
1400	16	408.6949	325.65	83.045	0.425	0.339	0.139	0.147	3.921
1400	16	421.708	325.65	96.058	0.438	0.339	0.161	0.142	3.39
1400	16	425.7192	325.65	100.069	0.443	0.339	0.167	0.141	3.254
1400	18	399.2352	321.73	77.508	0.427	0.344	0.134	0.15	4.151
1400	18	412.2483	321.73	90.521	0.441	0.344	0.157	0.146	3.554
1400	18	416.2595	321.73	94.533	0.445	0.344	0.164	0.144	3.403

1400	20	389.6661	316.98	72.69	0.427	0.348	0.13	0.154	4.361
1400	20	402.6793	316.98	85.704	0.442	0.348	0.154	0.149	3.699
1400	20	406.6905	316.98	89.715	0.446	0.348	0.161	0.148	3.533
1400	22	380.0992	311.66	68.439	0.427	0.35	0.126	0.158	4.554
1400	22	393.1123	311.66	81.453	0.442	0.35	0.15	0.153	3.826
1400	22	397.1235	311.66	85.464	0.447	0.35	0.158	0.151	3.647
1400	24	370.6017	305.96	64.645	0.427	0.352	0.123	0.162	4.733
1400	24	383.6148	305.96	77.659	0.442	0.352	0.147	0.156	3.94
1400	24	387.626	305.96	81.67	0.446	0.352	0.155	0.155	3.746
1400	26	361.2147	299.99	61.227	0.426	0.354	0.119	0.166	4.9
1400	26	374.2278	299.99	74.24	0.441	0.354	0.144	0.16	4.041
1400	26	378.239	299.99	78.251	0.446	0.354	0.152	0.159	3.834
1400	28	351.9627	293.84	58.122	0.424	0.354	0.116	0.17	5.056
1400	28	364.9759	293.84	71.135	0.44	0.354	0.142	0.164	4.131
1400	28	368.9871	293.84	75.146	0.445	0.354	0.15	0.163	3.91
1400	30	342.8599	287.58	55.282	0.422	0.354	0.112	0.175	5.202
1400	30	355.873	287.58	68.295	0.438	0.354	0.139	0.169	4.211
1400	30	359.8842	287.58	72.306	0.443	0.354	0.147	0.167	3.977
1600	2	455.9889	191.06	264.933	0.295	0.124	0.205	0.132	0.721
1600	2	469.0021	191.06	277.946	0.304	0.124	0.215	0.128	0.687
1600	2	473.0133	191.06	281.957	0.306	0.124	0.218	0.127	0.678
1600	4	531.3227	324.54	206.778	0.366	0.223	0.193	0.113	1.57
1600	4	544.3358	324.54	219.792	0.375	0.223	0.205	0.11	1.477
1600	4	548.347	324.54	223.803	0.377	0.223	0.209	0.109	1.45
1600	6	554.374	377.26	177.118	0.399	0.271	0.185	0.108	2.13
1600	6	567.3872	377.26	190.131	0.408	0.271	0.199	0.106	1.984
1600	6	571.3984	377.26	194.143	0.411	0.271	0.203	0.105	1.943
1600	8	561.3753	403.56	157.812	0.419	0.301	0.179	0.107	2.557
1600	8	574.3885	403.56	170.825	0.429	0.301	0.193	0.104	2.362
1600	8	578.3997	403.56	174.836	0.432	0.301	0.198	0.104	2.308

1600	10	561.4327	417.68	143.758	0.432	0.321	0.173	0.107	2.905
1600	10	574.4459	417.68	156.771	0.442	0.321	0.189	0.104	2.664
1600	10	578.4571	417.68	160.782	0.445	0.321	0.194	0.104	2.598
1600	12	557.9662	425.13	132.838	0.442	0.336	0.169	0.108	3.2
1600	12	570.9793	425.13	145.851	0.452	0.336	0.185	0.105	2.915
1600	12	574.9905	425.13	149.863	0.455	0.336	0.19	0.104	2.837
1600	14	552.5468	428.56	123.984	0.449	0.348	0.164	0.109	3.457
1600	14	565.5599	428.56	136.997	0.459	0.348	0.182	0.106	3.128
1600	14	569.5711	428.56	141.008	0.462	0.348	0.187	0.105	3.039
1600	16	545.9911	429.41	116.582	0.454	0.357	0.161	0.11	3.683
1600	16	559.0043	429.41	129.595	0.465	0.357	0.179	0.107	3.313
1600	16	563.0155	429.41	133.607	0.468	0.357	0.184	0.107	3.214
1600	18	538.7603	428.51	110.254	0.458	0.364	0.157	0.111	3.887
1600	18	551.7735	428.51	123.268	0.469	0.364	0.176	0.109	3.476
1600	18	555.7847	428.51	127.279	0.472	0.364	0.181	0.108	3.367
1600	20	531.1307	426.38	104.748	0.461	0.37	0.154	0.113	4.071
1600	20	544.1438	426.38	117.762	0.472	0.37	0.173	0.11	3.621
1600	20	548.155	426.38	121.773	0.475	0.37	0.179	0.109	3.501
1600	22	523.2749	423.38	99.89	0.463	0.374	0.151	0.115	4.239
1600	22	536.2881	423.38	112.903	0.474	0.374	0.171	0.112	3.75
1600	22	540.2993	423.38	116.915	0.478	0.374	0.177	0.111	3.621
1600	24	515.3048	419.75	95.554	0.464	0.378	0.148	0.116	4.393
1600	24	528.3179	419.75	108.567	0.476	0.378	0.168	0.114	3.866
1600	24	532.3291	419.75	112.578	0.48	0.378	0.174	0.113	3.729
1600	26	507.2939	415.65	91.647	0.465	0.381	0.145	0.118	4.535
1600	26	520.3071	415.65	104.66	0.477	0.381	0.166	0.115	3.971
1600	26	524.3183	415.65	108.672	0.481	0.381	0.172	0.114	3.825
1600	28	499.2919	411.19	88.098	0.466	0.384	0.143	0.12	4.667
1600	28	512.3051	411.19	101.112	0.478	0.384	0.164	0.117	4.067
1600	28	516.3163	411.19	105.123	0.482	0.384	0.17	0.116	3.912

1600	30	491.3323	406.48	84.853	0.466	0.386	0.14	0.122	4.79
1600	30	504.3455	406.48	97.866	0.479	0.386	0.162	0.119	4.153
1600	30	508.3567	406.48	101.877	0.483	0.386	0.168	0.118	3.99
1800	2	541.0309	224.02	317.014	0.303	0.125	0.213	0.111	0.707
1800	2	554.0441	224.02	330.027	0.31	0.125	0.221	0.108	0.679
1800	2	558.0553	224.02	334.038	0.312	0.125	0.224	0.108	0.671
1800	4	636.8487	385.26	251.59	0.376	0.227	0.203	0.094	1.531
1800	4	649.8618	385.26	264.603	0.384	0.227	0.213	0.092	1.456
1800	4	653.873	385.26	268.614	0.386	0.227	0.216	0.092	1.434
1800	6	670.3473	452.12	218.222	0.411	0.277	0.196	0.09	2.072
1800	6	683.3605	452.12	231.236	0.419	0.277	0.208	0.088	1.955
1800	6	687.3717	452.12	235.247	0.421	0.277	0.211	0.087	1.922
1800	8	684.149	487.65	196.503	0.432	0.308	0.191	0.088	2.482
1800	8	697.1621	487.65	209.516	0.441	0.308	0.203	0.086	2.327
1800	8	701.1733	487.65	213.527	0.443	0.308	0.207	0.086	2.284
1800	10	689.1568	508.47	180.692	0.447	0.33	0.186	0.087	2.814
1800	10	702.17	508.47	193.705	0.456	0.33	0.2	0.085	2.625
1800	10	706.1812	508.47	197.716	0.458	0.33	0.204	0.085	2.572
1800	12	689.5365	521.13	168.407	0.458	0.346	0.182	0.087	3.094
1800	12	702.5496	521.13	181.421	0.467	0.346	0.196	0.085	2.872
1800	12	706.5608	521.13	185.432	0.469	0.346	0.201	0.085	2.81
1800	14	687.236	528.79	158.446	0.466	0.359	0.179	0.087	3.337
1800	14	700.2492	528.79	171.459	0.475	0.359	0.194	0.086	3.084
1800	14	704.2604	528.79	175.47	0.478	0.359	0.198	0.085	3.014
1800	16	683.2874	533.17	150.119	0.473	0.369	0.176	0.088	3.552
1800	16	696.3005	533.17	163.133	0.482	0.369	0.191	0.086	3.268
1800	16	700.3117	533.17	167.144	0.485	0.369	0.196	0.086	3.19
1800	18	678.2855	535.28	143.001	0.478	0.377	0.173	0.088	3.743
1800	18	691.2986	535.28	156.014	0.487	0.377	0.189	0.087	3.431
1800	18	695.3098	535.28	160.025	0.49	0.377	0.194	0.086	3.345

1800	20	672.5952	535.79	136.806	0.482	0.384	0.17	0.089	3.916
1800	20	685.6084	535.79	149.82	0.492	0.384	0.187	0.088	3.576
1800	20	689.6196	535.79	153.831	0.494	0.384	0.192	0.087	3.483
1800	22	666.4507	535.11	131.341	0.486	0.39	0.168	0.09	4.074
1800	22	679.4639	535.11	144.354	0.495	0.39	0.185	0.088	3.707
1800	22	683.4751	535.11	148.365	0.498	0.39	0.19	0.088	3.607
1800	24	660.0078	533.55	126.463	0.488	0.395	0.166	0.091	4.219
1800	24	673.021	533.55	139.476	0.498	0.395	0.183	0.089	3.825
1800	24	677.0322	533.55	143.487	0.501	0.395	0.188	0.089	3.718
1800	26	653.3732	531.31	122.067	0.491	0.399	0.163	0.092	4.353
1800	26	666.3863	531.31	135.081	0.501	0.399	0.181	0.09	3.933
1800	26	670.3975	531.31	139.092	0.504	0.399	0.186	0.089	3.82
1800	28	646.6212	528.55	118.075	0.493	0.403	0.161	0.093	4.476
1800	28	659.6343	528.55	131.088	0.503	0.403	0.179	0.091	4.032
1800	28	663.6455	528.55	135.1	0.506	0.403	0.185	0.09	3.912
1800	30	639.8048	525.38	114.424	0.494	0.406	0.159	0.094	4.592
1800	30	652.818	525.38	127.437	0.504	0.406	0.178	0.092	4.123
1800	30	656.8292	525.38	131.448	0.507	0.406	0.183	0.091	3.997

For γ=1.5(for n=0,1,2)

TIT	rp1	wtot	wttot	wbtot	etot	etop	ebot	sfc	ratio
1000	2	187.3885	78.7	108.69	0.232	0.098	0.156	0.32	0.724
1000	2	200.4017	78.7	121.703	0.248	0.098	0.175	0.299	0.647
1000	2	204.4129	78.7	125.714	0.253	0.098	0.181	0.294	0.626
1000	4	181.3465	109	72.343	0.261	0.157	0.13	0.331	1.507
1000	4	194.3597	109	85.356	0.28	0.157	0.153	0.309	1.277
1000	4	198.3709	109	89.368	0.286	0.157	0.16	0.302	1.22
1000	6	157.5132	103.71	53.806	0.256	0.169	0.111	0.381	1.927
1000	6	170.5263	103.71	66.819	0.278	0.169	0.137	0.352	1.552
1000	6	174.5375	103.71	70.83	0.284	0.169	0.146	0.344	1.464

1000	8	130.9626	89.22	41.739	0.238	0.162	0.095	0.458	2.138
1000	8	143.9758	89.22	54.753	0.261	0.162	0.124	0.417	1.63
1000	8	147.987	89.22	58.764	0.268	0.162	0.134	0.405	1.518
1000	10	104.5852	71.63	32.955	0.21	0.144	0.081	0.574	2.174
1000	10	117.5984	71.63	45.969	0.236	0.144	0.113	0.51	1.558
1000	10	121.6096	71.63	49.98	0.244	0.144	0.123	0.493	1.433
1000	12	79.1261	53	26.131	0.175	0.117	0.069	0.758	2.028
1000	12	92.1393	53	39.144	0.204	0.117	0.103	0.651	1.354
1000	12	96.1505	53	43.155	0.213	0.117	0.113	0.624	1.228
1000	14	54.7602	34.16	20.596	0.134	0.083	0.057	1.096	1.659
1000	14	67.7734	34.16	33.61	0.165	0.083	0.094	0.885	1.016
1000	14	71.7846	34.16	37.621	0.175	0.083	0.105	0.836	0.908
1000	16	31.4823	15.51	15.971	0.085	0.042	0.047	1.906	0.971
1000	16	44.4955	15.51	28.984	0.12	0.042	0.085	1.348	0.535
1000	16	48.5067	15.51	32.995	0.13	0.042	0.097	1.237	0.47
1000	18	9.2287	-2.79	12.016	0.027	-0.008	0.037	6.501	-0.232
1000	18	22.2418	-2.79	25.029	0.066	-0.008	0.077	2.698	-0.111
1000	18	26.253	-2.79	29.04	0.078	-0.008	0.089	2.285	-0.096
1000	20	-12.0806	-20.66	8.575	-0.04	-0.068	0.027	-4.967	-2.409
1000	20	0.9325	-20.66	21.588	0.003	-0.068	0.069	64.34	-0.957
1000	20	4.9437	-20.66	25.599	0.016	-0.068	0.082	12.137	-0.807
1000	22	-32.5256	-38.06	5.538	-0.118	-0.139	0.018	-1.845	-6.873
1000	22	-19.5125	-38.06	18.551	-0.071	-0.139	0.061	-3.075	-2.052
1000	22	-15.5013	-38.06	22.563	-0.056	-0.139	0.075	-3.871	-1.687
1000	24	-52.1811	-55.01	2.828	-0.212	-0.223	0.01	-1.15	-19.451
1000	24	-39.1679	-55.01	15.841	-0.159	-0.223	0.054	-1.532	-3.473
1000	24	-35.1567	-55.01	19.852	-0.143	-0.223	0.068	-1.707	-2.771
1000	26	-71.1144	-71.5	0.386	-0.324	0.326	0.001	0.001	-185.095
1000	26	-58.1012	-71.5	13.399	-0.265	-0.326	0.047	-1.033	-5.336

1000	26	-54.09	-71.5	17.411	-0.246	-0.326	0.062	-1.109	-4.107
1000	28	-89.3858	-87.55	-1.832	-0.461	-0.451	-0.007	-0.671	47.8
1000	28	-76.3726	-87.55	11.181	-0.394	-0.451	0.041	-0.786	-7.83
1000	28	-72.3614	-87.55	15.193	-0.373	-0.451	0.055	-0.829	-5.763
1000	30	-107.0489	-103.19	-3.86	-0.631	-0.015	-0.015	-0.56	26.731
1000	30	-94.0357	-103.19	9.153	-0.554	0.608	0.034	-0.638	-11.274
1000	30	-90.0245	-103.19	13.164	-0.531	-0.608	0.049	-0.666	-7.839
1200	2	272.4305	111.66	160.771	0.26	0.107	0.18	0.22	0.695
1200	2	285.4437	111.66	173.784	0.272	0.107	0.194	0.21	0.643
1200	2	289.4549	111.66	177.795	0.276	0.107	0.199	0.207	0.628
1200	4	286.8725	169.72	117.155	0.307	0.181	0.161	0.209	1.449
1200	4	299.8857	169.72	130.168	0.321	0.181	0.179	0.2	1.304
1200	4	303.8969	169.72	134.179	0.325	0.181	0.184	0.197	1.265
1200	6	273.4865	178.58	94.91	0.32	0.209	0.148	0.219	1.882
1200	6	286.4997	178.58	107.923	0.335	0.209	0.168	0.209	1.655
1200	6	290.5109	178.58	111.934	0.339	0.209	0.174	0.207	1.595
1200	8	253.7363	173.31	80.43	0.32	0.219	0.137	0.236	2.155
1200	8	266.7495	173.31	93.443	0.336	0.219	0.159	0.225	1.855
1200	8	270.7607	173.31	97.455	0.342	0.219	0.166	0.222	1.778
1200	10	232.3093	162.42	69.889	0.314	0.22	0.128	0.258	2.324
1200	10	245.3225	162.42	82.903	0.332	0.22	0.151	0.245	1.959
1200	10	249.3337	162.42	86.914	0.337	0.22	0.159	0.241	1.869
1200	12	210.6965	149	61.7	0.304	0.215	0.12	0.285	2.415
1200	12	223.7096	149	74.713	0.323	0.215	0.145	0.268	1.994
1200	12	227.7208	149	78.724	0.329	0.215	0.152	0.263	1.893
1200	14	189.4495	134.39	55.059	0.291	0.206	0.112	0.317	2.441
1200	14	202.4627	134.39	68.072	0.311	0.206	0.139	0.296	1.974
1200	14	206.4739	134.39	72.083	0.317	0.206	0.147	0.291	1.864
1200	16	168.7786	119.27	49.508	0.275	0.194	0.105	0.355	2.409
1200	16	181.7917	119.27	62.521	0.296	0.194	0.133	0.33	1.908

1200	16	185.8029	119.27	66.532	0.303	0.194	0.142	0.323	1.793
1200	18	148.7538	103.99	44.762	0.257	0.18	0.099	0.403	2.323
1200	18	161.767	103.99	57.775	0.279	0.18	0.128	0.371	1.8
1200	18	165.7782	103.99	61.786	0.286	0.18	0.137	0.362	1.683
1200	20	129.3839	88.75	40.633	0.237	0.162	0.093	0.464	2.184
1200	20	142.3971	88.75	53.646	0.261	0.162	0.123	0.421	1.654
1200	20	146.4083	88.75	57.657	0.268	0.162	0.132	0.41	1.539
1200	22	110.6501	73.66	36.989	0.214	0.143	0.088	0.542	1.991
1200	22	123.6633	73.66	50.002	0.24	0.143	0.118	0.485	1.473
1200	22	127.6745	73.66	54.013	0.247	0.143	0.128	0.47	1.364
1200	24	92.522	58.79	33.737	0.19	0.12	0.082	0.648	1.742
1200	24	105.5352	58.79	46.75	0.216	0.12	0.114	0.569	1.257
1200	24	109.5464	58.79	50.761	0.225	0.12	0.124	0.548	1.158
1200	26	74.9649	44.16	30.807	0.163	0.096	0.077	0.8	1.433
1200	26	87.978	44.16	43.82	0.191	0.096	0.11	0.682	1.008
1200	26	91.9893	44.16	47.831	0.2	0.096	0.12	0.652	0.923
1200	28	57.9434	29.8	28.145	0.133	0.068	0.073	1.035	1.059
1200	28	70.9566	29.8	41.158	0.163	0.068	0.106	0.846	0.724
1200	28	74.9678	29.8	45.169	0.172	0.068	0.116	0.8	0.66
1200	30	41.4236	15.71	25.711	0.101	0.038	0.068	1.448	0.611
1200	30	54.4368	15.71	38.724	0.132	0.038	0.102	1.102	0.406
1200	30	58.448	15.71	42.735	0.142	0.038	0.113	1.027	0.368
1400	2	357.4725	144.62	212.852	0.277	0.112	0.195	0.168	0.679
1400	2	370.4857	144.62	225.865	0.287	0.112	0.207	0.162	0.64
1400	2	374.4969	144.62	229.876	0.29	0.112	0.21	0.16	0.629
1400	4	392.3985	230.43	161.967	0.333	0.196	0.18	0.153	1.423
1400	4	405.4117	230.43	174.98	0.345	0.196	0.195	0.148	1.317
1400	4	409.4229	230.43	178.991	0.348	0.196	0.199	0.147	1.287
1400	6	389.4598	253.45	136.014	0.355	0.231	0.17	0.154	1.863
1400	6	402.473	253.45	149.027	0.367	0.231	0.186	0.149	1.701

1400	6	406.4842	253.45	153.038	0.37	0.231	0.191	0.148	1.656
1400	8	376.5099	257.39	119.121	0.364	0.249	0.162	0.159	2.161
1400	8	389.5231	257.39	132.134	0.377	0.249	0.18	0.154	1.948
1400	8	393.5343	257.39	136.146	0.38	0.249	0.185	0.152	1.891
1400	10	360.0334	253.21	106.824	0.367	0.258	0.155	0.167	2.37
1400	10	373.0466	253.21	119.837	0.38	0.258	0.174	0.161	2.113
1400	10	377.0578	253.21	123.848	0.384	0.258	0.18	0.159	2.045
1400	12	342.2668	245	97.269	0.366	0.262	0.149	0.175	2.519
1400	12	355.28	245	110.282	0.38	0.262	0.169	0.169	2.222
1400	12	359.2912	245	114.293	0.384	0.262	0.175	0.167	2.144
1400	14	324.1387	234.62	89.521	0.363	0.263	0.144	0.185	2.621
1400	14	337.1519	234.62	102.534	0.378	0.263	0.165	0.178	2.288
1400	14	341.1631	234.62	106.546	0.382	0.263	0.171	0.176	2.202
1400	16	306.0748	223.03	83.045	0.358	0.261	0.139	0.196	2.686
1400	16	319.088	223.03	96.058	0.373	0.261	0.161	0.188	2.322
1400	16	323.0992	223.03	100.069	0.378	0.261	0.167	0.186	2.229
1400	18	288.279	210.77	77.508	0.351	0.257	0.134	0.208	2.719
1400	18	301.2921	210.77	90.521	0.367	0.257	0.157	0.199	2.328
1400	18	305.3033	210.77	94.533	0.372	0.257	0.164	0.197	2.23
1400	20	270.8484	198.16	72.69	0.344	0.251	0.13	0.222	2.726
1400	20	283.8616	198.16	85.704	0.36	0.251	0.154	0.211	2.312
1400	20	287.8728	198.16	89.715	0.365	0.251	0.161	0.208	2.209
1400	22	253.8259	185.39	68.439	0.335	0.245	0.126	0.236	2.709
1400	22	266.8391	185.39	81.453	0.352	0.245	0.15	0.225	2.276
1400	22	270.8503	185.39	85.464	0.357	0.245	0.158	0.222	2.169
1400	24	237.2251	172.58	64.645	0.325	0.237	0.123	0.253	2.67
1400	24	250.2383	172.58	77.659	0.343	0.237	0.147	0.24	2.222
1400	24	254.2495	172.58	81.67	0.349	0.237	0.155	0.236	2.113
1400	26	221.0441	159.82	61.227	0.315	0.228	0.119	0.271	2.61
1400	26	234.0573	159.82	74.24	0.333	0.228	0.144	0.256	2.153

1400	26	238.0685	159.82	78.251	0.339	0.228	0.152	0.252	2.042
1400	28	205.2727	147.15	58.122	0.303	0.217	0.116	0.292	2.532
1400	28	218.2858	147.15	71.135	0.322	0.217	0.142	0.275	2.069
1400	28	222.297	147.15	75.146	0.328	0.217	0.15	0.27	1.958
1400	30	189.8961	134.61	55.282	0.291	0.206	0.112	0.316	2.435
1400	30	202.9092	134.61	68.295	0.311	0.206	0.139	0.296	1.971
1400	30	206.9204	134.61	72.306	0.317	0.206	0.147	0.29	1.862
1600	2	442.5145	177.58	264.933	0.289	0.116	0.205	0.136	0.67
1600	2	455.5276	177.58	277.946	0.298	0.116	0.215	0.132	0.639
1600	2	459.5388	177.58	281.957	0.3	0.116	0.218	0.131	0.63
1600	4	497.9246	291.15	206.778	0.351	0.205	0.193	0.121	1.408
1600	4	510.9377	291.15	219.792	0.36	0.205	0.205	0.117	1.325
1600	4	514.9489	291.15	223.803	0.363	0.205	0.209	0.117	1.301
1600	6	505.4331	328.31	177.118	0.378	0.245	0.185	0.119	1.854
1600	6	518.4463	328.31	190.131	0.387	0.245	0.199	0.116	1.727
1600	6	522.4575	328.31	194.143	0.39	0.245	0.203	0.115	1.691
1600	8	499.2836	341.47	157.812	0.391	0.268	0.179	0.12	2.164
1600	8	512.2967	341.47	170.825	0.402	0.268	0.193	0.117	1.999
1600	8	516.3079	341.47	174.836	0.405	0.268	0.198	0.116	1.953
1600	10	487.7575	344	143.758	0.399	0.281	0.173	0.123	2.393
1600	10	500.7707	344	156.771	0.41	0.281	0.189	0.12	2.194
1600	10	504.7819	344	160.782	0.413	0.281	0.194	0.119	2.14
1600	12	473.8371	341	132.838	0.403	0.29	0.169	0.127	2.567
1600	12	486.8503	341	145.851	0.414	0.29	0.185	0.123	2.338
1600	12	490.8615	341	149.863	0.417	0.29	0.19	0.122	2.275
1600	14	458.828	334.84	123.984	0.404	0.295	0.164	0.131	2.701
1600	14	471.8412	334.84	136.997	0.416	0.295	0.182	0.127	2.444
1600	14	475.8524	334.84	141.008	0.42	0.295	0.187	0.126	2.375
1600	16	443.3711	326.79	116.582	0.404	0.298	0.161	0.135	2.803
1600	16	456.3842	326.79	129.595	0.416	0.298	0.179	0.131	2.522

1600	16	460.3954	326.79	133.607	0.42	0.298	0.184	0.13	2.446
1600	18	427.8041	317.55	110.254	0.403	0.299	0.157	0.14	2.88
1600	18	440.8173	317.55	123.268	0.415	0.299	0.176	0.136	2.576
1600	18	444.8285	317.55	127.279	0.419	0.299	0.181	0.135	2.495
1600	20	412.313	307.56	104.748	0.401	0.299	0.154	0.146	2.936
1600	20	425.3261	307.56	117.762	0.413	0.299	0.173	0.141	2.612
1600	20	429.3373	307.56	121.773	0.417	0.299	0.179	0.14	2.526
1600	22	397.0017	297.11	99.89	0.397	0.297	0.151	0.151	2.974
1600	22	410.0149	297.11	112.903	0.41	0.297	0.171	0.146	2.632
1600	22	414.0261	297.11	116.915	0.414	0.297	0.177	0.145	2.541
1600	24	381.9282	286.37	95.554	0.393	0.295	0.148	0.157	2.997
1600	24	394.9414	286.37	108.567	0.407	0.295	0.168	0.152	2.638
1600	24	398.9526	286.37	112.578	0.411	0.295	0.174	0.15	2.544
1600	26	367.1234	275.48	91.647	0.389	0.292	0.145	0.163	3.006
1600	26	380.1365	275.48	104.66	0.403	0.292	0.166	0.158	2.632
1600	26	384.1477	275.48	108.672	0.407	0.292	0.172	0.156	2.535
1600	28	352.6019	264.5	88.098	0.384	0.288	0.143	0.17	3.002
1600	28	365.6151	264.5	101.112	0.398	0.288	0.164	0.164	2.616
1600	28	369.6263	264.5	105.123	0.402	0.288	0.17	0.162	2.516
1600	30	338.3685	253.52	84.853	0.378	0.284	0.14	0.177	2.988
1600	30	351.3817	253.52	97.866	0.393	0.284	0.162	0.171	2.59
1600	30	355.3929	253.52	101.877	0.398	0.284	0.168	0.169	2.488
1800	2	527.5565	210.54	317.014	0.298	0.119	0.213	0.114	0.664
1800	2	540.5696	210.54	330.027	0.305	0.119	0.221	0.111	0.638
1800	2	544.5808	210.54	334.038	0.307	0.119	0.224	0.11	0.63
1800	4	603.4506	351.86	251.59	0.364	0.212	0.203	0.099	1.399
1800	4	616.4637	351.86	264.603	0.371	0.212	0.213	0.097	1.33
1800	4	620.4749	351.86	268.614	0.374	0.212	0.216	0.097	1.31
1800	6	621.4064	403.18	218.222	0.393	0.255	0.196	0.097	1.848
1800	6	634.4196	403.18	231.236	0.401	0.255	0.208	0.095	1.744

1800	6	638.4308	403.18	235.247	0.404	0.255	0.211	0.094	1.714
1800	8	622.0572	425.55	196.503	0.41	0.28	0.191	0.096	2.166
1800	8	635.0704	425.55	209.516	0.419	0.28	0.203	0.094	2.031
1800	8	639.0816	425.55	213.527	0.421	0.28	0.207	0.094	1.993
1800	10	615.4816	434.79	180.692	0.42	0.297	0.186	0.097	2.406
1800	10	628.4948	434.79	193.705	0.429	0.297	0.2	0.095	2.245
1800	10	632.506	434.79	197.716	0.432	0.297	0.204	0.095	2.199
1800	12	605.4074	437	168.407	0.427	0.308	0.182	0.099	2.595
1800	12	618.4206	437	181.421	0.436	0.308	0.196	0.097	2.409
1800	12	622.4318	437	185.432	0.439	0.308	0.201	0.096	2.357
1800	14	593.5173	435.07	158.446	0.431	0.316	0.179	0.101	2.746
1800	14	606.5304	435.07	171.459	0.441	0.316	0.194	0.099	2.537
1800	14	610.5416	435.07	175.47	0.444	0.316	0.198	0.098	2.479
1800	16	580.6673	430.55	150.119	0.434	0.322	0.176	0.103	2.868
1800	16	593.6805	430.55	163.133	0.444	0.322	0.191	0.101	2.639
1800	16	597.6917	430.55	167.144	0.447	0.322	0.196	0.1	2.576
1800	18	567.3293	424.33	143.001	0.435	0.326	0.173	0.106	2.967
1800	18	580.3424	424.33	156.014	0.445	0.326	0.189	0.103	2.72
1800	18	584.3536	424.33	160.025	0.448	0.326	0.194	0.103	2.652
1800	20	553.7775	416.97	136.806	0.436	0.328	0.17	0.108	3.048
1800	20	566.7907	416.97	149.82	0.446	0.328	0.187	0.106	2.783
1800	20	570.8019	416.97	153.831	0.449	0.328	0.192	0.105	2.711
1800	22	540.1775	408.84	131.341	0.435	0.33	0.168	0.111	3.113
1800	22	553.1906	408.84	144.354	0.446	0.33	0.185	0.108	2.832
1800	22	557.2018	408.84	148.365	0.449	0.33	0.19	0.108	2.756
1800	24	526.6313	400.17	126.463	0.434	0.33	0.166	0.114	3.164
1800	24	539.6444	400.17	139.476	0.445	0.33	0.183	0.111	2.869
1800	24	543.6556	400.17	143.487	0.448	0.33	0.188	0.11	2.789
1800	26	513.2026	391.14	122.067	0.433	0.33	0.163	0.117	3.204
1800	26	526.2158	391.14	135.081	0.444	0.33	0.181	0.114	2.896

1800	26	530.227	391.14	139.092	0.447	0.33	0.186	0.113	2.812
1800	28	499.9311	381.86	118.075	0.431	0.329	0.161	0.12	3.234
1800	28	512.9443	381.86	131.088	0.442	0.329	0.179	0.117	2.913
1800	28	516.9555	381.86	135.1	0.446	0.329	0.185	0.116	2.826
1800	30	486.841	372.42	114.424	0.429	0.328	0.159	0.123	3.255
1800	30	499.8542	372.42	127.437	0.44	0.328	0.178	0.12	2.922
1800	30	503.8654	372.42	131.448	0.444	0.328	0.183	0.119	2.833

For γ=1.6(for n=0,1,2)

TIT	rp1	wtot	wttot	wbtot	etot	etop	ebot	sfc	ratio
1000	2	175.0479	66.36	108.69	0.221	0.084	0.156	0.343	0.611
1000	2	188.0611	66.36	121.703	0.237	0.084	0.175	0.319	0.545
1000	2	192.0723	66.36	125.714	0.242	0.084	0.181	0.312	0.528
1000	4	149.7983	77.45	72.343	0.227	0.117	0.13	0.401	1.071
1000	4	162.8114	77.45	85.356	0.246	0.117	0.153	0.369	0.907
1000	4	166.8226	77.45	89.368	0.252	0.117	0.16	0.36	0.867
1000	6	110.4396	56.63	53.806	0.195	0.1	0.111	0.543	1.053
1000	6	123.4528	56.63	66.819	0.218	0.1	0.137	0.486	0.848
1000	6	127.464	56.63	70.83	0.225	0.1	0.146	0.471	0.8
1000	8	70.4693	28.73	41.739	0.144	0.059	0.095	0.851	0.688
1000	8	83.4824	28.73	54.753	0.171	0.059	0.124	0.719	0.525
1000	8	87.4936	28.73	58.764	0.179	0.059	0.134	0.686	0.489
1000	10	32.0892	-0.87	32.955	0.076	-0.002	0.081	1.87	-0.026
1000	10	45.1023	-0.87	45.969	0.107	-0.002	0.113	1.33	-0.019
1000	10	49.1135	-0.87	49.98	0.116	-0.002	0.123	1.222	-0.017
1000	12	-4.3316	-30.46	26.131	-0.012	-0.084	0.069	-13.852	-1.166
1000	12	8.6816	-30.46	39.144	0.024	-0.084	0.103	6.911	-0.778
1000	12	12.6928	-30.46	43.155	0.035	-0.084	0.113	4.727	-0.706
1000	14	-38.8514	-59.45	20.596	-0.124	-0.19	0.057	-1.544	-2.886
1000	14	-25.8382	-59.45	33.61	-0.083	-0.19	0.094	-2.322	-1.769

1000	14	-21.827	-59.45	37.621	-0.07	-0.19	0.105	-2.749	-1.58
1000	16	-71.6319	-87.6	15.971	-0.271	-0.331	0.047	-0.838	-5.485
1000	16	-58.6187	-87.6	28.984	-0.221	-0.331	0.085	-1.024	-3.022
1000	16	-54.6075	-87.6	32.995	-0.206	-0.331	0.097	-1.099	-2.655
1000	18	-102.8482	-114.86	12.016	-0.466	-0.521	0.037	-0.583	-9.559
1000	18	-89.8351	-114.86	25.029	-0.407	-0.521	0.077	-0.668	-4.589
1000	18	-85.8239	-114.86	29.04	-0.389	-0.521	0.089	-0.699	-3.955
1000	20	-132.6629	-141.24	8.575	-0.739	-0.787	0.027	-0.452	-16.472
1000	20	-119.6497	-141.24	21.588	-0.667	-0.787	0.069	-0.501	-6.542
1000	20	-115.6385	-141.24	25.599	-0.645	-0.787	0.082	-0.519	-5.517
1000	22	-161.2192	-166.76	5.538	-1.145	-1.185	0.018	-0.372	-30.111
1000	22	-148.206	-166.76	18.551	-1.053	-1.185	0.061	-0.405	-8.989
1000	22	-144.1948	-166.76	22.563	-1.024	-1.185	0.075	-0.416	-7.391
1000	24	-188.6418	-191.47	2.828	-1.81	-1.837	0.01	-0.318	-67.702
1000	24	-175.6286	-191.47	15.841	-1.685	-1.837	0.054	-0.342	-12.087
1000	24	-171.6174	-191.47	19.852	-1.646	-1.837	0.068	-0.35	-9.645
1000	26	-215.0381	-215.42	0.386	-3.091	-3.096	-0.001	-0.279	-557.672
1000	26	-202.025	-215.42	13.399	-2.904	-3.096	0.047	-0.297	-16.077
1000	26	-198.0138	-215.42	17.411	-2.846	-3.096	0.062	-0.303	-12.373
1000	28	-240.5014	-238.67	-1.832	-6.581	-6.531	-0.007	-0.249	130.302
1000	28	-227.4882	-238.67	11.181	-6.225	-6.531	0.041	-0.264	-21.345
1000	28	-223.477	-238.67	15.193	-6.115	-6.531	0.055	-0.268	-15.71
1000	30	-265.1122	-261.25	-3.86	-53.517	-52.738	-0.015	-0.226	67.678
1000	30	-252.0991	-261.25	9.153	-50.89	-52.738	0.034	-0.238	-28.543
1000	30	-248.0879	-261.25	13.164	-50.081	-52.738	0.049	-0.242	-19.846
1200	2	260.0899	99.32	160.771	0.251	0.096	0.18	0.231	0.618
1200	2	273.1031	99.32	173.784	0.264	0.096	0.194	0.22	0.572
1200	2	277.1143	99.32	177.795	0.268	0.096	0.199	0.217	0.559
1200	4	255.3243	138.17	117.155	0.283	0.153	0.161	0.235	1.179

1200	4	268.3374	138.17	130.168	0.297	0.153	0.179	0.224	1.061
1200	4	272.3486	138.17	134.179	0.302	0.153	0.184	0.22	1.03
1200	6	226.4129	131.5	94.91	0.281	0.163	0.148	0.265	1.386
1200	6	239.4261	131.5	107.923	0.297	0.163	0.168	0.251	1.218
1200	6	243.4373	131.5	111.934	0.302	0.163	0.174	0.246	1.175
1200	8	193.2429	112.81	80.43	0.265	0.155	0.137	0.31	1.403
1200	8	206.2561	112.81	93.443	0.283	0.155	0.159	0.291	1.207
1200	8	210.2673	112.81	97.455	0.288	0.155	0.166	0.285	1.158
1200	10	159.8133	89.92	69.889	0.241	0.135	0.128	0.375	1.287
1200	10	172.8264	89.92	82.903	0.26	0.135	0.151	0.347	1.085
1200	10	176.8376	89.92	86.914	0.266	0.135	0.159	0.339	1.035
1200	12	127.2387	65.54	61.7	0.21	0.108	0.12	0.472	1.062
1200	12	140.2519	65.54	74.713	0.231	0.108	0.145	0.428	0.877
1200	12	144.2631	65.54	78.724	0.238	0.108	0.152	0.416	0.833
1200	14	95.8379	40.78	55.059	0.173	0.074	0.112	0.626	0.741
1200	14	108.851	40.78	68.072	0.197	0.074	0.139	0.551	0.599
1200	14	112.8622	40.78	72.083	0.204	0.074	0.147	0.532	0.566
1200	16	65.6644	16.16	49.508	0.13	0.032	0.105	0.914	0.326
1200	16	78.6775	16.16	62.521	0.155	0.032	0.133	0.763	0.258
1200	16	82.6887	16.16	66.532	0.163	0.032	0.142	0.726	0.243
1200	18	36.6769	-8.09	44.762	0.079	-0.017	0.099	1.636	-0.181
1200	18	49.6901	-8.09	57.775	0.108	-0.017	0.128	1.207	-0.14
1200	18	53.7013	-8.09	61.786	0.116	-0.017	0.137	1.117	-0.131
1200	20	8.8017	-31.83	40.633	0.021	-0.076	0.093	6.817	-0.783
1200	20	21.8148	-31.83	53.646	0.052	-0.076	0.123	2.75	-0.593
1200	20	25.826	-31.83	57.657	0.061	-0.076	0.132	2.323	-0.552
1200	22	-18.0434	-55.03	36.989	-0.047	-0.144	0.088	-3.325	-1.488
1200	22	-5.0303	-55.03	50.002	-0.013	-0.144	0.118	-11.928	-1.101
1200	22	-1.0191	-55.03	54.013	-0.003	-0.144	0.128	-58.878	-1.019
1200	24	-43.9387	-77.68	33.737	-0.127	-0.225	0.082	-1.366	-2.302

1200	24	-30.9255	-77.68	46.75	-0.089	-0.225	0.114	-1.94	-1.662
1200	24	-26.9143	-77.68	50.761	-0.078	-0.225	0.124	-2.229	-1.53
1200	26	-68.9589	-99.77	30.807	-0.222	-0.321	0.077	-0.87	-3.238
1200	26	-55.9457	-99.77	43.82	-0.18	-0.321	0.11	-1.072	-2.277
1200	26	-51.9345	-99.77	47.831	-0.167	-0.321	0.12	-1.155	-2.086
1200	28	-93.1721	-121.32	28.145	-0.335	-0.436	0.073	-0.644	-4.31
1200	28	-80.159	-121.32	41.158	-0.288	-0.436	0.106	-0.749	-2.948
1200	28	-76.1478	-121.32	45.169	-0.274	-0.436	0.116	-0.788	-2.686
1200	30	-116.6398	-142.35	25.711	-0.473	-0.578	0.068	-0.514	-5.537
1200	30	-103.6266	-142.35	38.724	-0.421	-0.578	0.102	-0.579	-3.676
1200	30	-99.6154	-142.35	42.735	-0.404	-0.578	0.113	-0.602	-3.331
1400	2	345.1319	132.28	212.852	0.27	0.104	0.195	0.174	0.621
1400	2	358.1451	132.28	225.865	0.281	0.104	0.207	0.168	0.586
1400	2	362.1563	132.28	229.876	0.284	0.104	0.21	0.166	0.575
1400	4	360.8503	198.88	161.967	0.315	0.174	0.18	0.166	1.228
1400	4	373.8635	198.88	174.98	0.327	0.174	0.195	0.16	1.137
1400	4	377.8747	198.88	178.991	0.33	0.174	0.199	0.159	1.111
1400	6	342.3863	206.37	136.014	0.327	0.197	0.17	0.175	1.517
1400	6	355.3994	206.37	149.027	0.339	0.197	0.186	0.169	1.385
1400	6	359.4106	206.37	153.038	0.343	0.197	0.191	0.167	1.348
1400	8	316.0166	196.9	119.121	0.325	0.203	0.162	0.19	1.653
1400	8	329.0297	196.9	132.134	0.339	0.203	0.18	0.182	1.49
1400	8	333.0409	196.9	136.146	0.343	0.203	0.185	0.18	1.446
1400	10	287.5374	180.71	106.824	0.318	0.2	0.155	0.209	1.692
1400	10	300.5505	180.71	119.837	0.332	0.2	0.174	0.2	1.508
1400	10	304.5617	180.71	123.848	0.336	0.2	0.18	0.197	1.459
1400	12	258.8091	161.54	97.269	0.305	0.191	0.149	0.232	1.661
1400	12	271.8222	161.54	110.282	0.321	0.191	0.169	0.221	1.465
1400	12	275.8334	161.54	114.293	0.325	0.191	0.175	0.218	1.413
1400	14	230.5271	141.01	89.521	0.29	0.177	0.144	0.26	1.575

1400	14	243.5403	141.01	102.534	0.306	0.177	0.165	0.246	1.375
1400	14	247.5515	141.01	106.546	0.311	0.177	0.171	0.242	1.323
1400	16	202.9606	119.92	83.045	0.271	0.16	0.139	0.296	1.444
1400	16	215.9738	119.92	96.058	0.289	0.16	0.161	0.278	1.248
1400	16	219.985	119.92	100.069	0.294	0.16	0.167	0.273	1.198
1400	18	176.2021	98.69	77.508	0.25	0.14	0.134	0.341	1.273
1400	18	189.2152	98.69	90.521	0.269	0.14	0.157	0.317	1.09
1400	18	193.2264	98.69	94.533	0.275	0.14	0.164	0.311	1.044
1400	20	150.2662	77.58	72.69	0.227	0.117	0.13	0.399	1.067
1400	20	163.2794	77.58	85.704	0.247	0.117	0.154	0.367	0.905
1400	20	167.2906	77.58	89.715	0.253	0.117	0.161	0.359	0.865
1400	22	125.1324	56.69	68.439	0.201	0.091	0.126	0.479	0.828
1400	22	138.1455	56.69	81.453	0.222	0.091	0.15	0.434	0.696
1400	22	142.1567	56.69	85.464	0.228	0.091	0.158	0.422	0.663
1400	24	100.7644	36.12	64.645	0.172	0.062	0.123	0.595	0.559
1400	24	113.7775	36.12	77.659	0.194	0.062	0.147	0.527	0.465
1400	24	117.7887	36.12	81.67	0.201	0.062	0.155	0.509	0.442
1400	26	77.1203	15.89	61.227	0.14	0.029	0.119	0.778	0.26
1400	26	90.1335	15.89	74.24	0.163	0.029	0.144	0.666	0.214
1400	26	94.1447	15.89	78.251	0.17	0.029	0.152	0.637	0.203
1400	28	54.1571	-3.96	58.122	0.104	-0.008	0.116	1.108	-0.068
1400	28	67.1702	-3.96	71.135	0.129	-0.008	0.142	0.893	-0.056
1400	28	71.1814	-3.96	75.146	0.137	-0.008	0.15	0.843	-0.053
1400	30	31.8327	-23.45	55.282	0.065	-0.048	0.112	1.885	-0.424
1400	30	44.8459	-23.45	68.295	0.092	-0.048	0.139	1.338	-0.343
1400	30	48.8571	-23.45	72.306	0.1	-0.048	0.147	1.228	-0.324
1600	2	430.1739	165.24	264.933	0.283	0.109	0.205	0.139	0.624
1600	2	443.1871	165.24	277.946	0.292	0.109	0.215	0.135	0.595
1600	2	447.1983	165.24	281.957	0.295	0.109	0.218	0.134	0.586
1600	4	466.3763	259.6	206.778	0.337	0.187	0.193	0.129	1.255

1600	4	479.3895	259.6	219.792	0.346	0.187	0.205	0.125	1.181
1600	4	483.4007	259.6	223.803	0.349	0.187	0.209	0.124	1.16
1600	6	458.3596	281.24	177.118	0.355	0.218	0.185	0.131	1.588
1600	6	471.3727	281.24	190.131	0.365	0.218	0.199	0.127	1.479
1600	6	475.3839	281.24	194.143	0.369	0.218	0.203	0.126	1.449
1600	8	438.7902	280.98	157.812	0.362	0.232	0.179	0.137	1.78
1600	8	451.8034	280.98	170.825	0.373	0.232	0.193	0.133	1.645
1600	8	455.8146	280.98	174.836	0.376	0.232	0.198	0.132	1.607
1600	10	415.2615	271.5	143.758	0.362	0.237	0.173	0.144	1.889
1600	10	428.2746	271.5	156.771	0.373	0.237	0.189	0.14	1.732
1600	10	432.2858	271.5	160.782	0.377	0.237	0.194	0.139	1.689
1600	12	390.3794	257.54	132.838	0.358	0.236	0.169	0.154	1.939
1600	12	403.3925	257.54	145.851	0.37	0.236	0.185	0.149	1.766
1600	12	407.4037	257.54	149.863	0.374	0.236	0.19	0.147	1.719
1600	14	365.2164	241.23	123.984	0.352	0.233	0.164	0.164	1.946
1600	14	378.2295	241.23	136.997	0.365	0.233	0.182	0.159	1.761
1600	14	382.2407	241.23	141.008	0.369	0.233	0.187	0.157	1.711
1600	16	340.2568	223.67	116.582	0.344	0.226	0.161	0.176	1.919
1600	16	353.27	223.67	129.595	0.357	0.226	0.179	0.17	1.726
1600	16	357.2812	223.67	133.607	0.361	0.226	0.184	0.168	1.674
1600	18	315.7272	205.47	110.254	0.334	0.217	0.157	0.19	1.864
1600	18	328.7404	205.47	123.268	0.348	0.217	0.176	0.183	1.667
1600	18	332.7516	205.47	127.279	0.352	0.217	0.181	0.18	1.614
1600	20	291.7307	186.98	104.748	0.323	0.207	0.154	0.206	1.785
1600	20	304.7439	186.98	117.762	0.337	0.207	0.173	0.197	1.588
1600	20	308.7551	186.98	121.773	0.342	0.207	0.179	0.194	1.536
1600	22	268.3081	168.42	99.89	0.31	0.195	0.151	0.224	1.686
1600	22	281.3213	168.42	112.903	0.325	0.195	0.171	0.213	1.492
1600	22	285.3325	168.42	116.915	0.33	0.195	0.177	0.21	1.441
1600	24	245.4675	149.91	95.554	0.296	0.181	0.148	0.244	1.569

1600	24	258.4806	149.91	108.567	0.312	0.181	0.168	0.232	1.381
1600	24	262.4918	149.91	112.578	0.317	0.181	0.174	0.229	1.332
1600	26	223.1996	131.55	91.647	0.281	0.166	0.145	0.269	1.435
1600	26	236.2127	131.55	104.66	0.298	0.166	0.166	0.254	1.257
1600	26	240.2239	131.55	108.672	0.303	0.166	0.172	0.25	1.211
1600	28	201.4863	113.39	88.098	0.265	0.149	0.143	0.298	1.287
1600	28	214.4995	113.39	101.112	0.282	0.149	0.164	0.28	1.121
1600	28	218.5107	113.39	105.123	0.287	0.149	0.17	0.275	1.079
1600	30	180.3052	95.45	84.853	0.247	0.131	0.14	0.333	1.125
1600	30	193.3183	95.45	97.866	0.265	0.131	0.162	0.31	0.975
1600	30	197.3295	95.45	101.877	0.271	0.131	0.168	0.304	0.937
1800	2	515.2159	198.2	317.014	0.293	0.113	0.213	0.116	0.625
1800	2	528.2291	198.2	330.027	0.3	0.113	0.221	0.114	0.601
1800	2	532.2403	198.2	334.038	0.302	0.113	0.224	0.113	0.593
1800	4	571.9023	320.31	251.59	0.352	0.197	0.203	0.105	1.273
1800	4	584.9155	320.31	264.603	0.36	0.197	0.213	0.103	1.211
1800	4	588.9267	320.31	268.614	0.362	0.197	0.216	0.102	1.192
1800	6	574.3329	356.11	218.222	0.375	0.233	0.196	0.104	1.632
1800	6	587.3461	356.11	231.236	0.384	0.233	0.208	0.102	1.54
1800	6	591.3573	356.11	235.247	0.386	0.233	0.211	0.101	1.514
1800	8	561.5638	365.06	196.503	0.386	0.251	0.191	0.107	1.858
1800	8	574.577	365.06	209.516	0.395	0.251	0.203	0.104	1.742
1800	8	578.5882	365.06	213.527	0.398	0.251	0.207	0.104	1.71
1800	10	542.9856	362.29	180.692	0.391	0.261	0.186	0.111	2.005
1800	10	555.9987	362.29	193.705	0.4	0.261	0.2	0.108	1.87
1800	10	560.0099	362.29	197.716	0.403	0.261	0.204	0.107	1.832
1800	12	521.9497	353.54	168.407	0.392	0.266	0.182	0.115	2.099
1800	12	534.9629	353.54	181.421	0.402	0.266	0.196	0.112	1.949
1800	12	538.9741	353.54	185.432	0.405	0.266	0.201	0.111	1.907
1800	14	499.9056	341.46	158.446	0.391	0.267	0.179	0.12	2.155

1800	14	512.9188	341.46	171.459	0.401	0.267	0.194	0.117	1.991
1800	14	516.93	341.46	175.47	0.404	0.267	0.198	0.116	1.946
1800	16	477.5531	327.43	150.119	0.388	0.266	0.176	0.126	2.181
1800	16	490.5662	327.43	163.133	0.399	0.266	0.191	0.122	2.007
1800	16	494.5774	327.43	167.144	0.402	0.266	0.196	0.121	1.959
1800	18	455.2524	312.25	143.001	0.384	0.263	0.173	0.132	2.184
1800	18	468.2655	312.25	156.014	0.395	0.263	0.189	0.128	2.001
1800	18	472.2767	312.25	160.025	0.398	0.263	0.194	0.127	1.951
1800	20	433.1953	296.39	136.806	0.378	0.259	0.17	0.139	2.166
1800	20	446.2084	296.39	149.82	0.39	0.259	0.187	0.134	1.978
1800	20	450.2196	296.39	153.831	0.393	0.259	0.192	0.133	1.927
1800	22	411.4839	280.14	131.341	0.372	0.253	0.168	0.146	2.133
1800	22	424.4971	280.14	144.354	0.384	0.253	0.185	0.141	1.941
1800	22	428.5083	280.14	148.365	0.387	0.253	0.19	0.14	1.888
1800	24	390.1705	263.71	126.463	0.365	0.246	0.166	0.154	2.085
1800	24	403.1837	263.71	139.476	0.377	0.246	0.183	0.149	1.891
1800	24	407.1949	263.71	143.487	0.381	0.246	0.188	0.147	1.838
1800	26	369.2788	247.21	122.067	0.357	0.239	0.163	0.162	2.025
1800	26	382.292	247.21	135.081	0.369	0.239	0.181	0.157	1.83
1800	26	386.3032	247.21	139.092	0.373	0.239	0.186	0.155	1.777
1800	28	348.8155	230.74	118.075	0.348	0.23	0.161	0.172	1.954
1800	28	361.8287	230.74	131.088	0.361	0.23	0.179	0.166	1.76
1800	28	365.8399	230.74	135.1	0.365	0.23	0.185	0.164	1.708
1800	30	328.7776	214.35	114.424	0.339	0.221	0.159	0.182	1.873
1800	30	341.7908	214.35	127.437	0.352	0.221	0.178	0.176	1.682
1800	30	345.802	214.35	131.448	0.356	0.221	0.183	0.174	1.631

For7 γ=1.66(for n=0,1,2)

TIT	rp1	wtot	wttot	wbtot	etot	etop	ebot	sfc	ratio
1000	2	168.2877	59.6	108.69	0.214	0.076	0.156	0.357	0.548
1000	2	181.3008	59.6	121.703	0.23	0.076	0.175	0.331	0.49
1000	2	185.312	59.6	125.714	0.236	0.076	0.181	0.324	0.474
1000	4	132.1264	59.78	72.343	0.206	0.093	0.13	0.454	0.826
1000	4	145.1396	59.78	85.356	0.226	0.093	0.153	0.413	0.7
1000	4	149.1508	59.78	89.368	0.232	0.093	0.16	0.402	0.669
1000	6	83.726	29.92	53.806	0.156	0.056	0.111	0.717	0.556
1000	6	96.7392	29.92	66.819	0.18	0.056	0.137	0.62	0.448
1000	6	100.7504	29.92	70.83	0.187	0.056	0.146	0.596	0.422
1000	8	35.8221	-5.92	41.739	0.079	-0.013	0.095	1.675	-0.142
1000	8	48.8353	-5.92	54.753	0.108	-0.013	0.124	1.229	-0.108
1000	8	52.8465	-5.92	58.764	0.117	-0.013	0.134	1.135	-0.101
1000	10	-9.7301	-42.69	32.955	-0.026	-0.113	0.081	-6.166	-1.295
1000	10	3.283	-42.69	45.969	0.009	-0.113	0.113	18.276	-0.929
1000	10	7.2942	-42.69	49.98	0.019	-0.113	0.123	8.226	-0.854
1000	12	-52.7559	-78.89	26.131	-0.168	-0.251	0.069	-1.137	-3.019
1000	12	-39.7427	-78.89	39.144	-0.126	-0.251	0.103	-1.51	-2.015
1000	12	-35.7315	-78.89	43.155	-0.114	-0.251	0.113	-1.679	-1.828
1000	14	-93.4356	-114.03	20.596	-0.366	-0.446	0.057	-0.642	-5.536
1000	14	-80.4224	-114.03	33.61	-0.315	-0.446	0.094	-0.746	-3.393
1000	14	-76.4112	-114.03	37.621	-0.299	-0.446	0.105	-0.785	-3.031
1000	16	-132.0142	-147.98	15.971	-0.654	-0.733	0.047	-0.454	-9.266
1000	16	-119.001	-147.98	28.984	-0.59	-0.733	0.085	-0.504	-5.106
1000	16	-114.9898	-147.98	32.995	-0.57	-0.733	0.097	-0.522	-4.485
1000	18	-168.7264	-180.74	12.016	-1.11	-1.189	0.037	-0.356	-15.042
1000	18	-155.7133	-180.74	25.029	-1.025	-1.189	0.077	-0.385	-7.221
1000	18	-151.7021	-180.74	29.04	-0.998	-1.189	0.089	-0.396	-6.224

1000	20	-203.7794	-212.35	8.575	-1.934	-2.016	0.027	-0.294	-24.766
1000	20	-190.7662	-212.35	21.588	-1.811	-2.016	0.069	-0.315	-9.837
1000	20	-186.755	-212.35	25.599	-1.773	-2.016	0.082	-0.321	-8.295
1000	22	-237.351	-242.89	5.538	-3.862	-3.952	0.018	-0.253	-43.857
1000	22	-224.3378	-242.89	18.551	-3.65	-3.952	0.061	-0.267	-13.093
1000	22	-220.3266	-242.89	22.563	-3.585	-3.952	0.075	-0.272	-10.765
1000	24	-269.5929	-272.42	2.828	-13.535	-13.677	0.01	-0.223	-96.326
1000	24	-256.5797	-272.42	15.841	-12.881	-13.677	0.054	-0.234	-17.197
1000	24	-252.5685	-272.42	19.852	-12.68	-13.677	0.068	-0.238	-13.722
1000	26	-300.6349	-301.02	0.386	15.351	15.371	0.001	-0.2	-779.257
1000	26	-287.6217	-301.02	13.399	14.686	15.371	0.047	-0.209	-22.465
1000	26	-283.6105	-301.02	17.411	14.482	15.371	0.062	-0.212	-17.289
1000	28	-330.5881	-328.76	-1.832	5.77	5.738	-0.007	-0.181	179.485
1000	28	-317.5749	-328.76	11.181	5.543	5.738	0.041	-0.189	-29.402
1000	28	-313.5637	-328.76	15.193	5.473	5.738	0.055	-0.191	-21.639
1000	30	-359.5484	-355.69	-3.86	3.849	3.808	-0.015	-0.167	92.142
1000	30	-346.5353	-355.69	9.153	3.71	3.808	0.034	-0.173	-38.86
1000	30	-342.5241	-355.69	13.164	3.667	3.808	0.049	-0.175	-27.019
1200	2	253.3296	92.56	160.771	0.246	0.09	0.18	0.237	0.576
1200	2	266.3428	92.56	173.784	0.259	0.09	0.194	0.225	0.533
1200	2	270.354	92.56	177.795	0.263	0.09	0.199	0.222	0.521
1200	4	237.6525	120.5	117.155	0.269	0.136	0.161	0.252	1.029
1200	4	250.6656	120.5	130.168	0.284	0.136	0.179	0.239	0.926
1200	4	254.6768	120.5	134.179	0.288	0.136	0.184	0.236	0.898
1200	6	199.6993	104.79	94.91	0.256	0.135	0.148	0.3	1.104
1200	6	212.7125	104.79	107.923	0.273	0.135	0.168	0.282	0.971
1200	6	216.7237	104.79	111.934	0.278	0.135	0.174	0.277	0.936
1200	8	158.5958	78.17	80.43	0.229	0.113	0.137	0.378	0.972
1200	8	171.6089	78.17	93.443	0.247	0.113	0.159	0.35	0.837
1200	8	175.6201	78.17	97.455	0.253	0.113	0.166	0.342	0.802

1200	10	117.994	48.1	69.889	0.19	0.078	0.128	0.509	0.688
1200	10	131.0071	48.1	82.903	0.211	0.078	0.151	0.458	0.58
1200	10	135.0183	48.1	86.914	0.218	0.078	0.159	0.444	0.553
1200	12	78.8145	17.11	61.7	0.142	0.031	0.12	0.761	0.277
1200	12	91.8276	17.11	74.713	0.165	0.031	0.145	0.653	0.229
1200	12	95.8388	17.11	78.724	0.172	0.031	0.152	0.626	0.217
1200	14	41.2537	-13.81	55.059	0.083	-0.028	0.112	1.454	-0.251
1200	14	54.2668	-13.81	68.072	0.109	-0.028	0.139	1.106	-0.203
1200	14	58.278	-13.81	72.083	0.117	-0.028	0.147	1.03	-0.192
1200	16	5.282	-44.23	49.508	0.012	-0.1	0.105	11.359	-0.893
1200	16	18.2952	-44.23	62.521	0.041	-0.1	0.133	3.28	-0.707
1200	16	22.3064	-44.23	66.532	0.05	-0.1	0.142	2.69	-0.665
1200	18	-29.2013	-73.96	44.762	-0.074	-0.188	0.099	-2.055	-1.652
1200	18	-16.1881	-73.96	57.775	-0.041	-0.188	0.128	-3.706	-1.28
1200	18	-12.1769	-73.96	61.786	-0.031	-0.188	0.137	-4.927	-1.197
1200	20	-62.3149	-102.95	40.633	-0.18	-0.297	0.093	-0.963	-2.534
1200	20	-49.3017	-102.95	53.646	-0.142	-0.297	0.123	-1.217	-1.919
1200	20	-45.2905	-102.95	57.657	-0.131	-0.297	0.132	-1.325	-1.786
1200	22	-94.1752	-131.16	36.989	-0.311	-0.433	0.088	-0.637	-3.546
1200	22	-81.162	-131.16	50.002	-0.268	-0.433	0.118	-0.739	-2.623
1200	22	-77.1508	-131.16	54.013	-0.255	-0.433	0.128	-0.778	-2.428
1200	24	-124.8898	-158.63	33.737	-0.478	-0.607	0.082	-0.48	-4.702
1200	24	-111.8767	-158.63	46.75	-0.428	-0.607	0.114	-0.536	-3.393
1200	24	-107.8655	-158.63	50.761	-0.413	-0.607	0.124	-0.556	-3.125
1200	26	-154.5556	-185.36	30.807	-0.697	-0.835	0.077	-0.388	-6.017
1200	26	-141.5425	-185.36	43.82	-0.638	-0.835	0.11	-0.424	-4.23
1200	26	-137.5313	-185.36	47.831	-0.62	-0.835	0.12	-0.436	-3.875
1200	28	-183.2588	-211.4	28.145	-0.995	-1.148	0.073	-0.327	-7.511
1200	28	-170.2457	-211.4	41.158	-0.924	-1.148	0.106	-0.352	-5.136
1200	28	-166.2345	-211.4	45.169	-0.903	-1.148	0.116	-0.361	-4.68

1200	30	-211.076	-236.79	25.711	-1.426	-1.599	0.068	-0.284	-9.21
1200	30	-198.0628	-236.79	38.724	-1.338	-1.599	0.102	-0.303	-6.115
1200	30	-194.0516	-236.79	42.735	-1.311	-1.599	0.113	-0.309	-5.541
1400	2	338.3716	125.52	212.852	0.266	0.099	0.195	0.177	0.59
1400	2	351.3848	125.52	225.865	0.277	0.099	0.207	0.171	0.556
1400	2	355.396	125.52	229.876	0.28	0.099	0.21	0.169	0.546
1400	4	343.1785	181.21	161.967	0.305	0.161	0.18	0.175	1.119
1400	4	356.1916	181.21	174.98	0.317	0.161	0.195	0.168	1.036
1400	4	360.2028	181.21	178.991	0.32	0.161	0.199	0.167	1.012
1400	6	315.6726	179.66	136.014	0.309	0.176	0.17	0.19	1.321
1400	6	328.6858	179.66	149.027	0.322	0.176	0.186	0.183	1.206
1400	6	332.697	179.66	153.038	0.326	0.176	0.191	0.18	1.174
1400	8	281.3694	162.25	119.121	0.301	0.173	0.162	0.213	1.362
1400	8	294.3826	162.25	132.134	0.315	0.173	0.18	0.204	1.228
1400	8	298.3938	162.25	136.146	0.319	0.173	0.185	0.201	1.192
1400	10	245.7181	138.89	106.824	0.285	0.161	0.155	0.244	1.3
1400	10	258.7312	138.89	119.837	0.3	0.161	0.174	0.232	1.159
1400	10	262.7424	138.89	123.848	0.305	0.161	0.18	0.228	1.121
1400	12	210.3848	113.12	97.269	0.264	0.142	0.149	0.285	1.163
1400	12	223.398	113.12	110.282	0.28	0.142	0.169	0.269	1.026
1400	12	227.4092	113.12	114.293	0.285	0.142	0.175	0.264	0.99
1400	14	175.9429	86.42	89.521	0.238	0.117	0.144	0.341	0.965
1400	14	188.9561	86.42	102.534	0.256	0.117	0.165	0.318	0.843
1400	14	192.9673	86.42	106.546	0.261	0.117	0.171	0.311	0.811
1400	16	142.5783	59.53	83.045	0.208	0.087	0.139	0.421	0.717
1400	16	155.5914	59.53	96.058	0.227	0.087	0.161	0.386	0.62
1400	16	159.6026	59.53	100.069	0.233	0.087	0.167	0.376	0.595
1400	18	110.3239	32.82	77.508	0.174	0.052	0.134	0.544	0.423
1400	18	123.337	32.82	90.521	0.194	0.052	0.157	0.486	0.363
1400	18	127.3482	32.82	94.533	0.201	0.052	0.164	0.471	0.347

1400	20	79.1497	6.46	72.69	0.135	0.011	0.13	0.758	0.089
1400	20	92.1628	6.46	85.704	0.157	0.011	0.154	0.651	0.075
1400	20	96.174	6.46	89.715	0.163	0.011	0.161	0.624	0.072
1400	22	49.0006	-19.44	68.439	0.09	-0.036	0.126	1.224	-0.284
1400	22	62.0138	-19.44	81.453	0.114	-0.036	0.15	0.968	-0.239
1400	22	66.025	-19.44	85.464	0.121	-0.036	0.158	0.909	-0.227
1400	24	19.8133	-44.83	64.645	0.039	-0.089	0.123	3.028	-0.694
1400	24	32.8264	-44.83	77.659	0.065	-0.089	0.147	1.828	-0.577
1400	24	36.8376	-44.83	81.67	0.073	-0.089	0.155	1.629	-0.549
1400	26	-8.4764	-69.7	61.227	-0.018	-0.15	0.119	-7.078	-1.138
1400	26	4.5368	-69.7	74.24	0.01	-0.15	0.144	13.225	-0.939
1400	26	8.548	-69.7	78.251	0.018	-0.15	0.152	7.019	-0.891
1400	28	-35.9296	-94.05	58.122	-0.084	-0.221	0.116	-1.67	-1.618
1400	28	-22.9165	-94.05	71.135	-0.054	-0.221	0.142	-2.618	-1.322
1400	28	-18.9052	-94.05	75.146	-0.044	-0.221	0.15	-3.174	-1.252
1400	30	-62.6035	-117.89	55.282	-0.161	-0.303	0.112	-0.958	-2.132
1400	30	-49.5903	-117.89	68.295	-0.127	-0.303	0.139	-1.21	-1.726
1400	30	-45.5791	-117.89	72.306	-0.117	-0.303	0.147	-1.316	-1.63
1600	2	423.4136	158.48	264.933	0.28	0.105	0.205	0.142	0.598
1600	2	436.4268	158.48	277.946	0.289	0.105	0.215	0.137	0.57
1600	2	440.438	158.48	281.957	0.291	0.105	0.218	0.136	0.562
1600	4	448.7045	241.93	206.778	0.328	0.177	0.193	0.134	1.17
1600	4	461.7176	241.93	219.792	0.338	0.177	0.205	0.13	1.101
1600	4	465.7288	241.93	223.803	0.341	0.177	0.209	0.129	1.081
1600	6	431.646	254.53	177.118	0.342	0.202	0.185	0.139	1.437
1600	6	444.6591	254.53	190.131	0.352	0.202	0.199	0.135	1.339
1600	6	448.6703	254.53	194.143	0.356	0.202	0.203	0.134	1.311
1600	8	404.1431	246.33	157.812	0.343	0.209	0.179	0.148	1.561
1600	8	417.1562	246.33	170.825	0.355	0.209	0.193	0.144	1.442
1600	8	421.1674	246.33	174.836	0.358	0.209	0.198	0.142	1.409

1600	10	373.4422	229.68	143.758	0.338	0.208	0.173	0.161	1.598
1600	10	386.4553	229.68	156.771	0.35	0.208	0.189	0.155	1.465
1600	10	390.4665	229.68	160.782	0.354	0.208	0.194	0.154	1.429
1600	12	341.9551	209.12	132.838	0.329	0.201	0.169	0.175	1.574
1600	12	354.9683	209.12	145.851	0.342	0.201	0.185	0.169	1.434
1600	12	358.9795	209.12	149.863	0.346	0.201	0.19	0.167	1.395
1600	14	310.6322	186.65	123.984	0.317	0.19	0.164	0.193	1.505
1600	14	323.6453	186.65	136.997	0.33	0.19	0.182	0.185	1.362
1600	14	327.6565	186.65	141.008	0.334	0.19	0.187	0.183	1.324
1600	16	279.8745	163.29	116.582	0.302	0.176	0.161	0.214	1.401
1600	16	292.8877	163.29	129.595	0.316	0.176	0.179	0.205	1.26
1600	16	296.8989	163.29	133.607	0.321	0.176	0.184	0.202	1.222
1600	18	249.849	139.59	110.254	0.285	0.159	0.157	0.24	1.266
1600	18	262.8622	139.59	123.268	0.3	0.159	0.176	0.228	1.132
1600	18	266.8734	139.59	127.279	0.305	0.159	0.181	0.225	1.097
1600	20	220.6142	115.87	104.748	0.266	0.14	0.154	0.272	1.106
1600	20	233.6274	115.87	117.762	0.282	0.14	0.173	0.257	0.984
1600	20	237.6386	115.87	121.773	0.286	0.14	0.179	0.252	0.951
1600	22	192.1764	92.29	99.89	0.245	0.117	0.151	0.312	0.924
1600	22	205.1895	92.29	112.903	0.261	0.117	0.171	0.292	0.817
1600	22	209.2007	92.29	116.915	0.266	0.117	0.177	0.287	0.789
1600	24	164.5163	68.96	95.554	0.221	0.093	0.148	0.365	0.722
1600	24	177.5295	68.96	108.567	0.239	0.093	0.168	0.338	0.635
1600	24	181.5407	68.96	112.578	0.244	0.093	0.174	0.331	0.613
1600	26	137.6028	45.96	91.647	0.195	0.065	0.145	0.436	0.501
1600	26	150.616	45.96	104.66	0.214	0.065	0.166	0.398	0.439
1600	26	154.6272	45.96	108.672	0.219	0.065	0.172	0.388	0.423
1600	28	111.3996	23.3	88.098	0.167	0.035	0.143	0.539	0.264
1600	28	124.4128	23.3	101.112	0.187	0.035	0.164	0.482	0.23
1600	28	128.424	23.3	105.123	0.193	0.035	0.17	0.467	0.222

1600	30	85.869	1.02	84.853	0.136	0.002	0.14	0.699	0.012
1600	30	98.8821	1.02	97.866	0.157	0.002	0.162	0.607	0.01
1600	30	102.8933	1.02	101.877	0.163	0.002	0.168	0.583	0.01
1800	2	508.4556	191.44	317.014	0.29	0.109	0.213	0.118	0.604
1800	2	521.4688	191.44	330.027	0.298	0.109	0.221	0.115	0.58
1800	2	525.48	191.44	334.038	0.3	0.109	0.224	0.114	0.573
1800	4	554.2305	302.64	251.59	0.345	0.188	0.203	0.108	1.203
1800	4	567.2437	302.64	264.603	0.353	0.188	0.213	0.106	1.144
1800	4	571.2549	302.64	268.614	0.355	0.188	0.216	0.105	1.127
1800	6	547.6193	329.4	218.222	0.364	0.219	0.196	0.11	1.509
1800	6	560.6324	329.4	231.236	0.373	0.219	0.208	0.107	1.425
1800	6	564.6436	329.4	235.247	0.376	0.219	0.211	0.106	1.4
1800	8	526.9167	330.41	196.503	0.372	0.233	0.191	0.114	1.681
1800	8	539.9299	330.41	209.516	0.381	0.233	0.203	0.111	1.577
1800	8	543.9411	330.41	213.527	0.384	0.233	0.207	0.11	1.547
1800	10	501.1663	320.47	180.692	0.373	0.238	0.186	0.12	1.774
1800	10	514.1794	320.47	193.705	0.382	0.238	0.2	0.117	1.654
1800	10	518.1906	320.47	197.716	0.385	0.238	0.204	0.116	1.621
1800	12	473.5255	305.12	168.407	0.37	0.238	0.182	0.127	1.812
1800	12	486.5386	305.12	181.421	0.38	0.238	0.196	0.123	1.682
1800	12	490.5498	305.12	185.432	0.383	0.238	0.201	0.122	1.645
1800	14	445.3214	286.88	158.446	0.365	0.235	0.179	0.135	1.811
1800	14	458.3346	286.88	171.459	0.375	0.235	0.194	0.131	1.673
1800	14	462.3458	286.88	175.47	0.379	0.235	0.198	0.13	1.635
1800	16	417.1708	267.05	150.119	0.357	0.229	0.176	0.144	1.779
1800	16	430.1839	267.05	163.133	0.368	0.229	0.191	0.139	1.637
1800	16	434.1951	267.05	167.144	0.372	0.229	0.196	0.138	1.598
1800	18	389.3742	246.37	143.001	0.348	0.22	0.173	0.154	1.723
1800	18	402.3873	246.37	156.014	0.36	0.22	0.189	0.149	1.579
1800	18	406.3985	246.37	160.025	0.364	0.22	0.194	0.148	1.54

1800	20	362.0787	225.27	136.806	0.338	0.21	0.17	0.166	1.647
1800	20	375.0919	225.27	149.82	0.35	0.21	0.187	0.16	1.504
1800	20	379.1031	225.27	153.831	0.354	0.21	0.192	0.158	1.464
1800	22	335.3522	204.01	131.341	0.326	0.199	0.168	0.179	1.553
1800	22	348.3653	204.01	144.354	0.339	0.199	0.185	0.172	1.413
1800	22	352.3765	204.01	148.365	0.343	0.199	0.19	0.17	1.375
1800	24	309.2194	182.76	126.463	0.314	0.185	0.166	0.194	1.445
1800	24	322.2326	182.76	139.476	0.327	0.185	0.183	0.186	1.31
1800	24	326.2438	182.76	143.487	0.331	0.185	0.188	0.184	1.274
1800	26	283.6821	161.61	122.067	0.3	0.171	0.163	0.212	1.324
1800	26	296.6953	161.61	135.081	0.314	0.171	0.181	0.202	1.196
1800	26	300.7065	161.61	139.092	0.318	0.171	0.186	0.2	1.162
1800	28	258.7288	140.65	118.075	0.285	0.155	0.161	0.232	1.191
1800	28	271.742	140.65	131.088	0.299	0.155	0.179	0.221	1.073
1800	28	275.7532	140.65	135.1	0.304	0.155	0.185	0.218	1.041
1800	30	234.3414	119.92	114.424	0.269	0.137	0.159	0.256	1.048
1800	30	247.3546	119.92	127.437	0.284	0.137	0.178	0.243	0.941
1800	30	251.3658	119.92	131.448	0.288	0.137	0.183	0.239	0.912

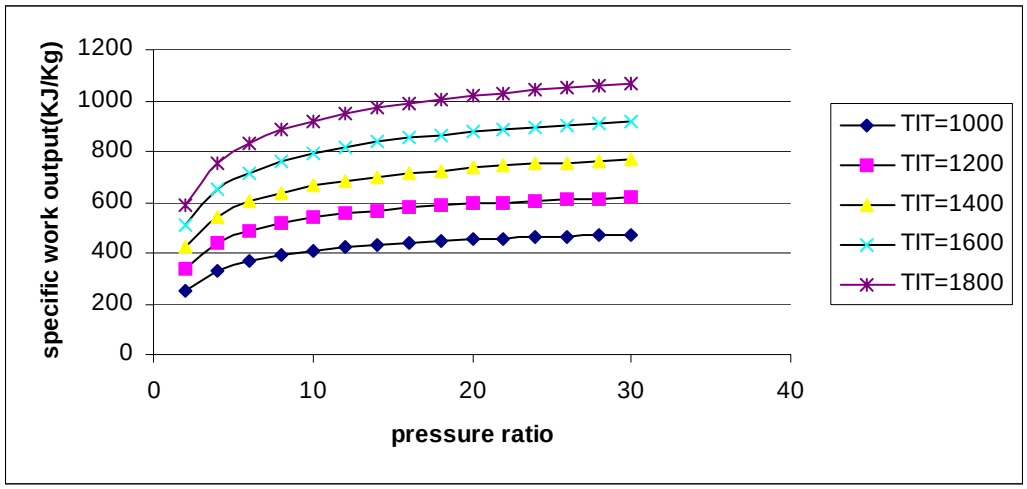

Fig 3.1.2a n=0

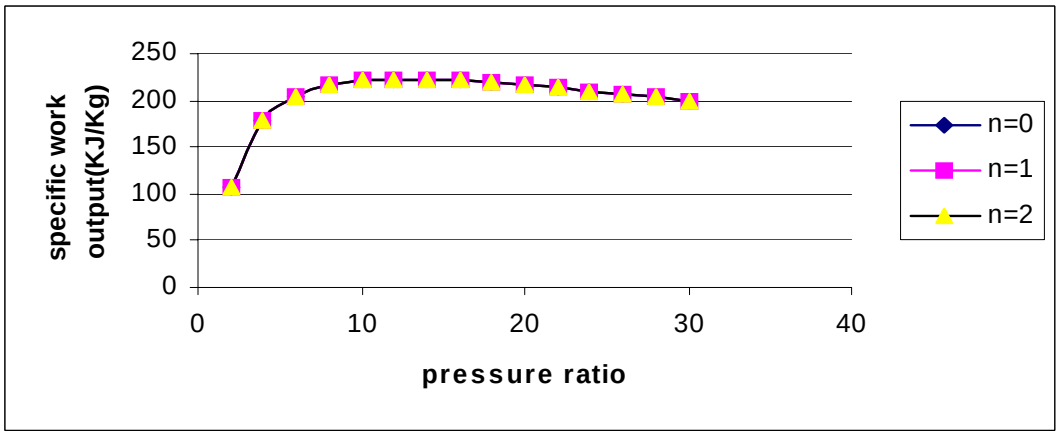

Fig 3.1.2b n=1

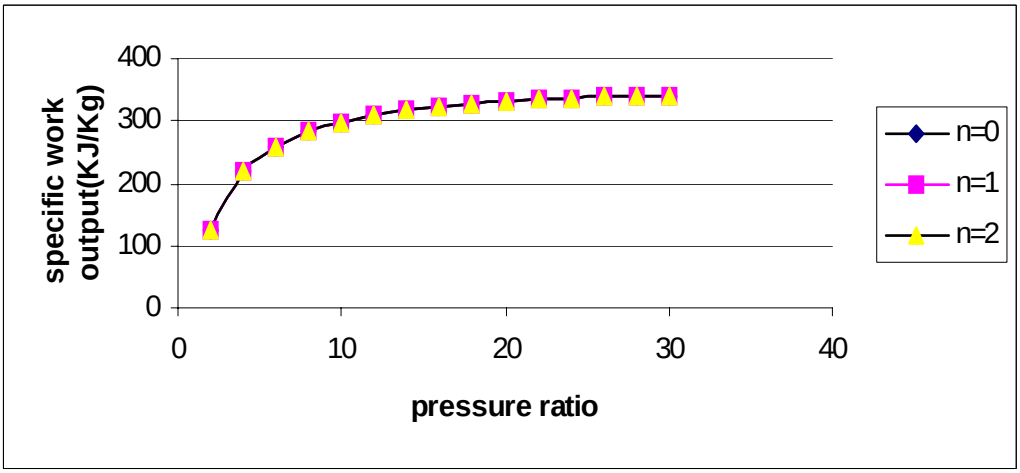

Fig 3.1.2c n=2

Fig 3.1.2 VARIATION OF SPECIFIC OUTPUT OF MIRROR GAS TURBINE VS PRESSURE RATIO (γ=1.1)

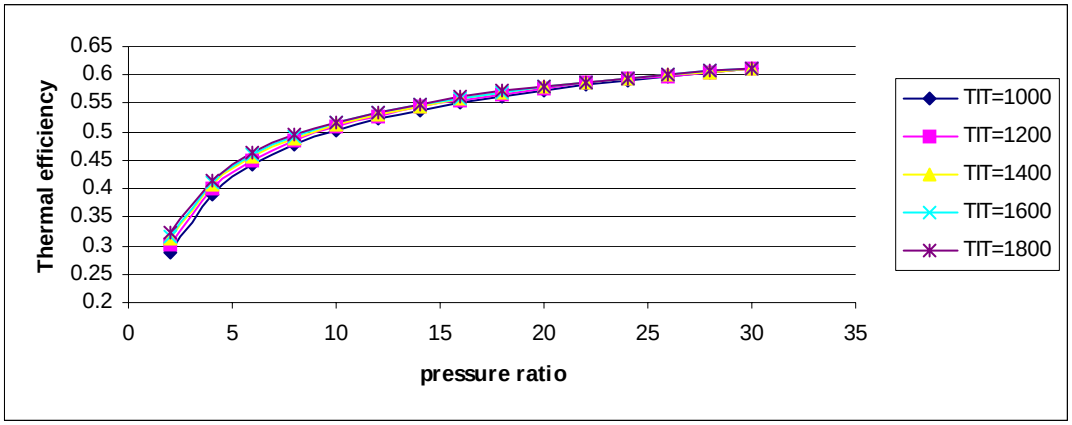

Fig 3.1.3a n=0

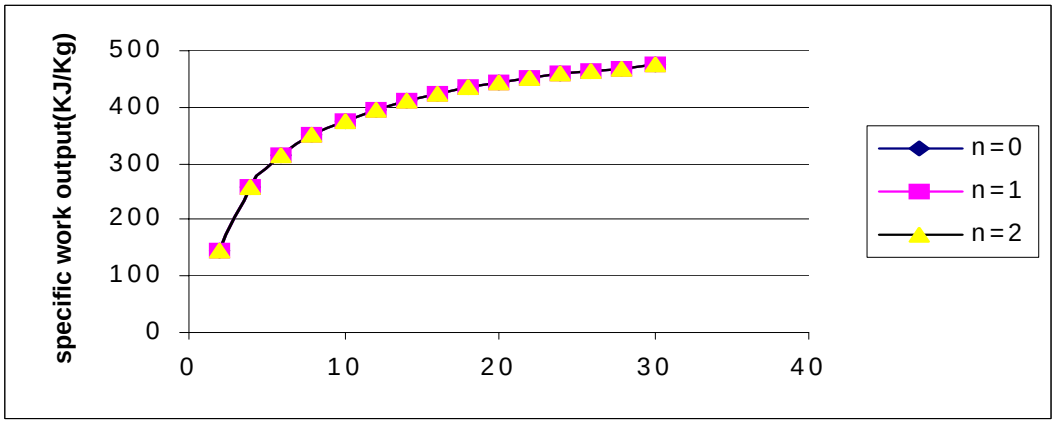

Fig 3.1.3b n=1

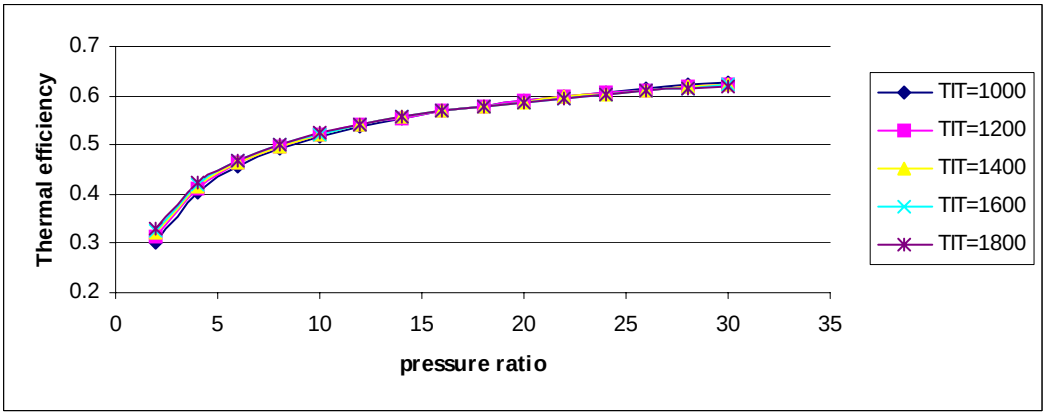

Fig 3.1.3c n=2

Fig 3.1.3 VARIATION OF THERMAL EFFICIENCY OF MIRROR GAS TURBINE VS PRESSURE RATIO (γ=1.1)

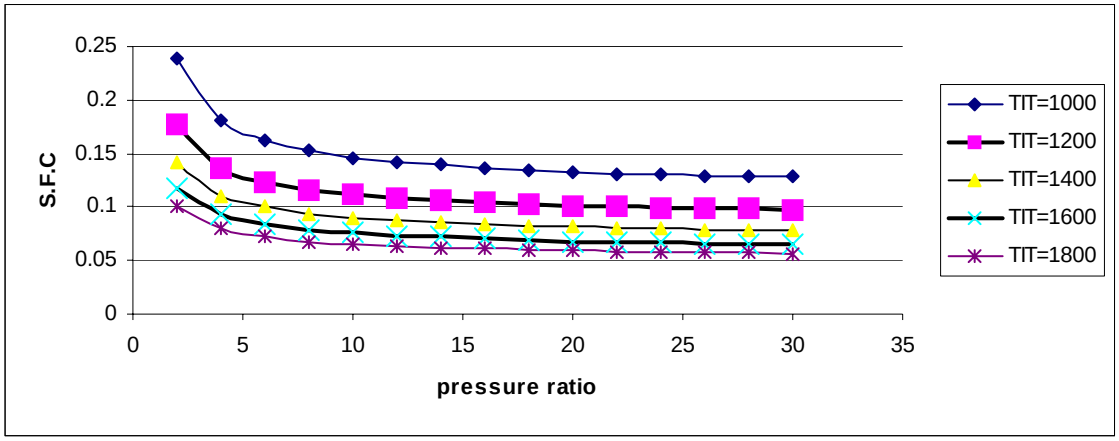

Fig 3.1.4a n=0

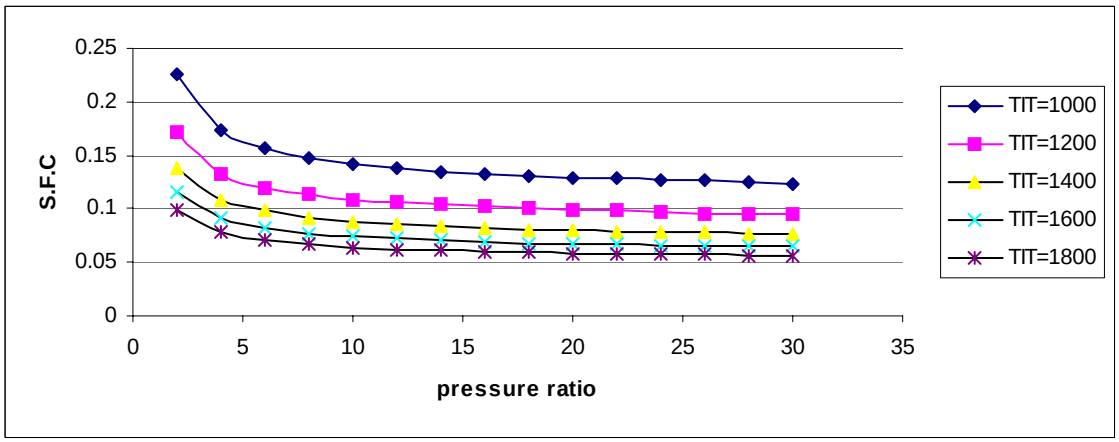

Fig 3.1.4b n=1

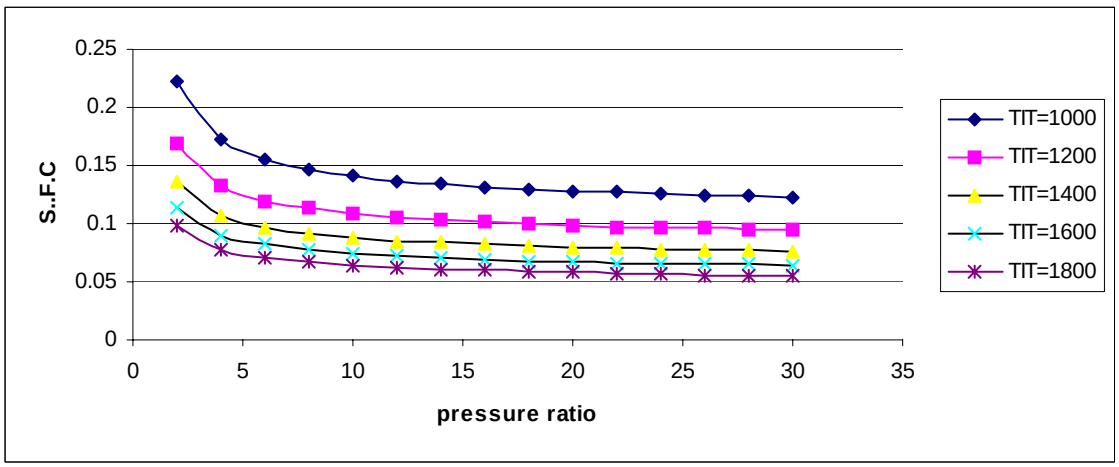

Fig 3.1.4c n=2

Fig 3.1.4 VARIATION OF S.F.C. OF MIRROR GAS TURBINE VS PRESSURE RATIO

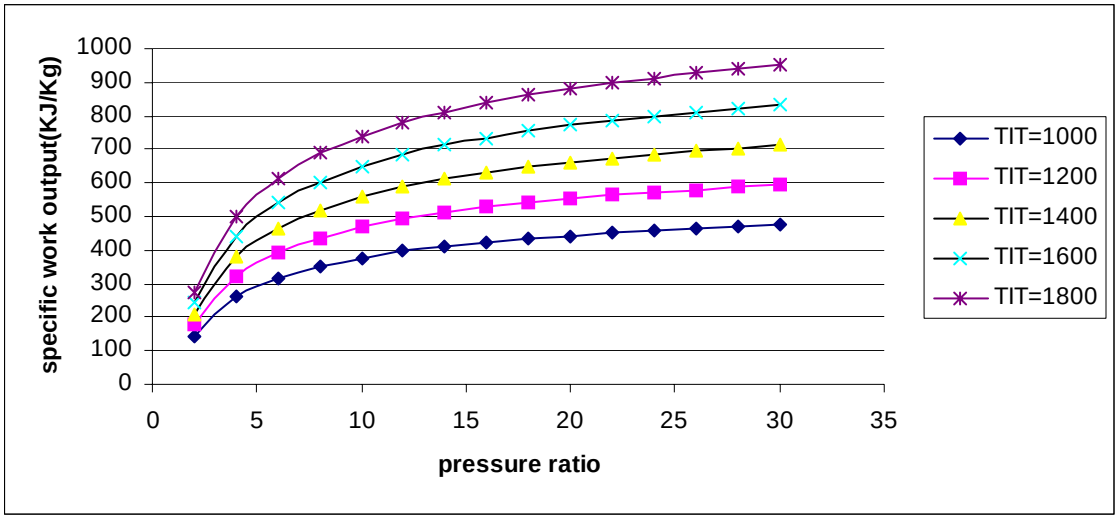

7

n=0,1,2

Fig 3.1.5 VARIATION OF SPECIFIC OUTPUT OF TOPPING CYCLE VS PRESSURE RATIO (γ=1.1)

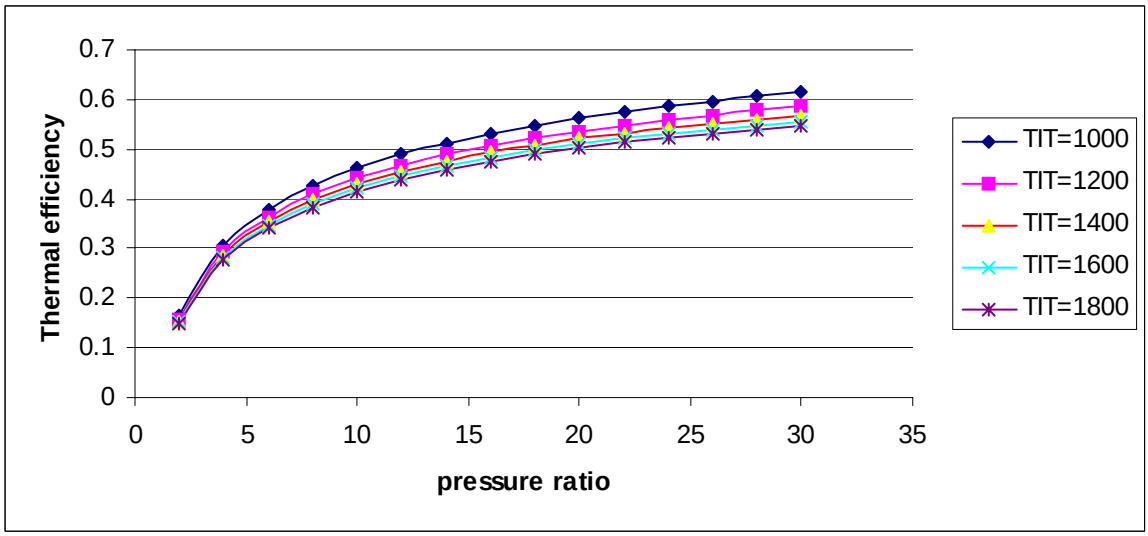

n=0,1,2

Fig 3.1.6 VARIATION OF THERMAL EFFICIENCY OF TOPPING CYCLE VS PRESSURE RATIO (γ=1.1)

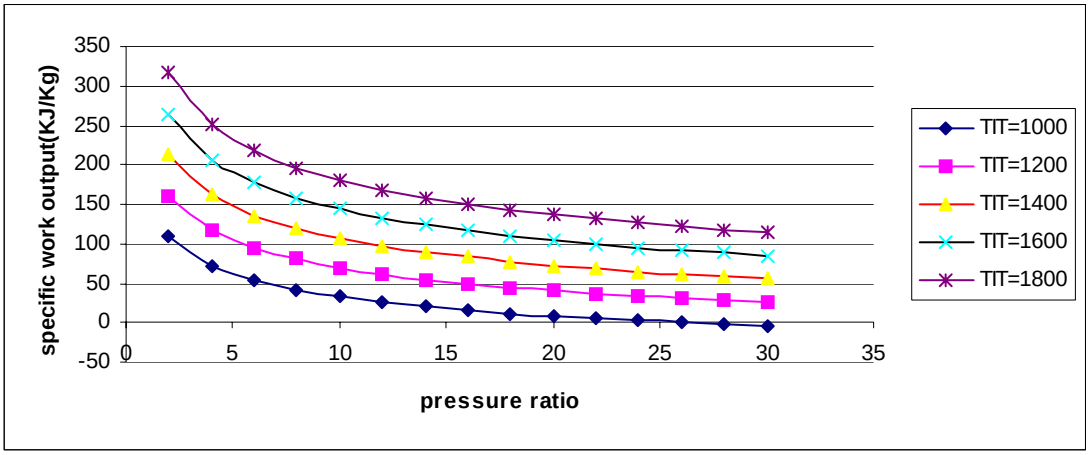

Fig 3.1.7a n=0

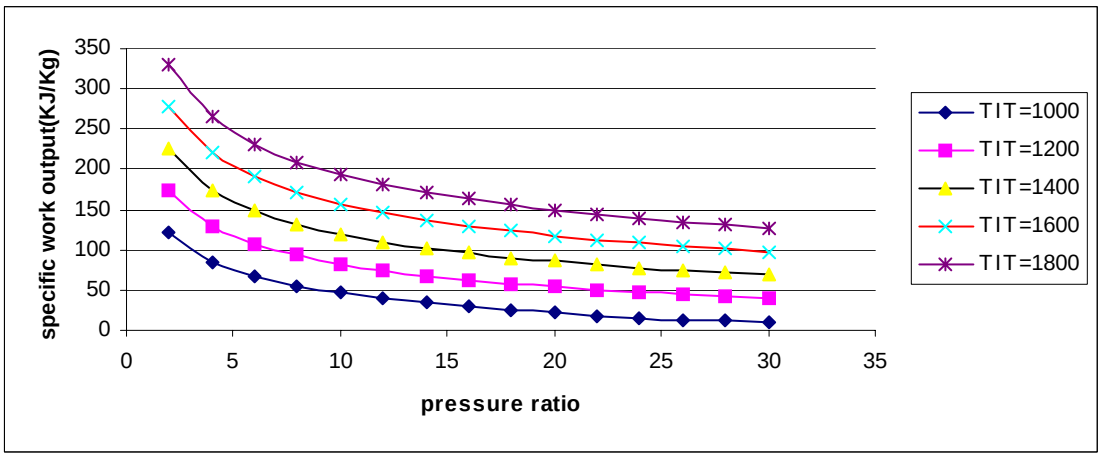

Fig 3.1.7b n=1

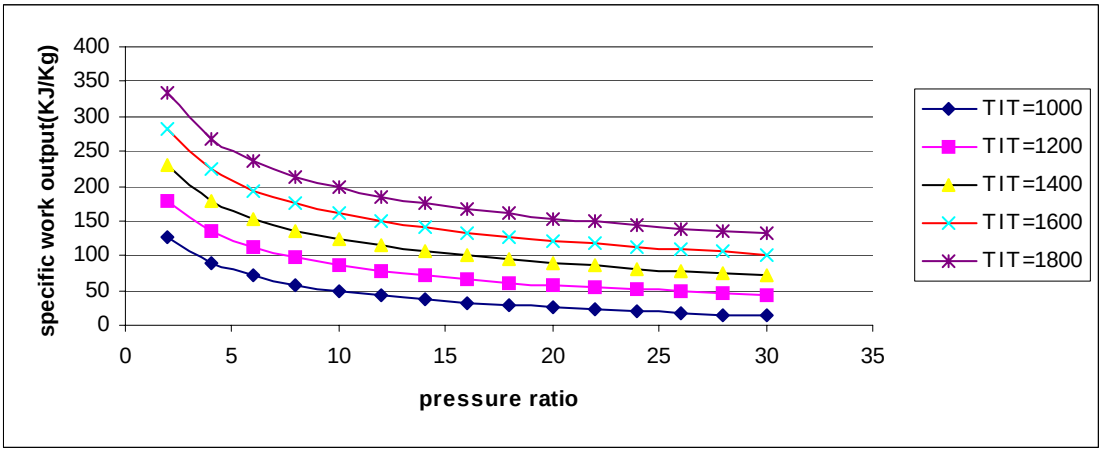

Fig 3.1.7c n=2

Fig 3.1.7 VARIATION OF SPECIFIC OUTPUT OF BOTTOMING CYCLE VS PRESSURE RATIO (γ=1.1)

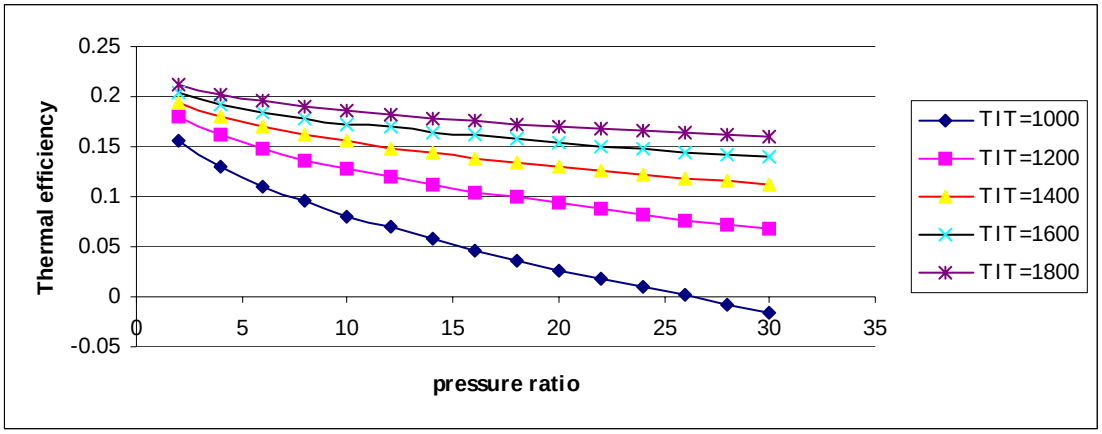

Fig 3.1.8a n=0

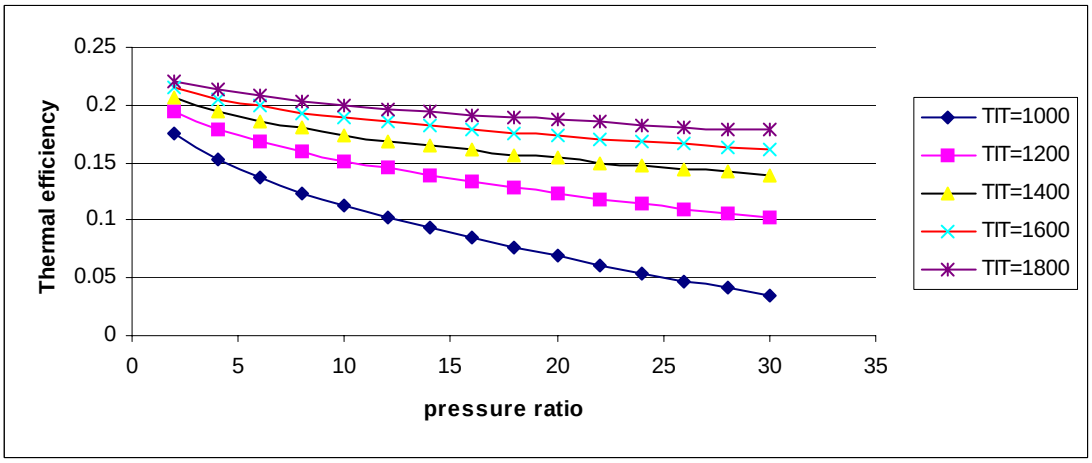

Fig 3.1.8b n=1

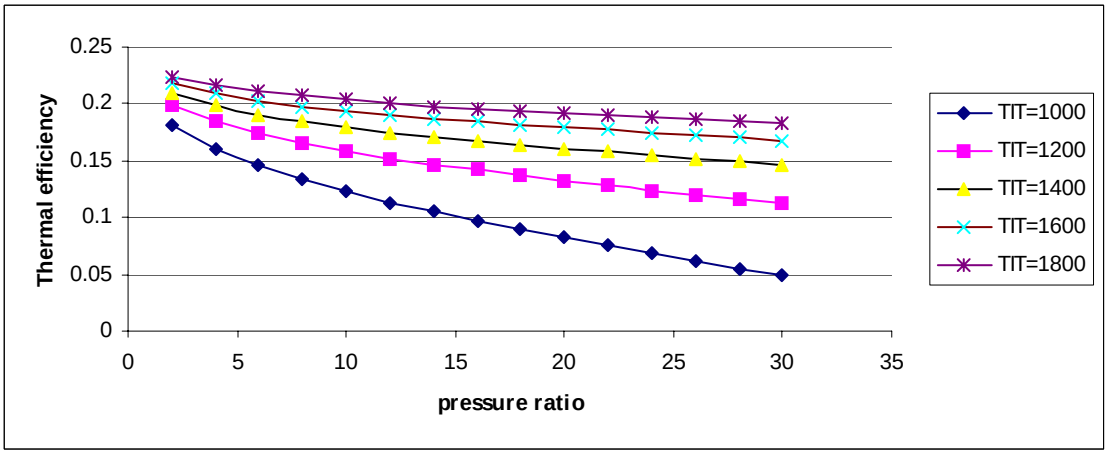

Fig 3.1.8c n=2

Fig 3.1.8 VARIATION OF THERMAL EFFICIENCY BOTTOMING CYCLE VS PRESSURE RATIO

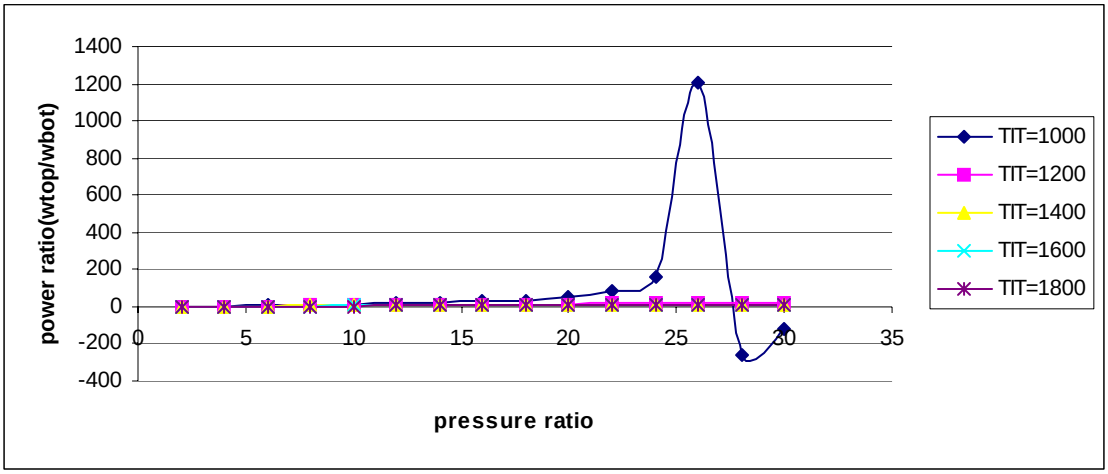

Fig 3.1.9a n=0

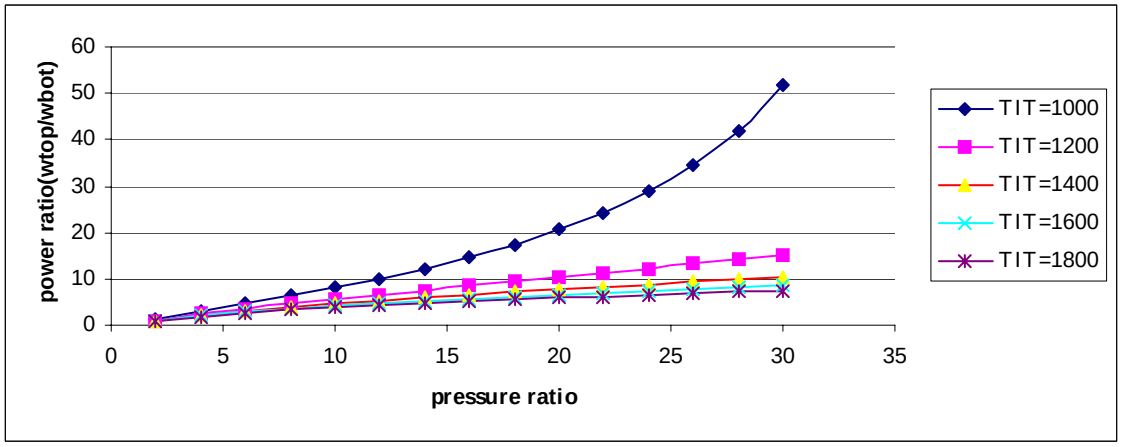

Fig 3.1.9b n=1

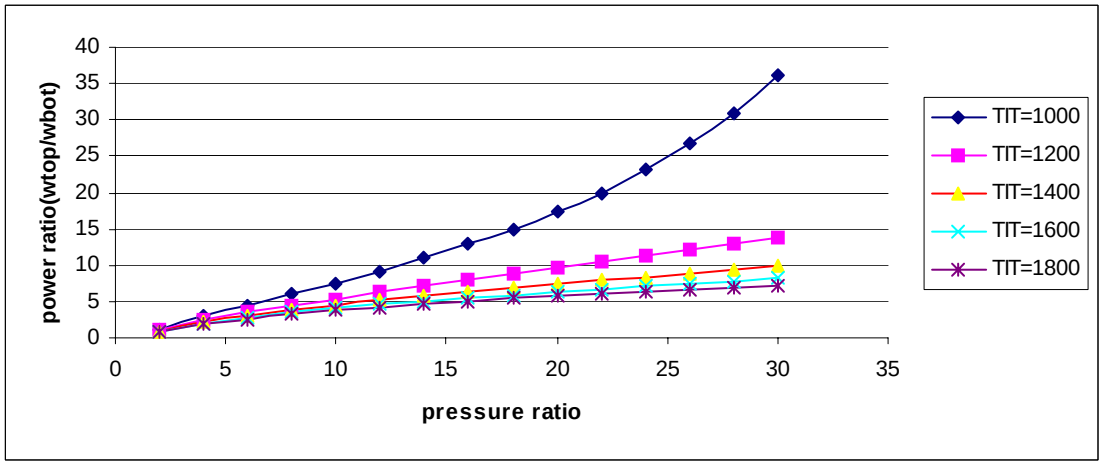

Fig 3.1.9c n=2

Fig 3.1.9 VARIATION OF POWER RATIO OF MIRROR GAS TURBINE VS PRESSURE RATIO (γ=1.1)

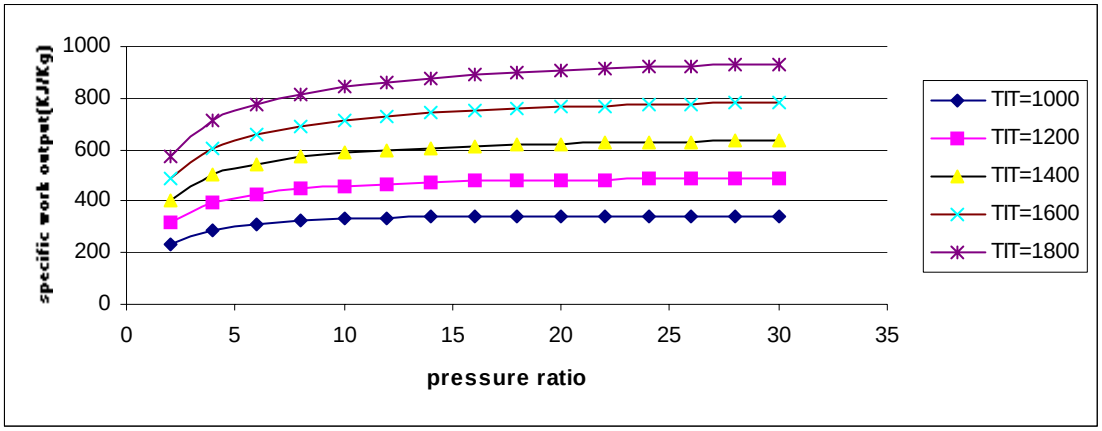

Fig 3.2.1a n=0

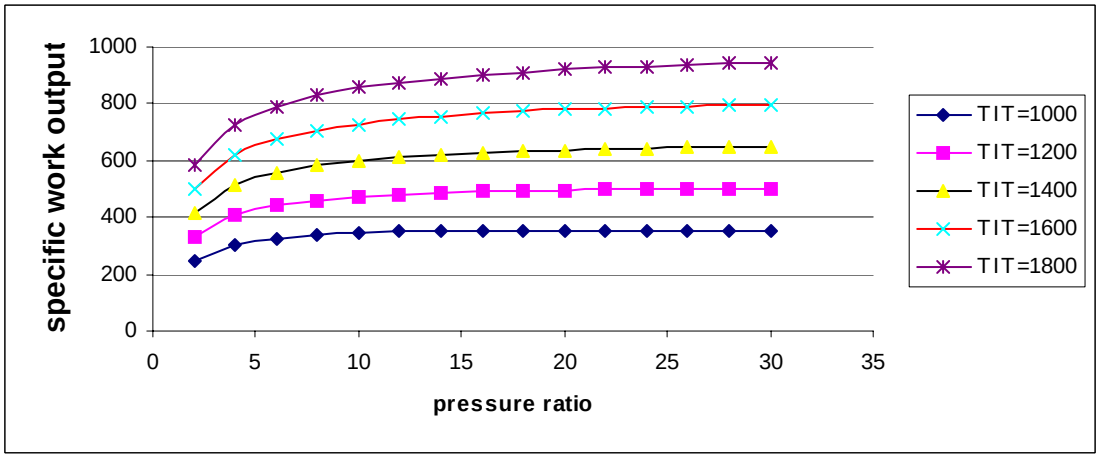

Fig 3.2.1b n=1

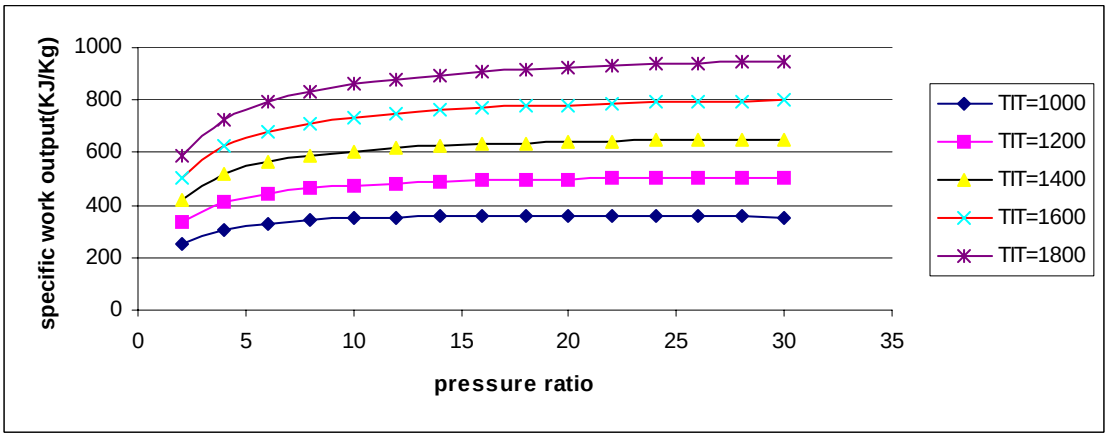

Fig 3.2.1c n=2

Fig 3.2.1 VARIATION OF SPECIFIC OUTPUT OF MIRROR GAS TURBINE VS PRESSURE RATIO(γ=1.2)

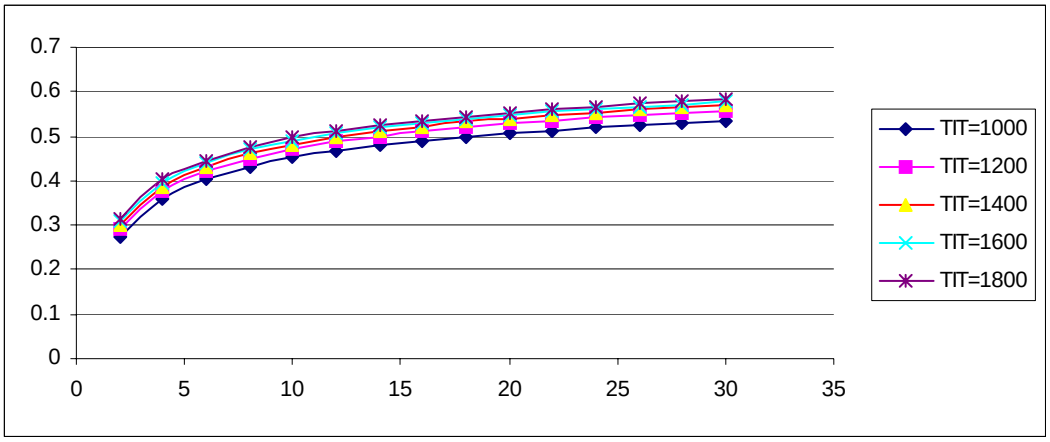

Fig 3.2.2a n=0

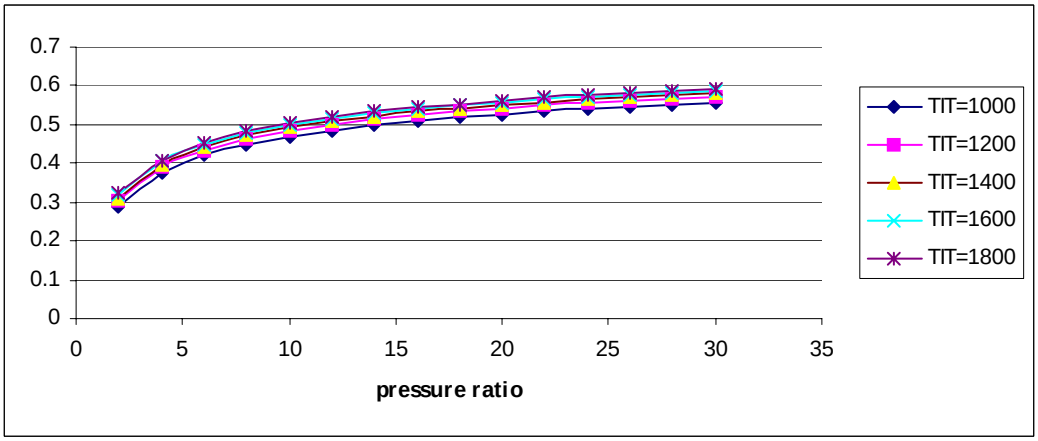

Fig 3.2.2b n=1

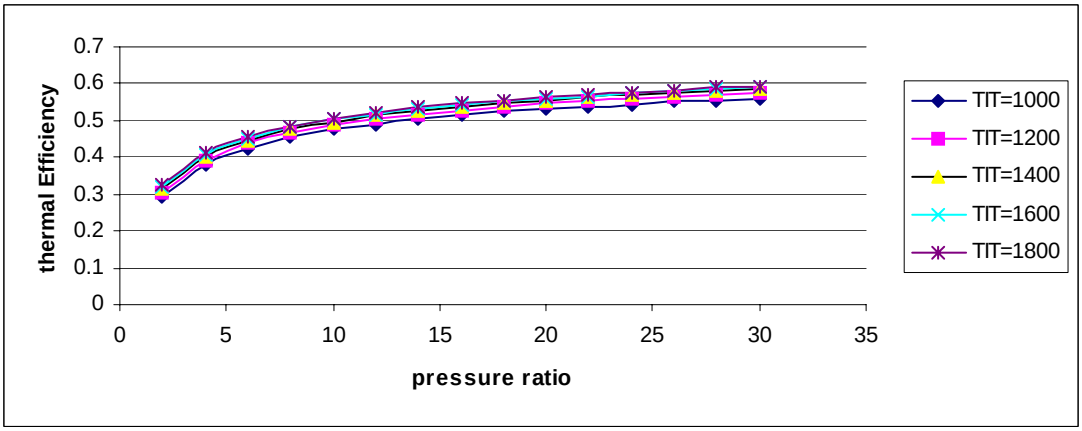

Fig 3.2.2c n=2

Fig 3.2.2 VARIATION OF THERMAL EFFICIENCY OF MIRROR GAS TURBINE VS PRESSURE RATIO(γ=1.2)

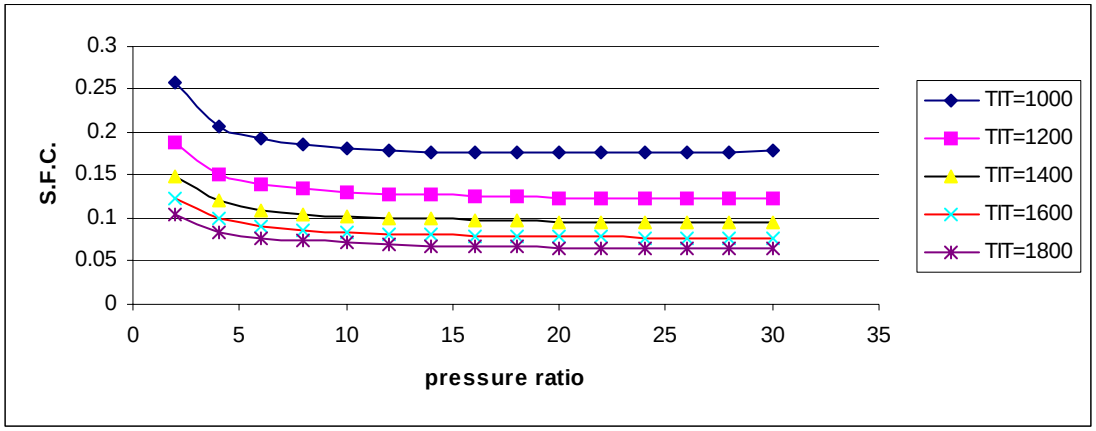

Fig 3.2.3a n=0

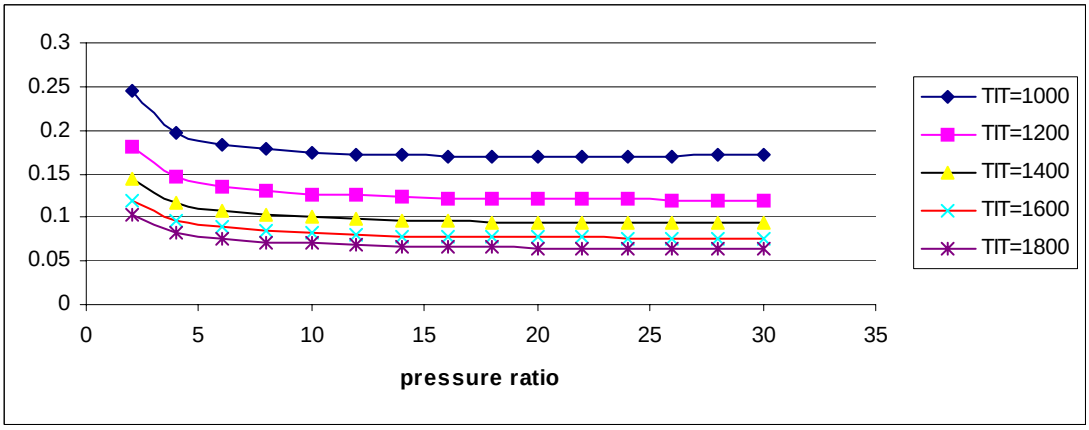

Fig 3.2.3b n=1

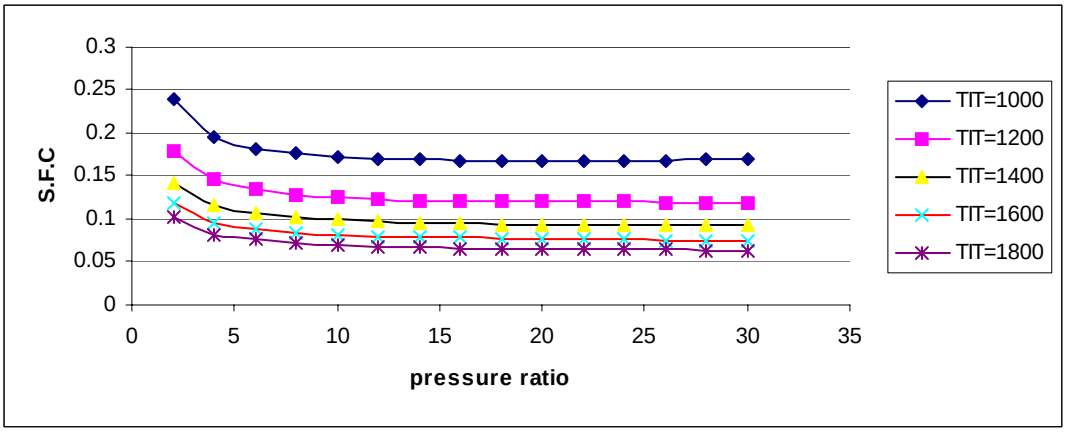

Fig 3.2.3c n=2

3.2.3 VARIATION OF S.F.C. OF MIRROR GAS TURBINE VS PRESSURE RATIO(γ=1.2)

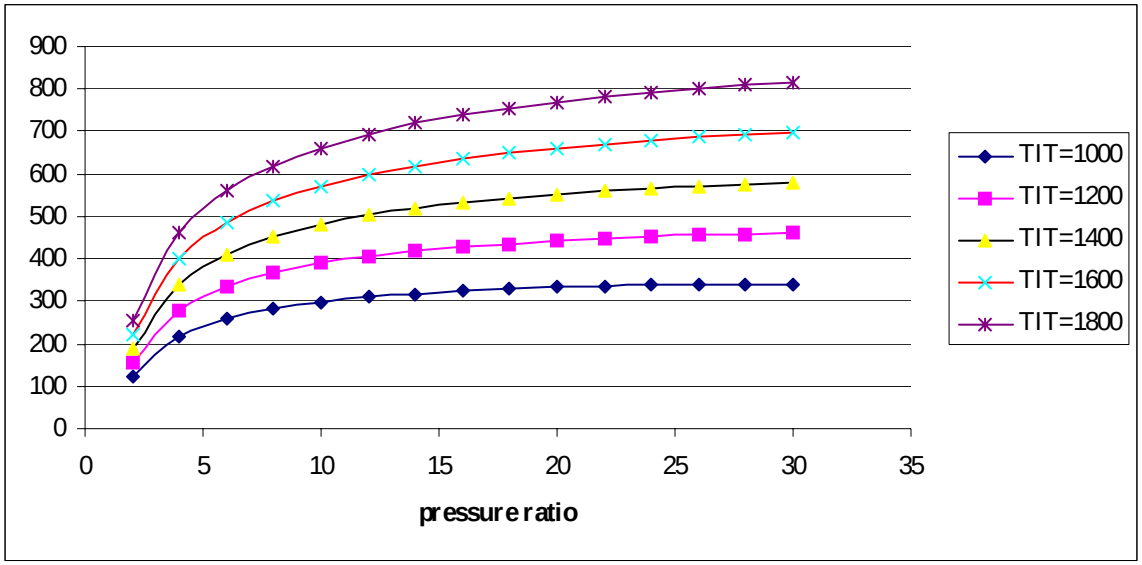

n=0,1,2

Fig 3.2.4 VARIATION OF SPECIFIC OUTPUT OF TOPPING CYCLE VS PRESSURE RATIO(γ=1.2)

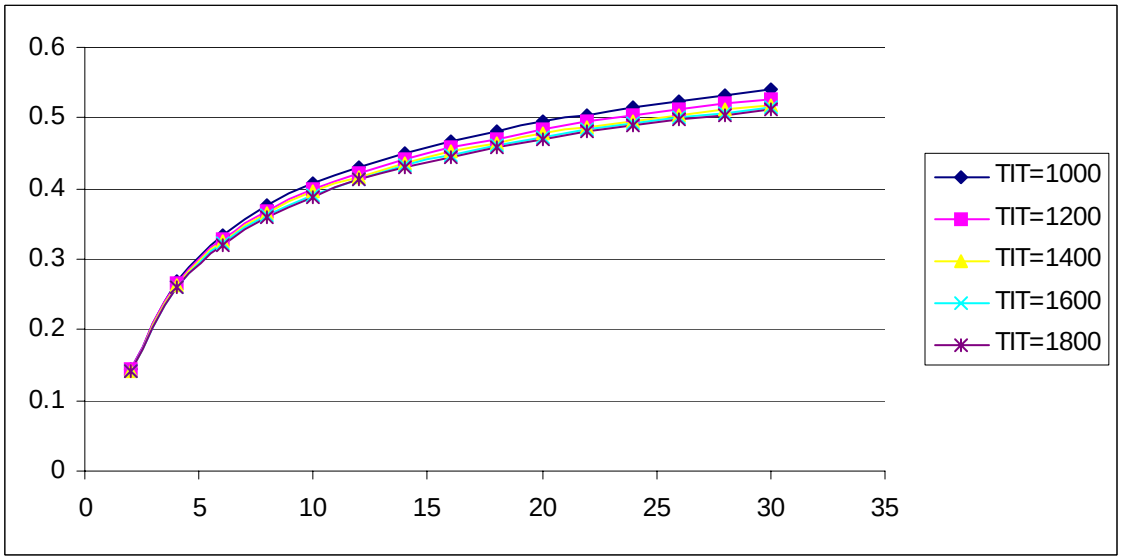

n=0,1,2

Fig 3.2.5 VARIATION OF THERMAL EFFICIENCY OF TOPPING CYCLE VS PRESSURE RATIO(γ=1.2)

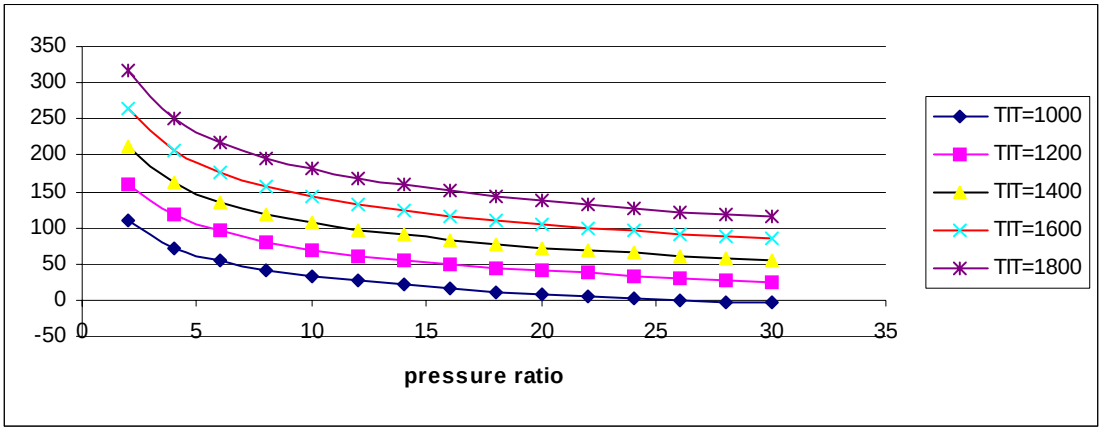

Fig 3.2.6a n=0

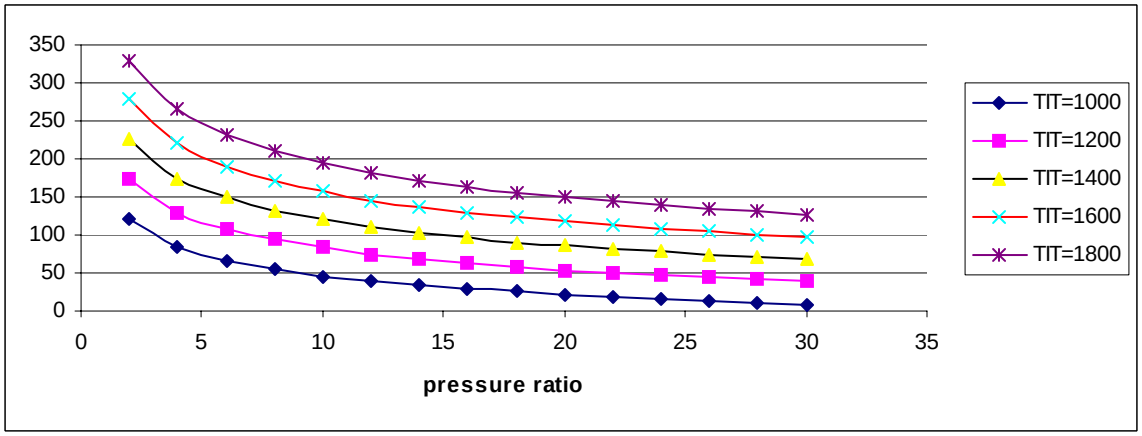

Fig 3.2.6b n=1

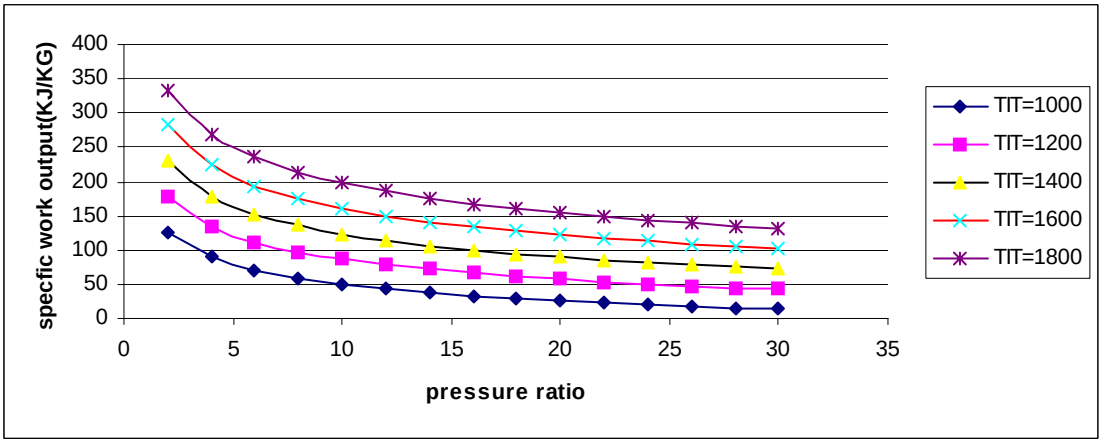

Fig 3.2.6c n=2

Fig 3.2.6 VARIATION OF SPECIFIC OUTPUT OF BOTTOMING CYCLE VS PRESSURE RATIO(γ=1.2)

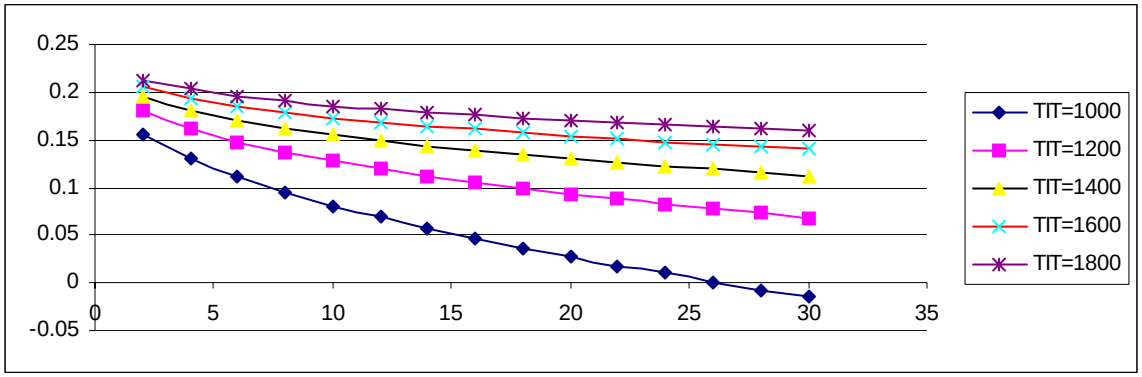

Fig 3.2.7a n=0

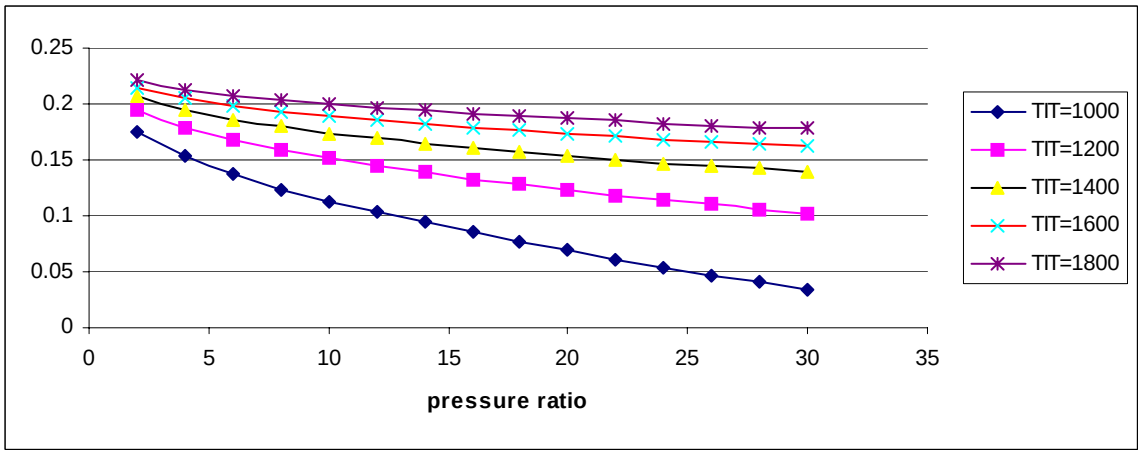

Fig 3.2.7b n=1

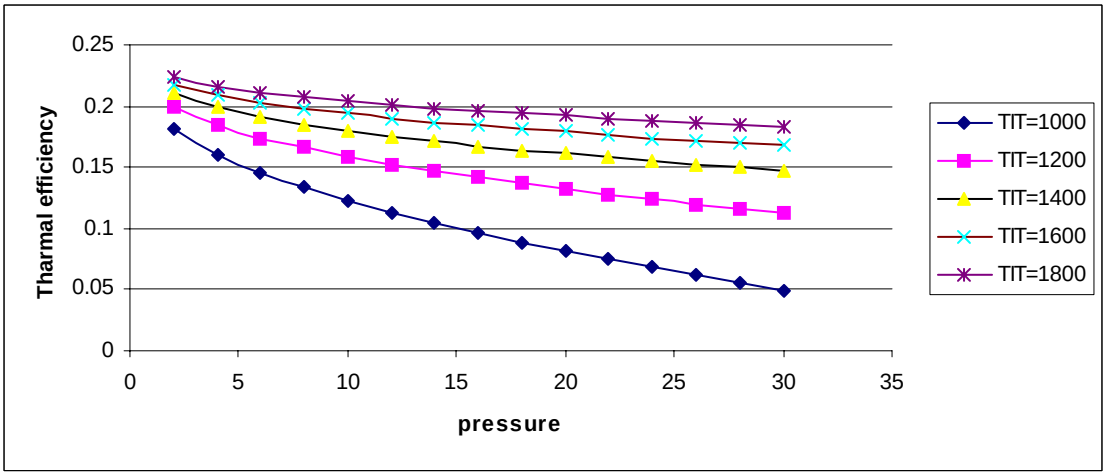

Fig 3.2.7c n=2

Fig 3.2.7 VARIATION OF THERMAL EFFICIENCY BOTTOMING CYCLE VS PRESSURE RATIO(γ=1.2)

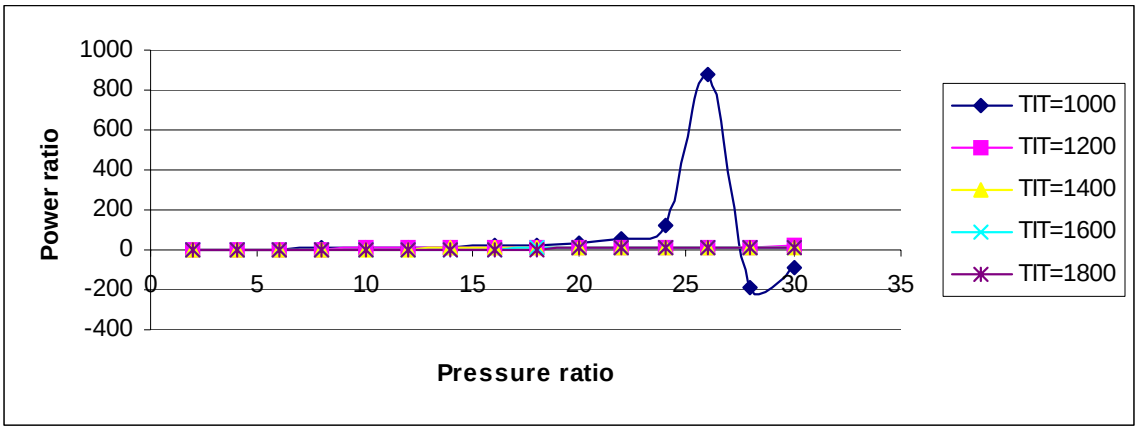

Fig 3.2.8a n=0

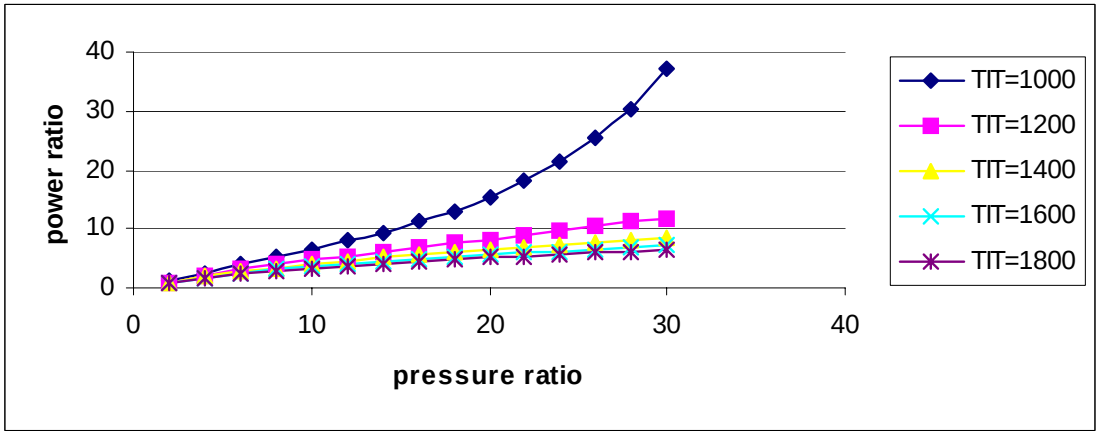

Fig 3.2.8b n=1

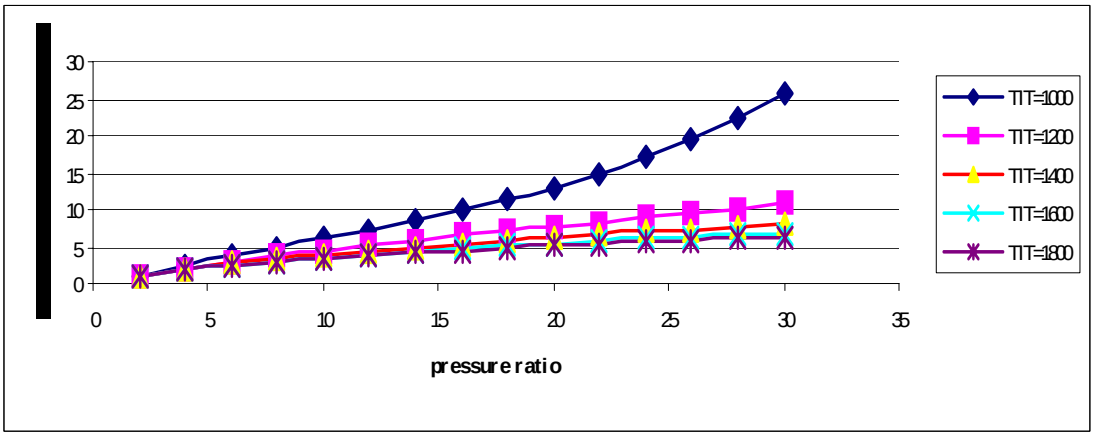

Fig 3.2.8c n=2

Fig 3.2.8 VARIATION OF POWER RATIO OF MIRROR GAS TURBINE VS PRESSURE RATIO(γ=1.2)

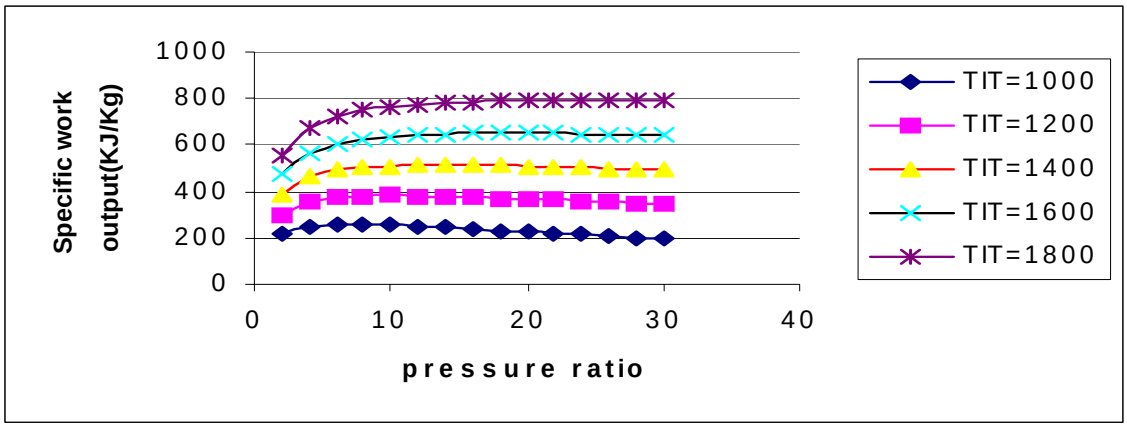

Fig 3.3.1a n=0

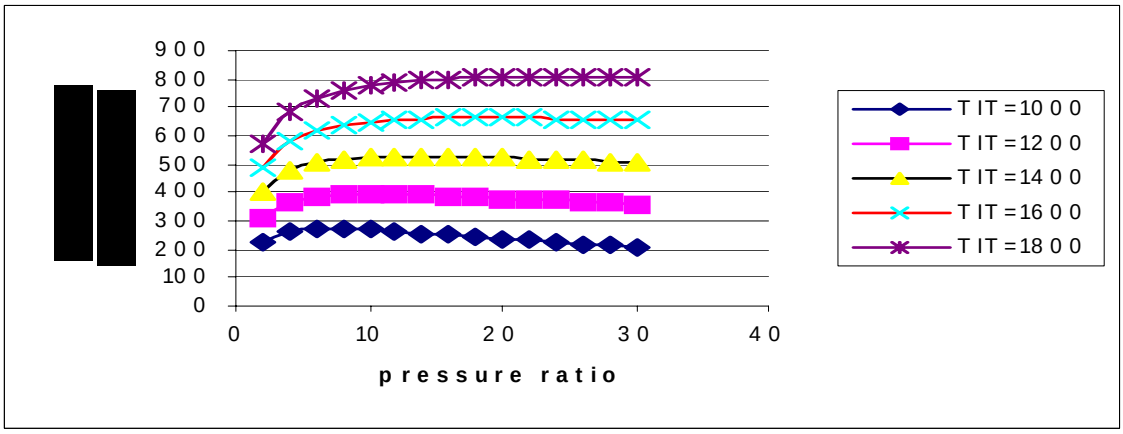

Fig 3.3.1b n=1

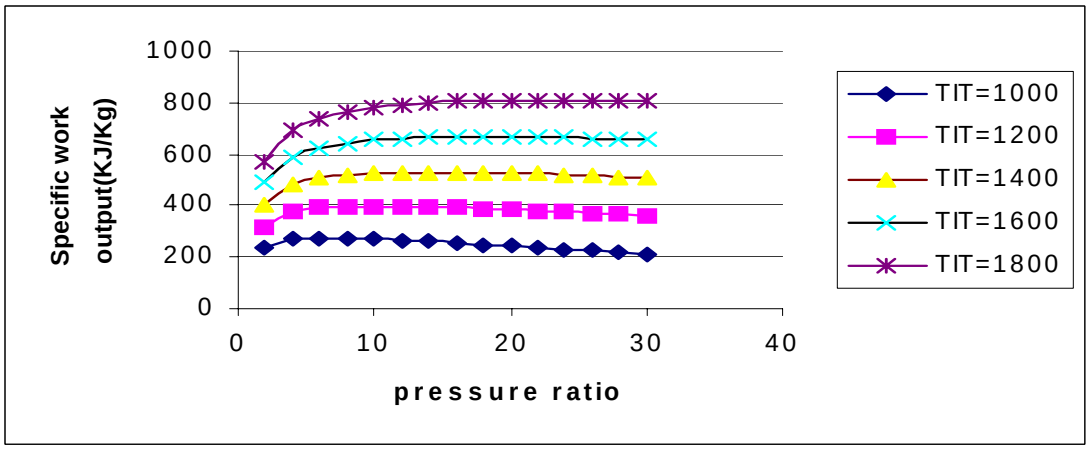

Fig 3.3.1c n=2

Fig 3.3.1 VARIATION OF SPECIFIC OUTPUT OF MIRROR GAS TURBINE VS PRESSURE RATIO (γ=1.3)

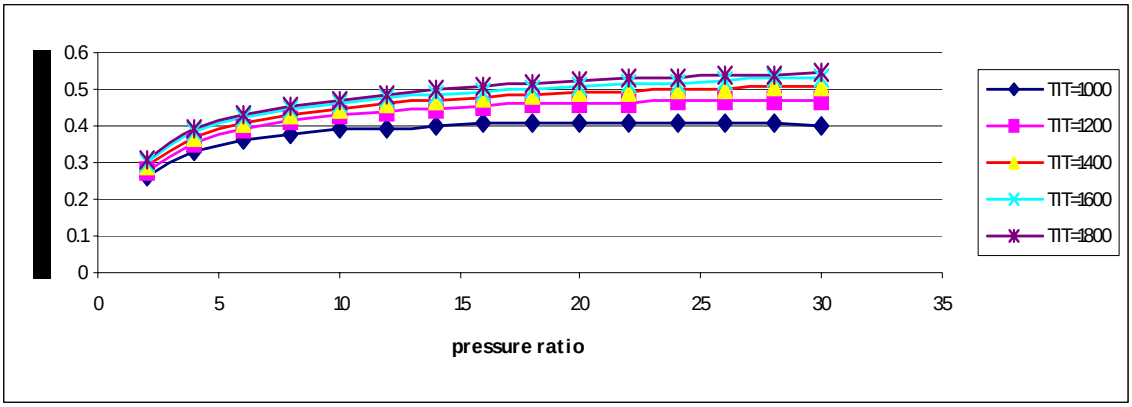

Fig 3.3.2a n=0

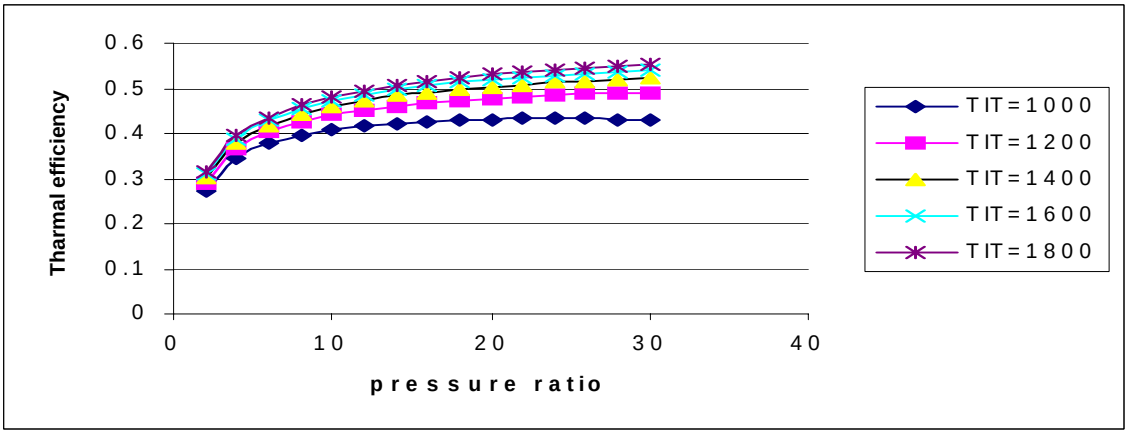

Fig 3.3.2b n=1

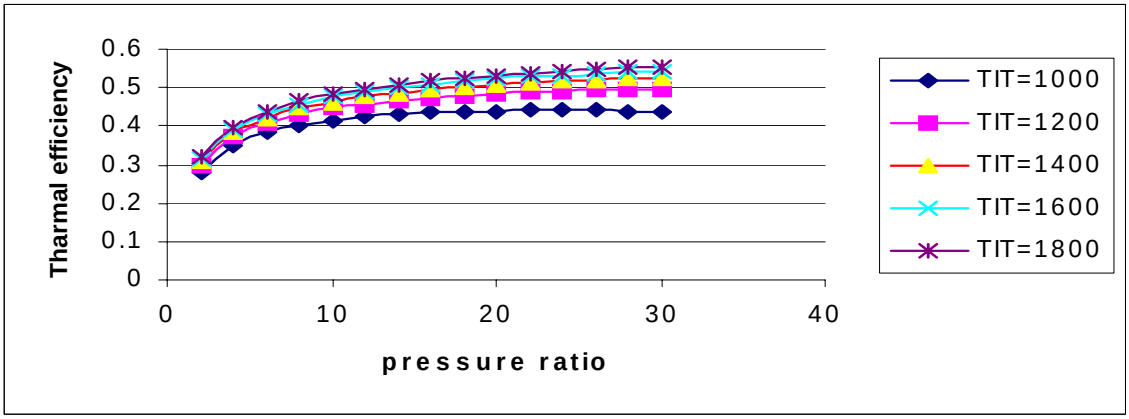

Fig 3.3.2c n=2

Fig 3.3.2 VARIATION OF THERMAL EFFICIENCY OF MIRROR GAS TURBINE VS PRESSURE RATIO(γ=1.3)

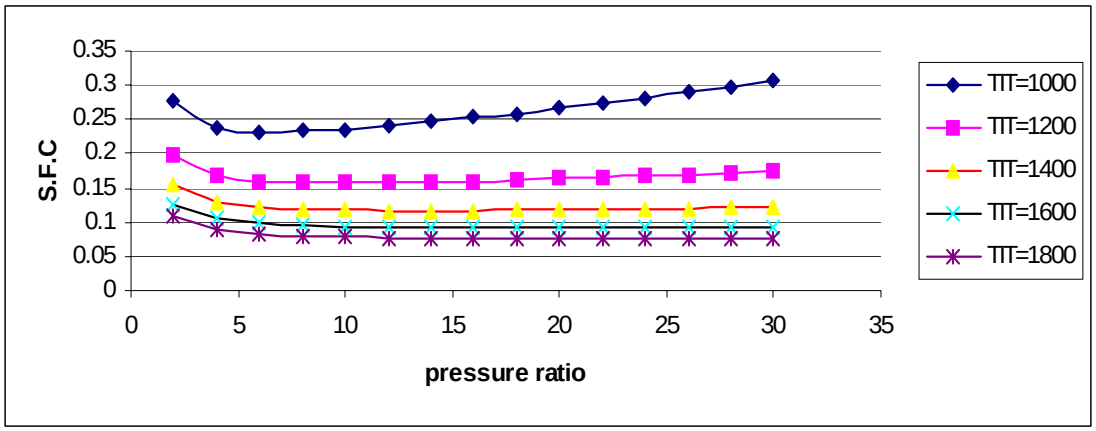

Fig 3.3.3a n=0

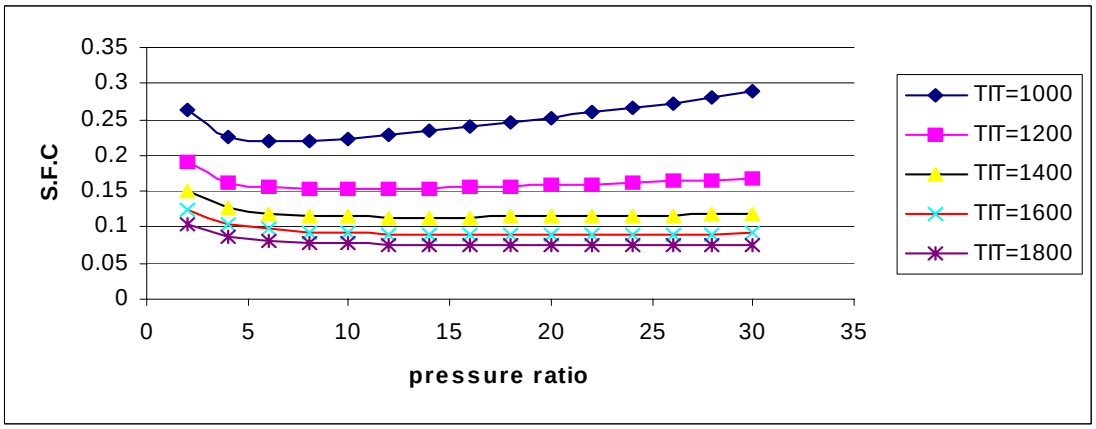

Fig 3.3.3b n=1

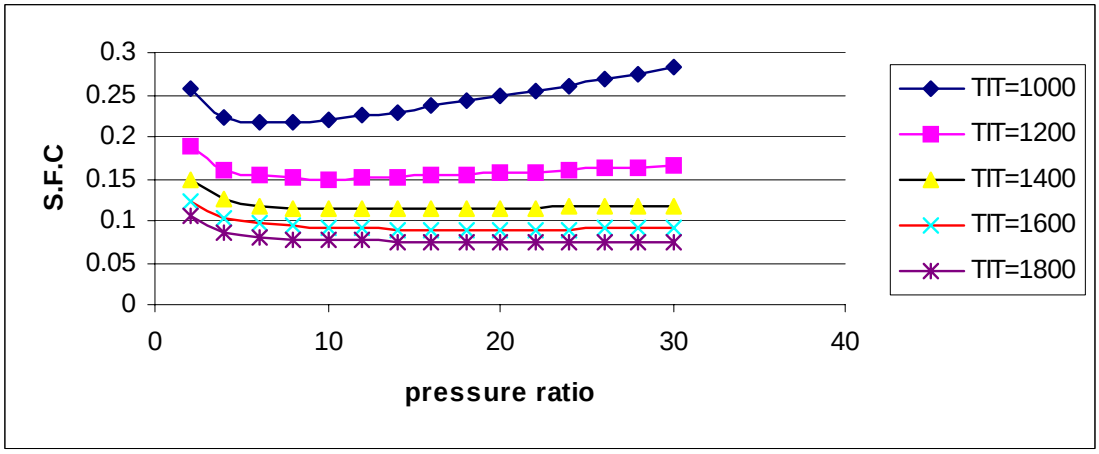

Fig 3.3.3c n=2

Fig 3.3.3 VARIATION OF S.F.C. OF MIRROR GAS TURBINE VS PRESSURE RATIO (γ=1.3)

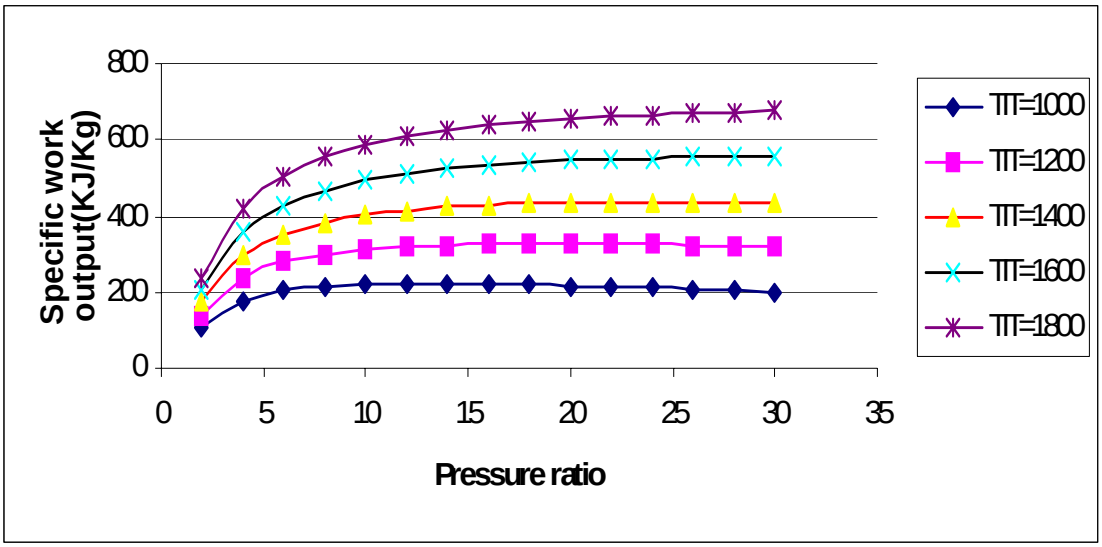

n=0,1,2

Fig 3.3.4 VARIATION OF SPECIFIC OUTPUT OF TOPPING CYCLE VS PRESSURE RATIO(γ=1.3)

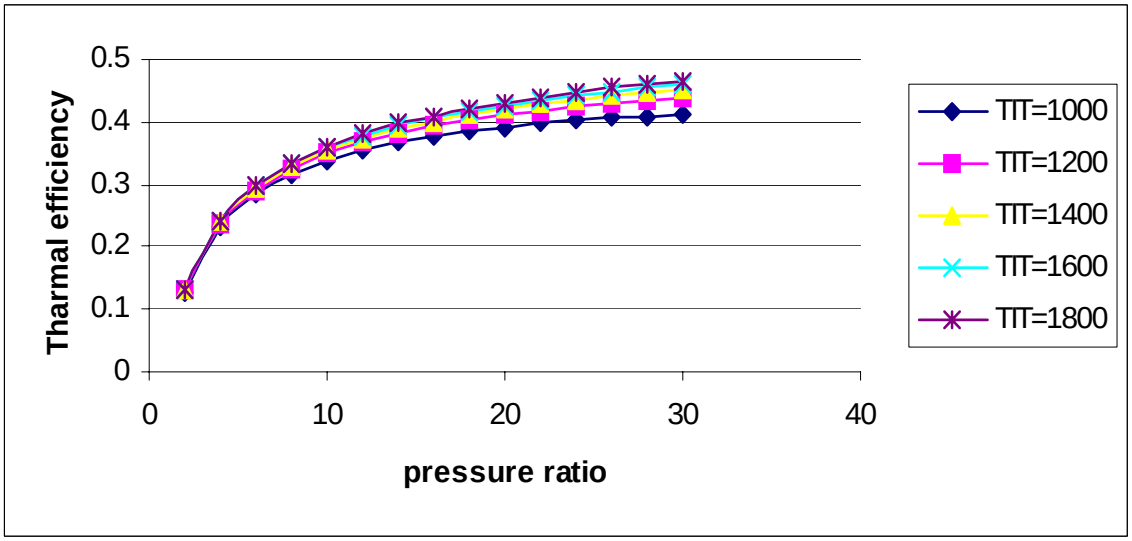

n=0,1,2

Fig 3.3.5 VARIATION OF THERMAL EFFICIENCY OF TOPPING CYCLE VS PRESSURE RATIO(γ=1.3)

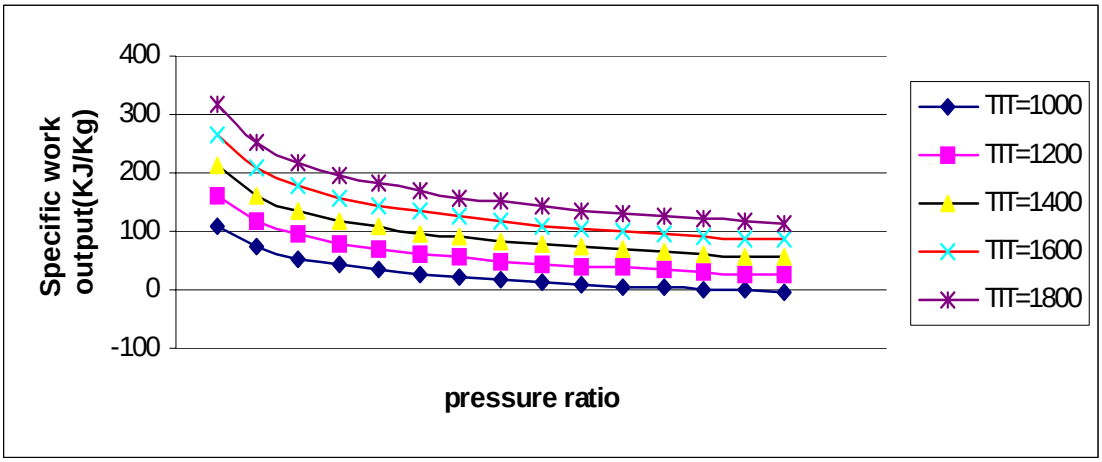

Fig 3.3.6a n=0

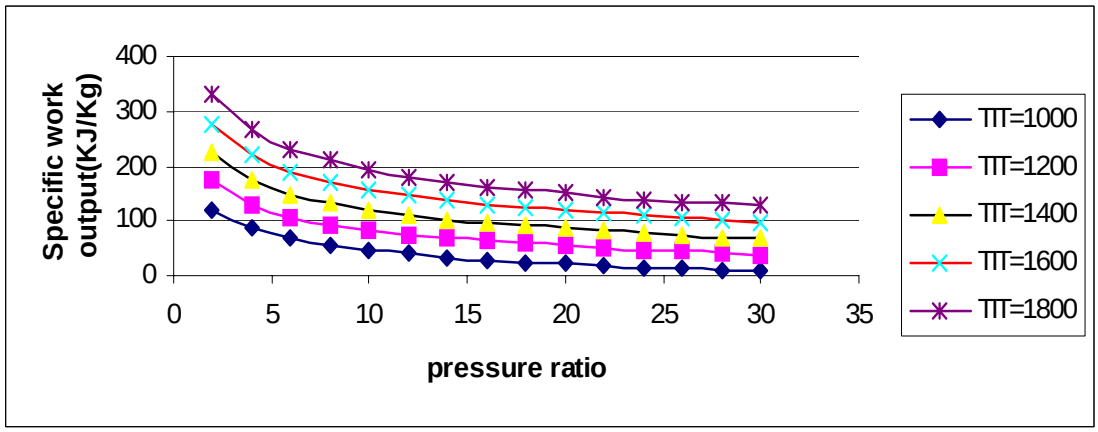

Fig 3.3.6b n=1

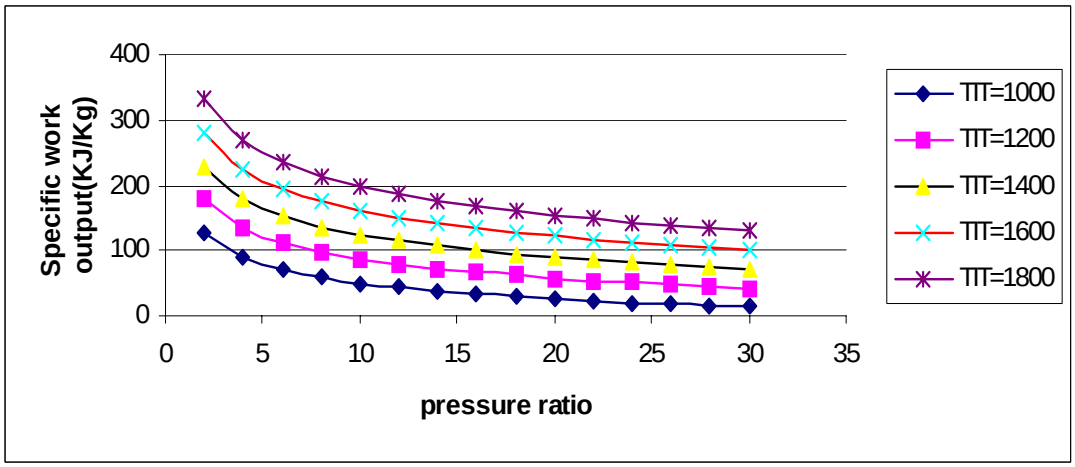

Fig 3.3.6c n=2

Fig 3.3.6 VARIATION OF SPECIFIC OUTPUT OF BOTTOMING CYCLE VS PRESSURE RATIO(γ=1.3)

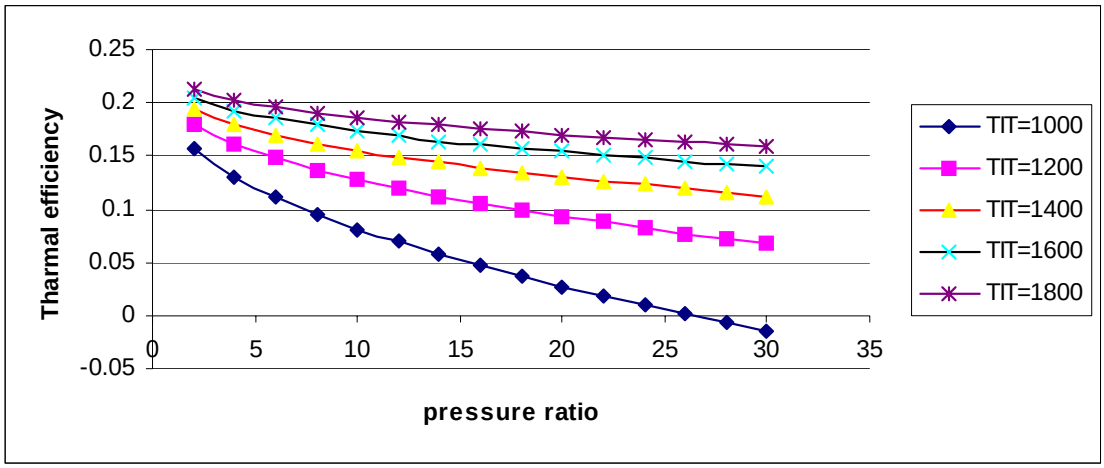

Fig 3.3.7a n=0

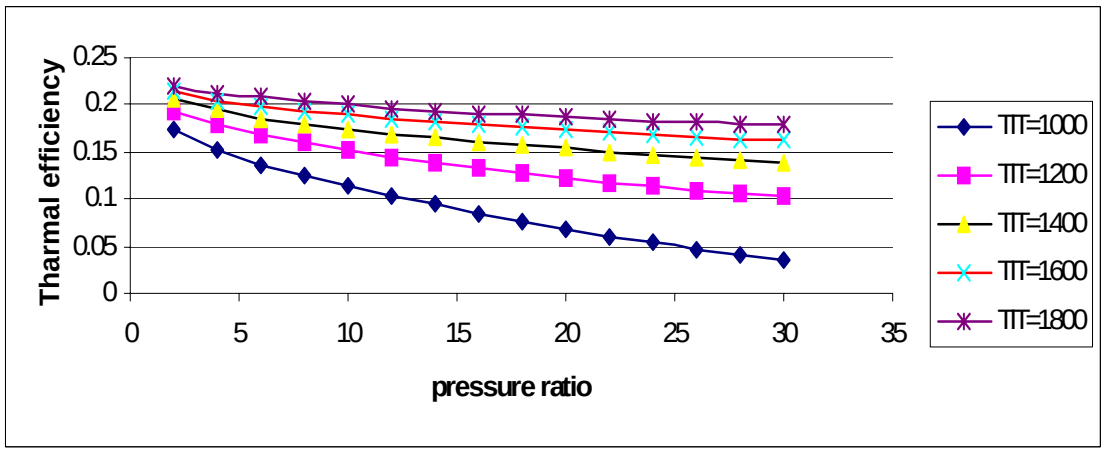

Fig 3.3.7b n=1

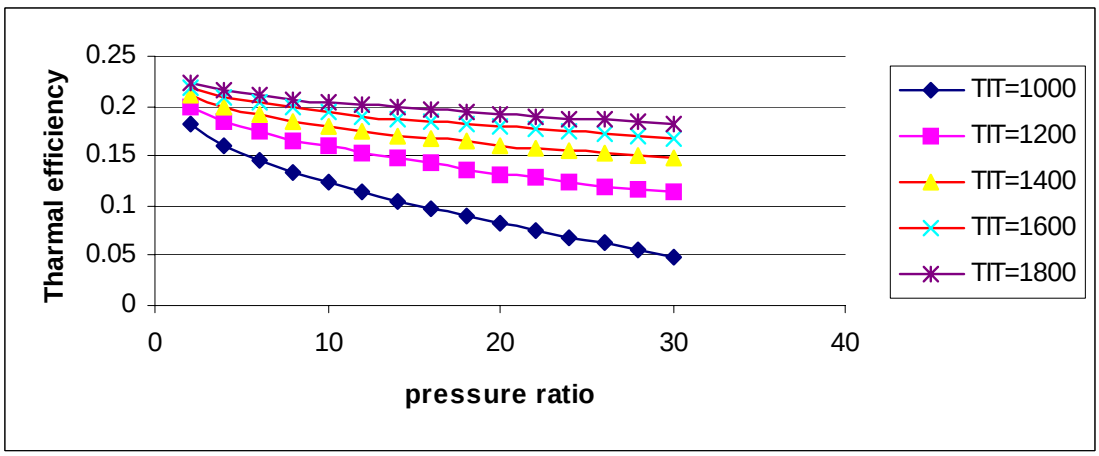

Fig 3.3.7c n=2

Fig 3.3.7 VARIATION OF THERMAL EFFICIENCY BOTTOMING CYCLE VS PRESSURE RATIO(γ=1.3)

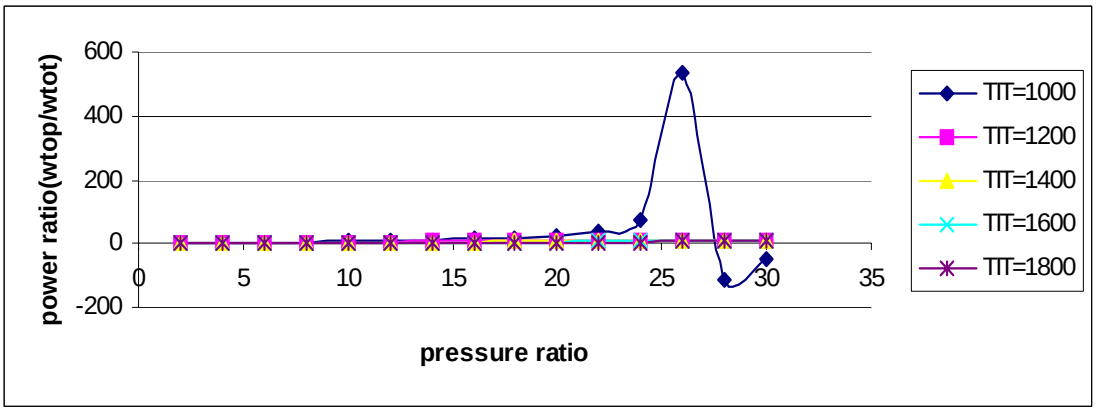

Fig 3.3.8a n=0

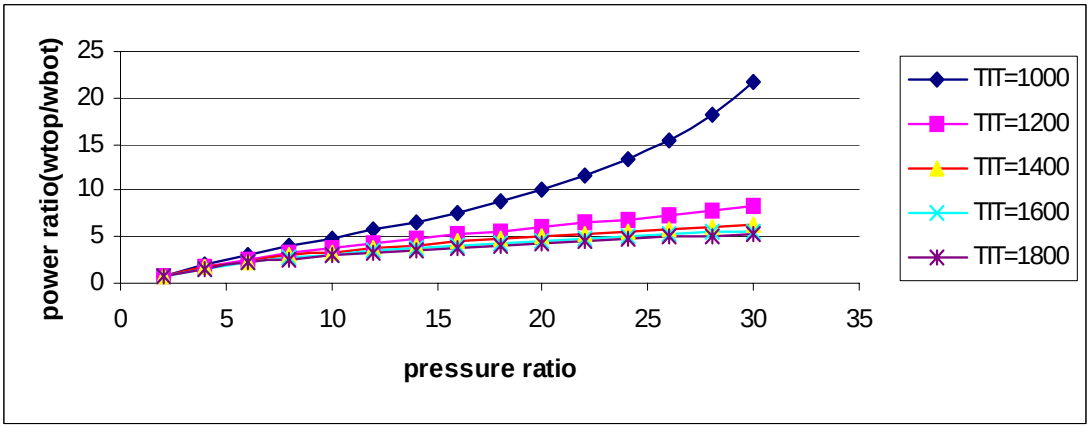

Fig 3.3.8b n=1

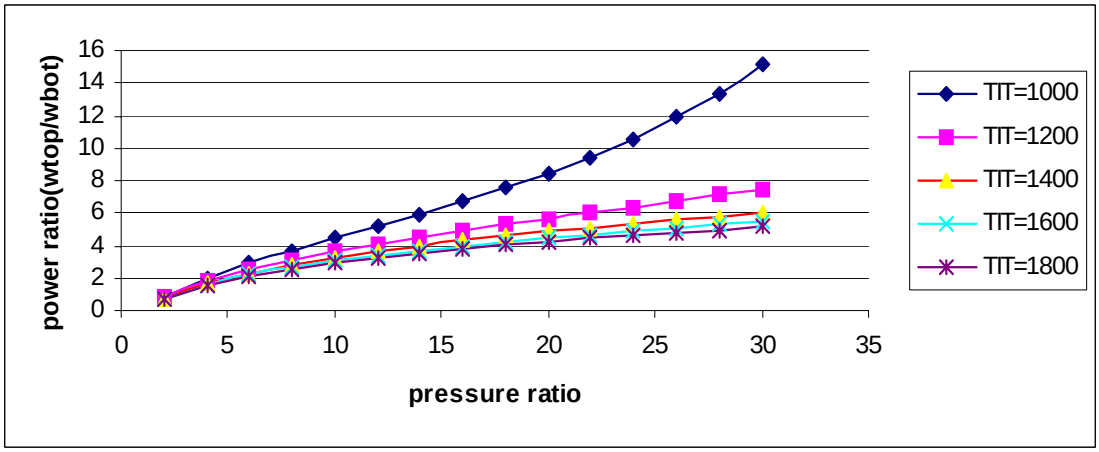

Fig 3.3.8c n=2

Fig 3.3.8 VARIATION OF POWER RATIO OF MIRROR GAS TURBINE VS PRESSURE RATIO(γ=1.3)

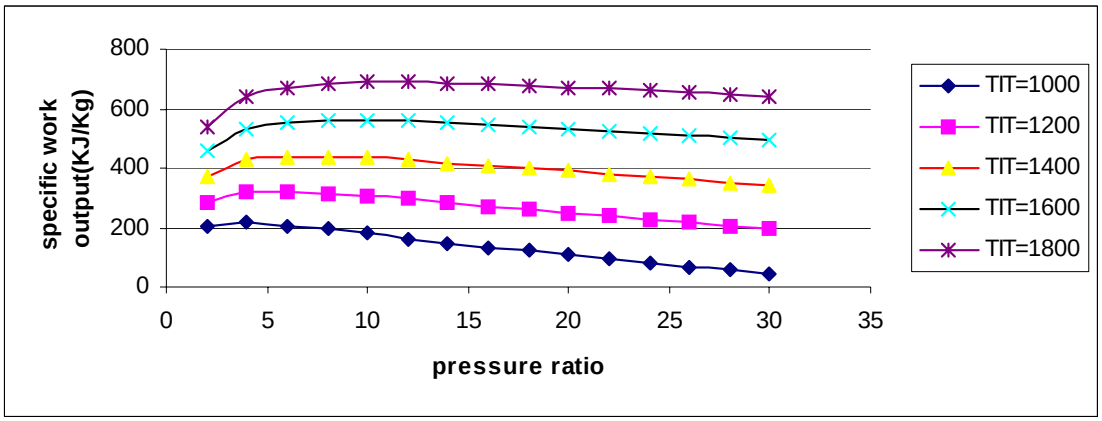

Fig 3.4.1a n=0

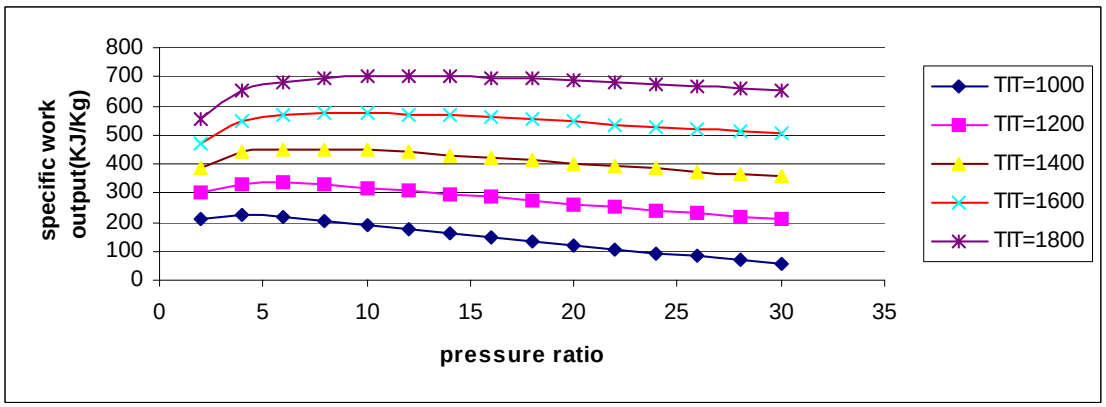

Fig 3.4.1b n=1

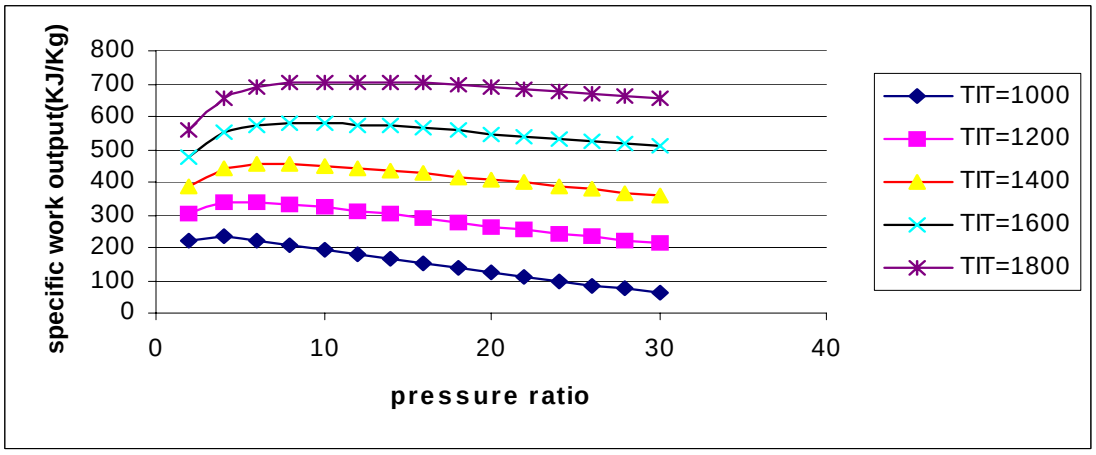

Fig 3.4.1c n=2

Fig 3.4.1 VARIATION OF SPECIFIC OUTPUT OF MIRROR GAS TURBINE VS PRESSURE RATIO(γ=1.4)

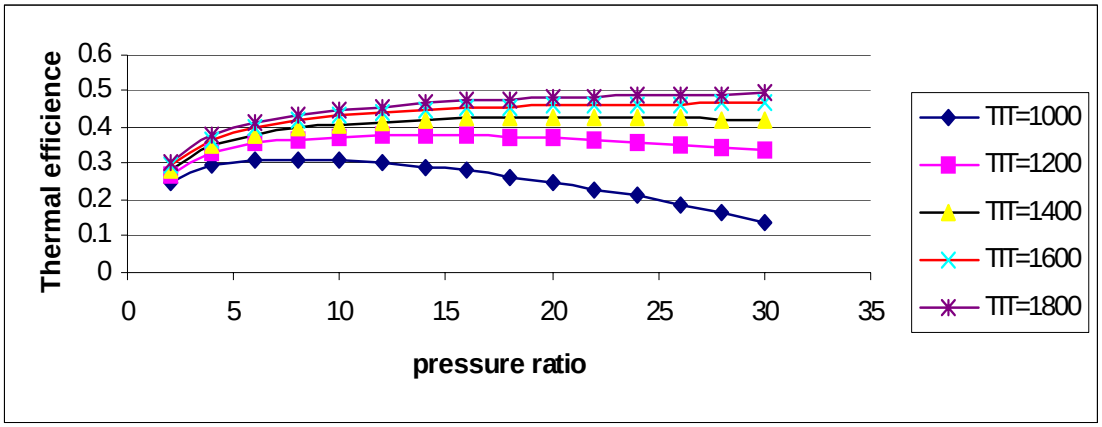

Fig 3.4.2a n=0

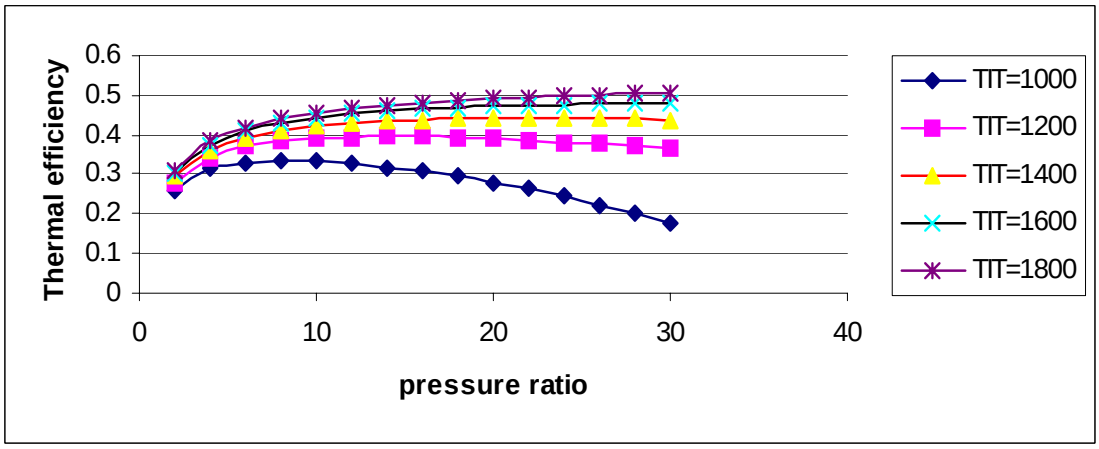

Fig 3.4.2b n=1

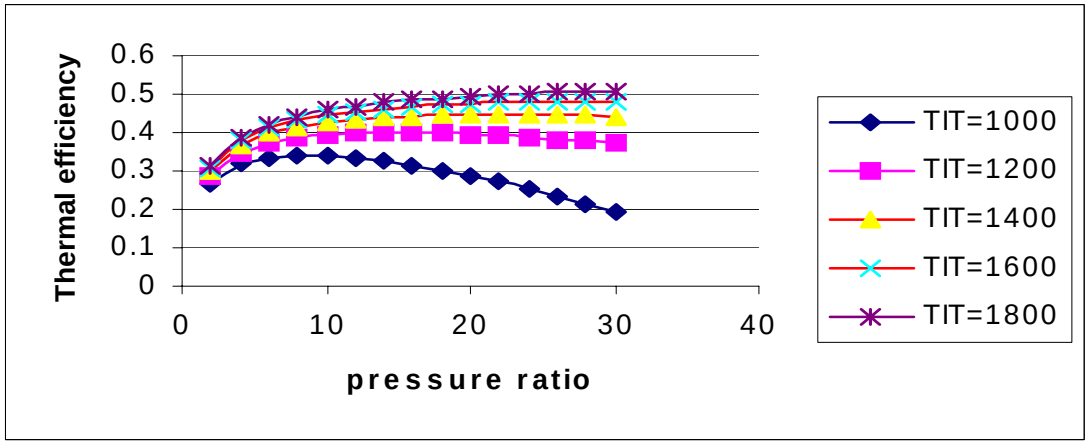

Fig 3.4.2c n=2

Fig 3.4.2 VARIATION OF THERMAL EFFICIENCY OF MIRROR GAS TURBINE VS PRESSURE RATIO(γ=1.4)

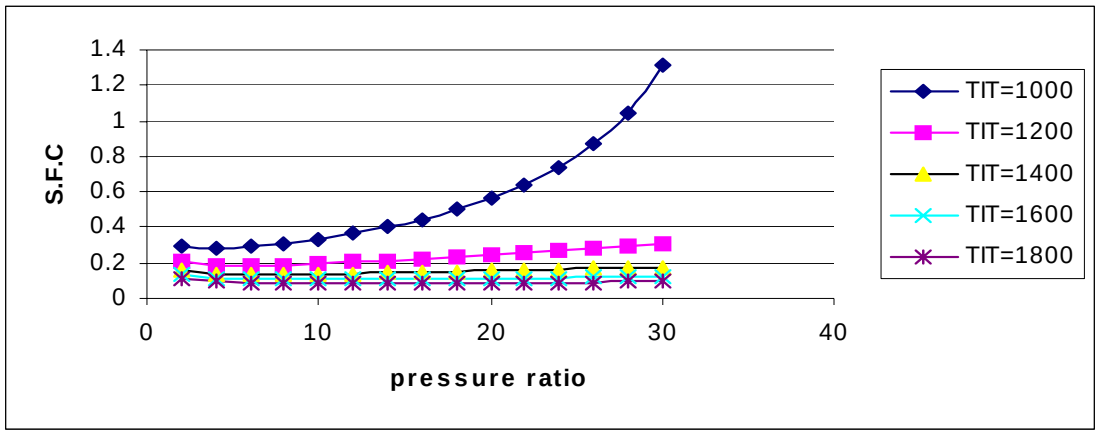

Fig 3.4.3a n=0

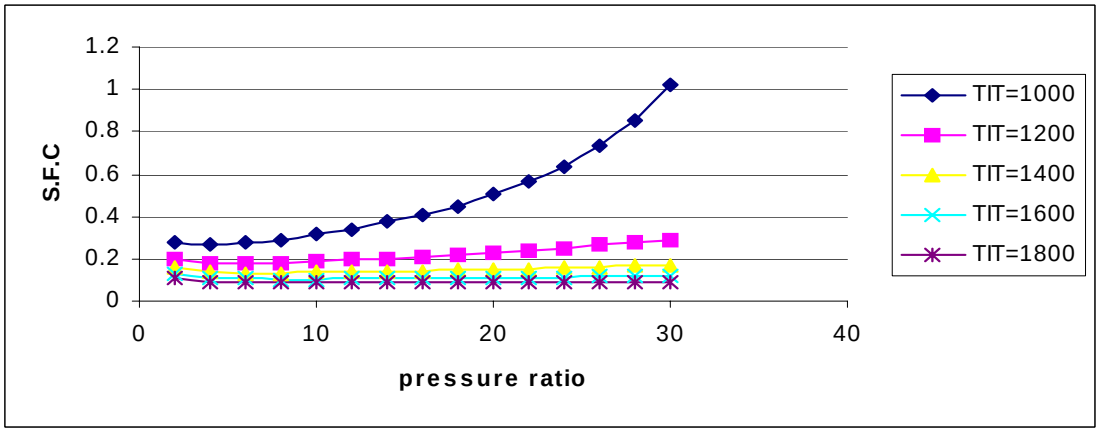

Fig 3.4.3b n=1

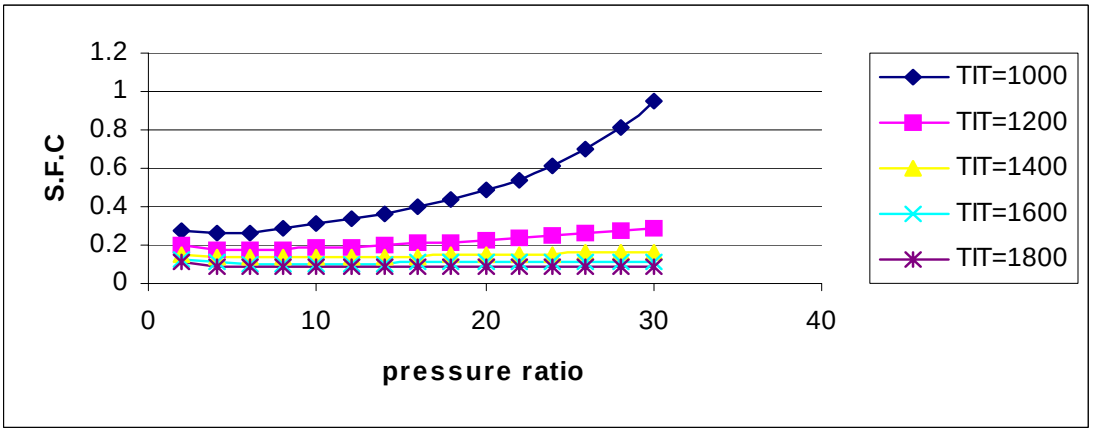

Fig 3.4.3c n=2

Fig 3.4.3 VARIATION OF S.F.C. OF MIRROR GAS TURBINE VS PRESSURE RATIO(γ=1.4)

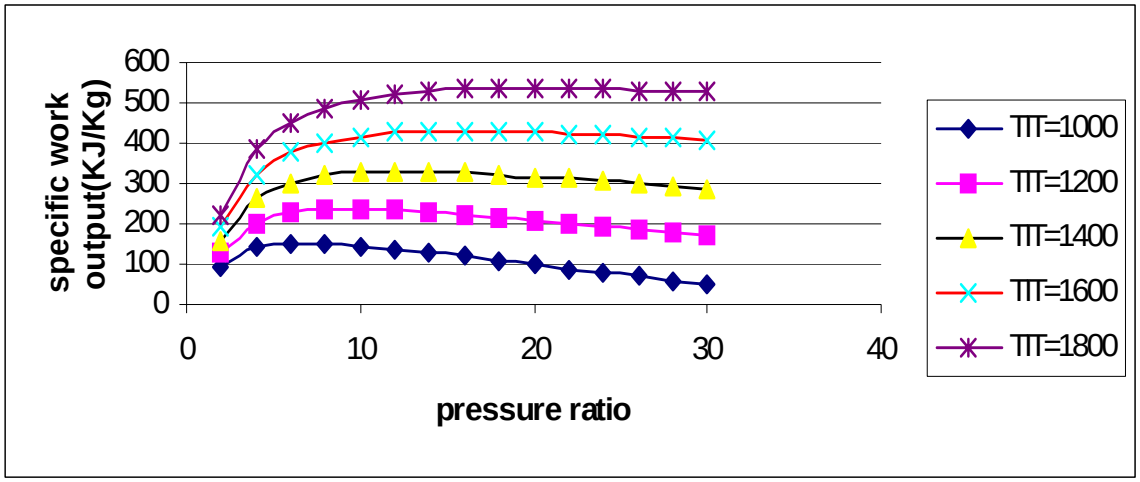

n=0,1,2

3.4.4 GRAPH SHOWING VARIATION OF SPECIFIC OUTPUT OF TOPPING CYCLE VS PRESSURE RATIO(γ=1.4)

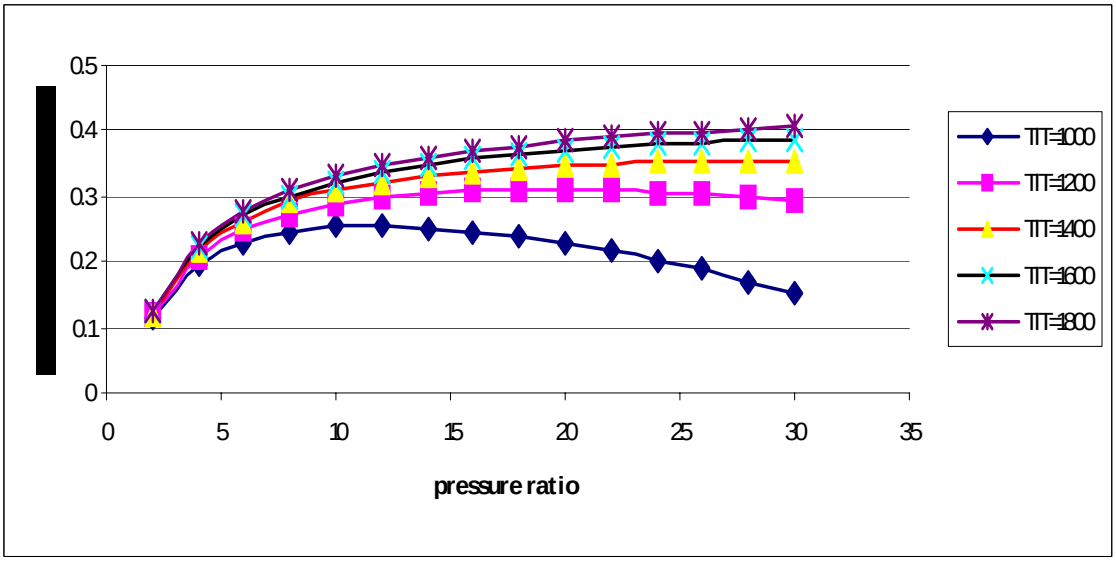

n=0,1,2

Fig 3.4.5 VARIATION OF THERMAL EFFICIENCY OF TOPPING CYCLE VS PRESSURE RATIO(γ=1.4)

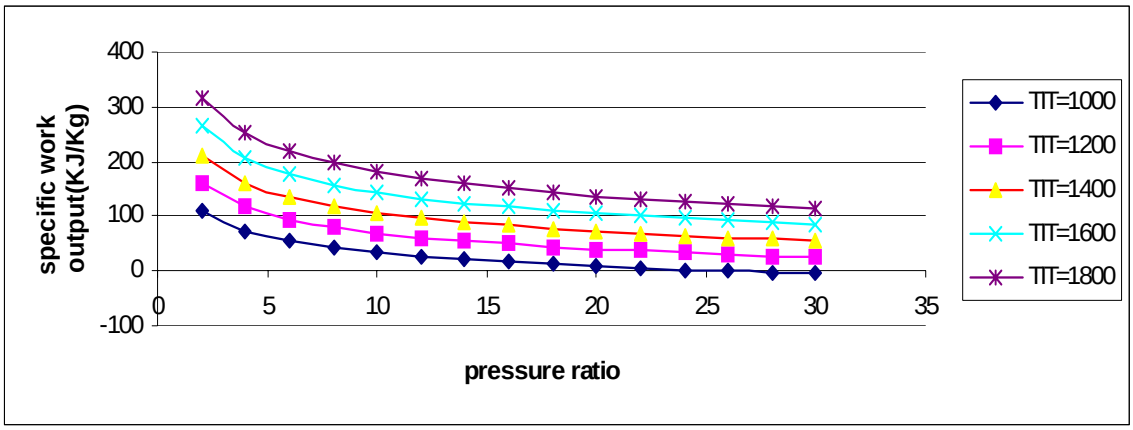

Fig 3.4.6a n=0

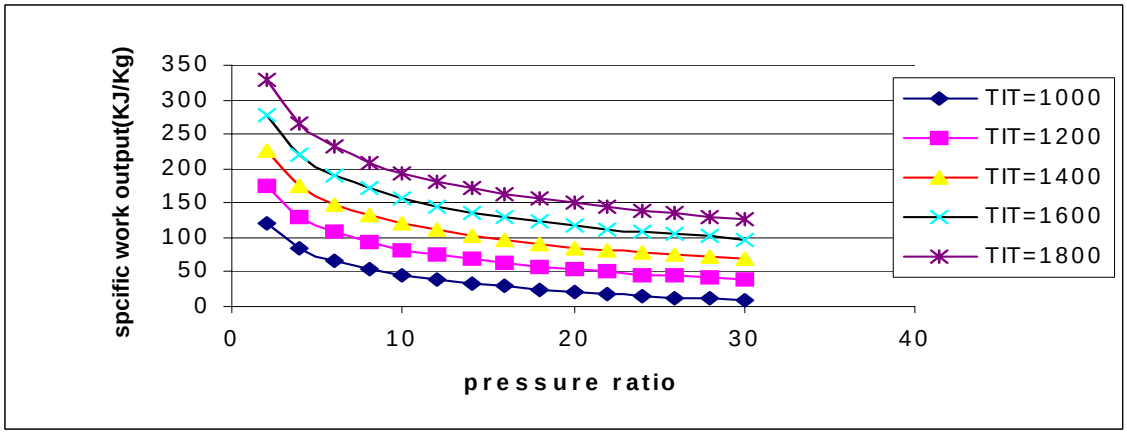

Fig 3.4.6b n=1

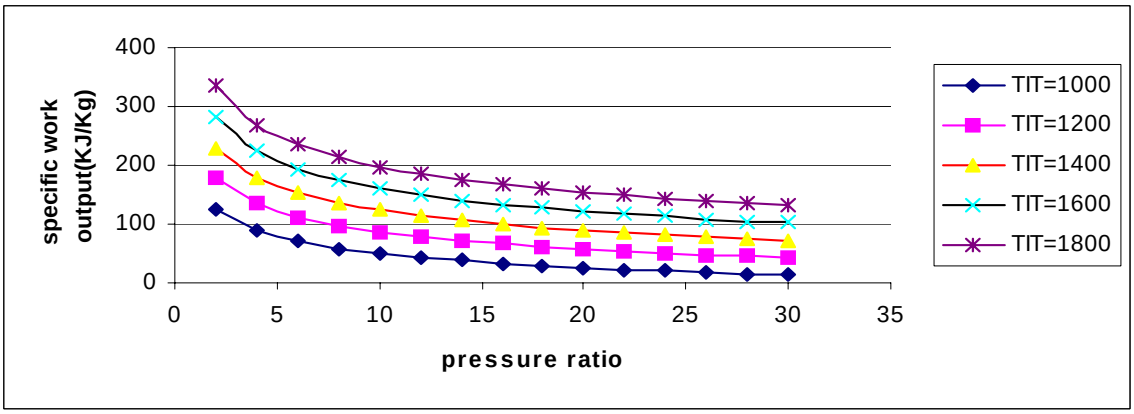

Fig 3.4.6c n=2

Fig 3.4.6 VARIATION OF SPECIFIC OUTPUT OF BOTTOMING CYCLE VS PRESSURE RATIO(γ=1.4)

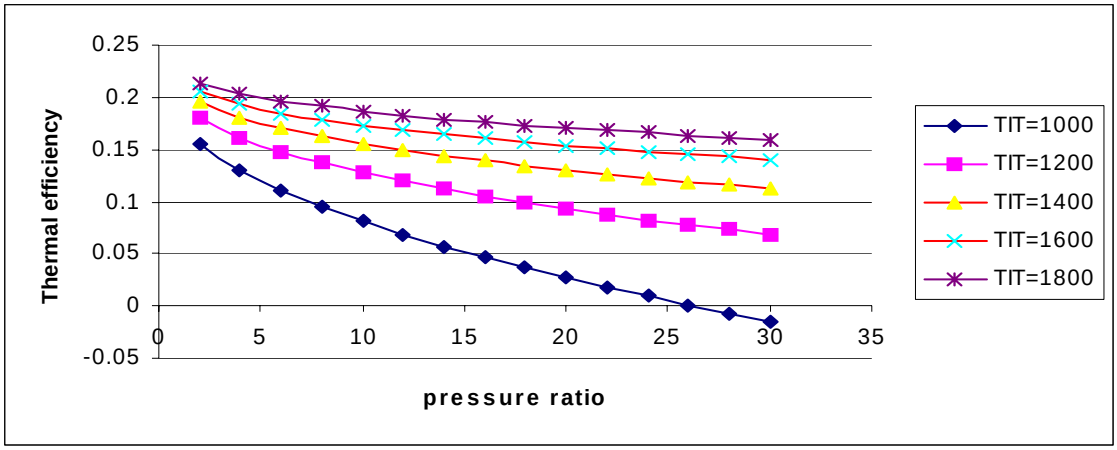

Fig 3.4.7a n=0

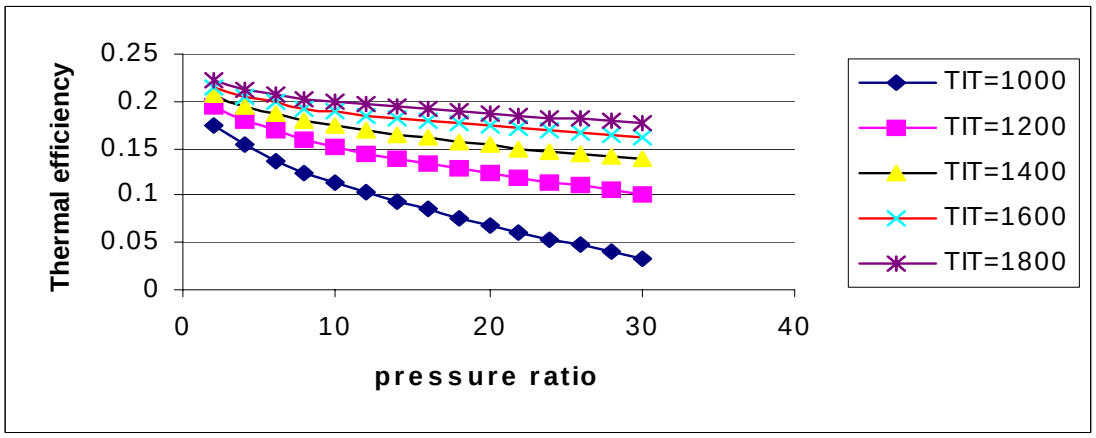

Fig 3.4.7b n=1

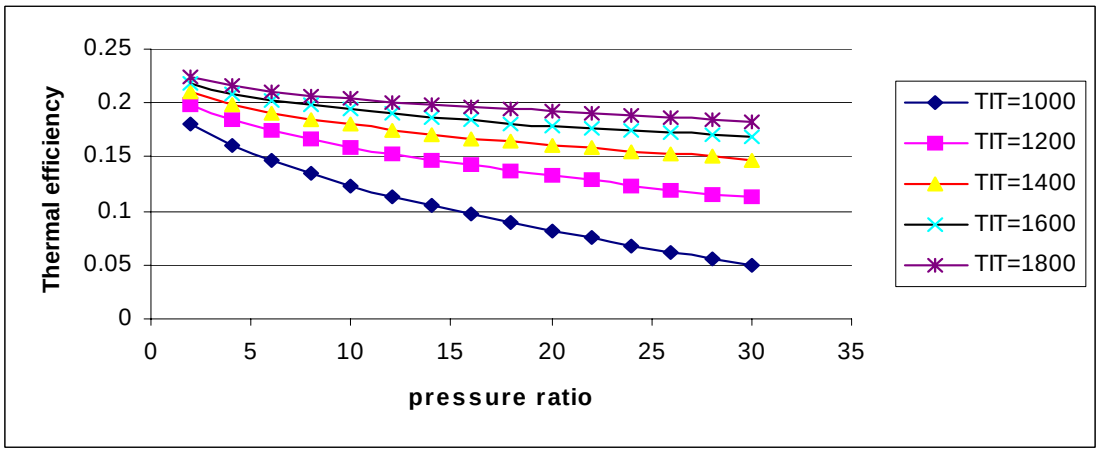

Fig 3.4.7c n=2

Fig 3.4.7 VARIATION OF THERMAL EFFICIENCY BOTTOMING CYCLE VS PRESSURE RATIO(γ=1.4)

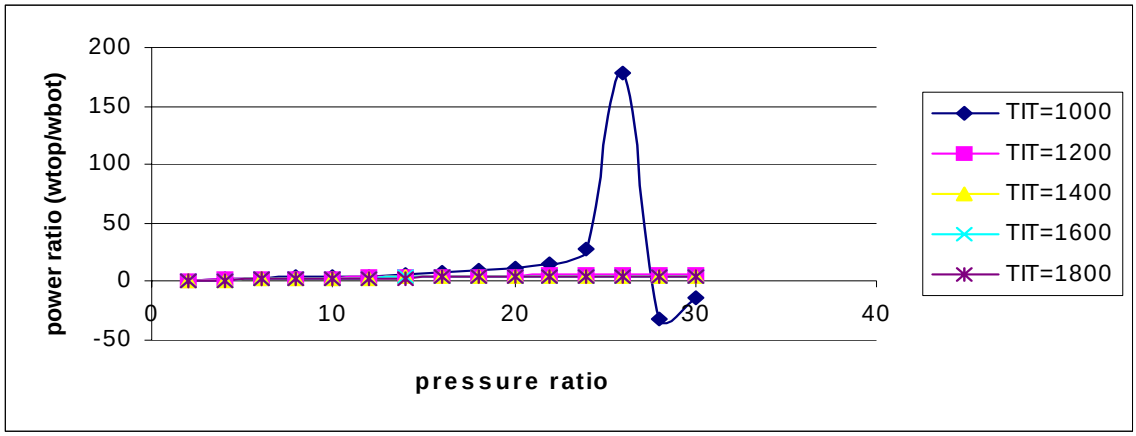

Fig 3.4.8a n=0

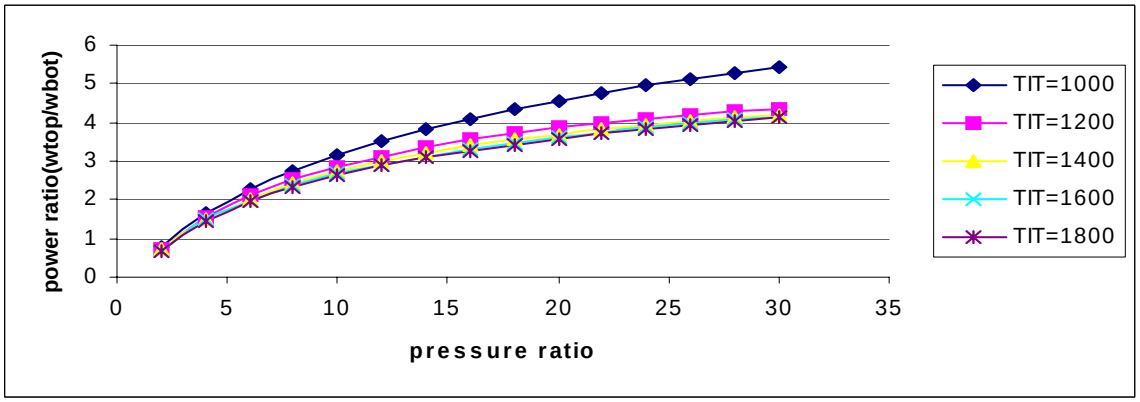

Fig 3.4.8b n=1

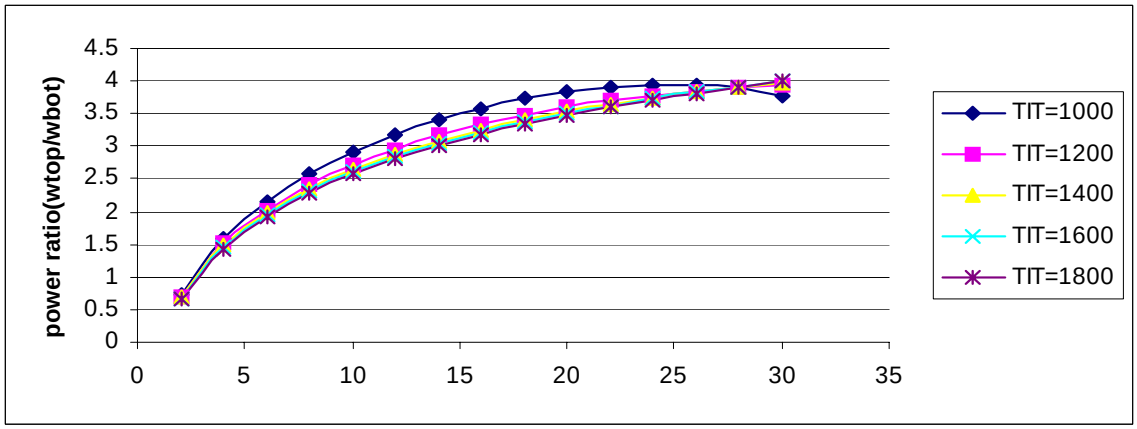

Fig 3.4.8c n=2

Fig 3.4.8 VARIATION OF POWER RATIO OF MIRROR GAS TURBINE VS PRESSURE RATIO(γ=1.4)

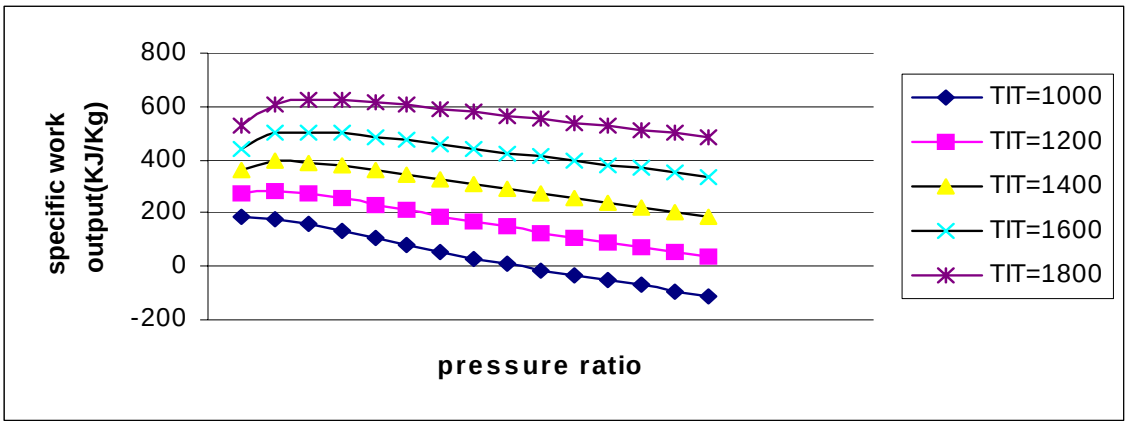

Fig 3.5.1a n=0

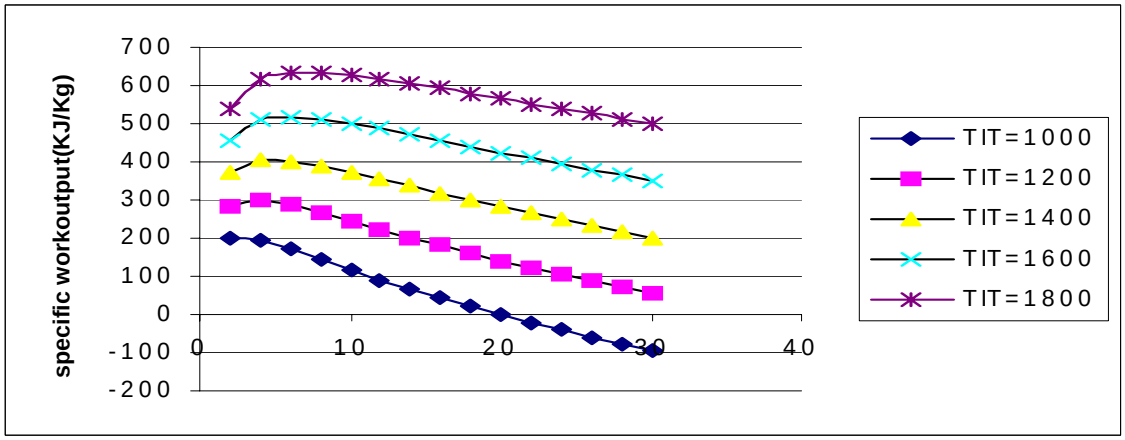

Fig 3.5.1b n=1

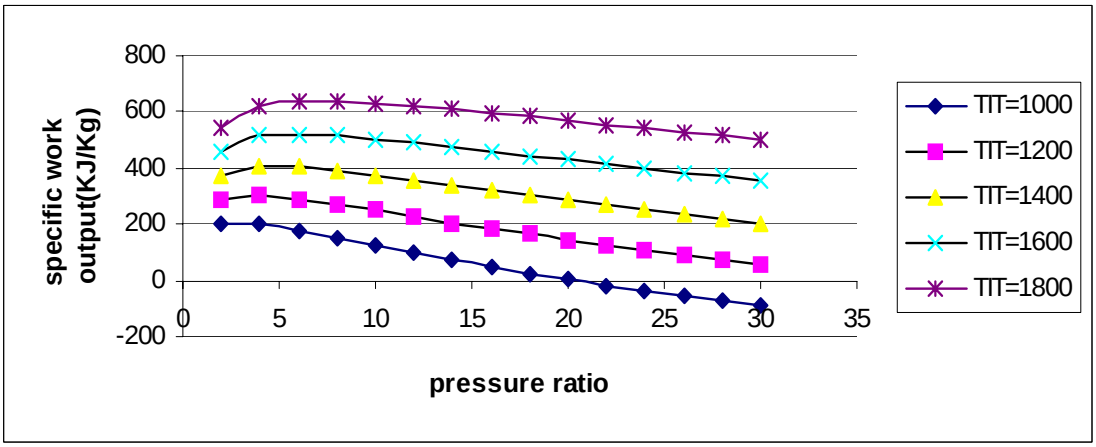

Fig 3.5.1c n=2

Fig 3.5.1 VARIATION OF SPECIFIC OUTPUT OF MIRROR GAS TURBINE VS PRESSURE RATIO(γ=1.5)

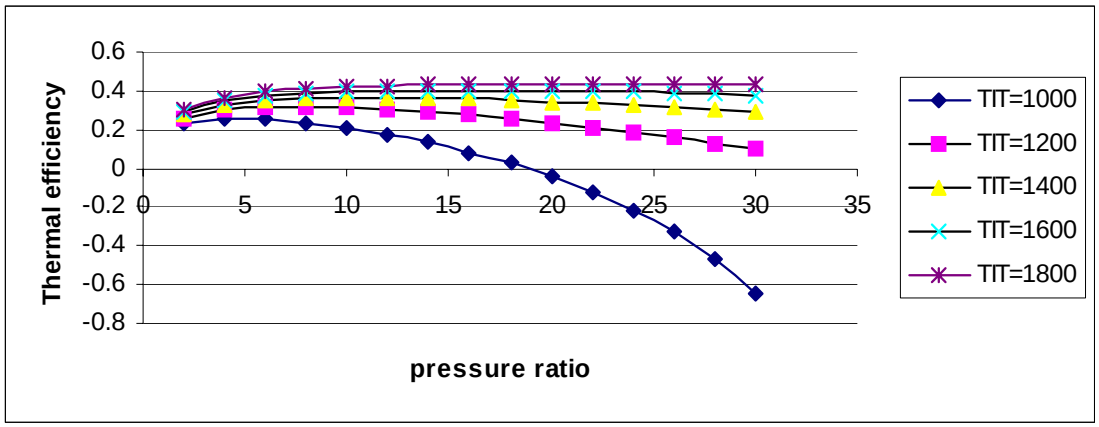

Fig 3.5.2a n=0

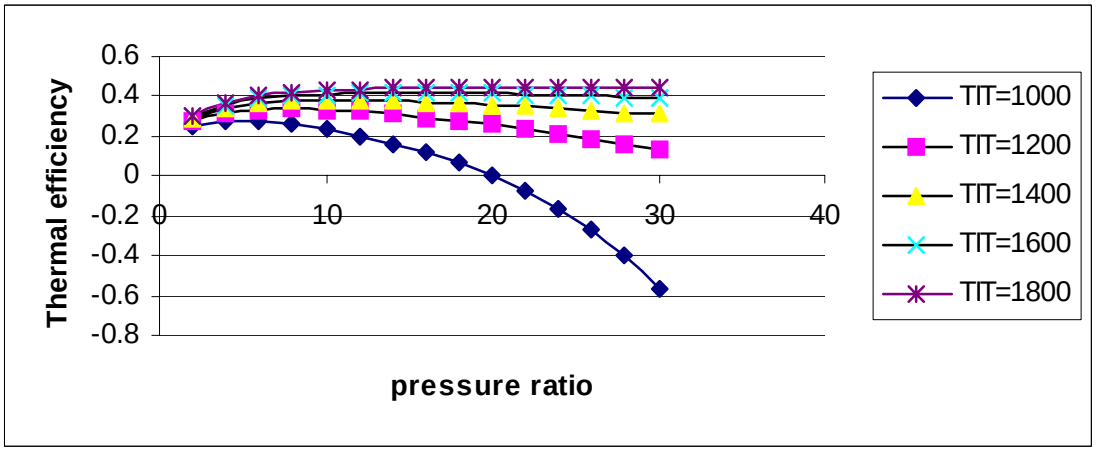

Fig 3.5.2b n=1

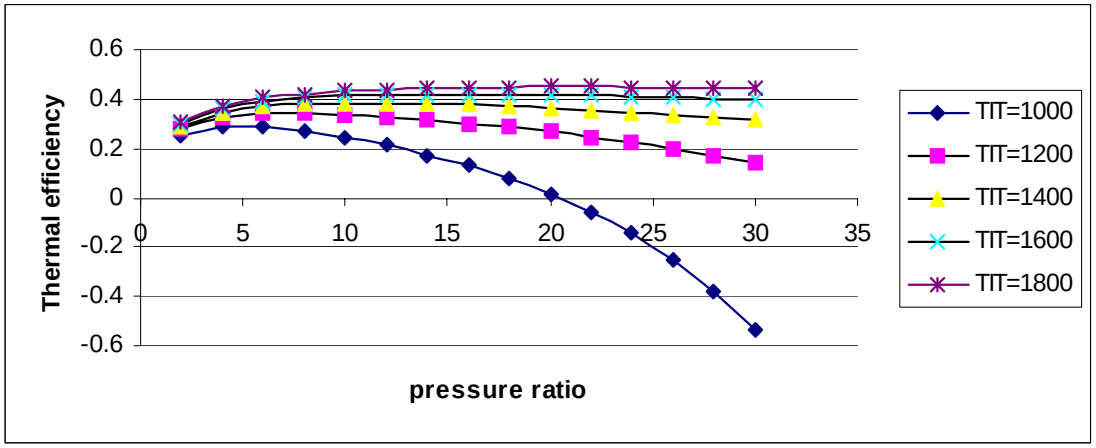

Fig 3.5.2c n=2

Fig 3.5.2 VARIATION OF THERMAL EFFICIENCY OF MIRROR GAS TURBINE VS PRESSURE RATIO (γ=1.5)

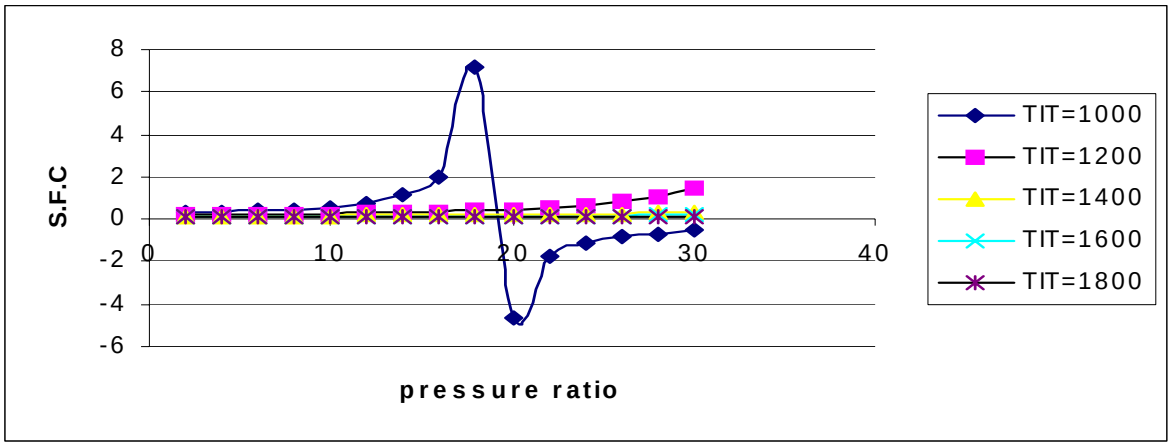

Fig 3.5.3a n=0

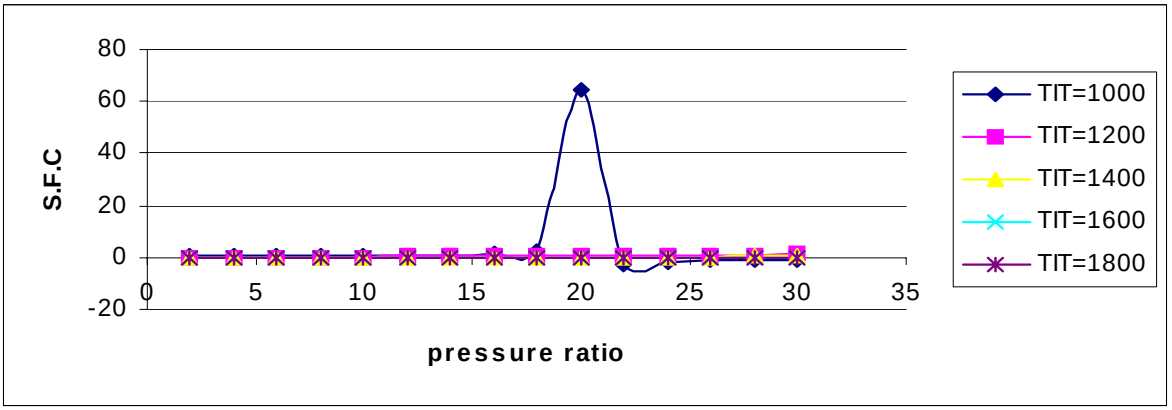

Fig 3.5.3b n=1

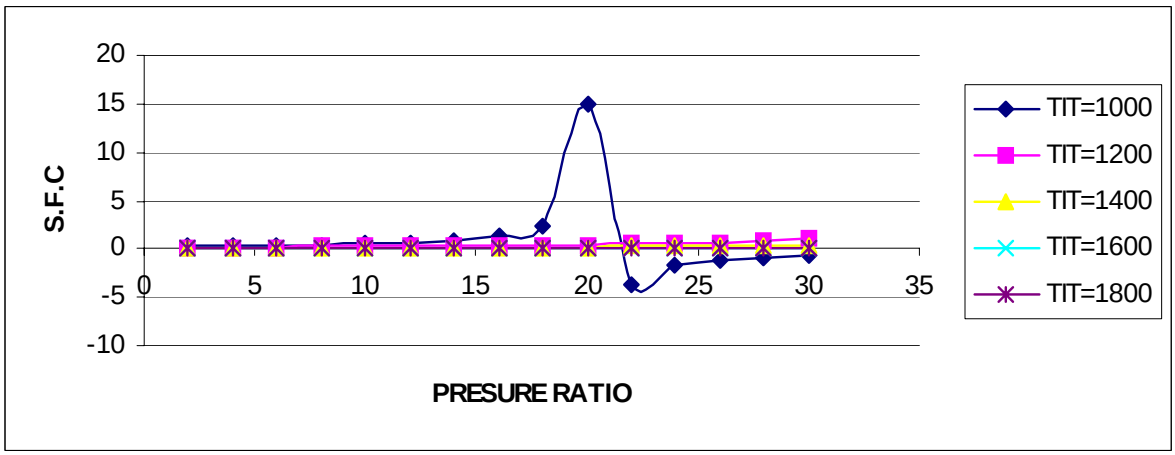

Fig 3.5.3 n=2

Fig.5.3 VARIATION OF S.F.C. OF MIRROR GAS TURBINE VS PRESSURE RATIO(γ=1.5)

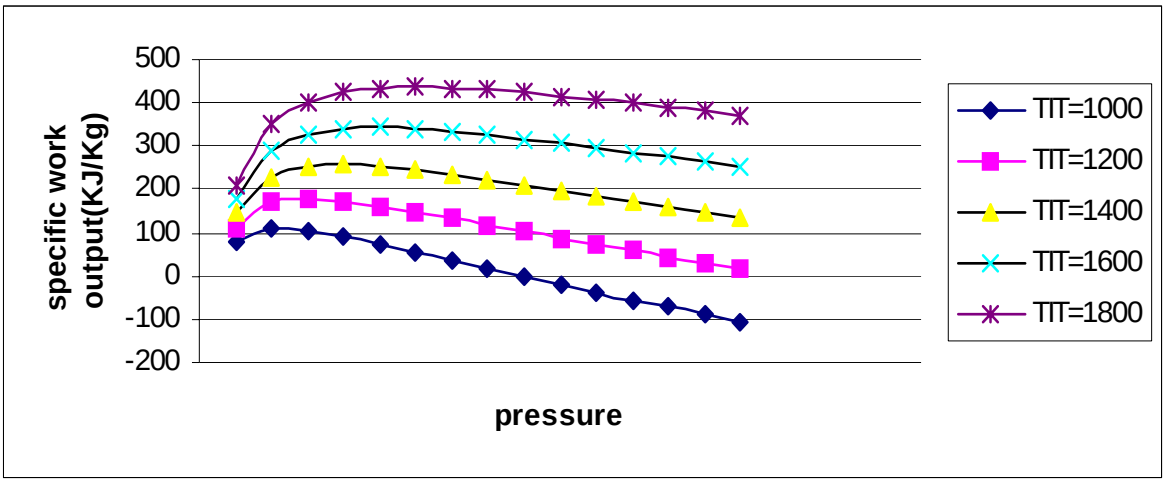

n=0,1,2

Fig 3.5.4 VARIATION OF SPECIFIC OUTPUT OF TOPPING CYCLE VS PRESSURE RATIO(γ=1.5)

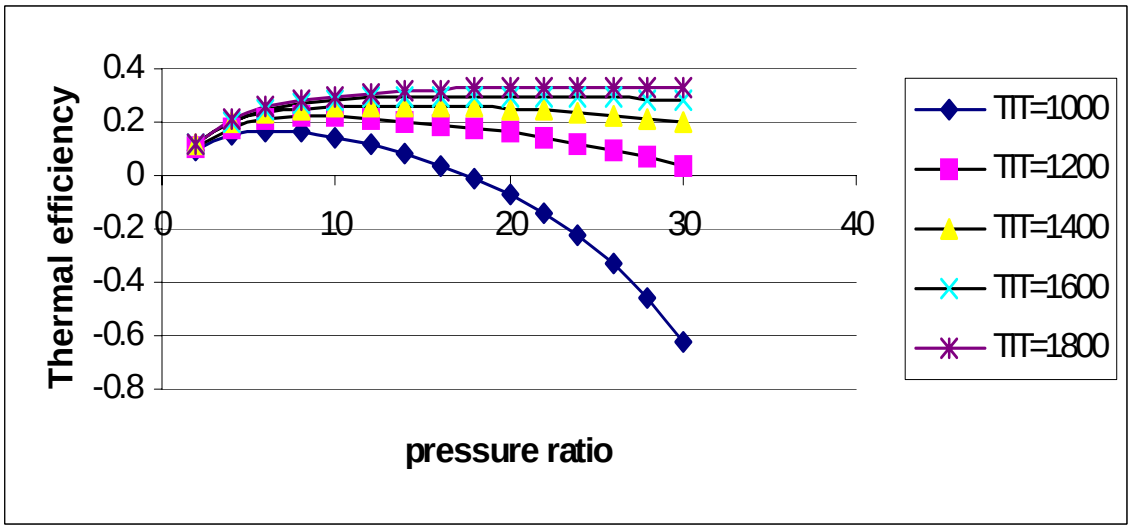

n=0,1,2

Fig 3.5.5 VARIATION OF THERMAL EFFICIENCY OF TOPPING CYCLE VS PRESSURE RATIO(γ=1.5)

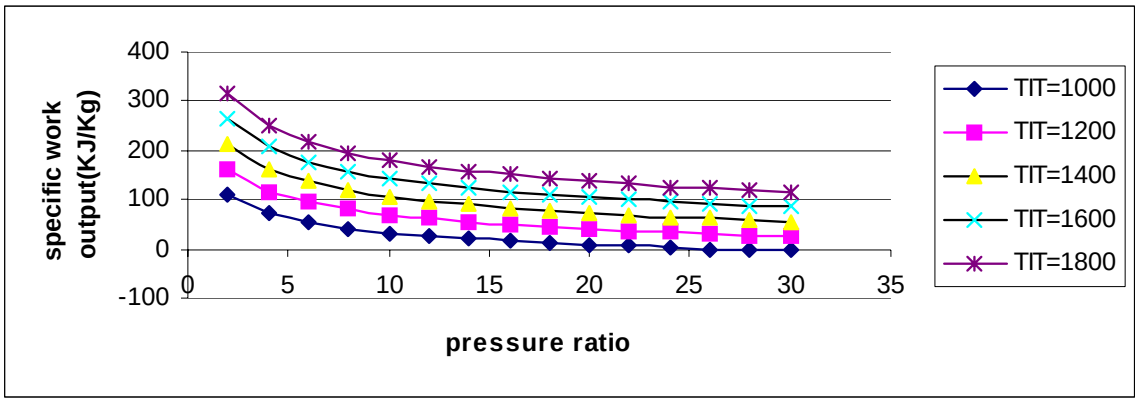

Fig 3.5.6a n=0

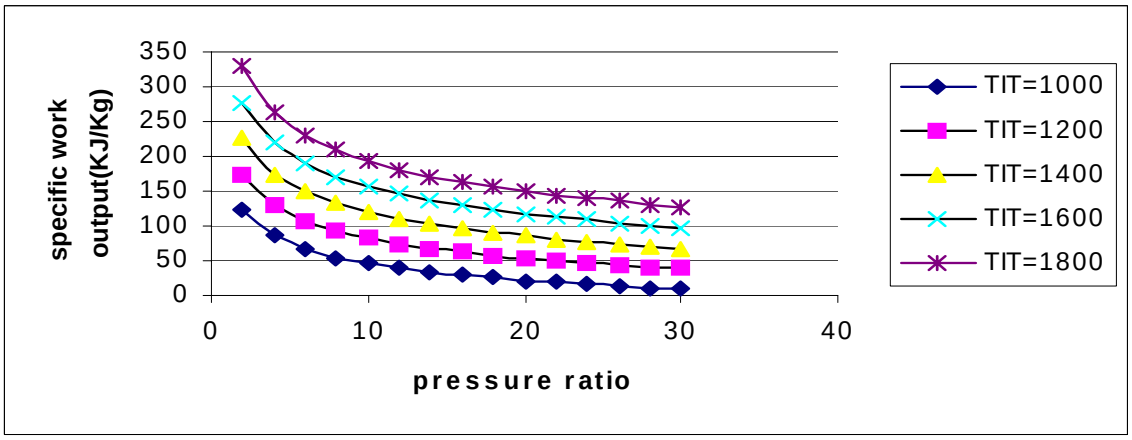

Fig 3.5.6b n=1

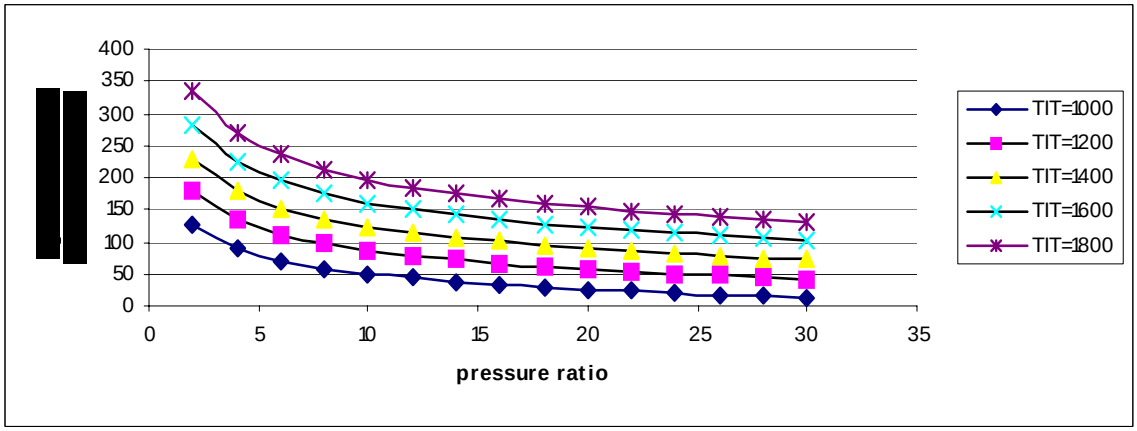

Fig 3.5.6c n=2

Fig 3.5.6 VARIATION OF SPECIFIC OUTPUT OF BOTTOMING CYCLE VS PRESSURE RATIO(γ=1.5)

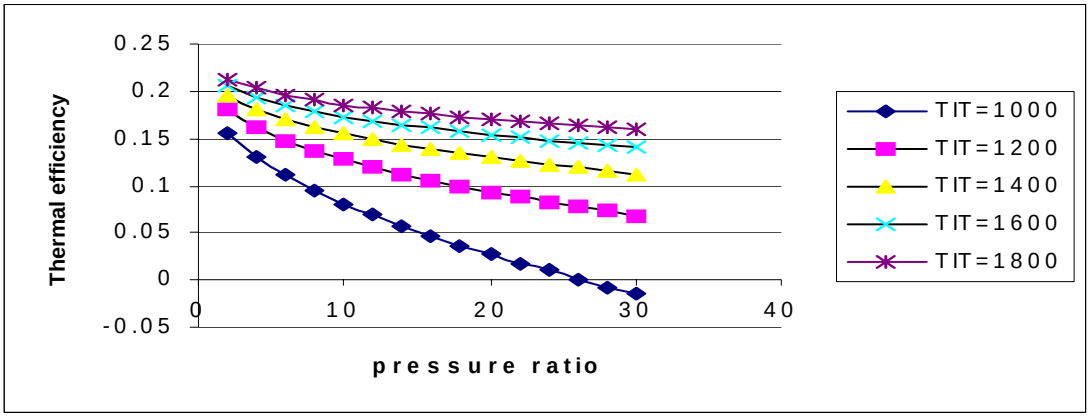

Fig 3.5.7a n=0

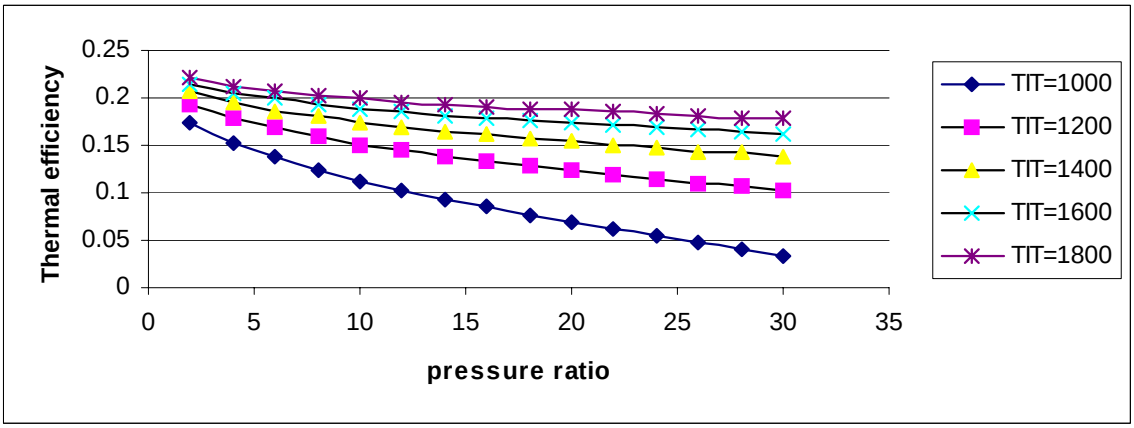

Fig 3.5.7b n=1

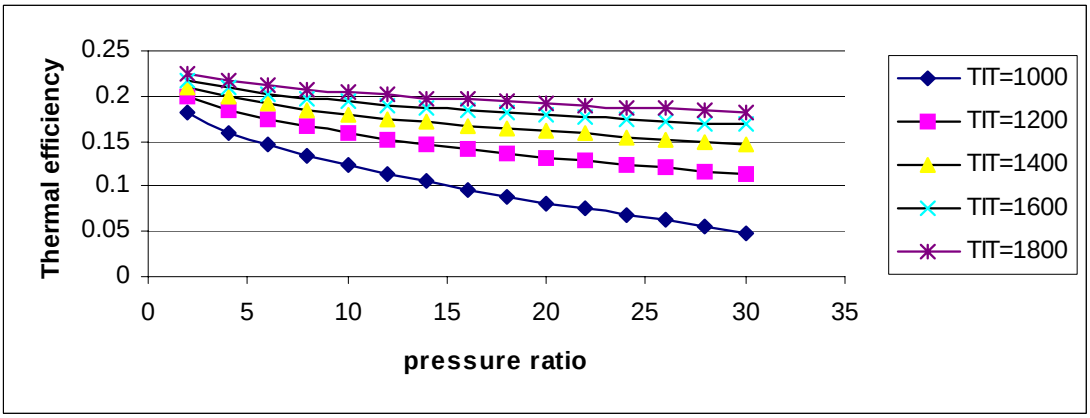

Fig 3.5.7c n=2

Fig 3.5.7 VARIATION OF THERMAL EFFICIENCY BOTTOMING CYCLE VS PRESSURE RATIO(γ=1.5)

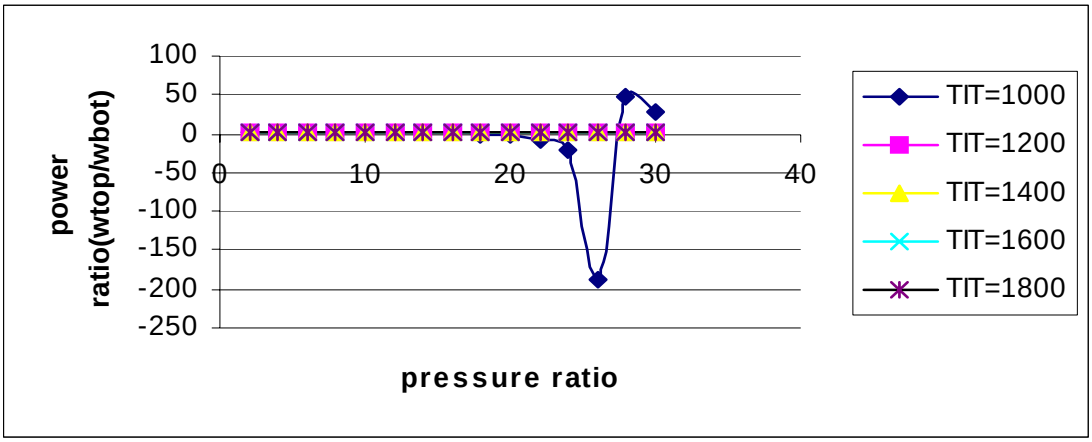

Fig 3.5.8a n=0

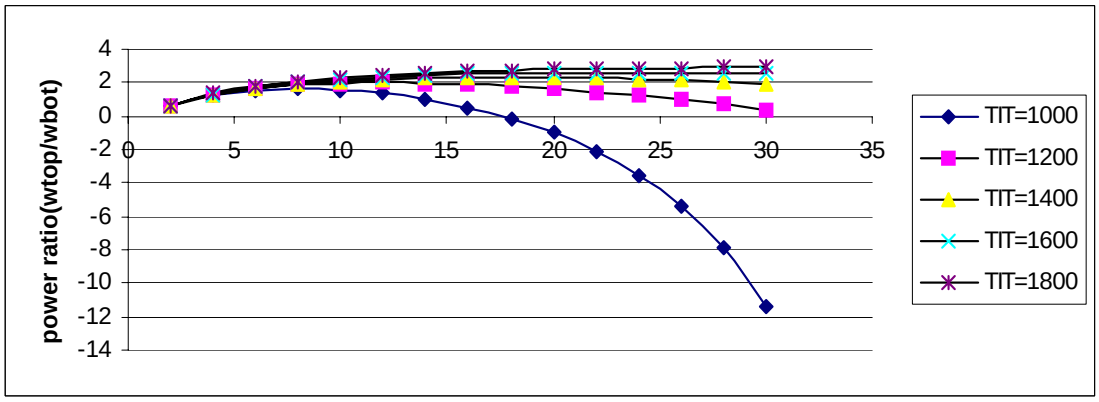

Fig 3.5.8b n=1

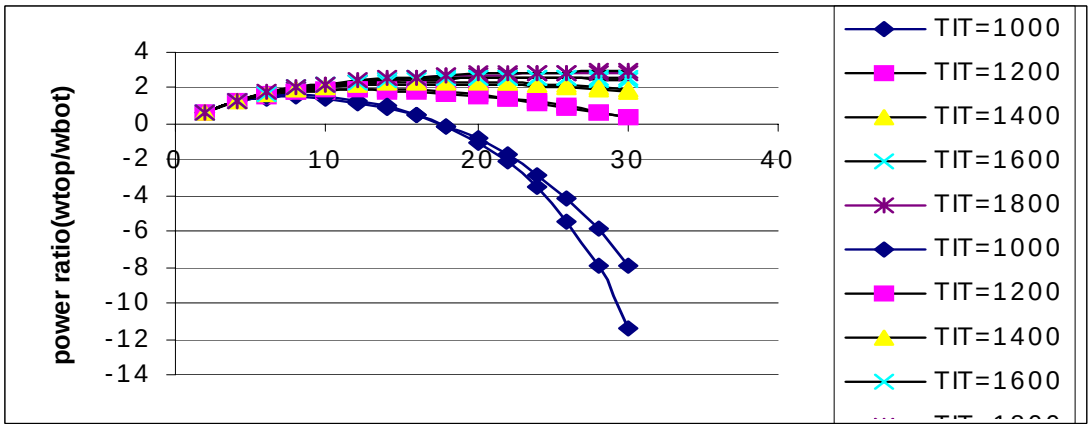

Fig 3.5.8c n=2

Fig 3.5.8 VARIATION OF POWER RATIO OF MIRROR GAS TURBINE VS PRESSURE RATIO(γ=1.5)

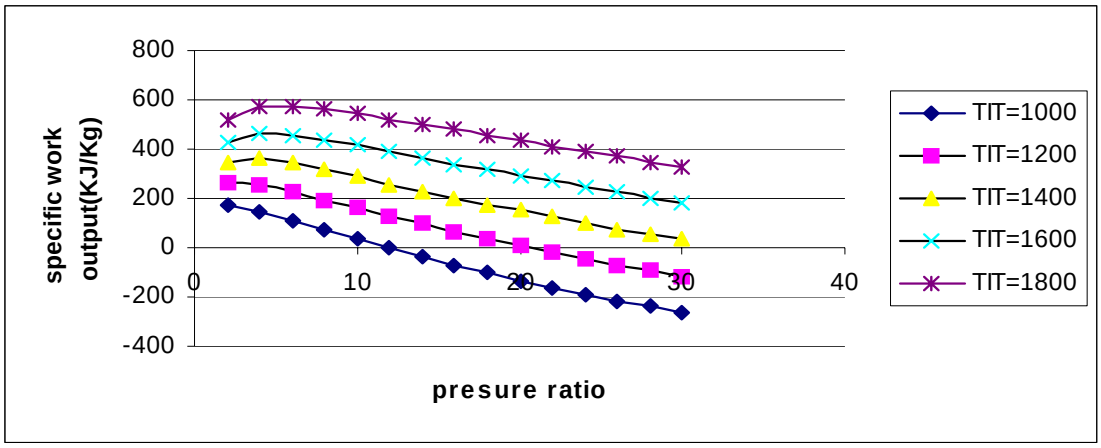

Fig 3.6.1a n=0

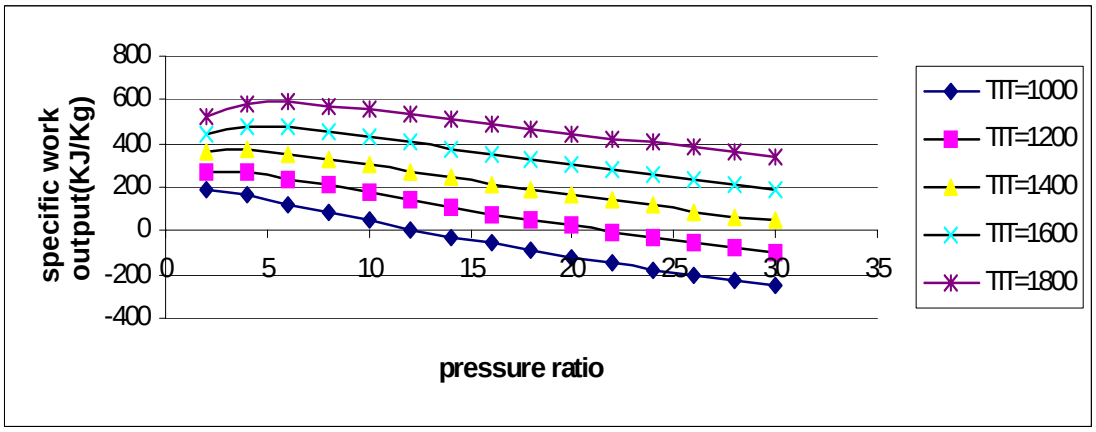

Fig 3.6.1b n=1

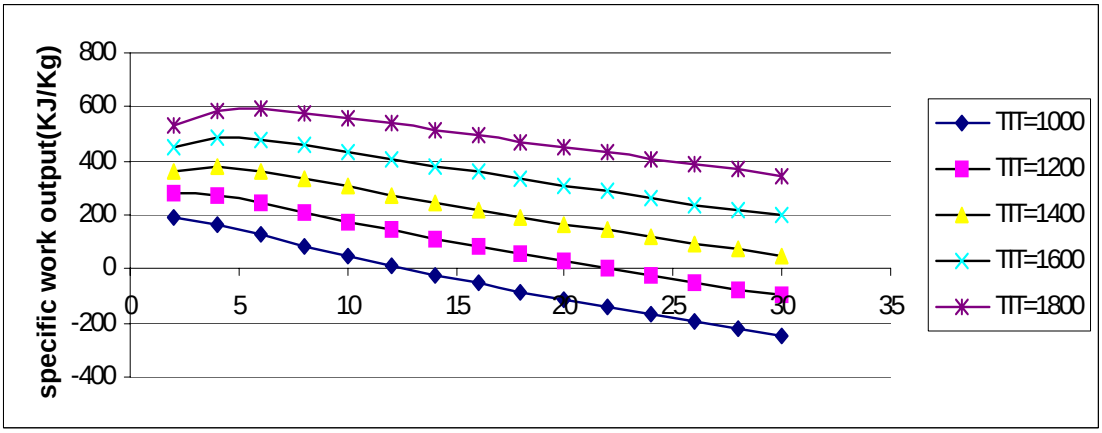

Fig 3.6.1c n=2

Fig 3.6.1 VARIATION OF SPECIFIC OUTPUT OF MIRROR GAS TURBINE VS PRESSURE RATIO(γ=1.6)

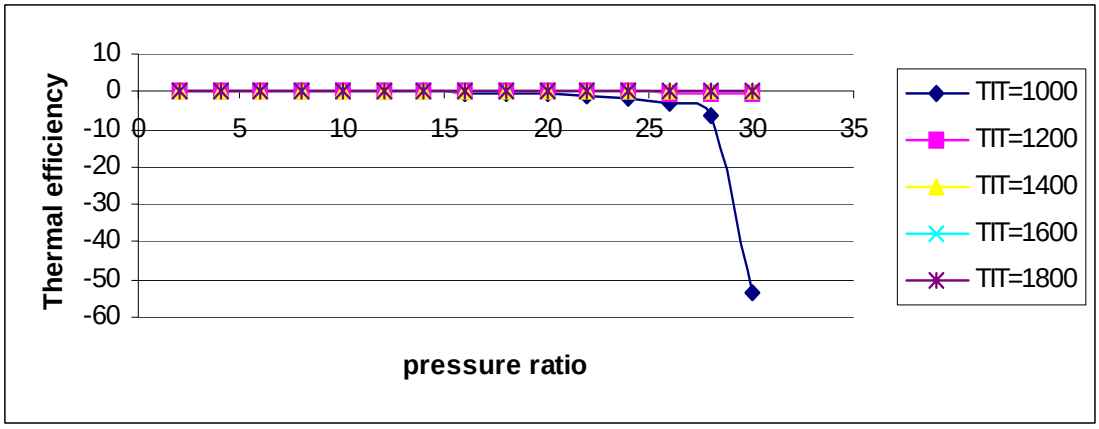

Fig 3.6.2a n=0

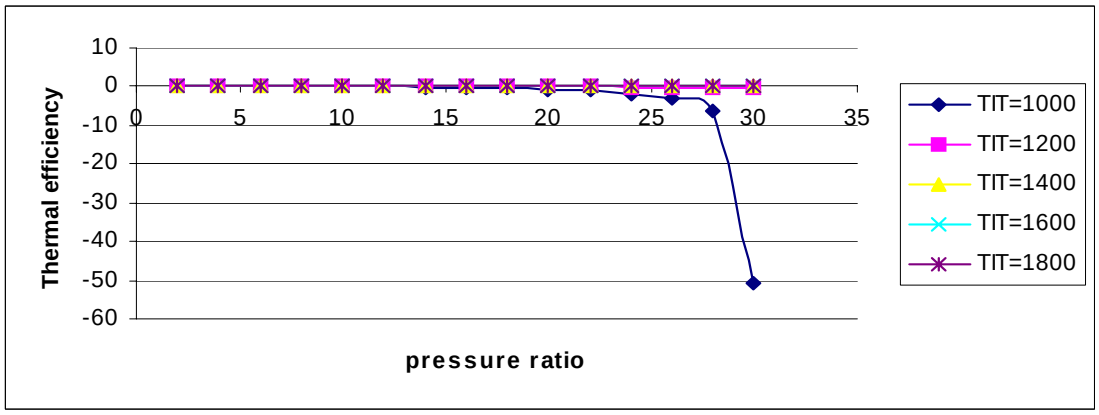

Fig 3.6.2b n=1

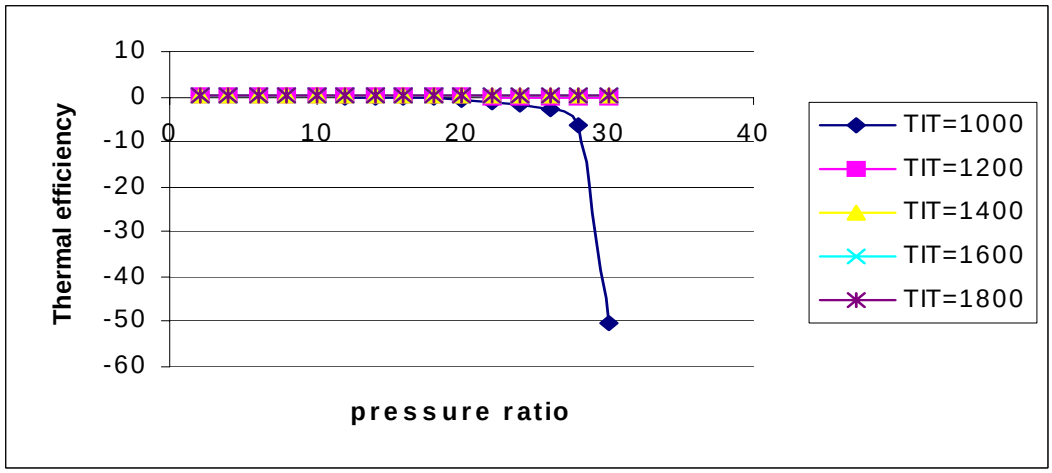

Fig 3.6.2c n=2

Fig 3.6.2 VARIATION OF THERMAL EFFICIENCY OF MIRROR GAS TURBINE VS PRESSURE RATIO(γ=1.6)

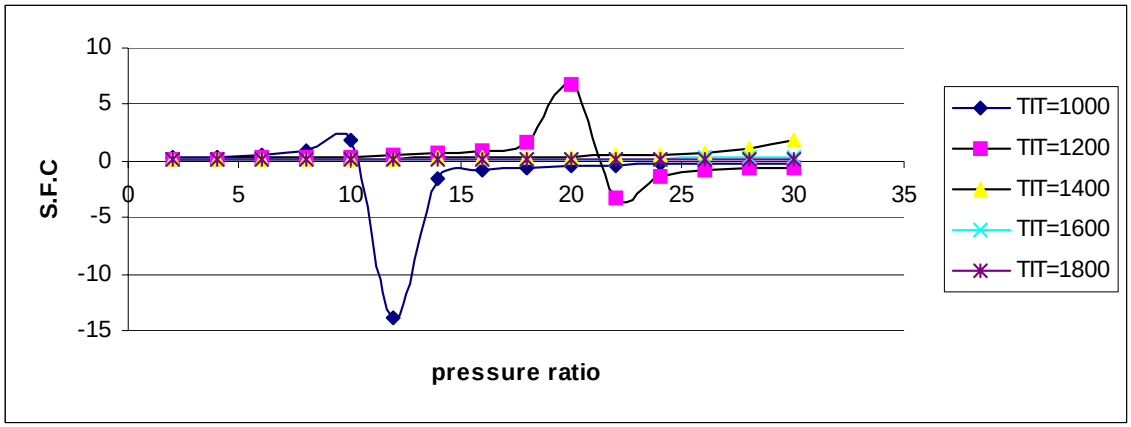

Fig 3.6.3a n=0

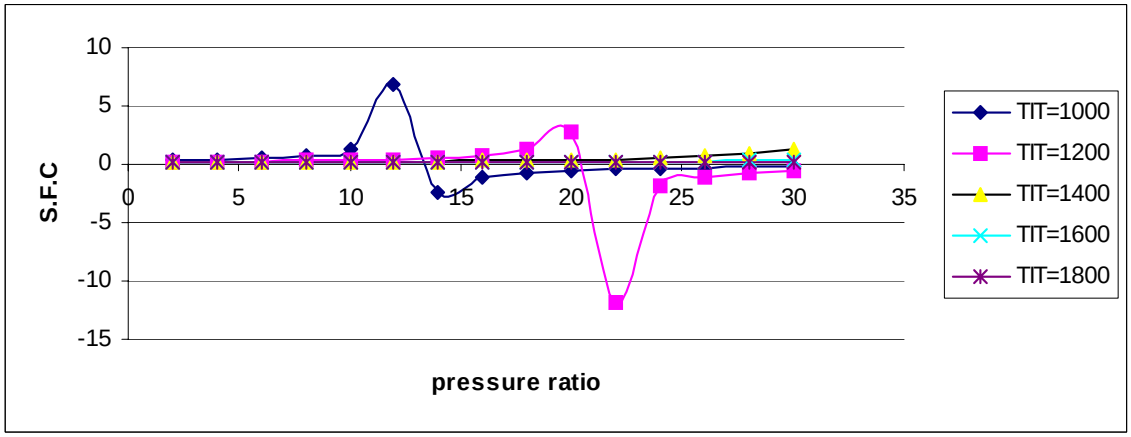

Fig 3.6.3b n=1

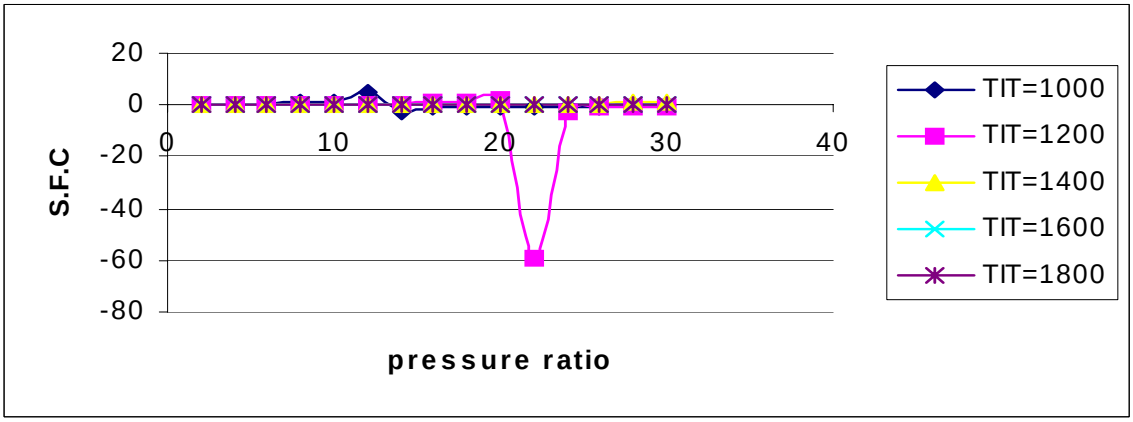

Fig 3.6.3c n=2

Fig 3.6.3 VARIATION OF S.F.C. OF MIRROR GAS TURBINE VS PRESSURE RATIO(γ=1.6)

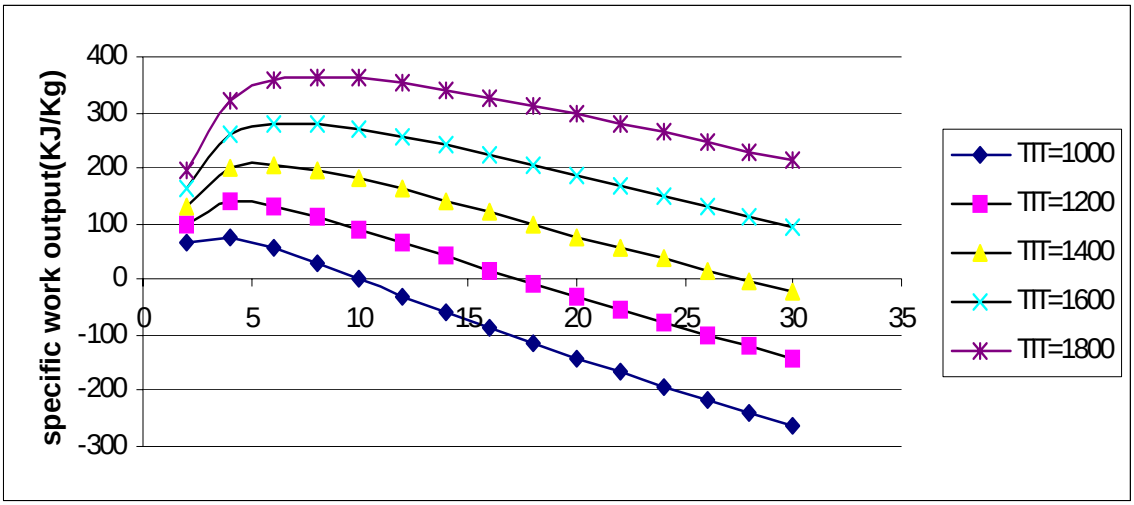

n=0,1,2

Fig 3.6.4 VARIATION OF SPECIFIC OUTPUT OF TOPPING CYCLE VS PRESSURE RATIO(γ=1.6)

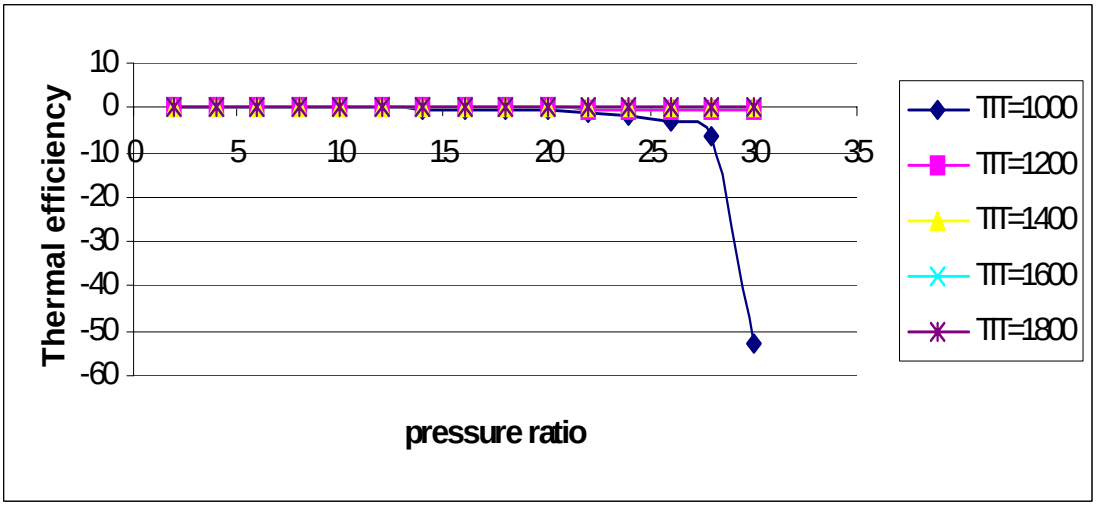

n=0,1,2

Fig 3.6.5 VARIATION OF THERMAL EFFICIENCY OF TOPPING CYCLE VS PRESSURE RATIO(γ=1.6)

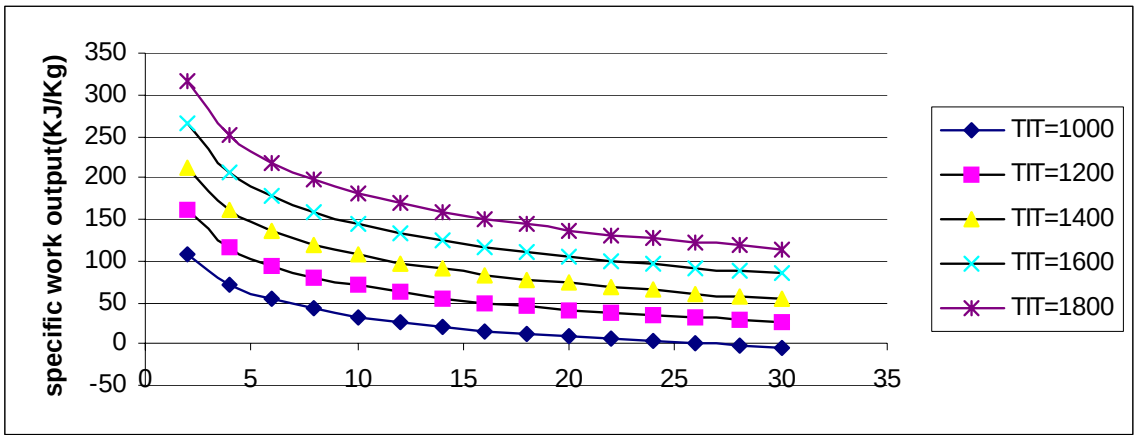

Fig 3.6.6a n=0

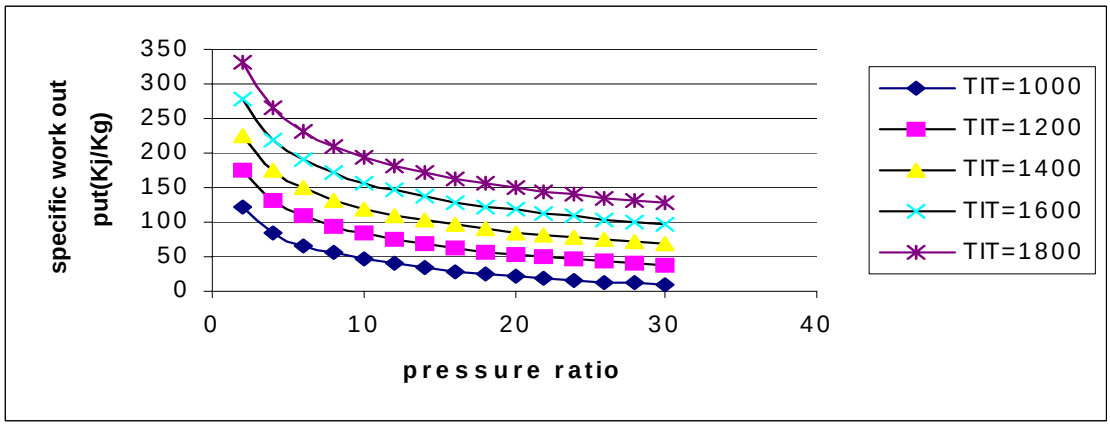

Fig 3.6.6b n=1

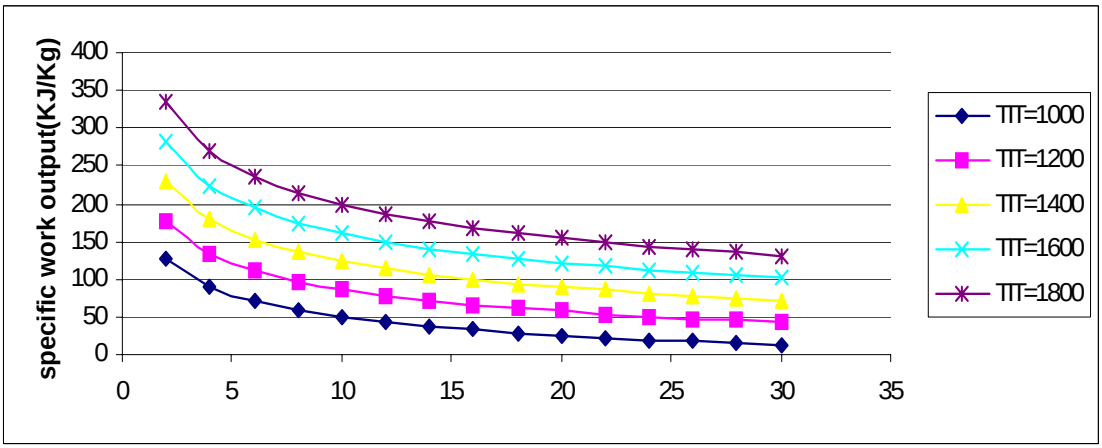

Fig 3.6.6c n=2

Fig 3.6.6 VARIATION OF SPECIFIC OUTPUT OF BOTTOMING CYCLE VS PRESSURE RATIO(γ=1.6)

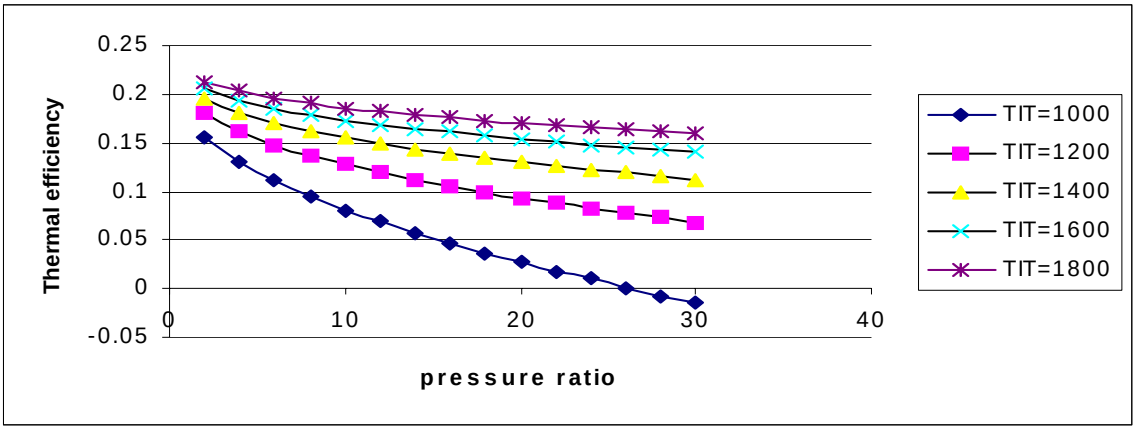

Fig 3.6.7a n=0

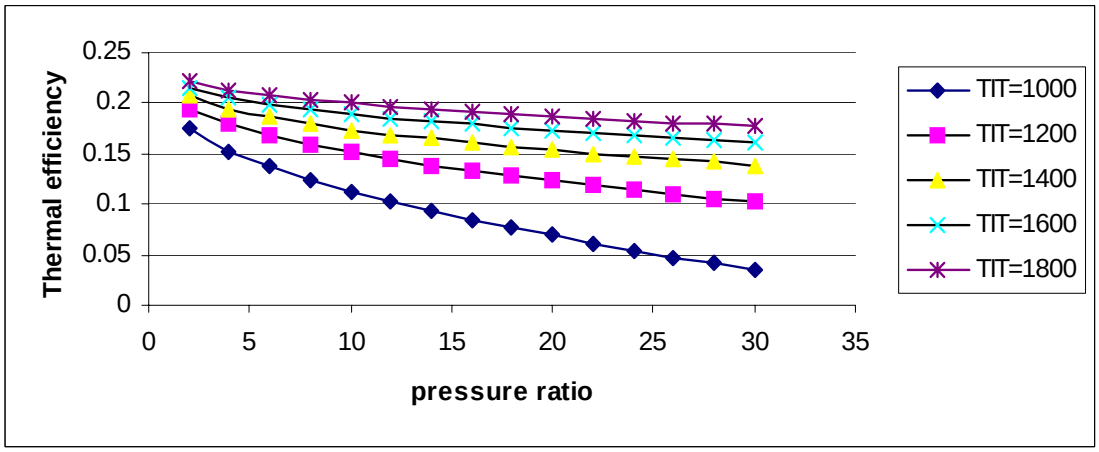

Fig 3.6.7b n=1

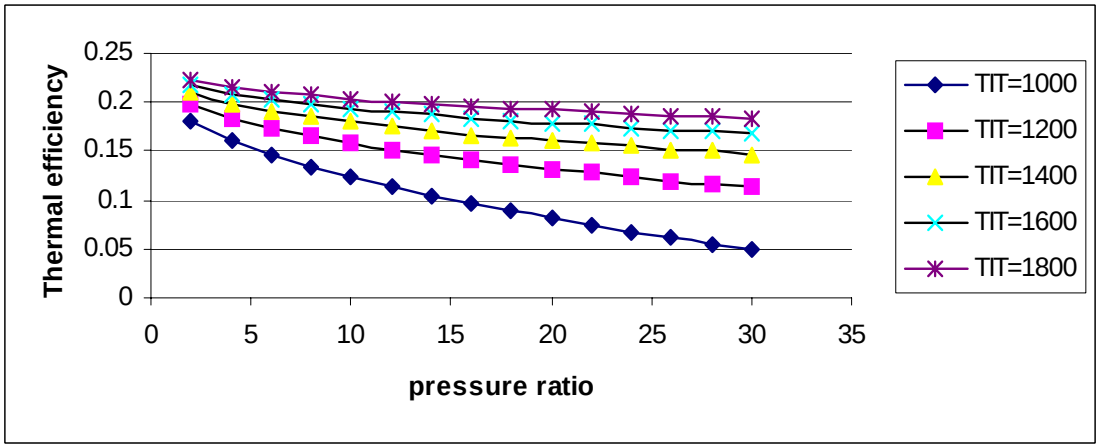

Fig 3.6.7c n=2

Fig 3.6.7 VARIATION OF THERMAL EFFICIENCY BOTTOMING CYCLE VS PRESSURE RATIO(γ=1.6)

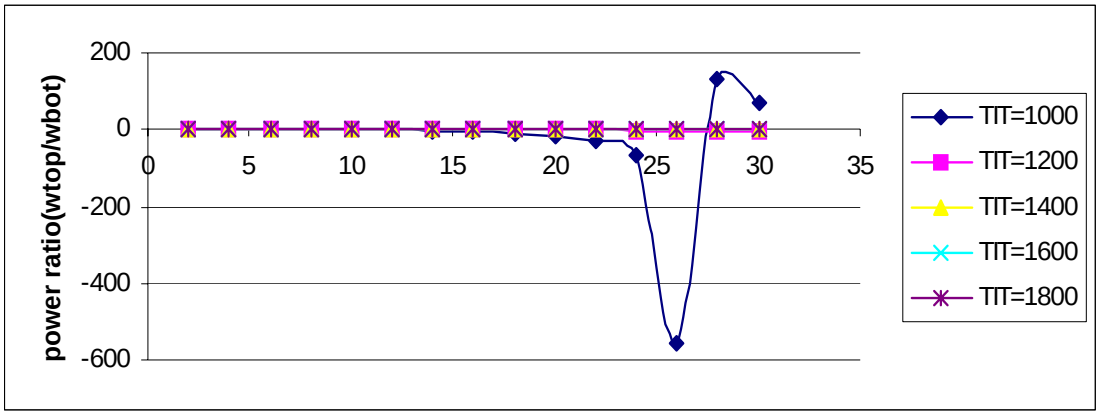

Fig 3.6.8a n=0

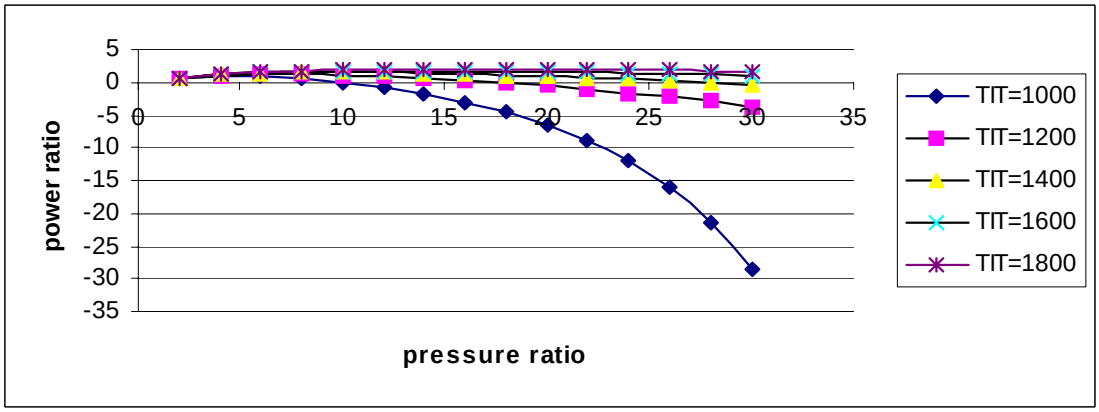

Fig 3.6.8b n=1

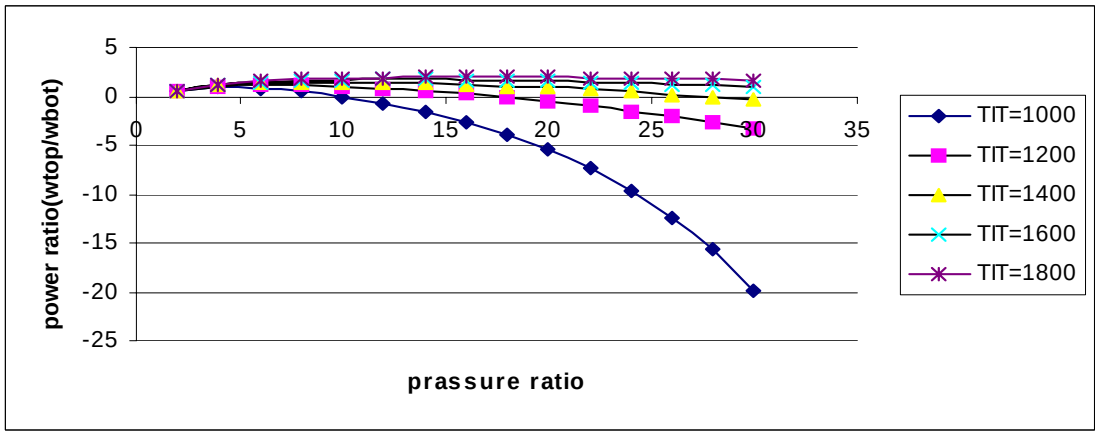

Fig 3.6.8c n=2

Fig 3.6.8 VARIATION OF POWER RATIO OF MIRROR GAS TURBINE VS PRESSURE RATIO(γ=1.6)

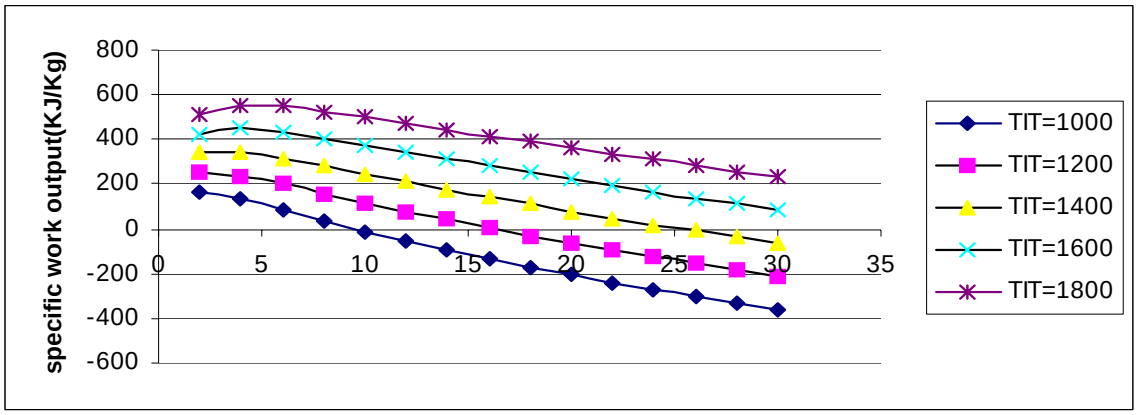

Fig 3.7.1a n=0

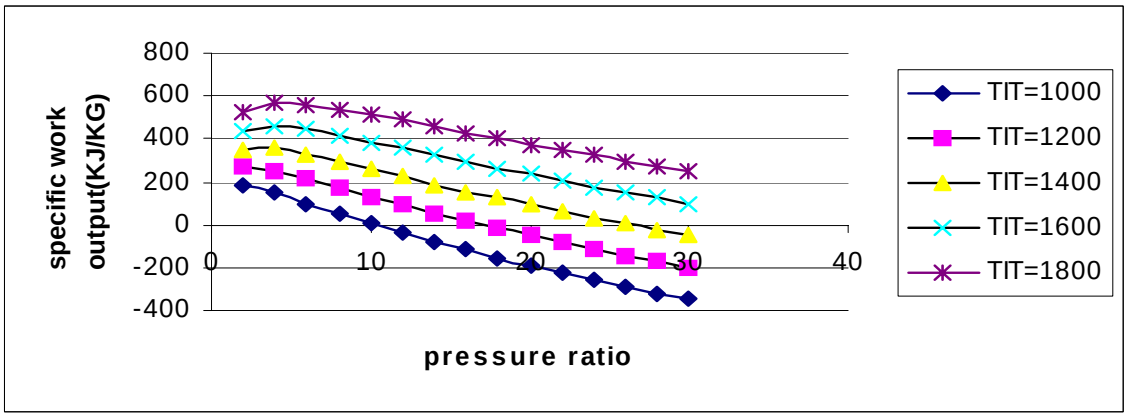

Fig 3.7.1b n=1

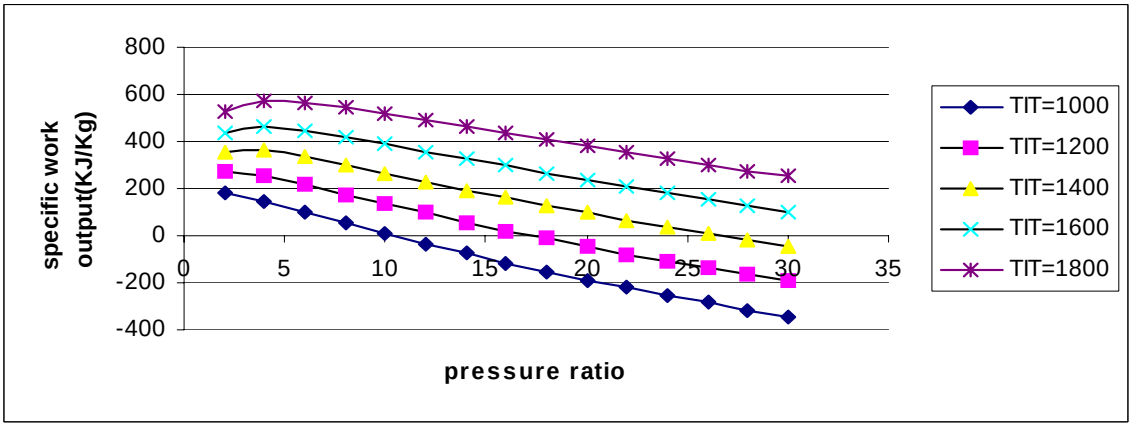

Fig 3.7.1c n=2

Fig 3.7.1 VARIATION OF SPECIFIC OUTPUT OF MIRROR GAS TURBINE VS PRESSURE RATIO(γ=1.66)

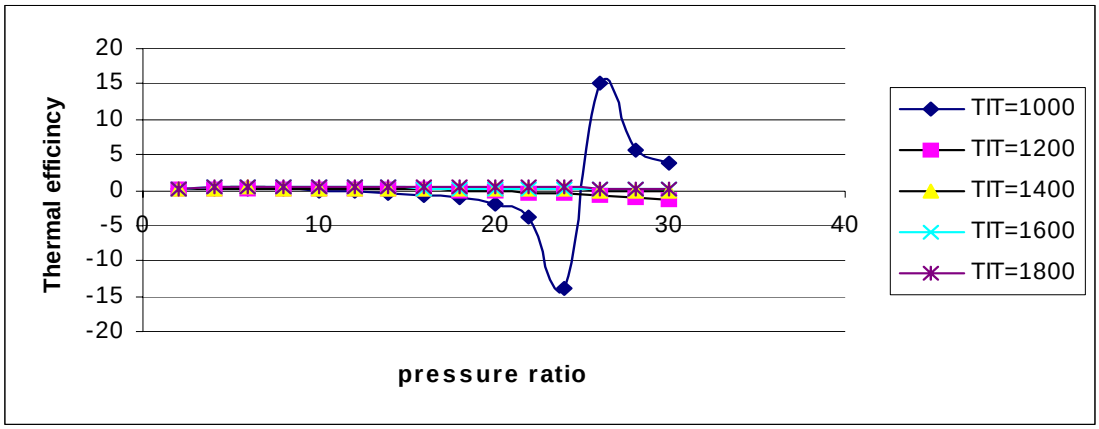

Fig 3.7.2a n=0

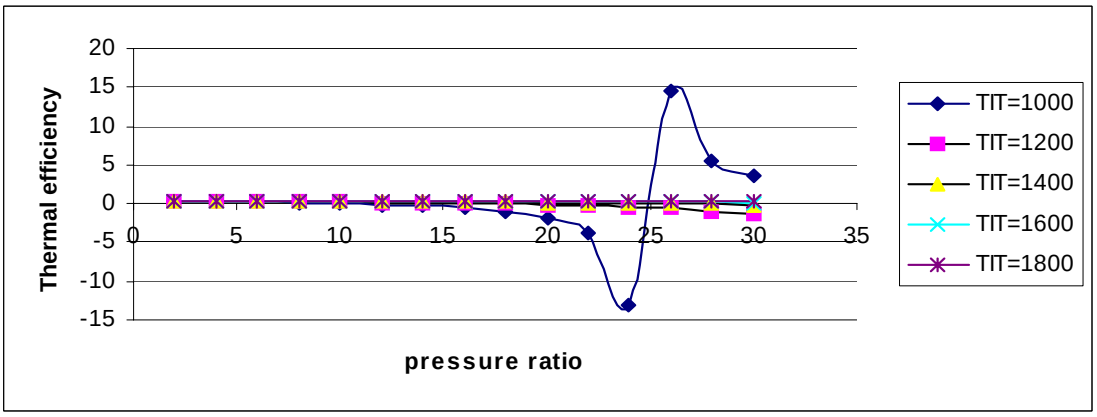

Fig 3.7.2b n=1

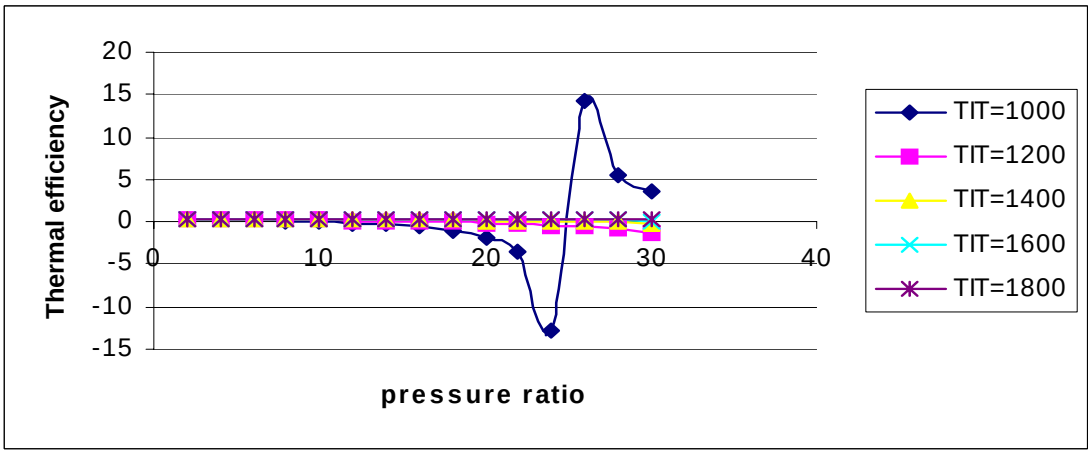

Fig 3.7.2c n=2

Fig 3.7.2 VARIATION OF THERMAL EFFICIENCY OF MIRROR GAS TURBINE VS PRESSURE RATIO(γ=1.66)

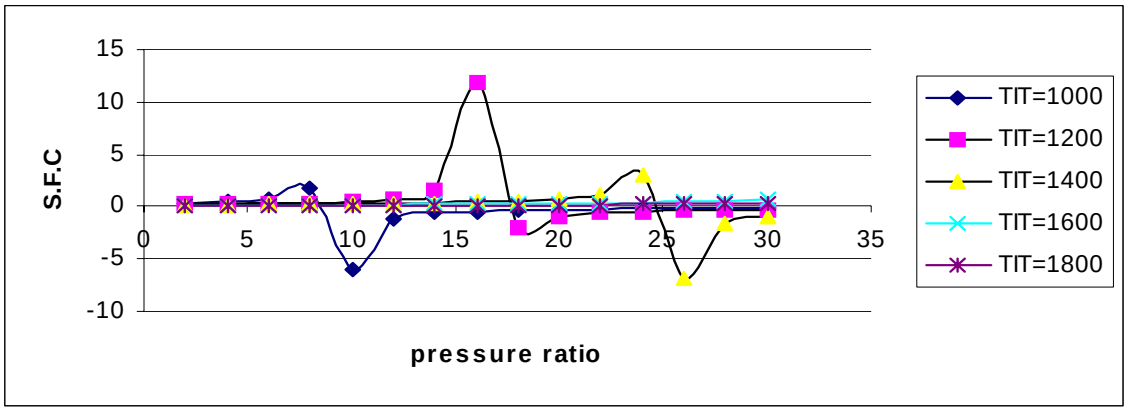

Fig 3.7.3a n=0

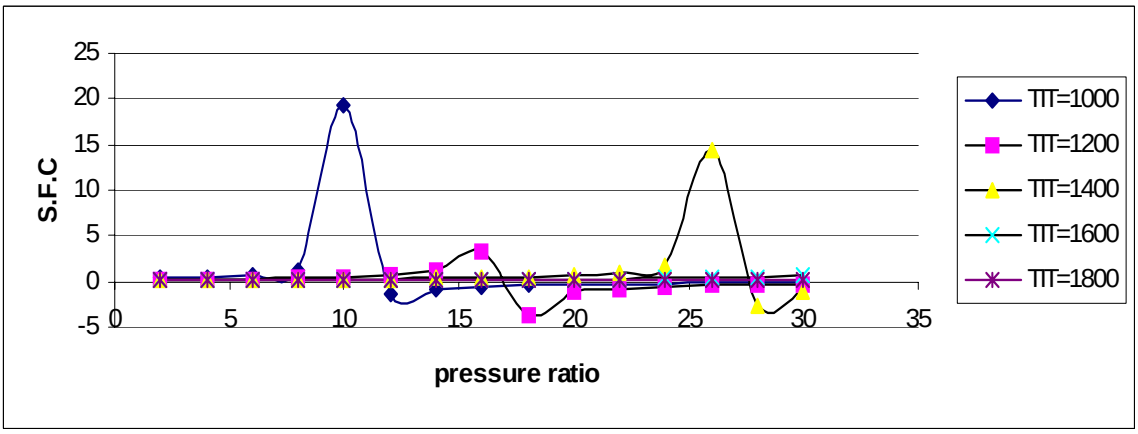

Fig 3.7.3b n=1

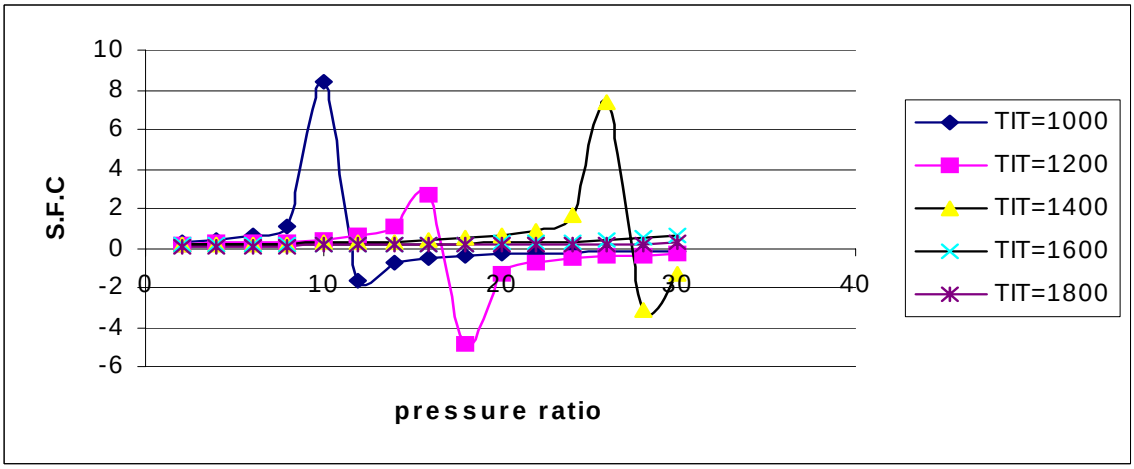

Fig 3.7.3c n=2

Fig 3.7.3 VARIATION OF S.F.C. OF MIRROR GAS TURBINE VS PRESSURE RATIO(γ=1.66)

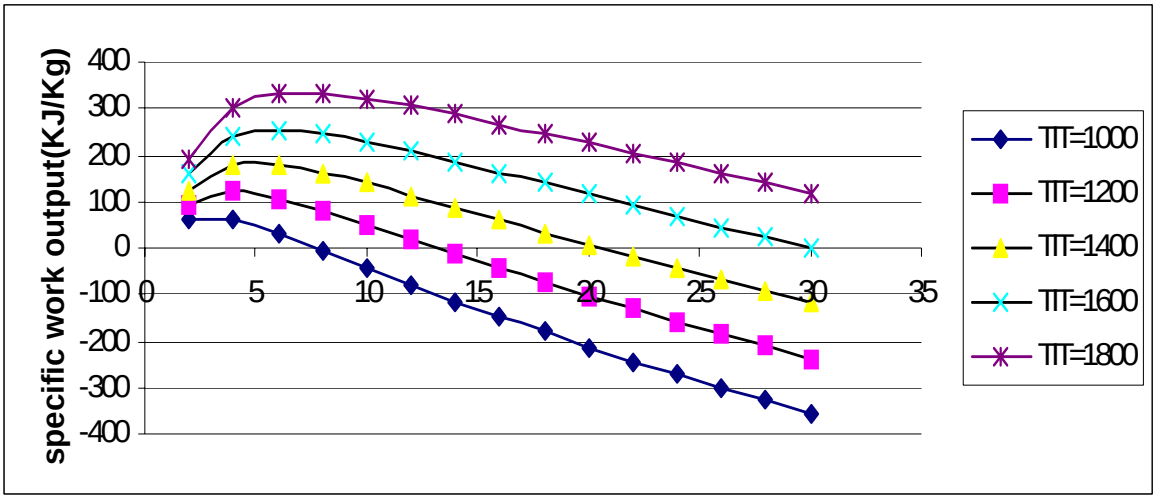

n=0,1,2

Fig 3.7.4 VARIATION OF SPECIFIC OUTPUT OF TOPPING CYCLE VS PRESSURE RATIO(γ=1.66)

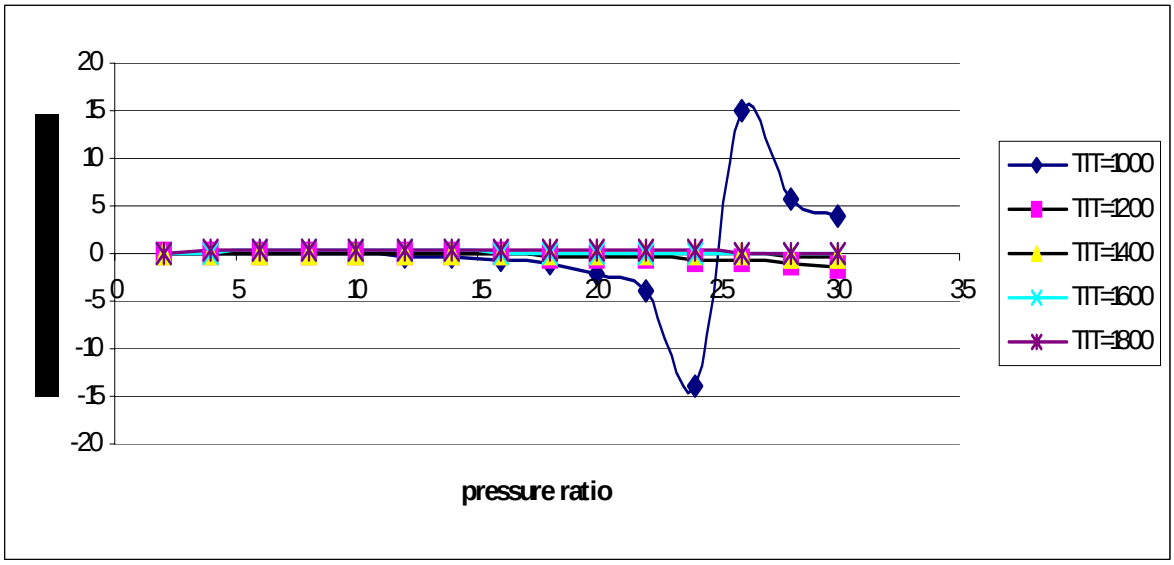

n=0,1,2

Fig 3.7.5 VARIATION OF THERMAL EFFICIENCY OF TOPPING CYCLE VS PRESSURE RATIO(γ=1.66)

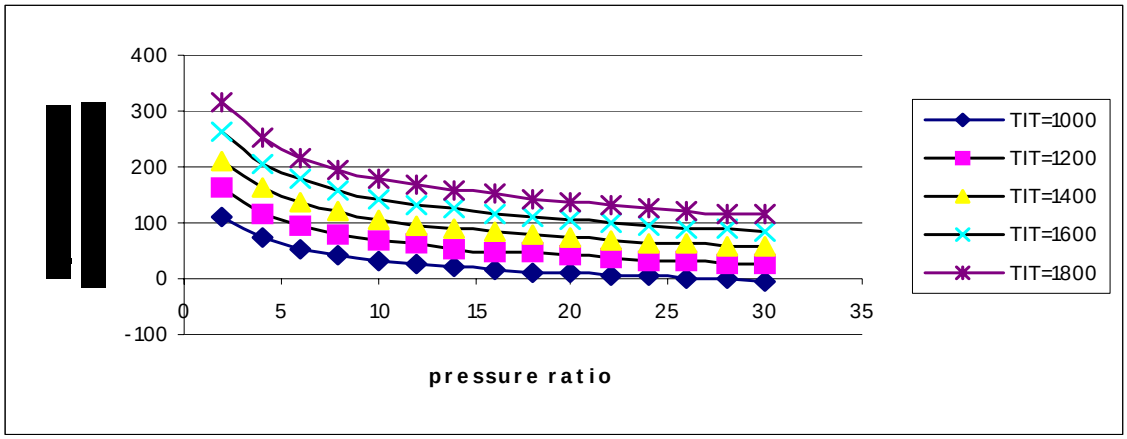

Fig 3.7.6a n=0

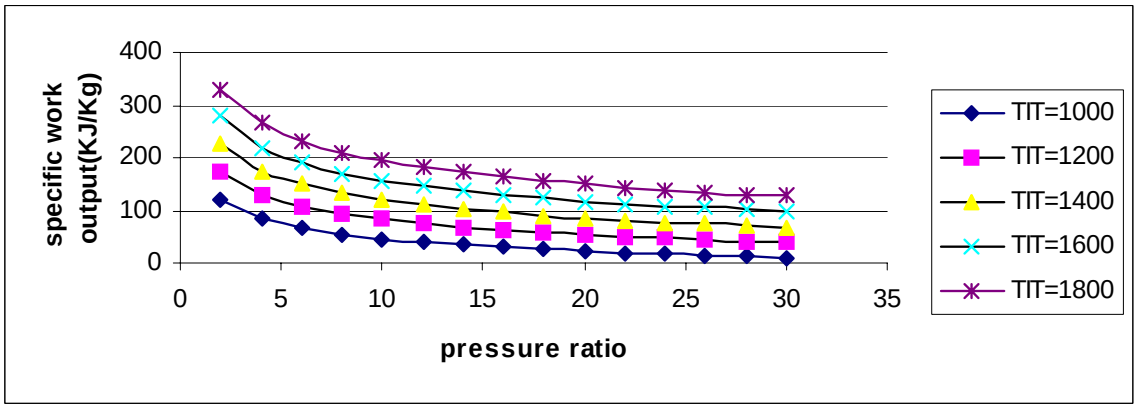

Fig 3.7.6b n=1

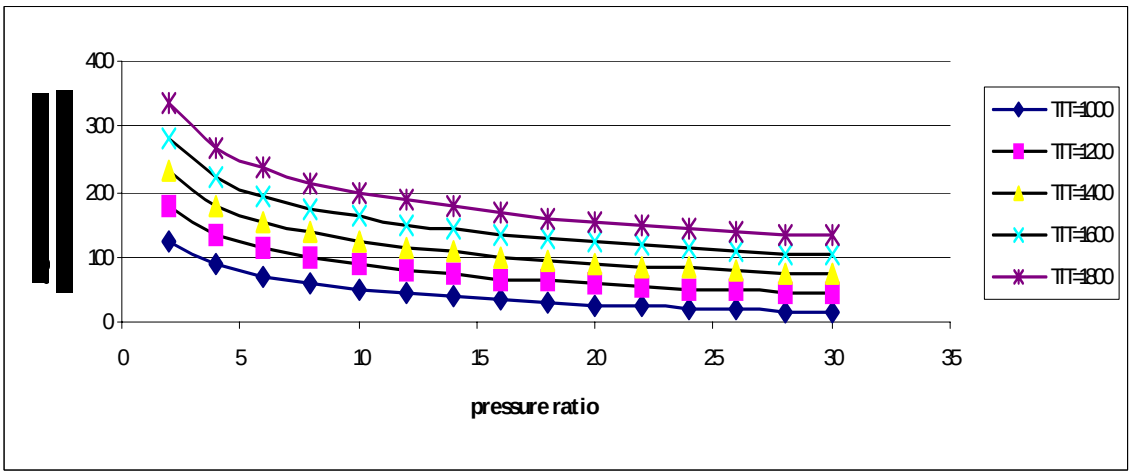

Fig 3.7.6c n=2

Fig 3.7.6 VARIATION OF SPECIFIC OUTPUT OF BOTTOMING CYCLE VS PRESSURE RATIO(γ=1.66)

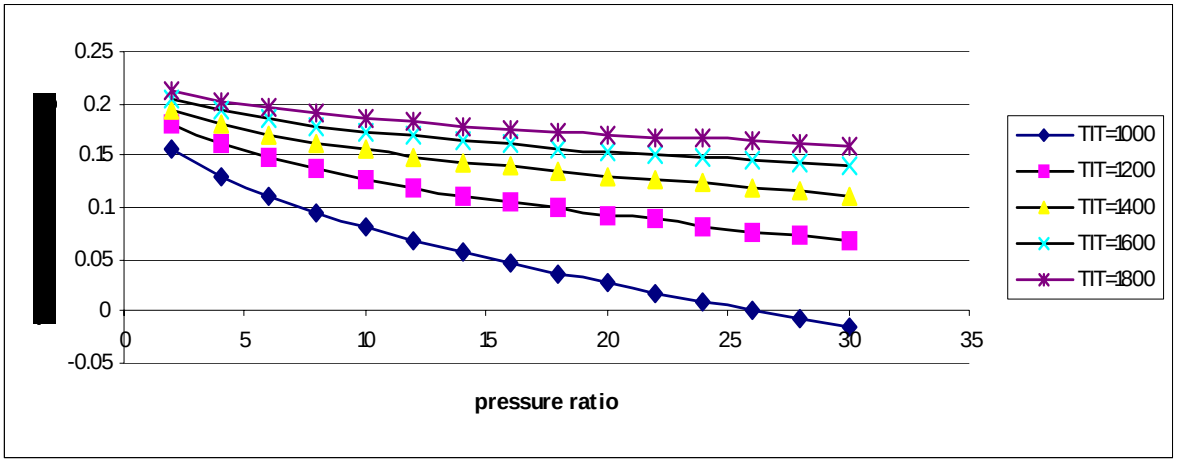

Fig 3.7.7a n=0

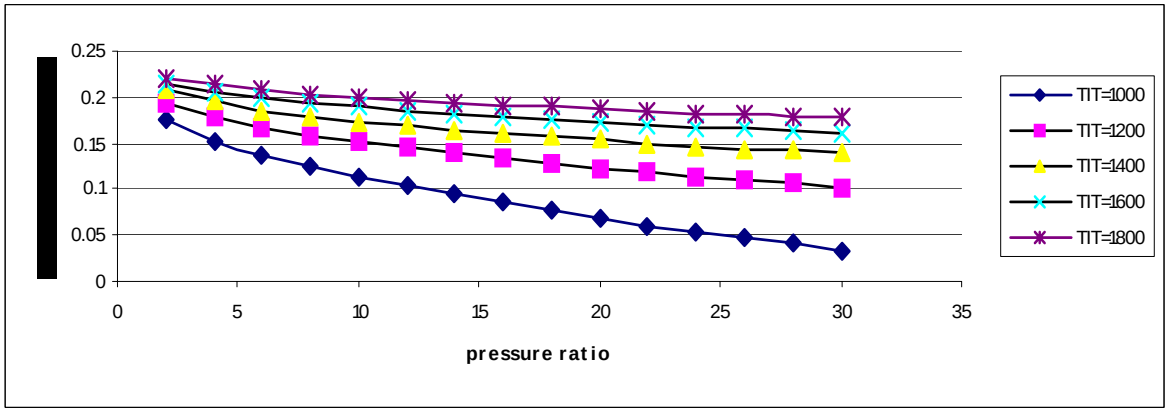

Fig 3.7.7b n=1

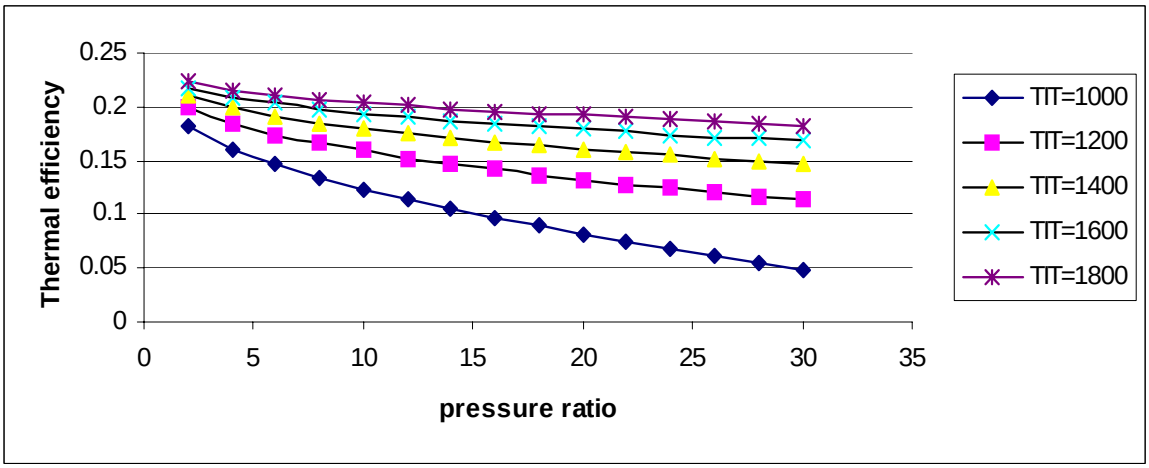

Fig 3.7.7c n=2

Fig 3.7.7 VARIATION OF THERMAL EFFICIENCY BOTTOMING CYCLE VS PRESSURE RATIO(γ=1.66)

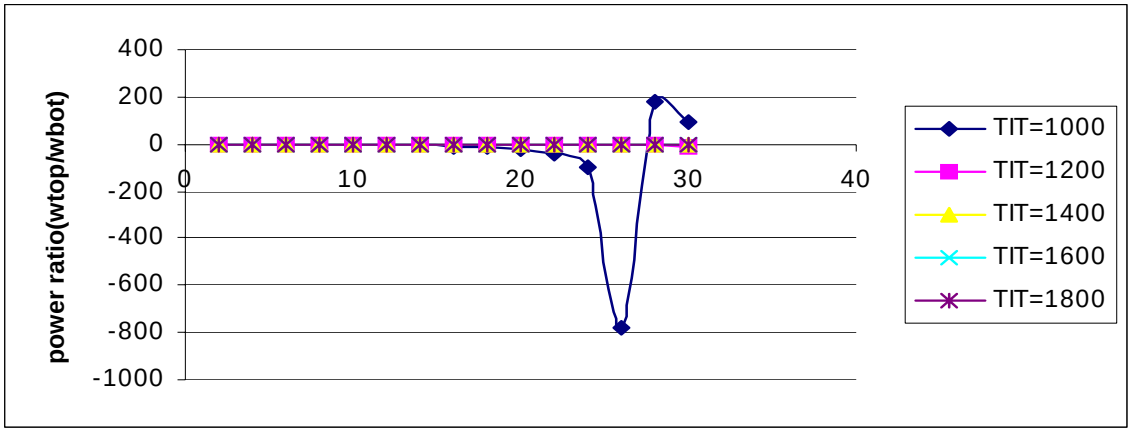

Fig 3.7.8a n=0

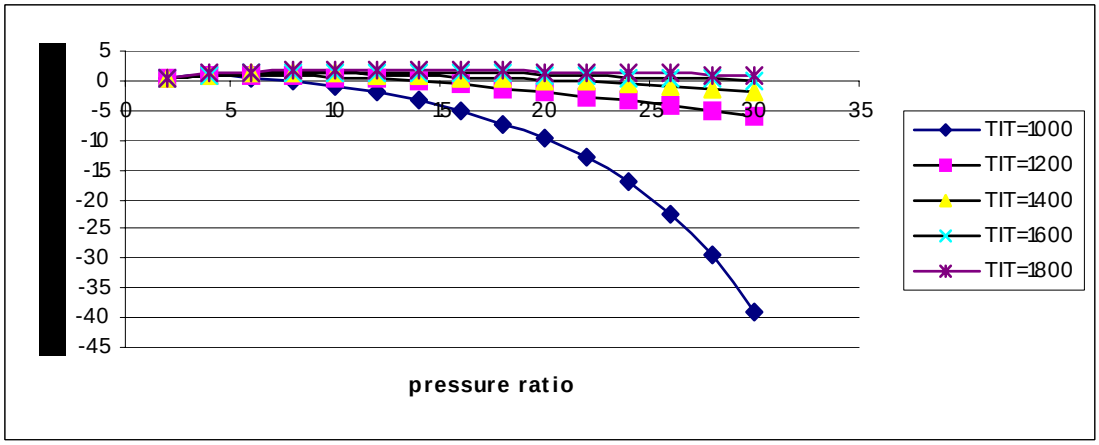

Fig 3.7.8b n=1

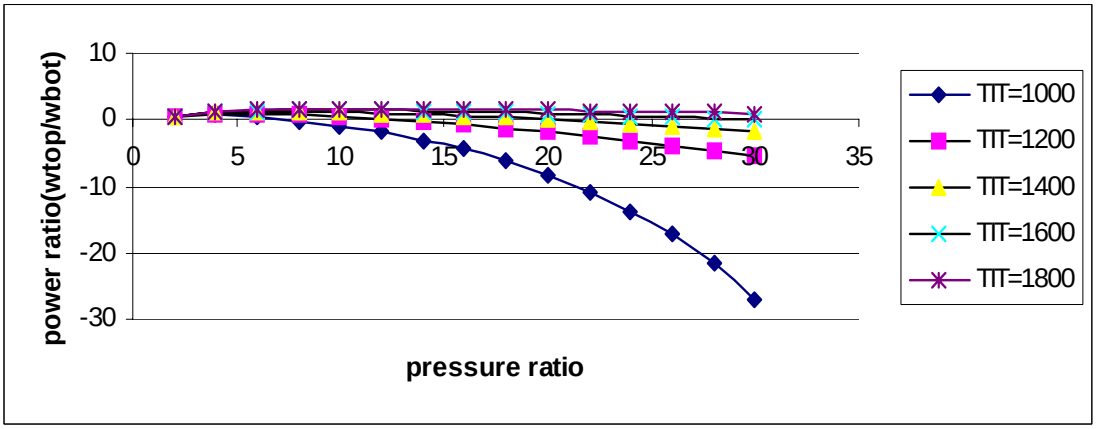

Fig 3.7.8c n=2

Fig 3.7.8 VARIATION OF POWER RATIO OF MIRROR GAS TURBINE VS PRESSURE RATIO(γ=1.66)

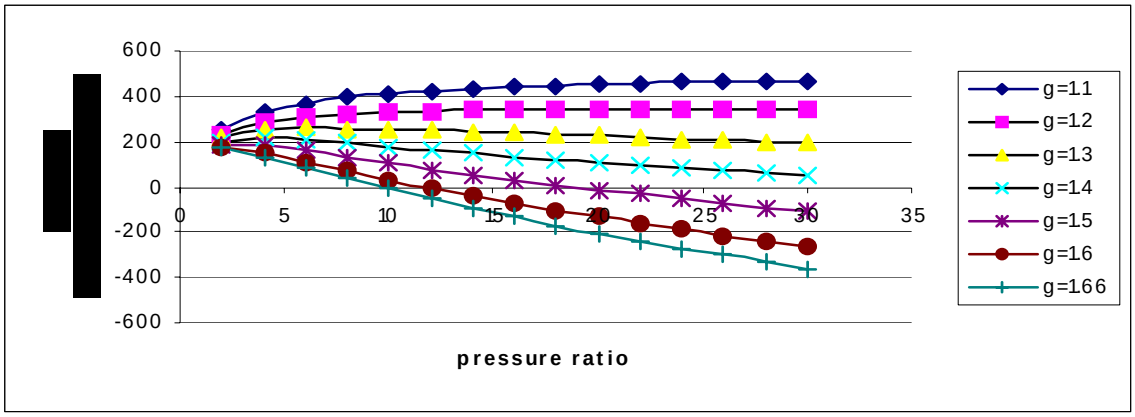

n=0

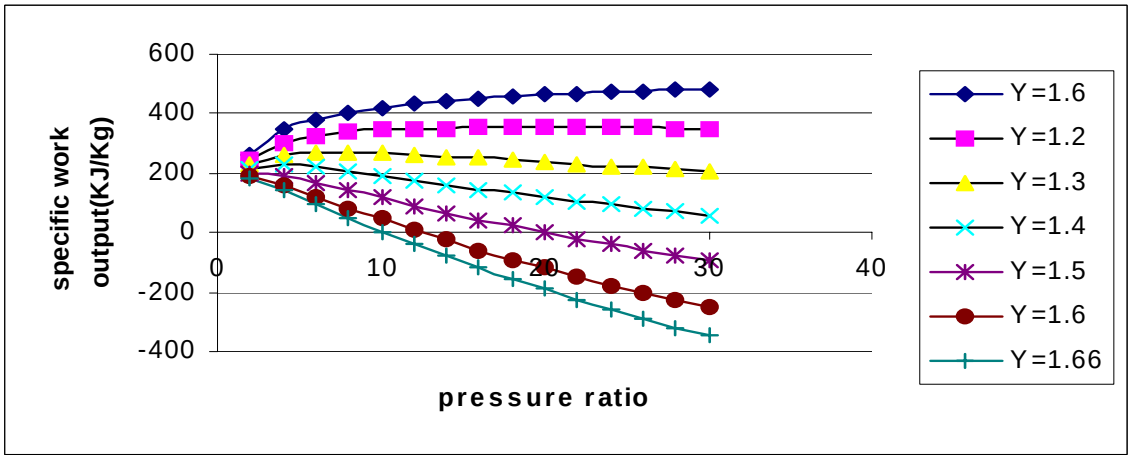

n=1

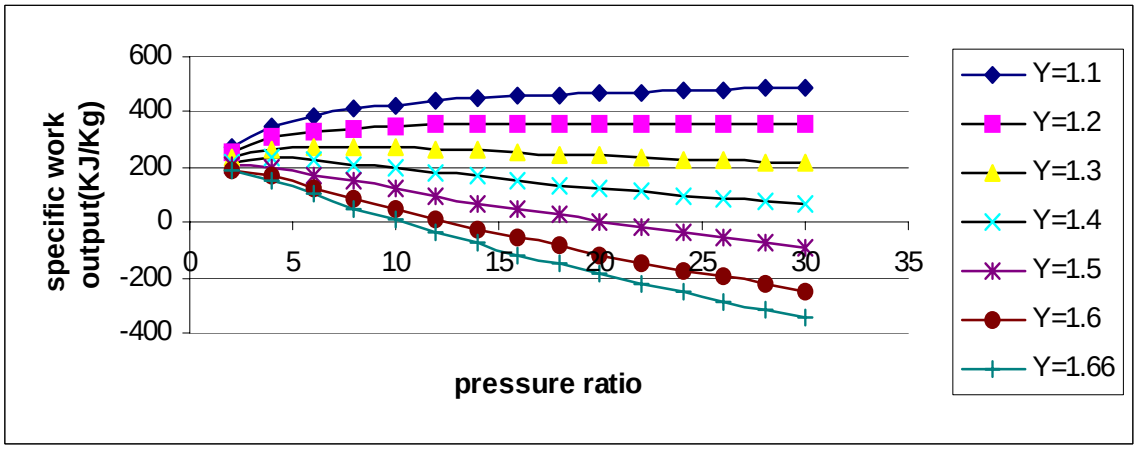

n=2

Fig 3.8.1. VARIATION OF SPECIFIC OUTPUT OF MIRROR GAS TURBINE VS PRESSURE RATIO AT VARIOUS SPECIFIC HEAT (γ=1.1 ,1.2,1.3,1.4,1.5,1.6,1.66) at TIT(1000K)

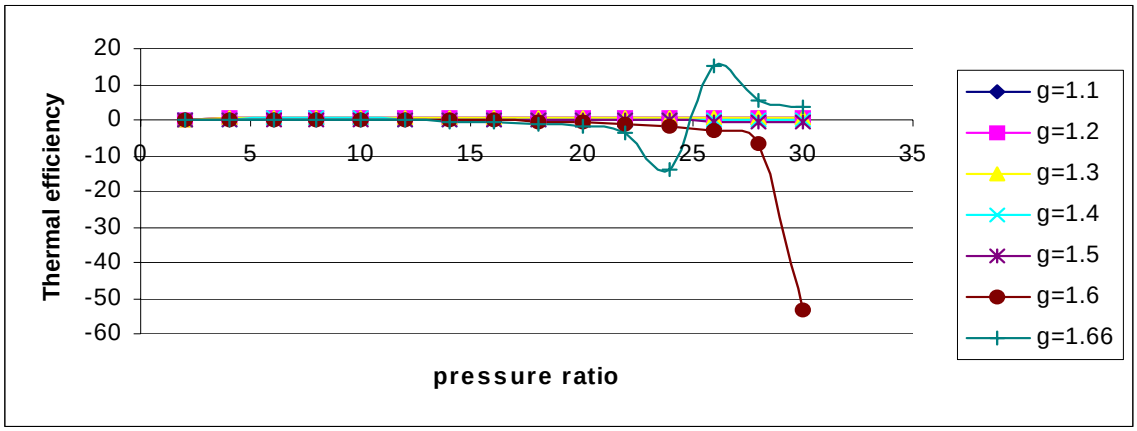

n=0

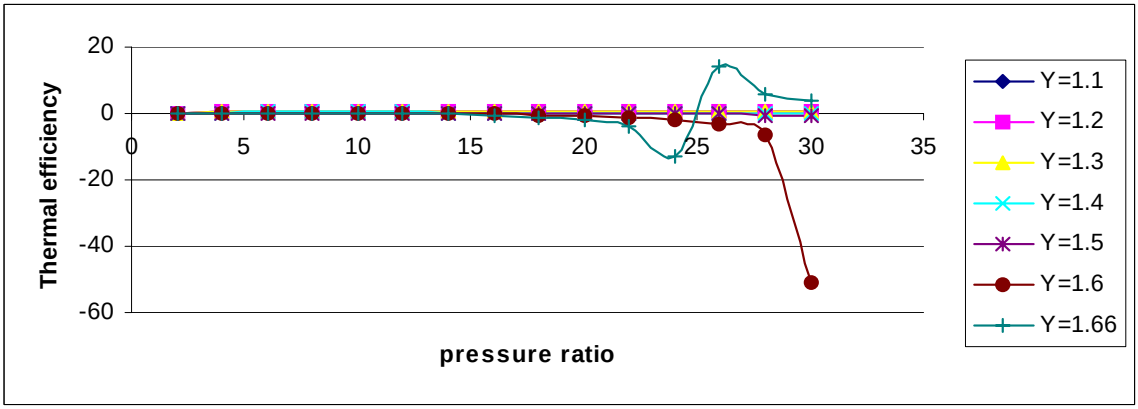

n=1

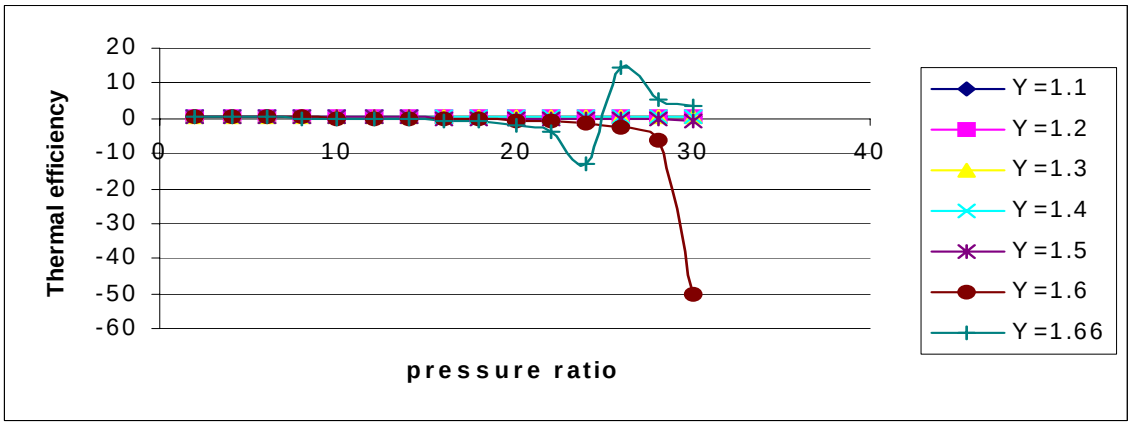

n=2

Fig 3.8.2 VARIATION OF THERMAL EFFICIENCY OF MIRROR GAS TURBINE VS PRESSURE RATIO AT VARIOUS SPECIFIC HEAT (γ=1.1 ,1.2,1.3,1.4,1.5,1.6,1.66) at TIT(1000K)

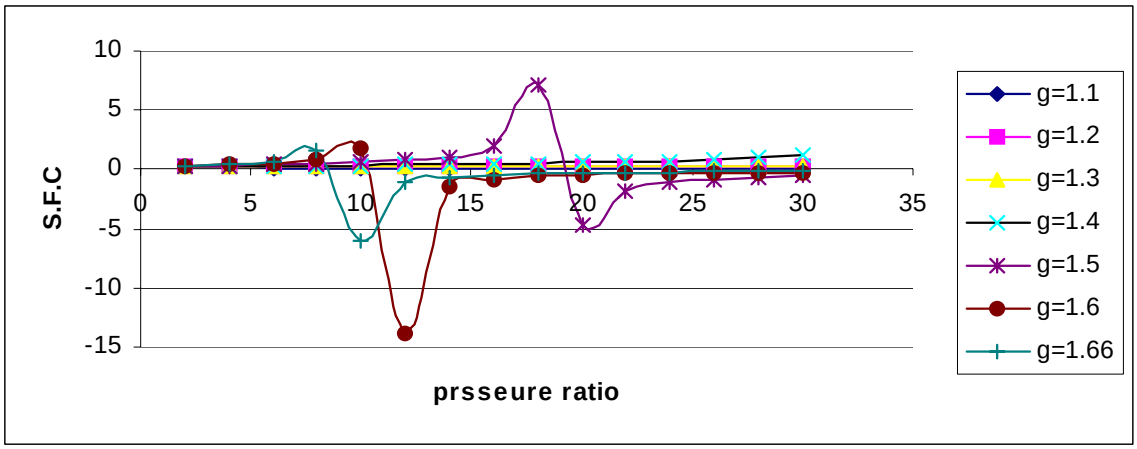

n=0

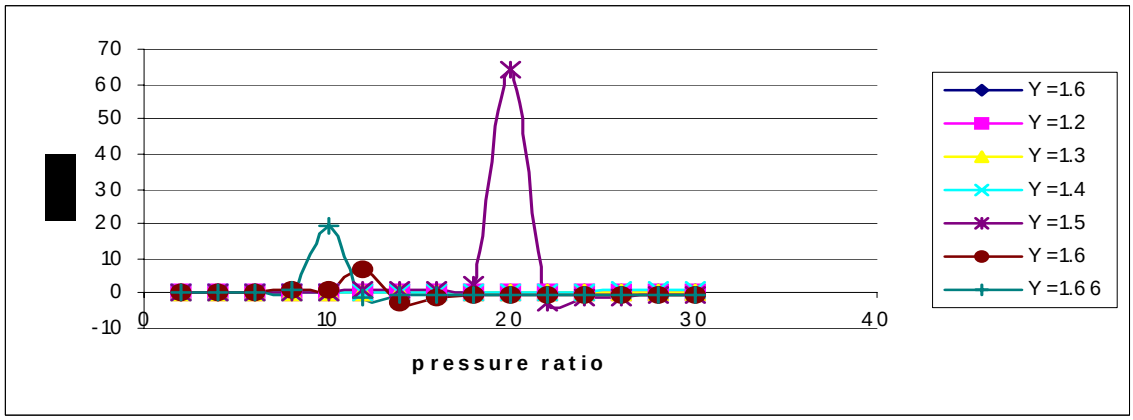

n=1

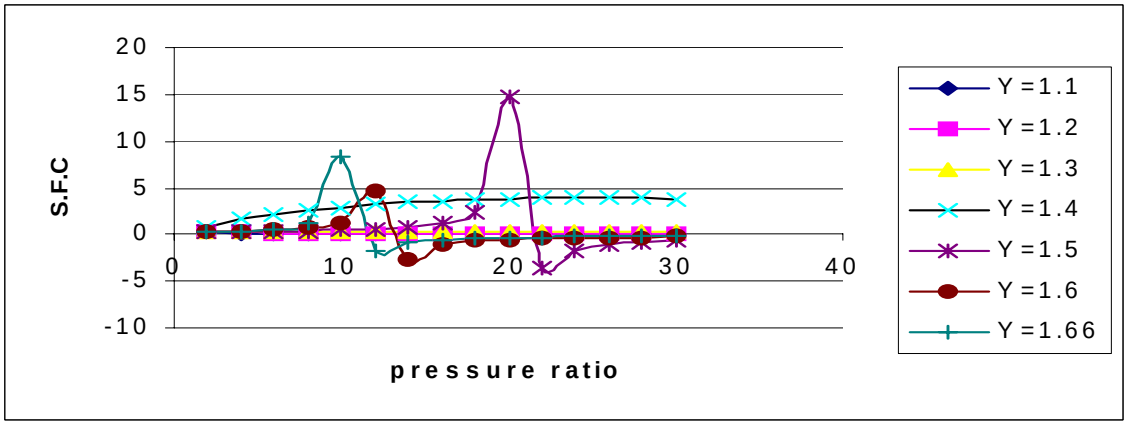

n=2

Fig 3.8.3 VARIATION OF S.F.C. OF MIRROR GAS TURBINE VS PRESSURE RATIO AT VARIOUS SPECIFIC HEAT (γ=1.1 ,1.2,1.3,1.4,1.5,1.6,1.66) at TIT(1000K)

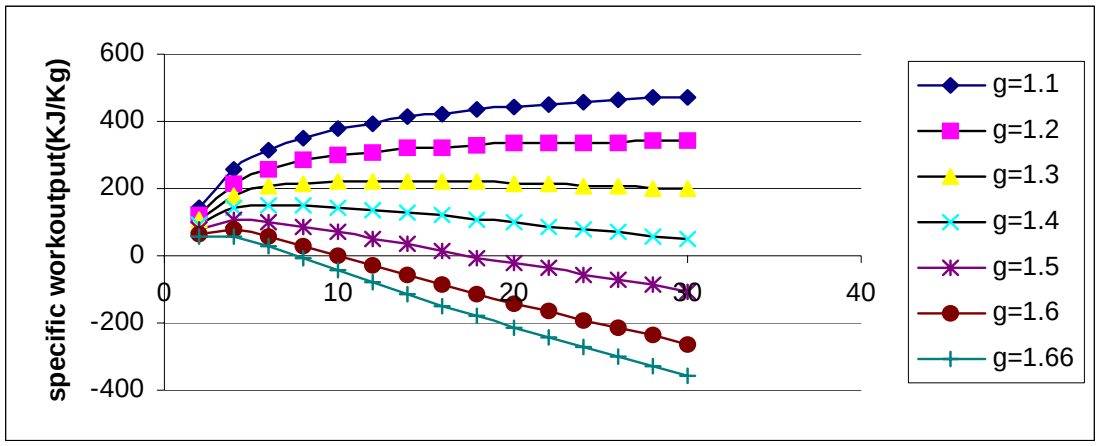

n=0,1,2

Fig 3.8.4 VARIATION OF SPECIFIC OUTPUT OF TOPPING CYCLE VS PRESSURE RATIO AT VARIOUS SPECIFIC HEAT (γ=1.1 ,1.2,1.3,1.4,1.5,1.6,1.66) at TIT(1000K)

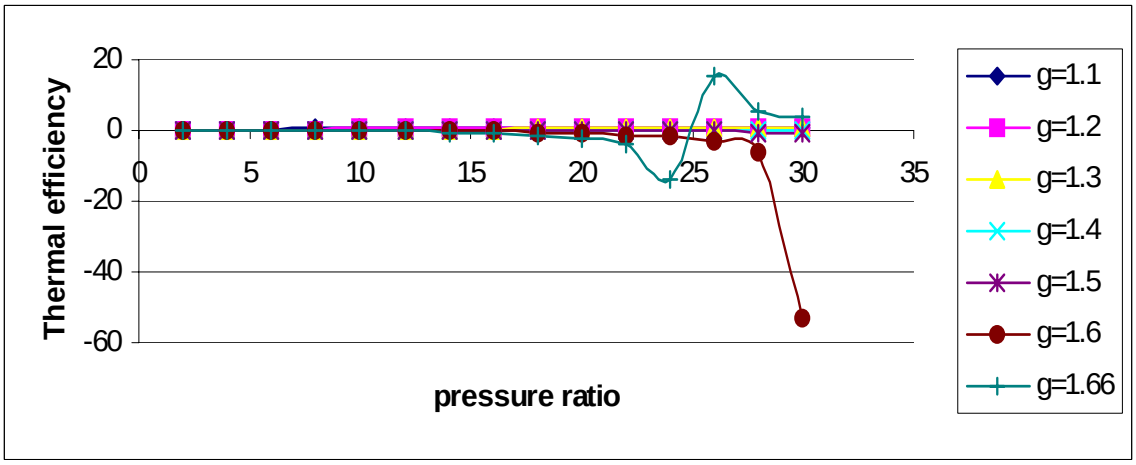

n=0,1,2

Fig 3.8.5 VARIATION OF THERMAL EFFICIENCY OF TOPPING CYCLE VS PRESSURE RATIO AT VARIOUS SPECIFIC HEAT (γ=1.1 ,1.2,1.3,1.4,1.5,1.6,1.66) at TIT(1000K)

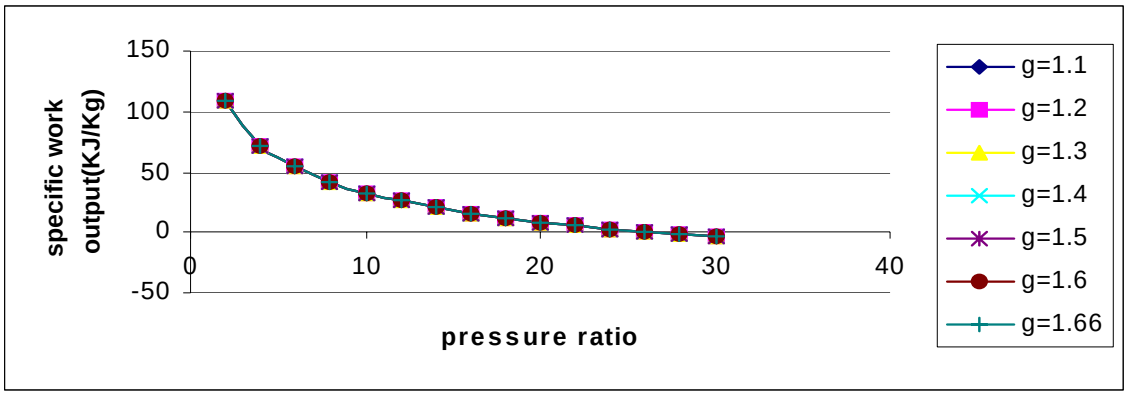

n=0

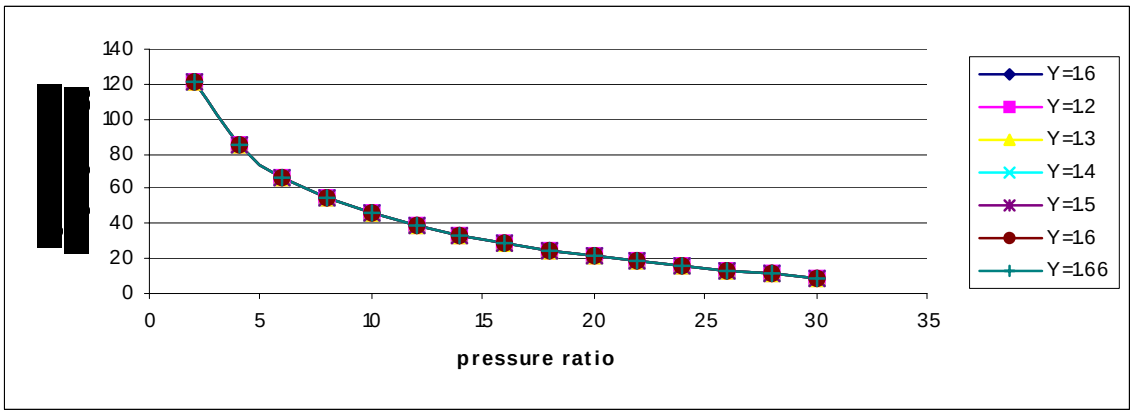

n=1

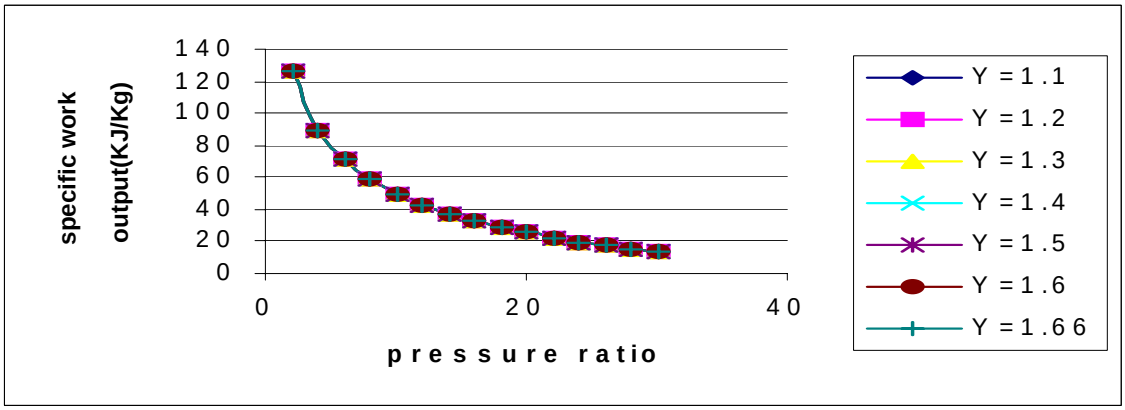

n=2

Fig 3.8.6 VARIATION OF SPECIFIC OUTPUT OF BOTTOMING CYCLE VS PRESSURE RATIO AT VARIOUS SPECIFIC HEAT (γ=1.1 ,1.2,1.3,1.4,1.5,1.6,1.66) at TIT(1000K)

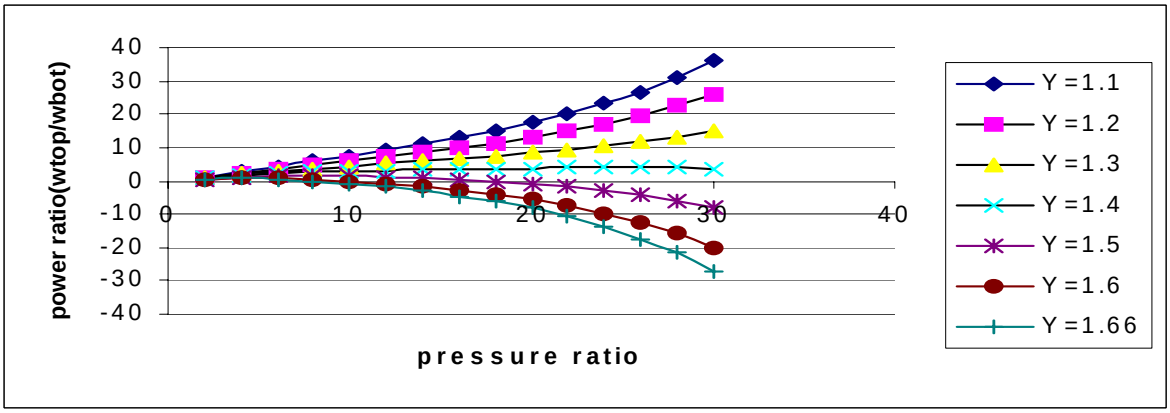

n=0

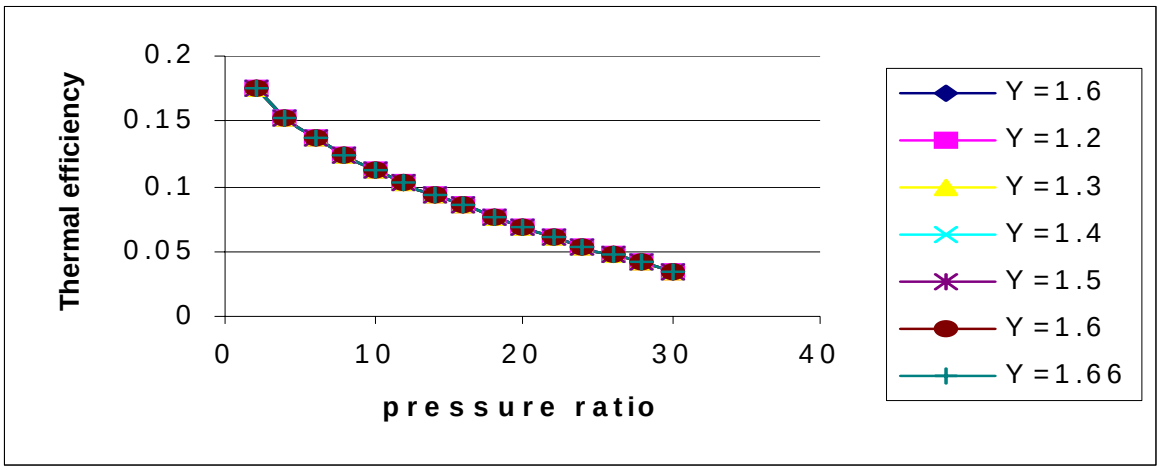

n=1

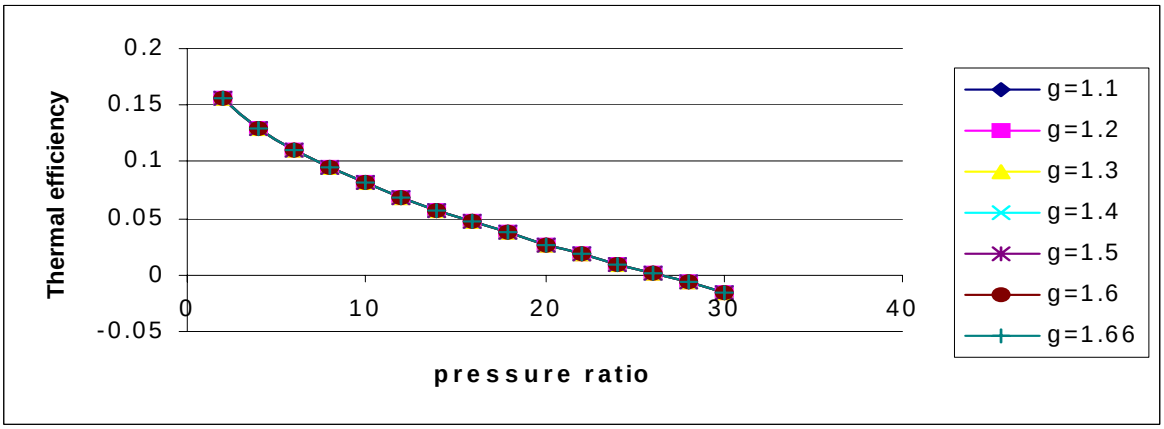

n=2

Fig 3.8.7 VARIATION OF THERMAL EFFICIENCY BOTTOMING CYCLE VS PRESSURE RATIO AT VARIOUS SPECIFIC HEAT (γ=1.1 ,1.2,1.3,1.4,1.5,1.6,1.66) at TIT(1000K)

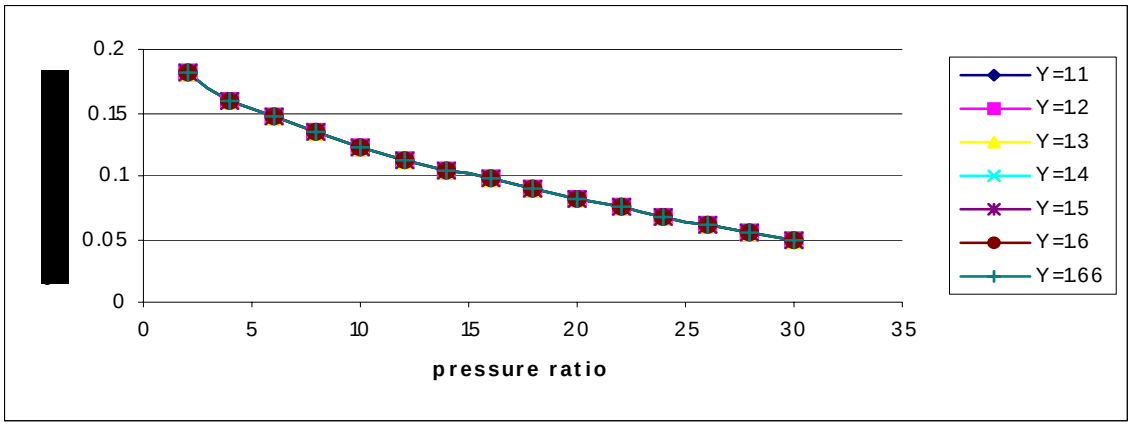

n=2

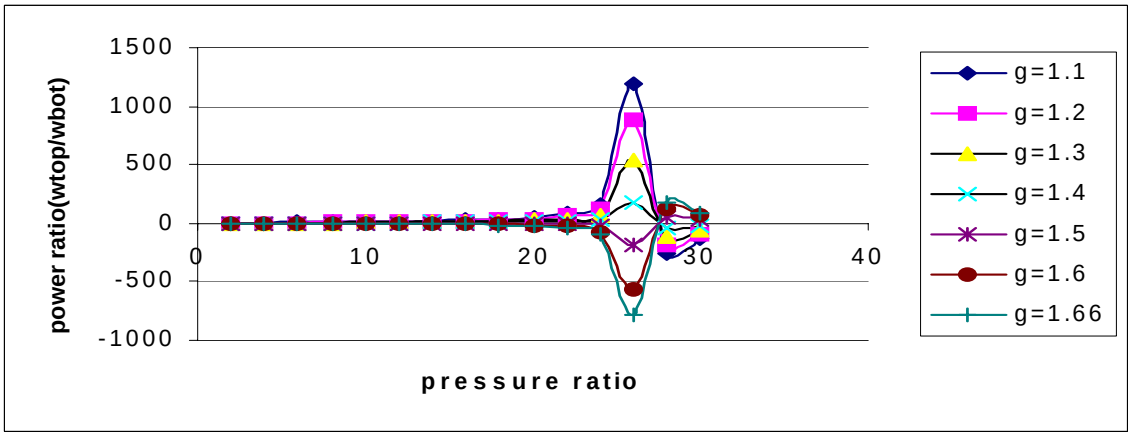

n=0

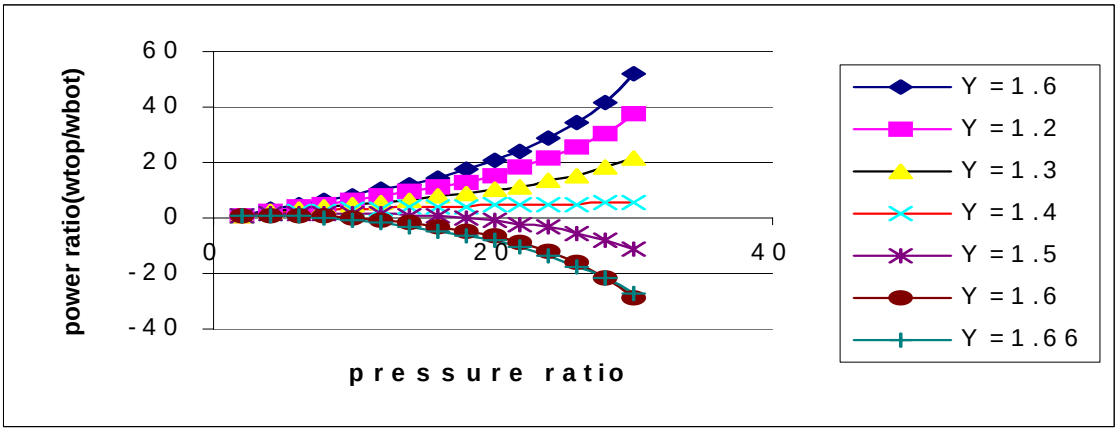

n=1

Fig 3.8.8 VARIATION OF POWER RATIO OF MIRROR GAS TURBINE VS PRESSURE RATIO AT VARIOUS SPECIFIC HEAT (γ=1.1 ,1.2,1.3,1.4,1.5,1.6,1.66) at TIT(1000K)

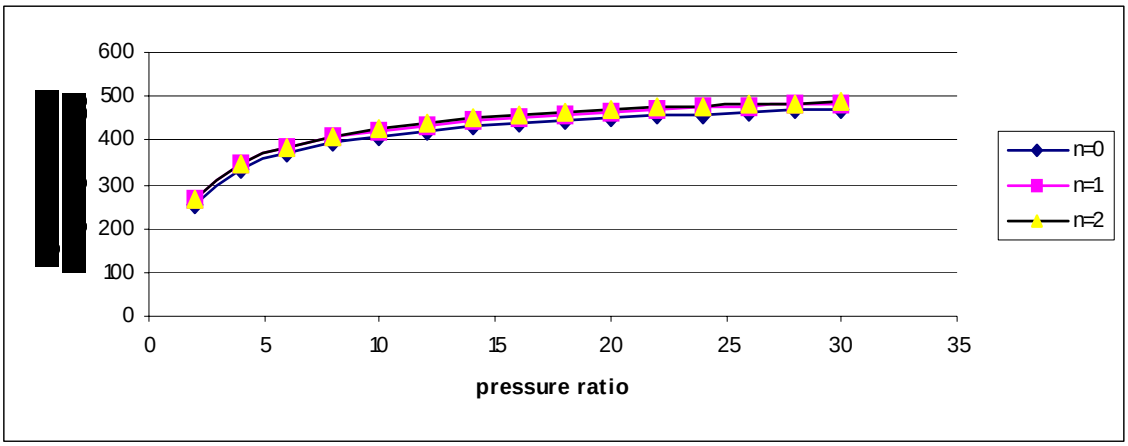

(γ=1.1) **Fig 3.9.1a**

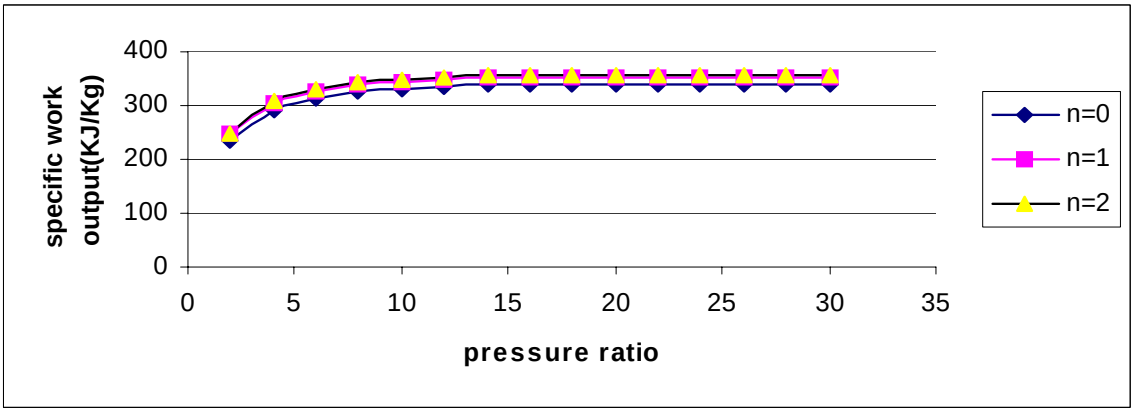

Fig 3.9.1b **(γ=1.2)**

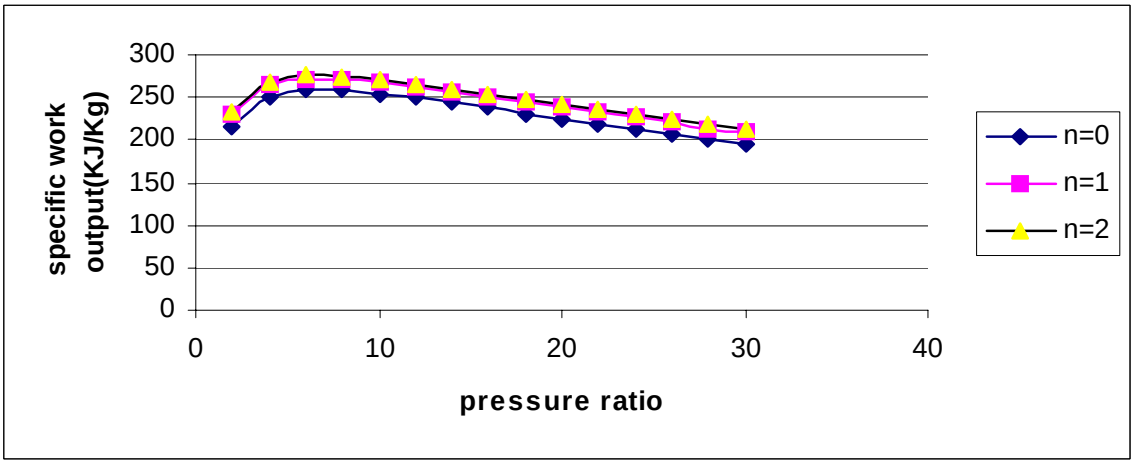

(γ=1.3) **Fig 3.9.1c**

Fig 3.9.1 VARIATION OF SPECIFIC OUTPUT OF MIRROR GAS TURBINE VS PRESSURE RATIO(1000K)

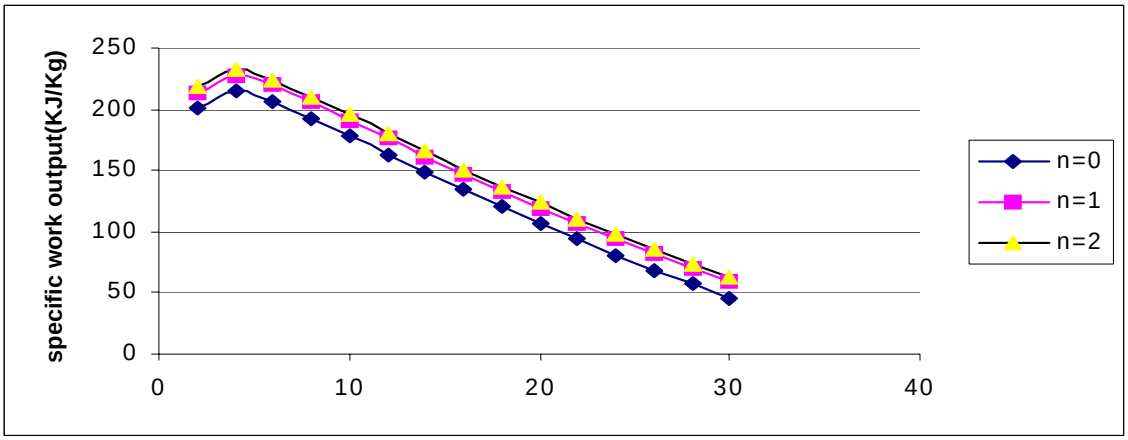

(γ=1.4) **Fig 3.9.1d**

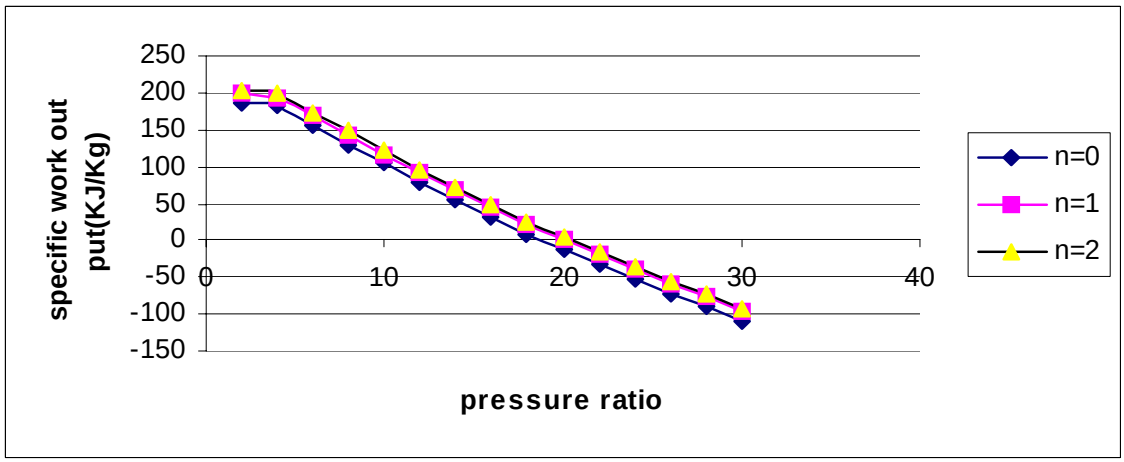

Fig 3.9.1e **(γ=1.5)**

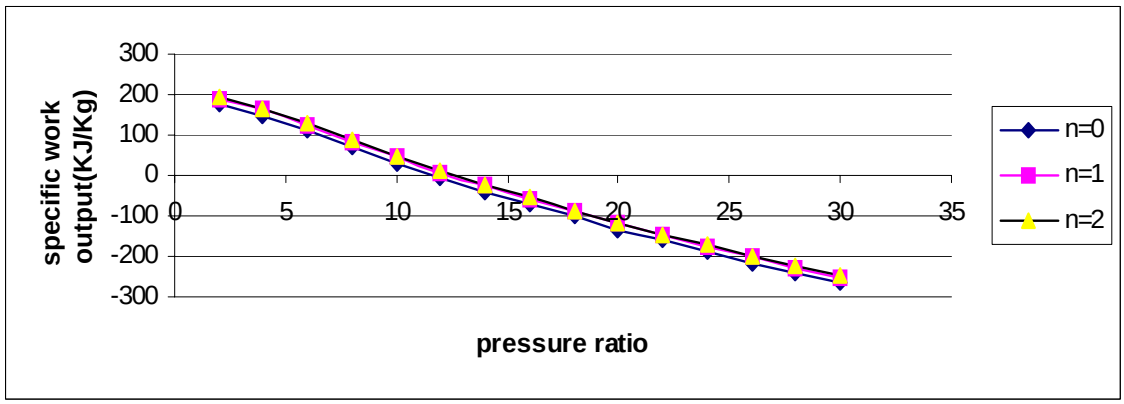

(γ=1.6) **Fig 3.9.1f**

Fig 3.9.1 VARIATION OF SPECIFIC OUTPUT OF MIRROR GAS TURBINE VS PRESSURE RATIO(1000K)

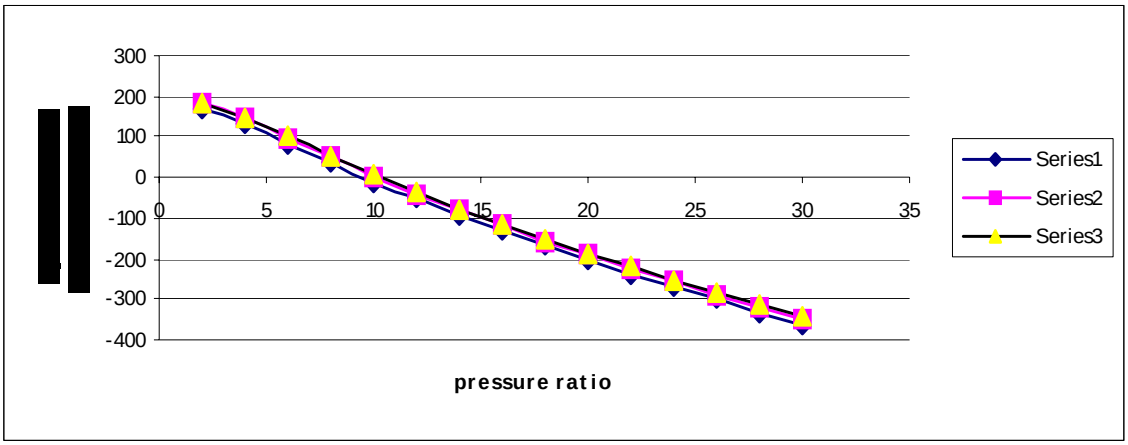

(γ=1.66) **Fig 3.9.1g**

Fig 3.9.1 VARIATION OF SPECIFIC OUTPUT OF MIRROR GAS TURBINE VS PRESSURE RATIO(TIT=1000K)

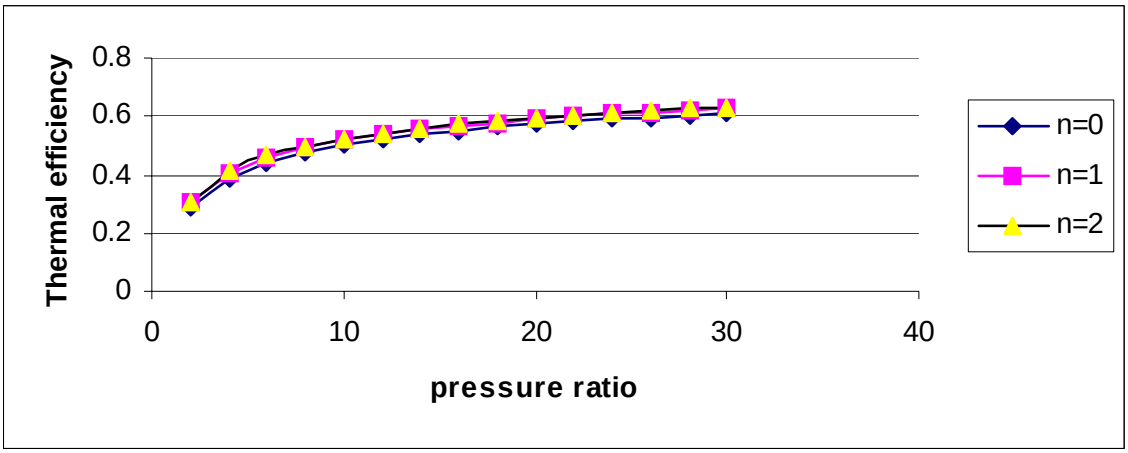

Fig 3.9.2a (γ=1.1)

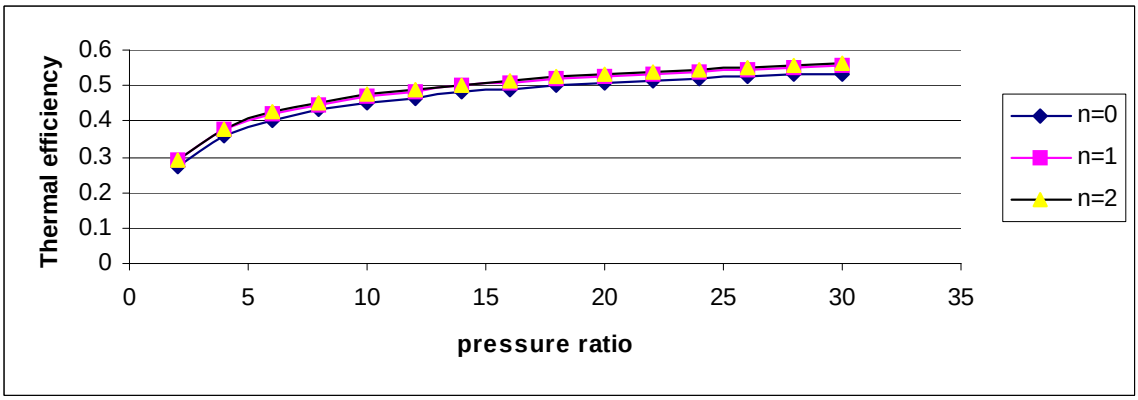

Fig 3.9.2b (γ=1.2)

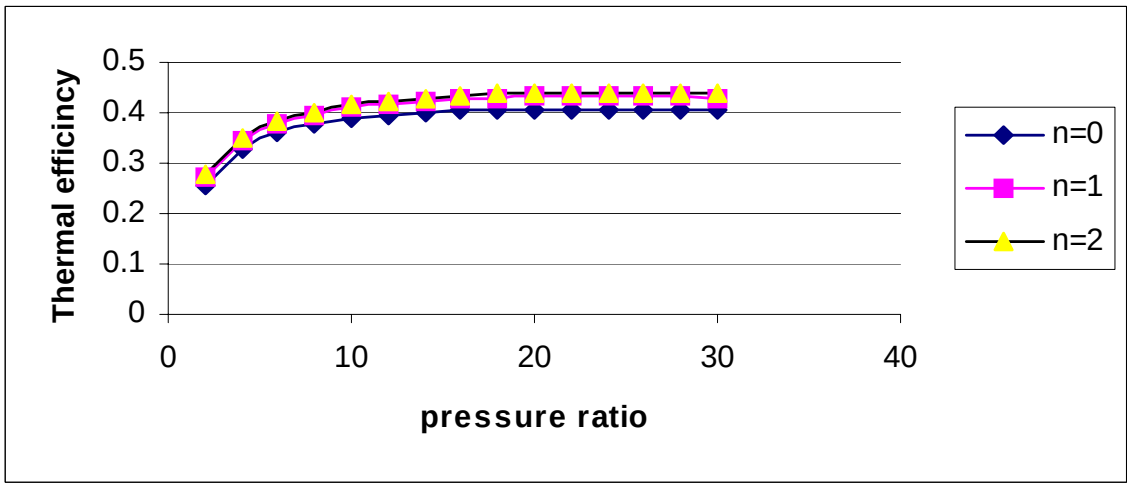

(γ=1.3) Fig 3.9.2c

Fig 3.9.2 VARIATION OF THERMAL EFFICIENCY OF MIRROR GAS TURBINE VS PRESSURE RATIO(TIT=1000K)

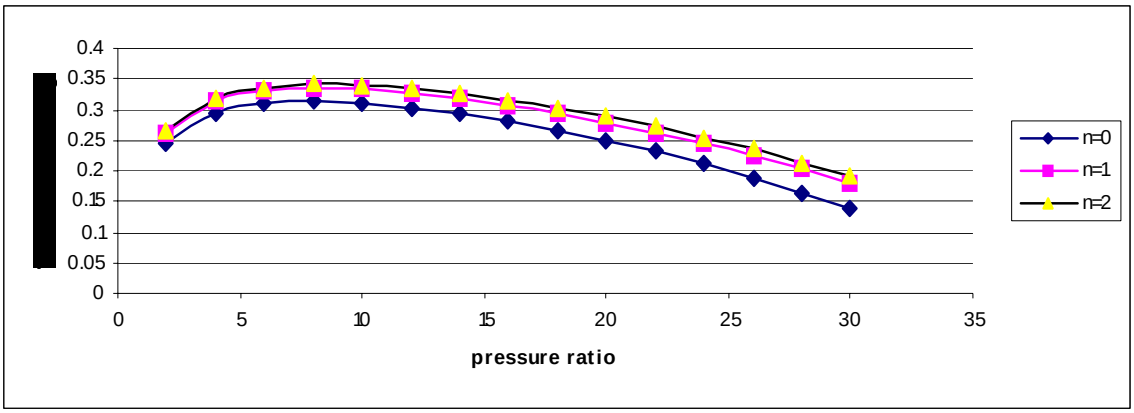

Fig 3.9.2d (γ=1.4)

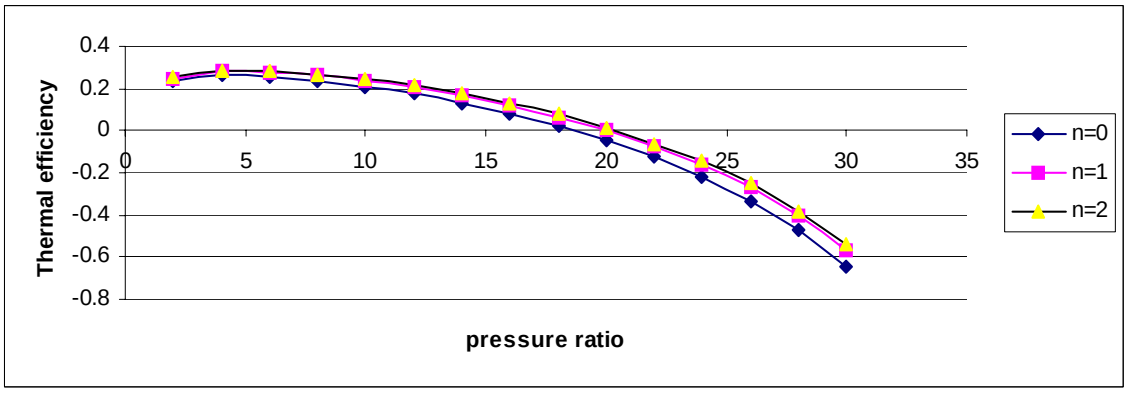

Fig 3.9.2e (γ=1.5)

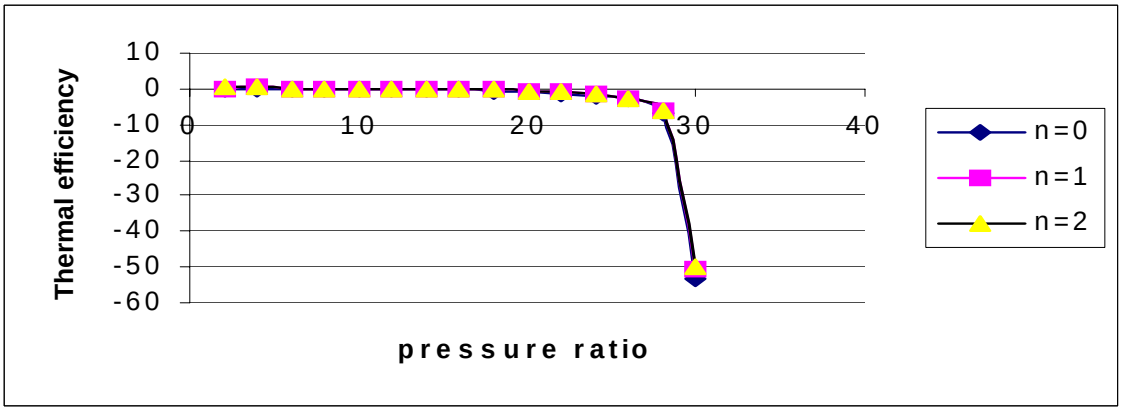

Fig 3.9.2f (γ=1.6)

Fig 3.9.2 VARIATION OF THERMAL EFFICIENCY OF MIRROR GAS TURBINE VS PRESSURE RATIO(TIT=1000K)

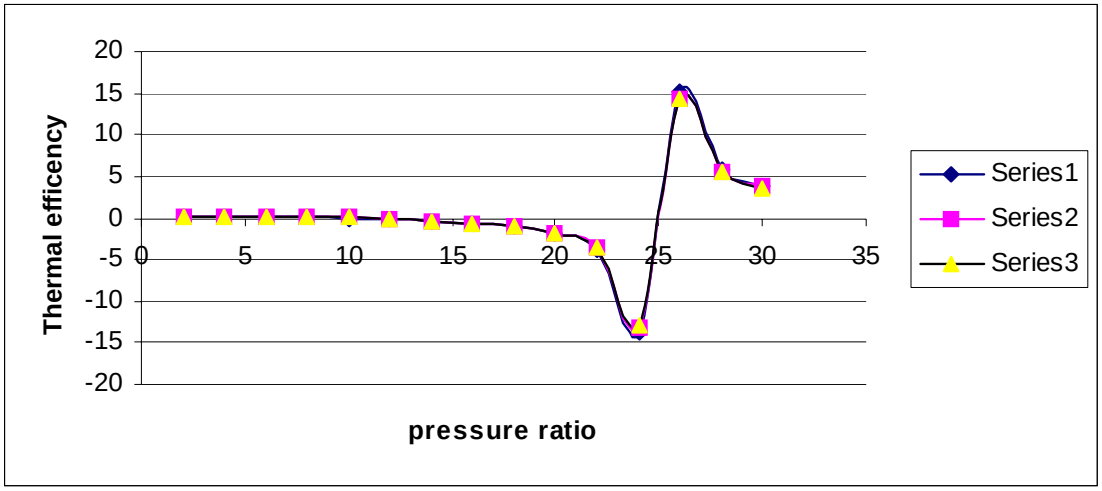

Fig 3.9.2g **(γ=1.66)**

Fig 3.9.2 VARIATION OF THERMAL EFFICIENCY OF MIRROR GAS TURBINE VS PRESSURE RATIO(TIT=1000K)

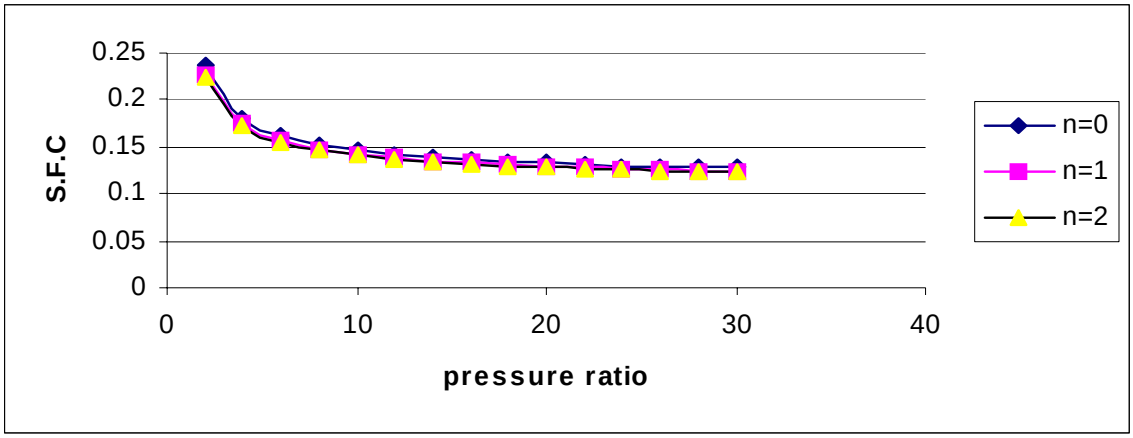

Fig 3.9.3a (γ=1.1)

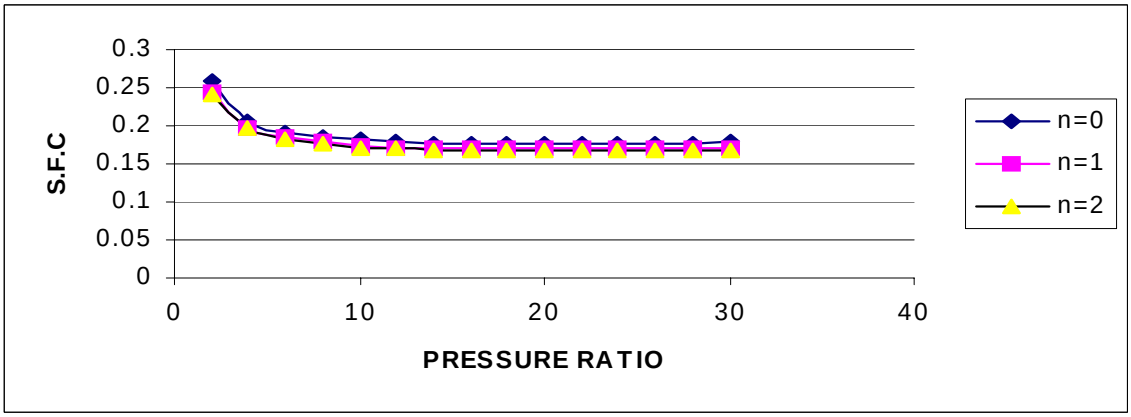

Fig 3.9.3b (γ=1.2)

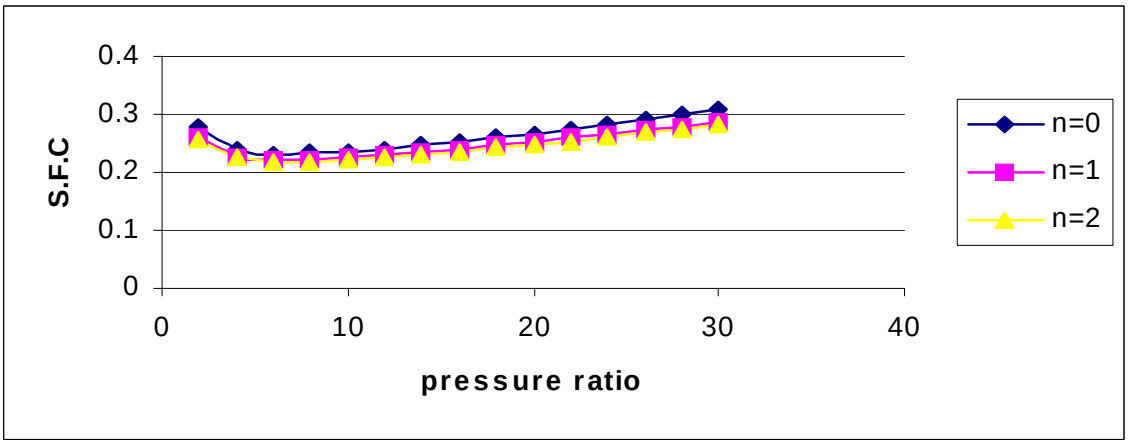

Fig 3.9.3c (γ=1.3)

Fig 3.9.3 VARIATION OF S.F.C. OF MIRROR GAS TURBINE VS PRESSURE RATIO(TIT=1000K)

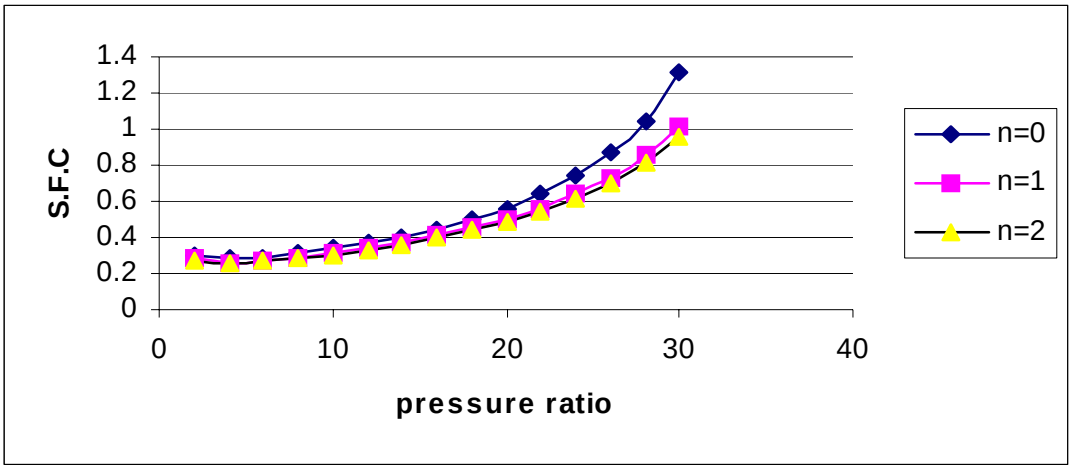

Fig 3.9.3d (γ=1.4)

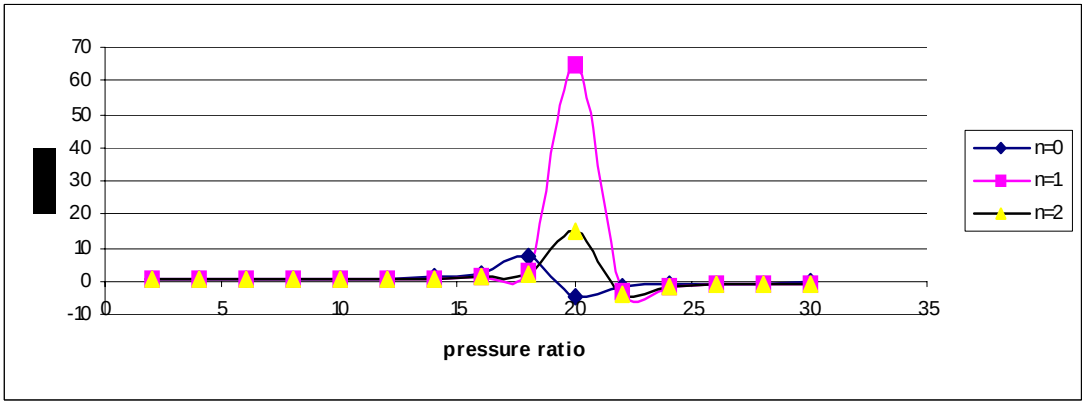

Fig 3.9.3e (γ=1.5)

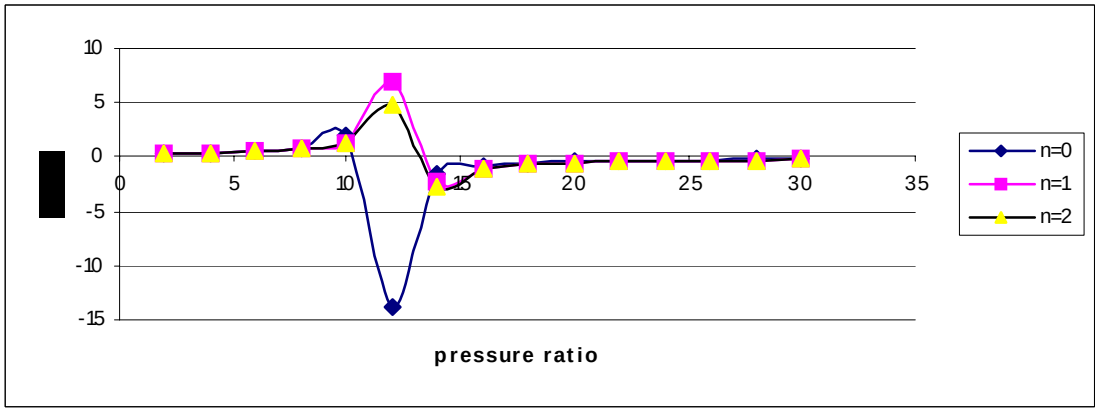

Fig 3.9.3f (γ=1.6)

Fig 3.9.3 VARIATION OF S.F.C. OF MIRROR GAS TURBINE VS PRESSURE RATIO(TIT=1000K)

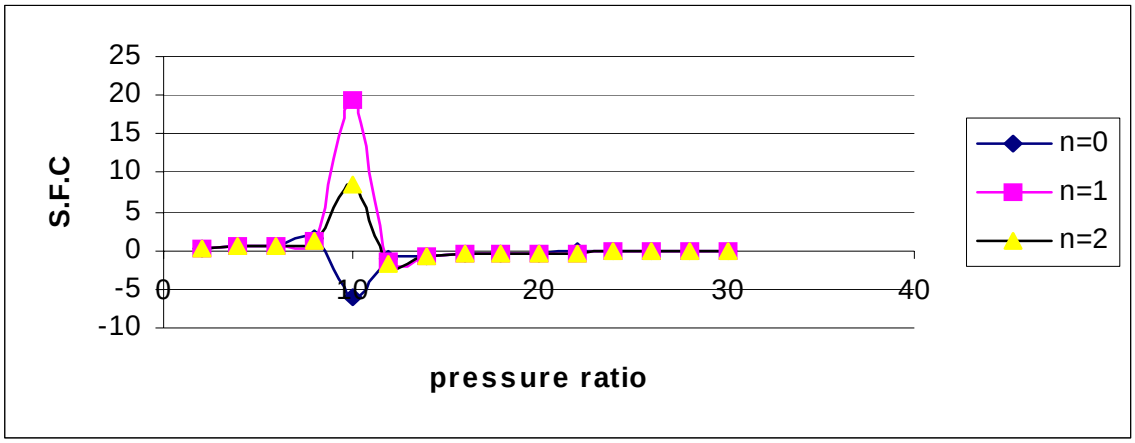

Fig 3.9.3g (γ=1.66)

Fig 3.9.3 VARIATION OF S.F.C. OF MIRROR GAS TURBINE VS PRESSURE RATIO(TIT=1000K)

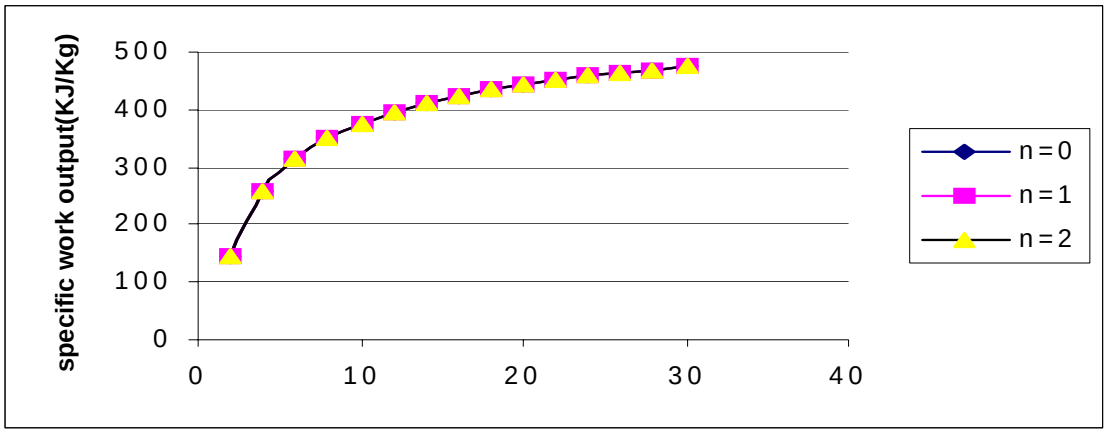

fig 3.9.4a **γ=1.1**

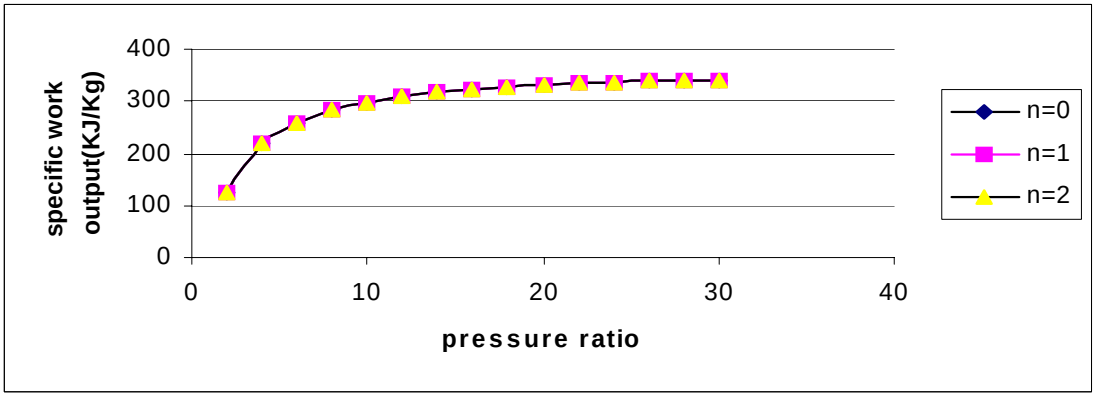

fig 3.9.4b **γ=1.2**

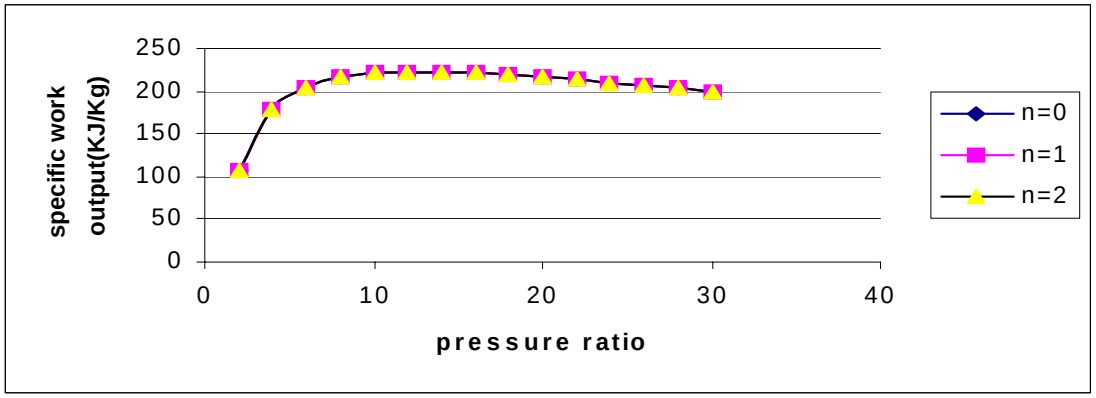

fig 3.9.4c **γ=1.3**

Fig 3.9.4 VARIATION OF SPECIFIC OUTPUT OF TOPPING CYCLE VS PRESSURE RATIO(TIT=1000K)

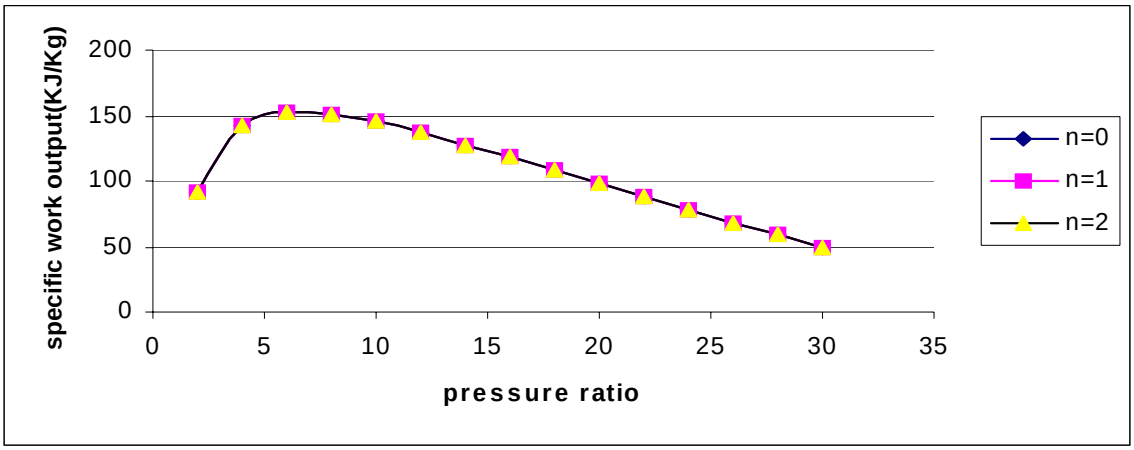

fig 3.9.4d γ=1.4

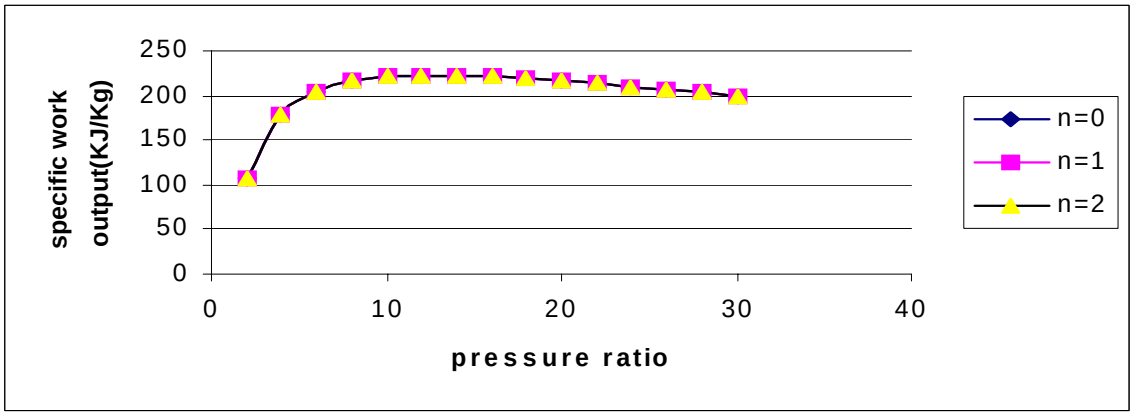

fig 3.9.4e γ=1.5

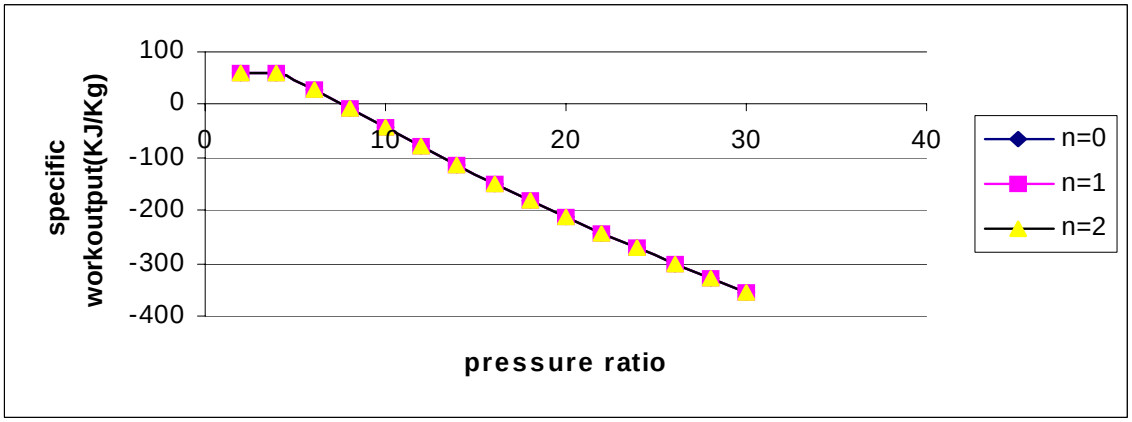

fig 3.9.4f γ=1.6

Fig 3.9.4 VARIATION OF SPECIFIC OUTPUT OF TOPPING CYCLE VS PRESSURE RATIO(TIT=1000K)

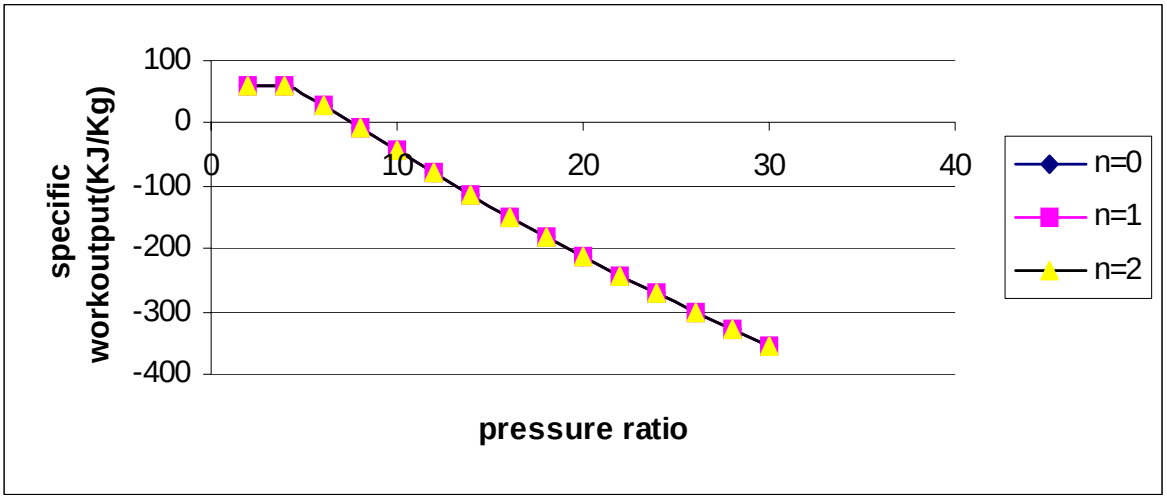

fig 3.9.4g **γ=1.66**

Fig 3.9.4 VARIATION OF SPECIFIC OUTPUT OF TOPPING CYCLE VS PRESSURE RATIO(TIT=1000K)

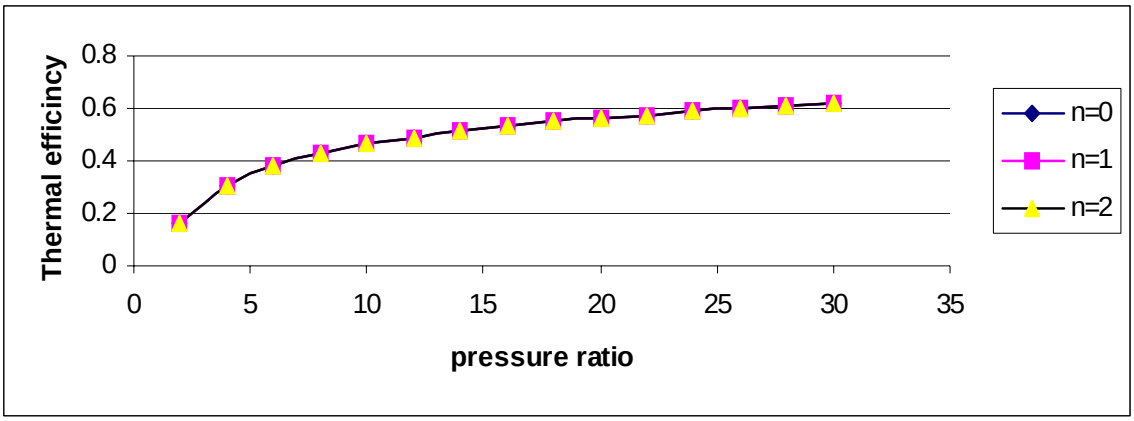

Fig3.9.5a (γ=1.1)

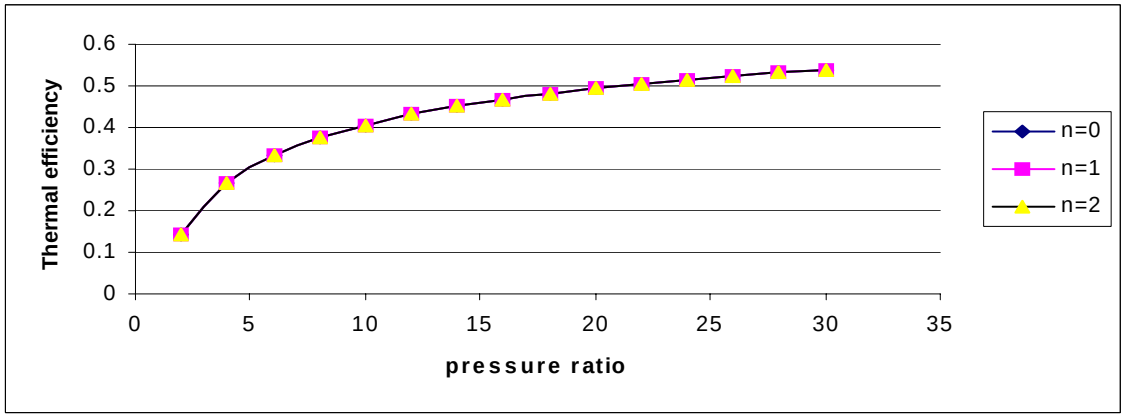

Fig3.9.5b (γ=1.2)

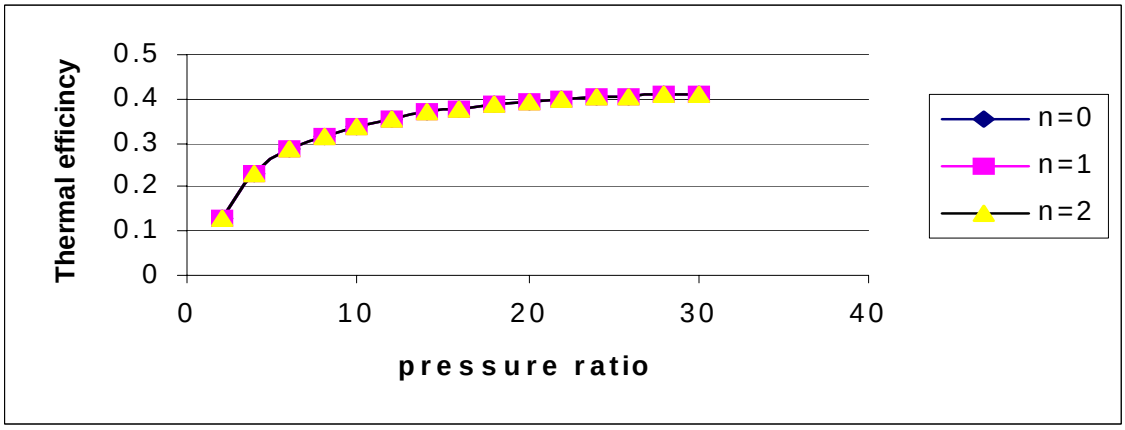

Fig3.9.5c (γ=1.3)

Fig 3.9.5 VARIATION OF THERMAL EFFICIENCY OF TOPPING CYCLE VS PRESSURE RATIO(TIT=1000K)

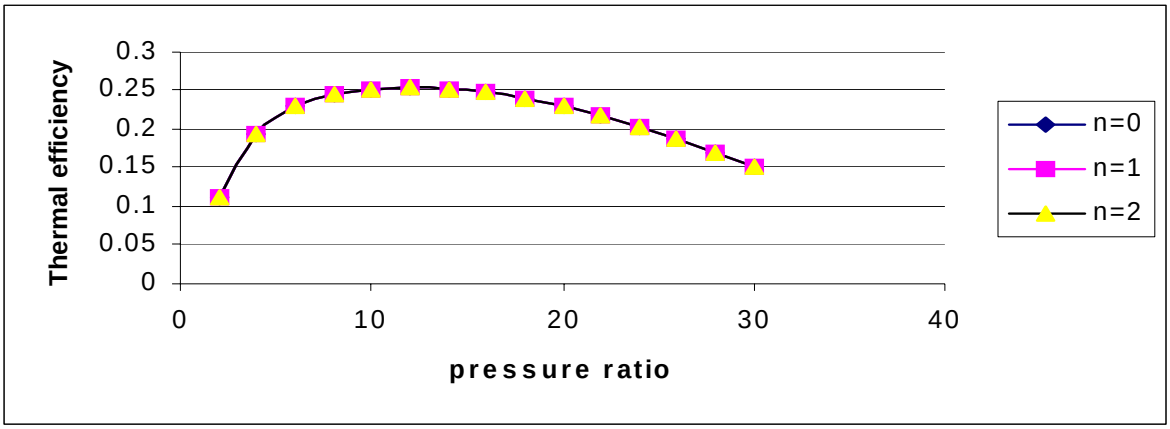

Fig3.9.5d (γ=1.4)

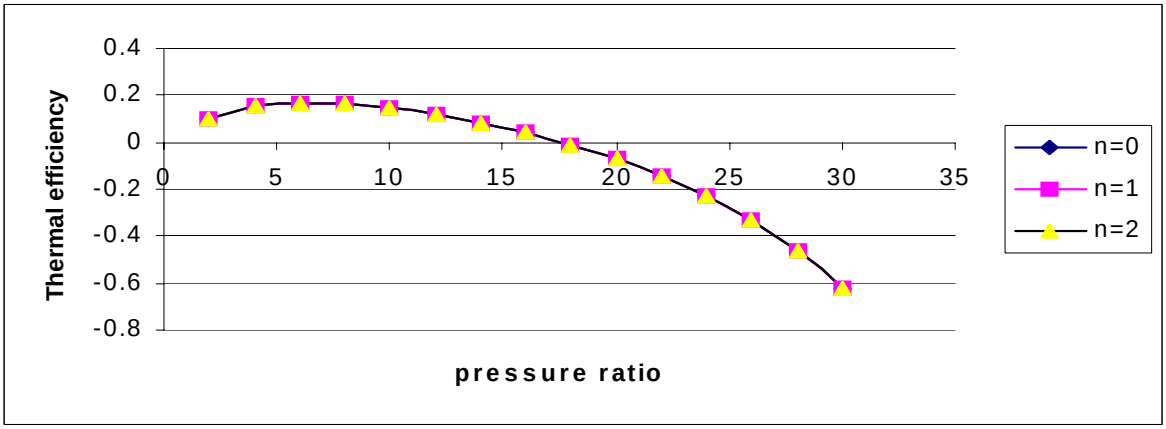

Fig3.9.5e (γ=1.5)

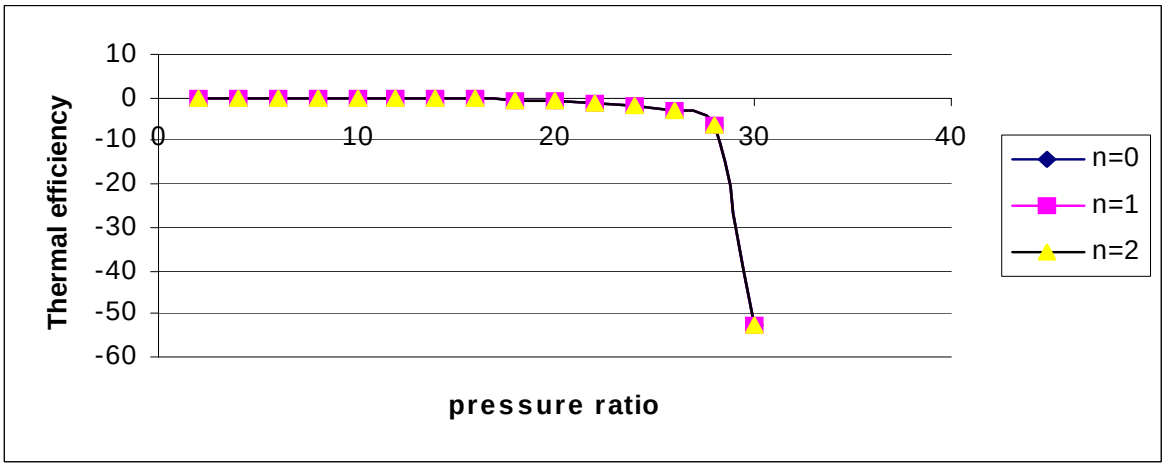

Fig3.9.5f (γ=1.6)

Fig 3.9.5 VARIATION OF THERMAL EFFICIENCY OF TOPPING CYCLE VS PRESSURE RATIO(TIT=1000K)

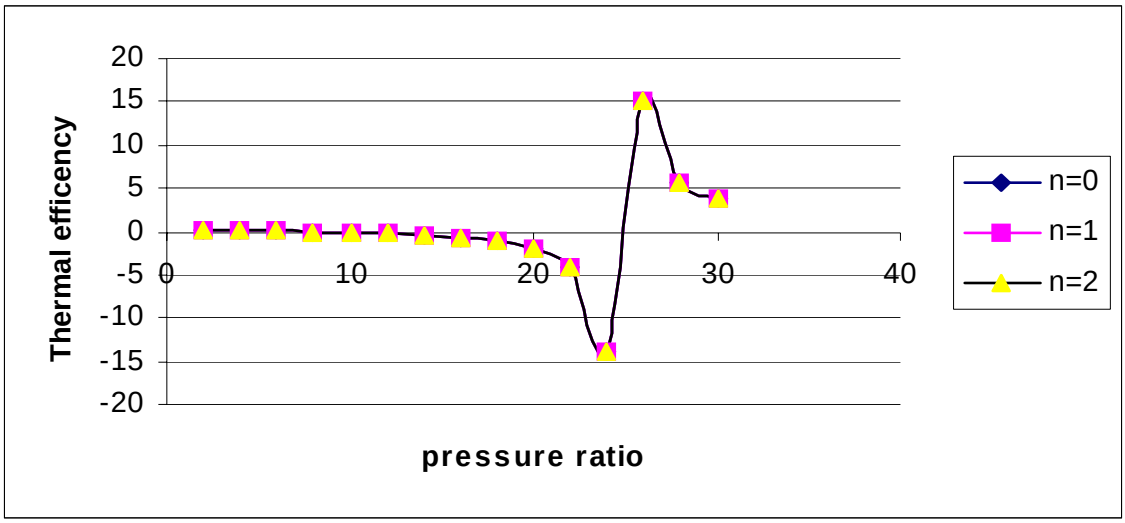

Fig3.9.5g (γ=1.66)

Fig 3.9.5 OF THERMAL EFFICIENCY OF TOPPING CYCLE VS PRESSURE RATIO(TIT=1000K)

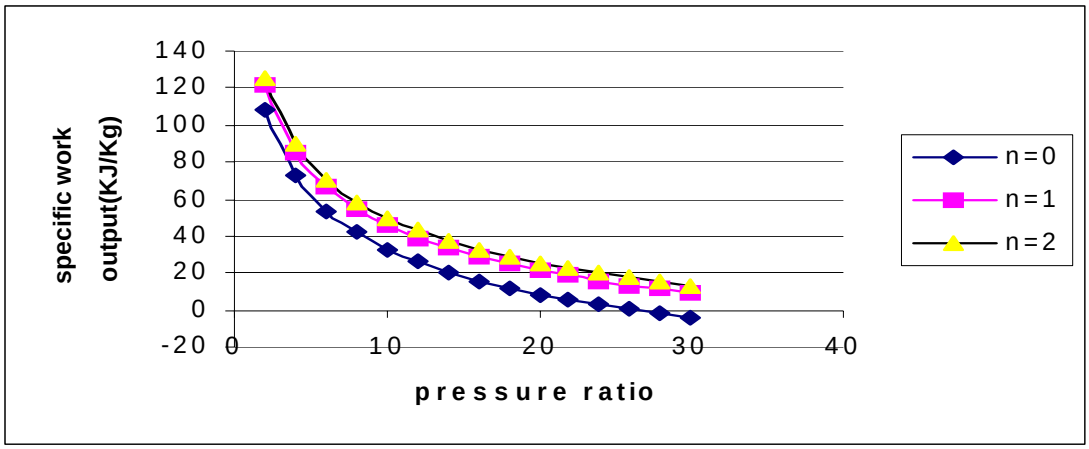

Fig 3.9.6a **γ=1.1**

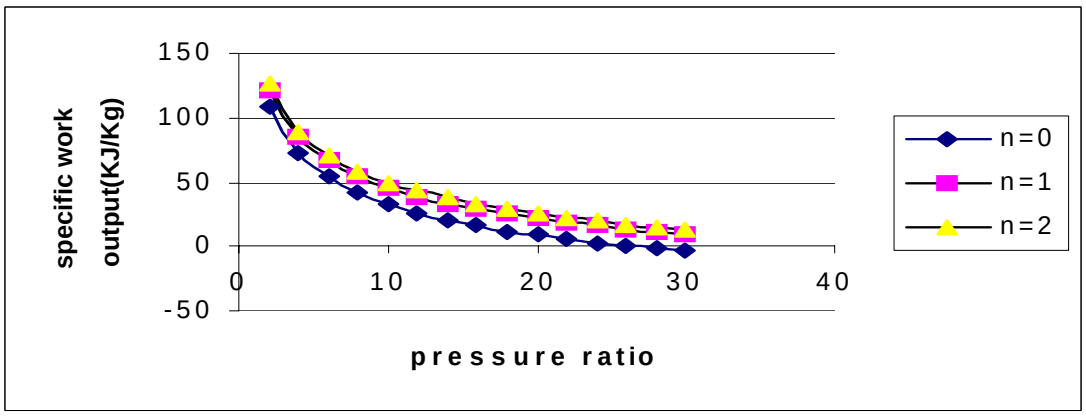

Fig 3.9.6b **(γ=1.2)**

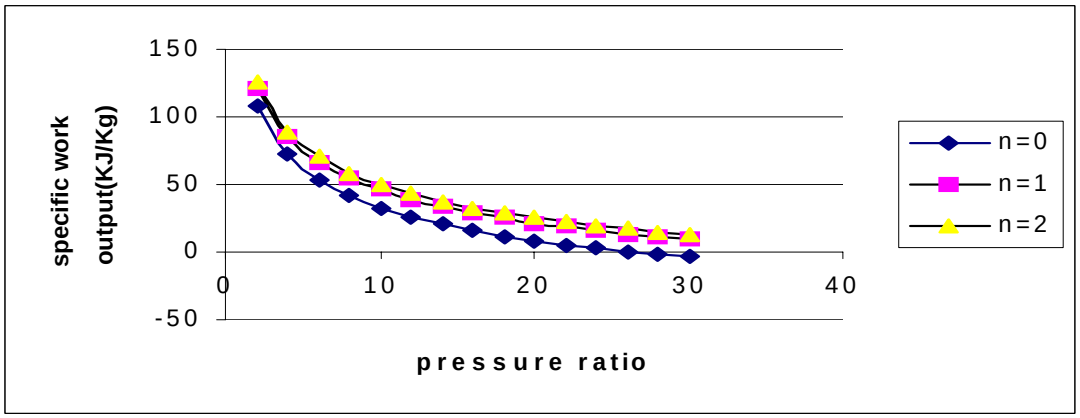

7

Fig 3.9.6c **(γ=1.3)**

Fig 3.9.6 VARIATION OF SPECIFIC OUTPUT OF BOTTOMING CYCLE VS PRESSURE RATIO(TIT=1000K)

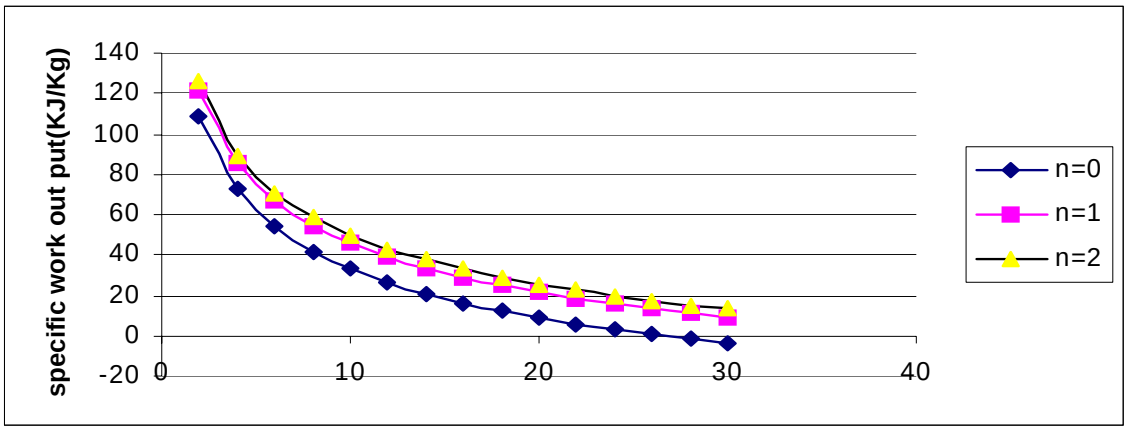

Fig 3.9.6d (γ=1.4)

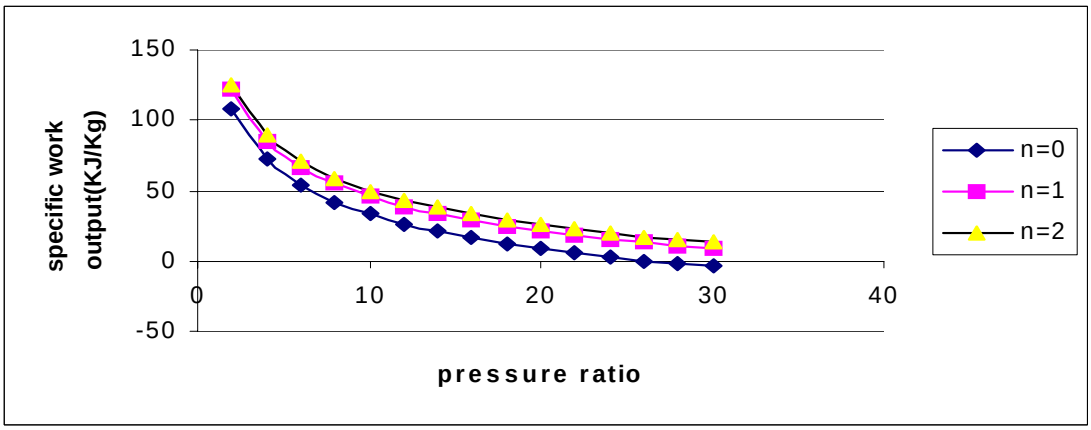

Fig 3.9.6e (γ=1.5)

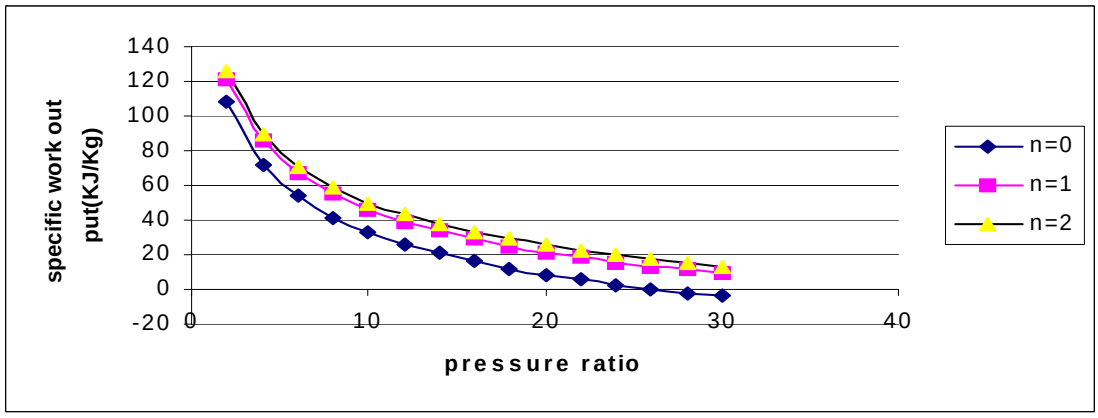

Fig 3.9.6f (γ=1.6)

Fig 3.9.6 VARIATION OF SPECIFIC OUTPUT OF BOTTOMING CYCLE VS PRESSURE RATIO(TIT=1000K)

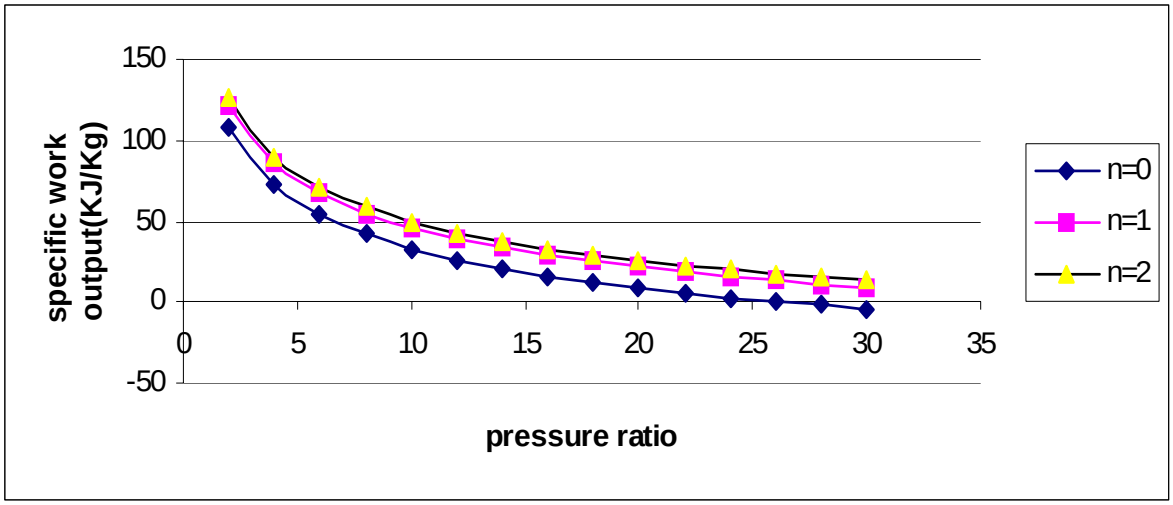

Fig 3.9.6g (γ=1.66)

Fig 3.9.6 VARIATION OF SPECIFIC OUTPUT OF BOTTOMING CYCLE VS PRESSURE RATIO(TIT=1000K)

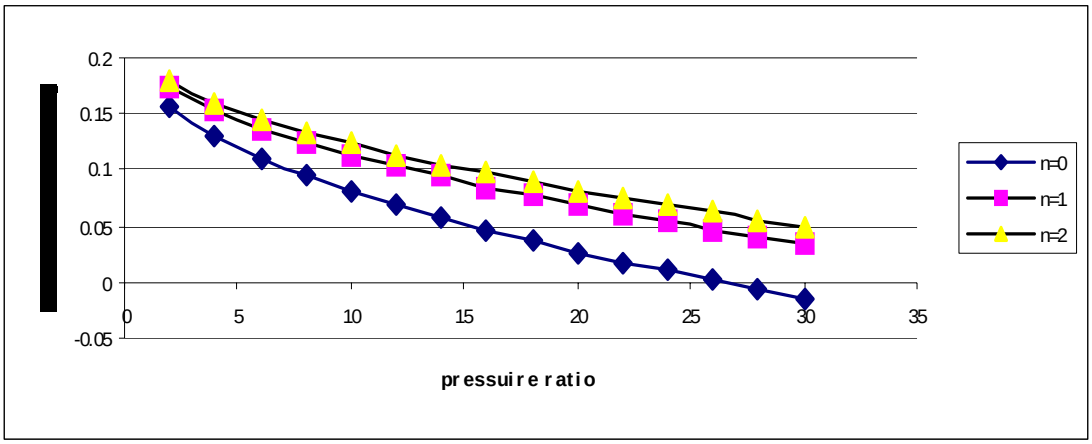

Fig 3.9.7a (γ=1.1)

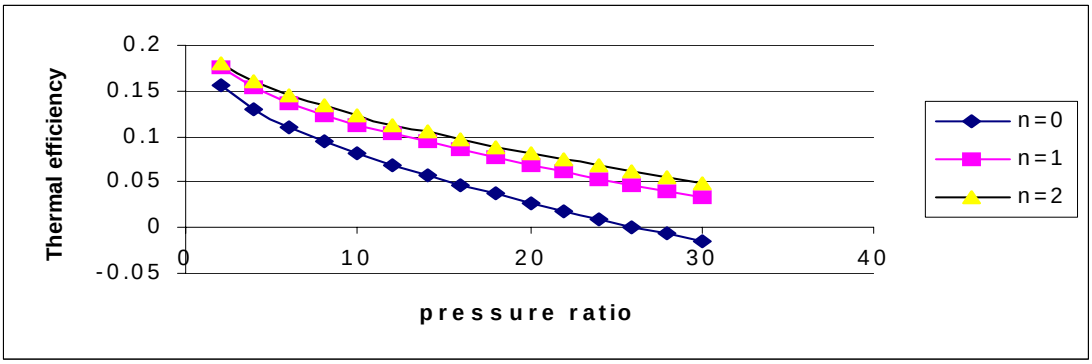

Fig 3.9.7b (γ=1.2)

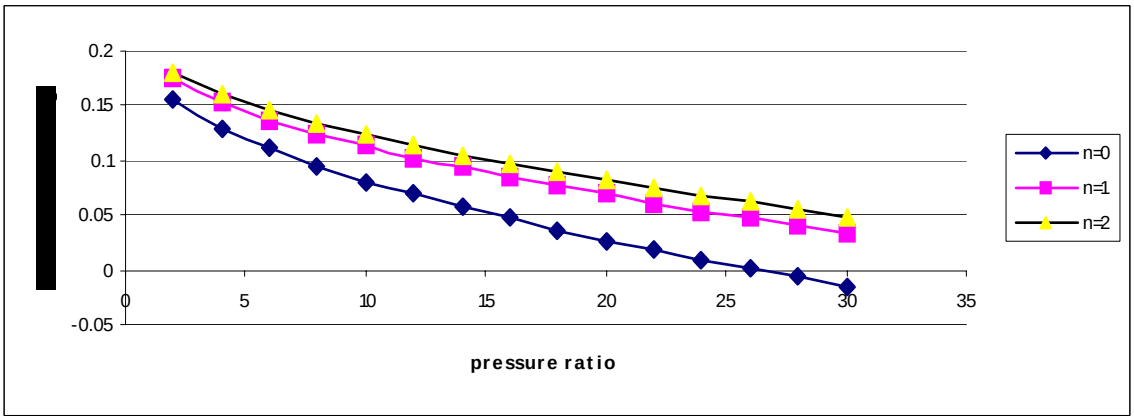

Fig 3.9.7c (γ=1.3)

Fig 3.9.7 VARIATION OF THERMAL EFFICIENCY OF BOTTOMING CYCLE VS PRESSURE RATIO(TIT=1000K)

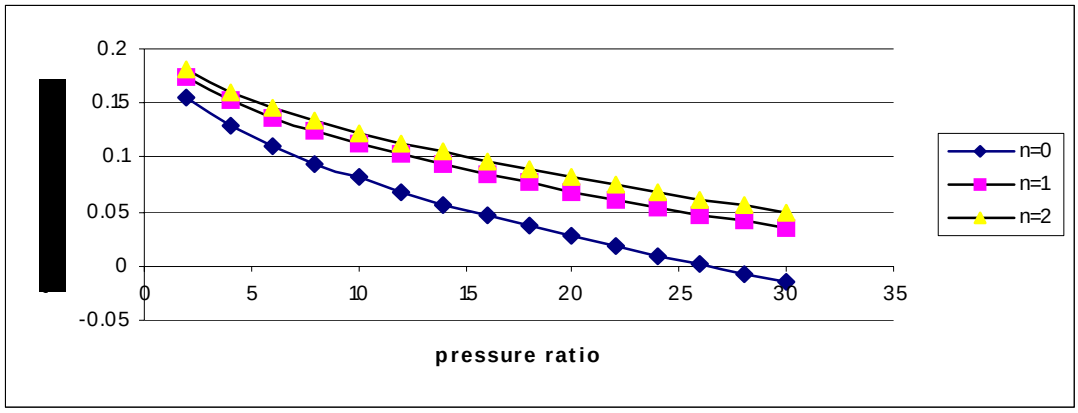

Fig 3.9.7d (γ=1.4)

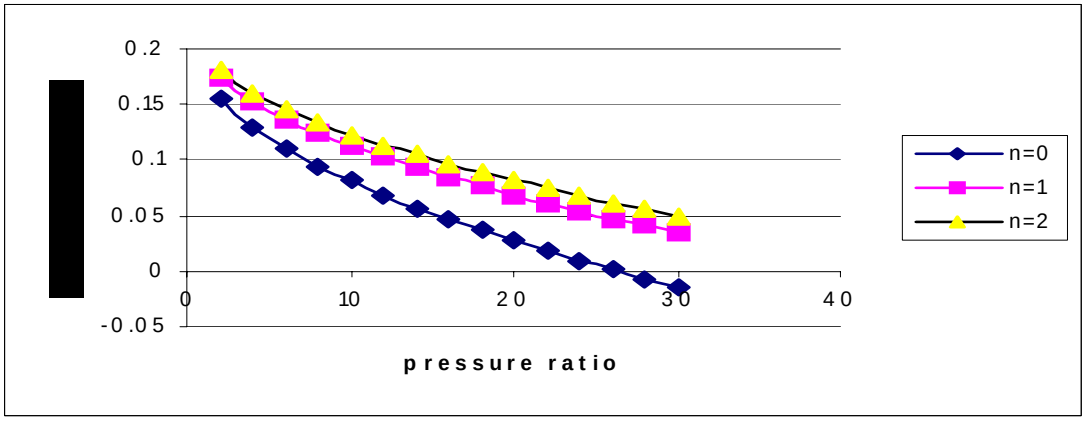

Fig 3.9.7e (γ=1.5)

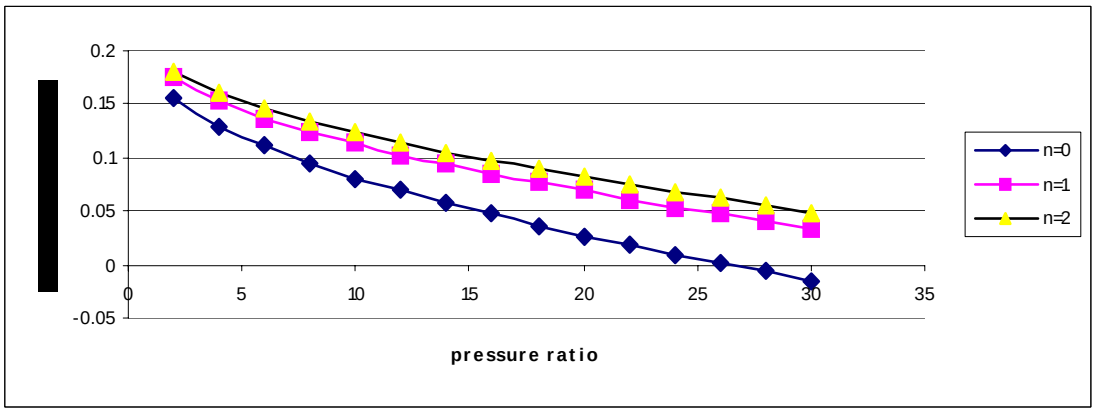

Fig 3.9.7f (γ=1.6)

Fig 3.9.7 VARIATION OF THERMAL EFFICIENCY OF BOTTOMING CYCLE VS PRESSURE RATIO(TIT=1000K)

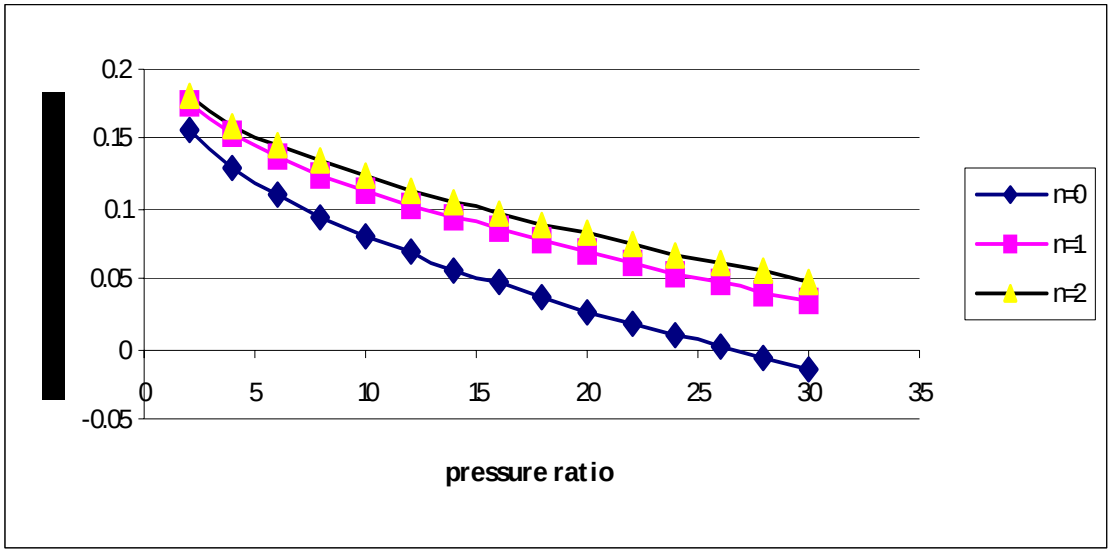

Fig 3.9.7g (γ=1.66)

Fig 3.9.7 VARIATION OF THERMAL EFFICIENCY OF BOTTOMING CYCLE VS PRESSURE RATIO(TIT=1000K)

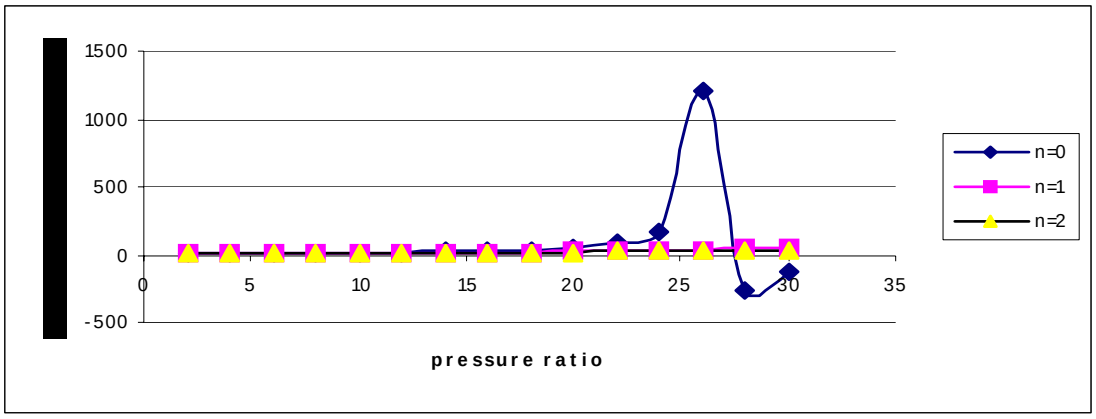

Fig 3.9.8a (γ=1.1)

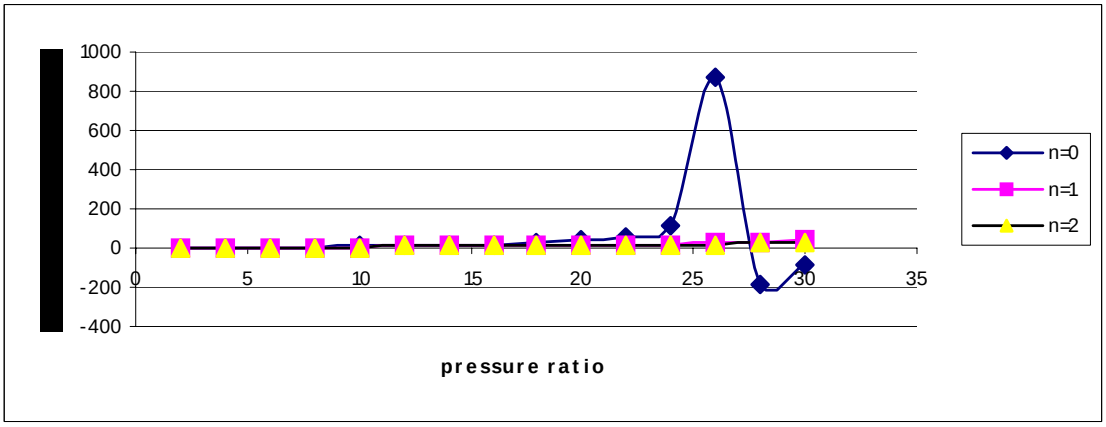

Fig 3.9.8b (γ=1.2)

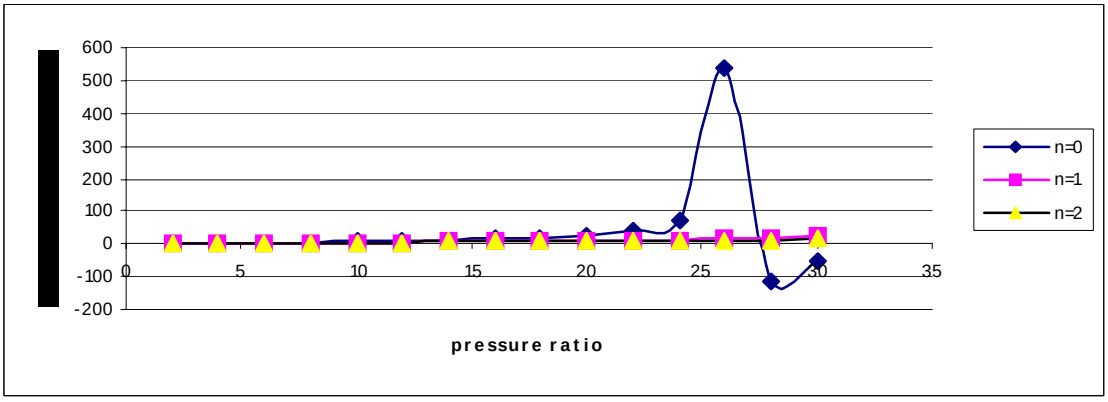

Fig 3.9.8c (γ=1.3)

Fig 3.9.8 VARIATION OF POWER RATIO OF MIRROR GAS TURBINE VS PRESSURE RATIO(TIT=1000K)

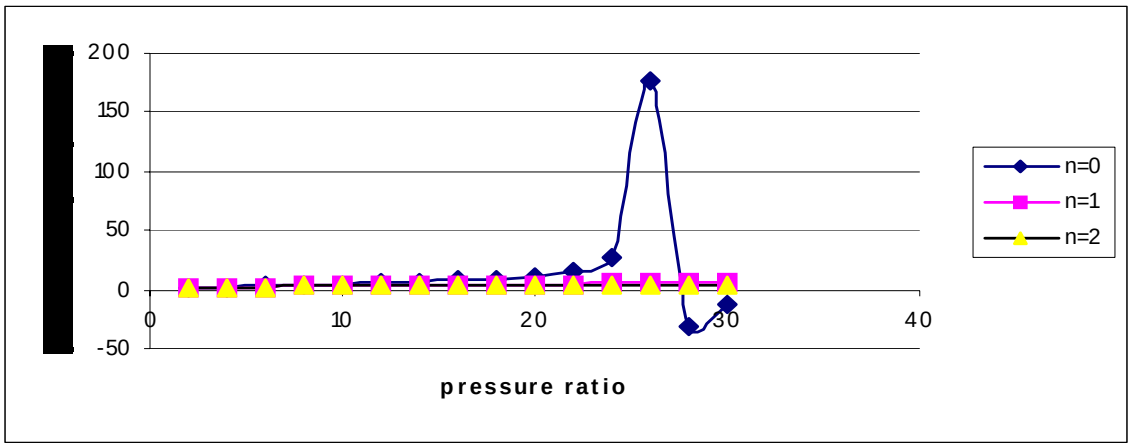

Fig 3.9.8d (γ=1.4)

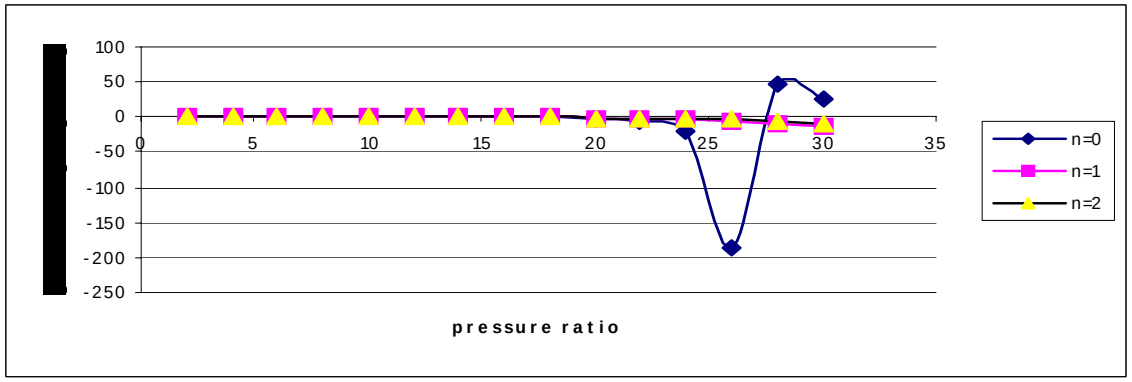

Fig 3.9.8e (γ=1.5)

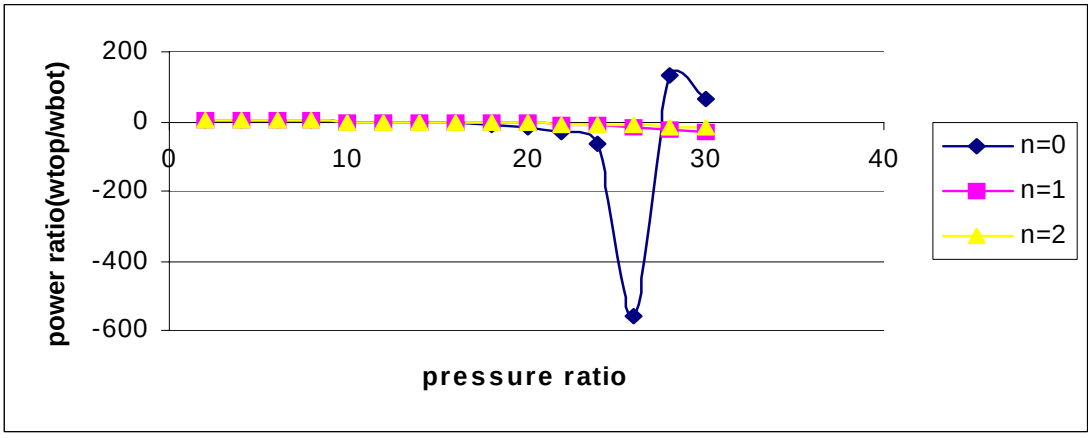

Fig 3.9.8f (γ=1.6)

Fig 3.9.8 VARIATION OF POWER RATIO OF MIRROR GAS TURBINE VS PRESSURE RATIO(TIT=1000K)

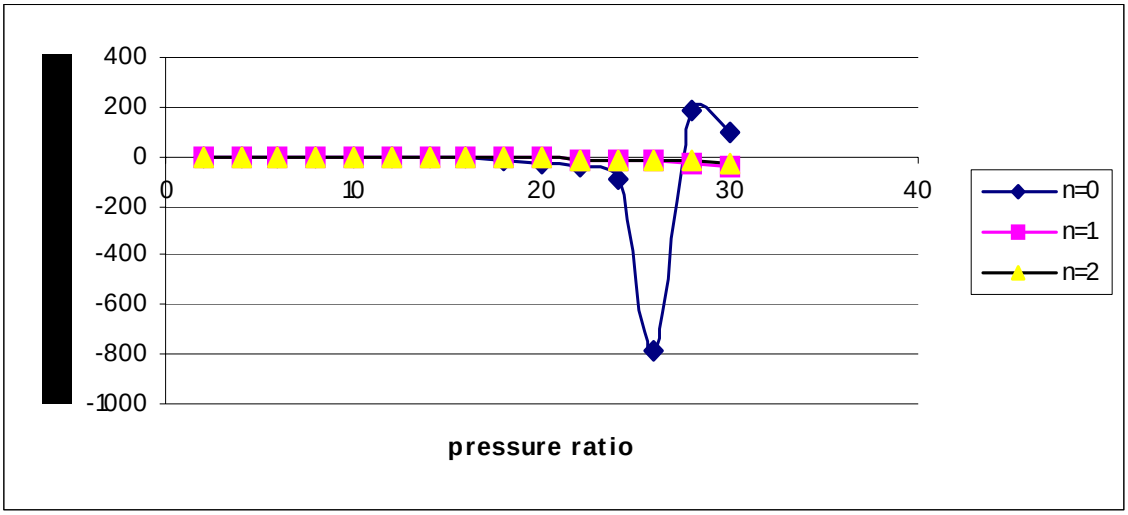

Fig 3.9.8g (γ=1.66)

Fig 3.9.8 VARIATION OF POWER RATIO OF MIRROR GAS TURBINE VS PRESSURE RATIO(TIT=1000K)

DISCUSSION OF RESULTS

From graph 3.1.2

- For each TIT, specific output mirror gas turbine increases with increases in pressure ratio of topping cycle (rp1).
- Specific output of mirror gas turbine is higher for higher TIT at particular pressure ratio (rp1).
- Optimum pressure ratio for maximum specific Work output (KJ/Kg) shifts towards higher-pressure ratio (rp1) with increase in TIT(K).
- With increase in number of intercooler in stages of compression of bottoming cycle, specific work output of mirror gas turbine increases, this is only due to decrease in work of compression in bottoming cycle.

From graph 3.1.3

- Thermal efficiency of mirror gas turbine is higher for higher TIT at particular pressure ratio(rp1).
- For higher TIT i.e.TIT=1600K &1800,thermal Efficiency of mirror gas turbine increases up to maximum value.
- With increase in number of intercooler in stages of compression of bottoming cycle, Thermal efficiency of mirror gas turbine increase, this is only due to decrease in work of compression in bottoming cycle.

From graph 3.1.4

- S.F.C is lower for higher TIT, at particular pressure ratio (rp1).
- S.F.C of mirror gas turbine decreases with intercooling in stages of compressor of bottoming cycle, this is only due to reduced work of compression of mirror gas

turbine.

From graph 3.1.5

- For each TIT, specific work output of topping cycle i.e. simple gas turbine cycle first increases with increase in pressure ratio of topping cycle (rp1)& then reaches maximum value at particular pressure ratio.
- Specific output of topping cycle i.e. simple gas turbine cycle is higher for higher TIT at particular pressure ratio.
- Optimum pressure ratio for maximum specific work output of topping cycle (KJ/Kg) shifts towards higher-pressure ratio with increase in TIT.
- There is no effect of increase in number of intercooling in stages of compression of bottoming cycle on specific work output of topping cycle, i.e. specific work output of topping cycle remains constant even with increase in no. of stages of intercooling.

From graph 3.1.6

- Thermal Efficiency of topping cycle decreases with increase inTIT.
- Thermal Efficiency of topping cycle is higher for higher TIT at particular pressure ratio (rp1).
- There is no effect of increase in number of intercooling in stages of compression of bottoming cycle on specific output of topping cycle, as a result thermal efficiency of topping cycle remains constant even with increase in no. of stages of intercooling.

From graph 3.1.7

- For each TIT, specific work output of bottoming cycle i.e. inverted gas turbine cycle first decreases with increase in pressure ratio of topping cycle (rp1)& then almost flattens with increase in pressure ratio (rp1).

- Specific work output of bottoming cycle i.e. inverted gas turbine cycle is higher for higher TIT at particular pressure ratio.

- With increase in number of intercooler in stage of compression of bottoming cycle, specific work output of bottoming cycle increases, due to decreases in work required for compression in bottoming cycle. As a result thermal efficiency of bottoming cycle increases with increase in no of intercooler in stage of compression.

From graph 3.1.8

- For each TIT, Thermal efficiency of bottoming cycle i.e. inverted gas turbine cycle first decreases with increase in pressure ratio of topping cycle (rp1)& then almost flattens with increase in pressure ratio (rp1).

- Thermal efficiency of bottoming cycle i.e. inverted gas turbine cycle is higher for higher TIT at particular pressure ratio.

- With increase in number of intercooler in stage of compression of bottoming cycle, specific work output of bottoming cycle increases, due to decreases in work required for compression in bottoming cycle. As a result thermal efficiency of bottoming cycle increases with increase in no of intercooler in stage of compression.

From graph 3.1.9

- For lower TIT i.e.TIT=1000K,power ratio (wtop/wbot)increase very rapidly with increase in pressure ratio (rp1) showing that load on topping cycle increases as compare to bottoming cycle with increase in pressure ratio &at pressure ratio (rp1) 25 power ratio reaches maximum value then starts decreasing with increase in pressure ratio(rp1) then starts increasing .

- For higher TITi.e.TIT1600K&1800K,power ratio (wtop/wbot) increases first with increase in pressure ratio &then almost flattens for higher pressure ratio

- Power ratio of mirror gas turbine is lower for higher TIT.

- With increase in number of intercooler in stage of compression of bottoming cycle, specific work output of bottoming cycle increase, due to decrease in work required for compression in bottoming cycle. As a result of this power ratio will decreases with increase in no of intercooling for particular TIT & pressure ratio.

From graph3.2.1

- For each TIT, specific output mirror gas turbine increases with increases in pressure ratio of topping cycle (rp1) and then reaches maximum value at particular pressure ratio (rp1). This value of pressure ratio (rp1) is called as optimum pressure ratio with respect to work.

- Specific output of mirror gas turbine is higher for higher TIT at particular pressure ratio (rp1).

- Optimum pressure ratio for maximum specific Work output (KJ/Kg) shifts towards higher-pressure ratio (rp1) with increase in TIT (K).

- With increase in number of intercooler in stages of compression of bottoming cycle, specific work output of mirror gas turbine increases, this is only due to decrease in work of compression in bottoming cycle.

From graph 3.2.2

- Thermal efficiency of mirror gas turbine is higher for higher TIT at particular pressure ratio (rp1).

- For higher TIT i.e. IT=1600K &1800,thermal Efficiency of mirror gas turbine increases up to maximum value.

- With increase in number of intercooler in stages of compression of bottoming cycle, Thermal efficiency of mirror gas turbine increase, this is only due to decrease in work of compression in bottoming cycle.

From graph 3.2.3

- S.F.C is lower for higher TIT, at particular pressure ratio (rp1).
- S.F.C of mirror gas turbine decreases with intercooling in stages of compressor of bottoming cycle, this is only due to reduced work of compression of mirror gas turbine.

From graph 3.2.4

- For each TIT, specific work output of topping cycle i.e. simple gas turbine cycle first increases with increase in pressure ratio of topping cycle (rp1)& then reaches maximum value at particular pressure ratio.
- Specific output of topping cycle i.e. simple gas turbine cycle is higher for higher TIT at particular pressure ratio.
- Optimum pressure ratio for maximum specific work output of topping cycle (KJ/Kg) shifts towards higher-pressure ratio with increase in TIT.
- There is no effect of increase in number of intercooling in stages of compression of bottoming cycle on specific work output of topping cycle, i.e. specific work output of topping cycle remains constant even with increase in no. of stages of intercooling.

From graph 3.2.5

- Thermal Efficiency of topping cycle decreases with increase inTIT.
- Thermal Efficiency of topping cycle is higher for higher TIT at particular pressure ratio (rp1).
- There is no effect of increase in number of intercooling in stages of compression of bottoming cycle on specific output of topping cycle, as a result thermal efficiency of topping cycle remains constant even with increase in no. of stages of intercooling.

From graph 3.2.6

- For each TIT, specific work output of bottoming cycle i.e. inverted gas turbine cycle first decreases with increase in pressure ratio of topping cycle (rp1)& then almost flattens with increase in pressure ratio (rp1).

- specific work output of bottoming cycle i.e. inverted gas turbine cycle is higher for higher TIT at particular pressure ratio.

- With increase in number of intercooler in stage of compression of bottoming cycle, specific work output of bottoming cycle increases, due to decreases in work required for compression in bottoming cycle. As a result thermal efficiency of bottoming cycle increases with increase in no of intercooler in stage of compression.

From graph 3.2.7

- For each TIT, Thermal efficiency of bottoming cycle i.e. inverted gas turbine cycle first decreases with increase in pressure ratio of topping cycle (rp1)& then almost flattens with increase in pressure ratio (rp1).

- Thermal efficiency of bottoming cycle i.e. inverted gas turbine cycle is higher for higher TIT at particular pressure ratio.

- With increase in number of intercooler in stage of compression of bottoming cycle, specific work output of bottoming cycle increases, due to decreases in work required for compression in bottoming cycle. As a result thermal efficiency of bottoming cycle increases with increase in no of intercooler in stage of compression.

From graph 3.2.8

- For lower TIT i.e.TIT=1000K,power ratio (wtop/wbot) increase very rapidly with increase in pressure ratio (rp1) showing that load on topping cycle increases as compare to bottoming cycle with increase in pressure ratio & at pressure ratio (rp1) 25 power ratio reaches maximum value then starts decreasing with increase in

pressure ratio (rp1) then starts increasing.

- For higher TITi.e.TIT1600K&1800K,power ratio (wtop/wbot) increases first with increase in pressure ratio &then almost flattens for higher pressure ratio

- Power ratio of mirror gas turbine is lower for higher TIT.

- With increase in number of intercooler in stage of compression of bottoming cycle, specific work output of bottoming cycle increase, due to decrease in work required for compression in bottoming cycle. As a result of this power ratio will decreases with increase in no of intercooling for particular TIT & pressure ratio.

From graph3.3.1

- For each TIT, specific output mirror gas turbine increases with increases in pressure ratio of topping cycle (rp1) and then reaches maximum value at particular pressure ratio (rp1) then almost flattens with increase in pressure ratio(rp1).. This value of pressure ratio (rp1) is called as optimum pressure ratio with respect to work.

- Specific output of mirror gas turbine is higher for higher TIT at particular pressure ratio (rp1).

- Optimum pressure ratio for maximum specific Work output (KJ/Kg) shifts towards higher-pressure ratio (rp1) with increase in TIT (K).

- With increase in number of intercooler in stages of compression of bottoming cycle, specific work output of mirror gas turbine increases, this is only due to decrease in work of compression in bottoming cycle.

From graph 3.3.2

- Thermal efficiency of mirror gas turbine is higher for higher TIT at particular pressure ratio (rp1).

- For higher TIT i.e. IT=1600K &1800,thermal Efficiency of mirror gas turbine

increases up to maximum value.

- With increase in number of intercooler in stages of compression of bottoming cycle, Thermal efficiency of mirror gas turbine increase, this is only due to decrease in work of compression in bottoming cycle.

From graph 3.3.3

- For lower TIT i.e.TIT=100K & 1200K S.F.C(Kg/K W. hr) of mirror gas turbine decrease up to minimum value with increase in pressure ratio of topping cycle (rp1)& then increase in S.F.C occur with further rise in pressure ratio(rp1).

- For higher TIT i.e.TIT=1600K & 1800K,S.F.C of mirror gas turbine decreases up to minimum value & then flattens with increase in pressure ratio(rp1).

- S.F.C is lower for higher TIT, at particular pressure ratio (rp1).

- S.F.C of mirror gas turbine decreases with intercooling in stages of compressor of bottoming cycle, this is only due to reduced work of compression of mirror gas turbine.

From graph 3.3.4

- For each TIT, specific work output of topping cycle i.e. simple gas turbine cycle first increases with increase in pressure ratio of topping cycle (rp1)& then reaches maximum value at particular pressure ratio.
- Specific output of topping cycle i.e. simple gas turbine cycle is higher for higher TIT at particular pressure ratio.
- Optimum pressure ratio for maximum specific work output of topping cycle (KJ/Kg) shifts towards higher-pressure ratio with increase in TIT.
- There is no effect of increase in number of intercooling in stages of compression of bottoming cycle on specific work output of topping cycle, i.e. specific work output of topping cycle remains constant even with increase in no. of stages of intercooling.

From graph 3.3.5

- Thermal Efficiency of topping cycle decreases with increase inTIT.
- Thermal Efficiency of topping cycle is higher for higher TIT at particular pressure ratio (rp1).
- There is no effect of increase in number of intercooling in stages of compression of bottoming cycle on specific output of topping cycle, as a result thermal efficiency of topping cycle remains constant even with increase in no. of stages of intercooling.

From graph 3.3.6

- For each TIT, specific work output of bottoming cycle i.e. inverted gas turbine cycle first decreases with increase in pressure ratio of topping cycle (rp1)& then almost flattens with increase in pressure ratio(rp1).
- Specific work output of bottoming cycle i.e. inverted gas turbine cycle is higher for

higher TIT at particular pressure ratio.

- With increase in number of intercooler in stage of compression of bottoming cycle, specific work output of bottoming cycle increases, due to decreases in work required for compression in bottoming cycle. As a result thermal efficiency of bottoming cycle increases with increase in no of intercooler in stage of compression.

From graph 3.3.7

- For each TIT, Thermal efficiency of bottoming cycle i.e. inverted gas turbine cycle first decreases with increase in pressure ratio of topping cycle (rp1)& then almost flattens with increase in pressure ratio (rp1).

- Thermal efficiency of bottoming cycle i.e. inverted gas turbine cycle is higher for higher TIT at particular pressure ratio.

- With increase in number of intercooler in stage of compression of bottoming cycle, specific work output of bottoming cycle increases, due to decreases in work required for compression in bottoming cycle. As a result thermal efficiency of bottoming cycle increases with increase in no of intercooler in stage of compression.

From graph 3.3.8

- For lower TIT i.e.TIT=1000K,power ratio (wtop/wbot) increase very rapidly with increase in pressure ratio (rp1) showing that load on topping cycle increases as compare to bottoming cycle with increase in pressure ratio &at pressure ratio (rp1) 25 power ratio reaches maximum value then starts decreasing with increase in pressure ratio (rp1) then starts increasing.

- For higher TITi.e.TIT1600K&1800K,power ratio (wtop/wbot) increases first with increase in pressure ratio &then almost flattens for higher pressure ratio

- Power ratio of mirror gas turbine is lower for higher TIT.

- With increase in number of intercooler in stage of compression of bottoming cycle, specific work output of bottoming cycle increase, due to decrease in work required for compression in bottoming cycle. As a result of this power ratio will decreases with increase in no of intercooling for particular TIT & pressure ratio.

From graph3.4.1

- For each TIT, specific output mirror gas turbine increases with increases in pressure ratio of topping cycle (rp1) and then reaches maximum value at particular pressure ratio (rp1) then almost flattens with increase in pressure ratio(rp1). This value of pressure ratio (rp1) is called as optimum pressure ratio with respect to work.

- Specific output of mirror gas turbine is higher for higher TIT at particular pressure ratio (rp1).

- Optimum pressure ratio for maximum specific Work output (KJ/Kg) shifts towards higher-pressure ratio (rp1) with increase in TIT (K).

- With increase in number of intercooler in stages of compression of bottoming cycle, specific work output of mirror gas turbine increases, this is only due to decrease in work of compression in bottoming cycle.

From graph 3.4.2

- Thermal efficiency of mirror gas turbine is higher for higher TIT at particular pressure ratio (rp1).

- For lower TIT i.e.TIT=100K & 1200K Thermal efficiency of mirror gas turbine increases up to maximum value with increase in pressure ratio of topping cycle(rp1)& then decrease in efficiency occur with further rise in pressure ratio(rp1).

- For higher TIT i.e. IT=1600K &1800,thermal Efficiency of mirror gas turbine increases up to maximum value.

- With increase in number of intercooler in stages of compression of bottoming cycle, Thermal efficiency of mirror gas turbine increase, this is only due to decrease in work of compression in bottoming cycle.

From graph 3.4.3

- For lower TIT i.e.TIT=100K & 1200K ,S.F.C(Kg/K W. hr)of mirror gas turbine decrease up to minimum value with increase in pressure ratio of topping cycle(rp1)& then increase in S.F.C occur with further rise in pressure ratio(rp1).

- For higher TIT i.e.TIT=1600K & 1800K, S.F.C of mirror gas turbine decreases up to minimum value & then flattens with increase in pressure ratio(rp1).

- S.F.C is lower for higher TIT, at particular pressure ratio (rp1).

- S.F.C of mirror gas turbine decreases with intercooling in stages of compressor of bottoming cycle, this is only due to reduced work of compression of mirror gas turbine.

From graph 3.4.4

- For each TIT, specific work output of topping cycle i.e. simple gas turbine cycle first increases with increase in pressure ratio of topping cycle (rp1)& then reaches maximum value at particular pressure ratio then decreases with increase in pressure ratio.

- Specific output of topping cycle i.e. simple gas turbine cycle is higher for higher TIT at particular pressure ratio.

- Optimum pressure ratio for maximum specific work output of topping cycle (KJ/Kg) shifts towards higher-pressure ratio with increase in TIT.

- There is no effect of increase in number of intercooling in stages of compression of bottoming cycle on specific work output of topping cycle, i.e. specific work output of

topping cycle remains constant even with increase in no. of stages of intercooling.

From graph 3.4.5

- Thermal Efficiency of topping cycle increases with increase inTIT.
- Thermal Efficiency of topping cycle is higher for higher TIT at particular pressure ratio (rp1).
- There is no effect of increase in number of intercooling in stages of compression of bottoming cycle on specific output of topping cycle, as a result thermal efficiency of topping cycle remains constant even with increase in no. of stages of intercooling.

From graph 3.4.6

- For each TIT, specific work output of bottoming cycle i.e. inverted gas turbine cycle first decreases with increase in pressure ratio of topping cycle (rp1)& then almost flattens with increase in pressure ratio (rp1).
- Specific work output of bottoming cycle i.e. inverted gas turbine cycle is higher for higher TIT at particular pressure ratio.
- With increase in number of intercooler in stage of compression of bottoming cycle, specific work output of bottoming cycle increases, due to decreases in work required for compression in bottoming cycle. As a result thermal efficiency of bottoming cycle increases with increase in no of intercooler in stage of compression.

From graph 3.4.7

- For each TIT, Thermal efficiency of bottoming cycle i.e. inverted gas turbine cycle first decreases with increase in pressure ratio of topping cycle (rp1)& then almost flattens with increase in pressure ratio (rp1).
- Thermal efficiency of bottoming cycle i.e. inverted gas turbine cycle is higher for higher TIT at particular pressure ratio.

- With increase in number of intercooler in stage of compression of bottoming cycle, specific work output of bottoming cycle increases, due to decreases in work required for compression in bottoming cycle. As a result thermal efficiency of bottoming cycle increases with increase in no of intercooler in stage of compression.

From graph 3.4.8

- For lower TIT i.e.TIT=1000K,power ratio (wtop/wbot)(n=0) increase very rapidly with increase in pressure ratio (rp1) showing that load on topping cycle increases as compare to bottoming cycle with increase in pressure ratio &at pressure ratio (rp1) 25 power ratio reaches maximum value then starts decreasing with increase in pressure ratio (rp1) then starts increasing.

- For higher TITi.e.TIT1600K&1800K,power ratio (wtop/wbot) increases first with increase in pressure ratio &then almost flattens for higher pressure ratio

- Power ratio of mirror gas turbine is lower for higher TIT.

- With increase in number of intercooler in stage of compression of bottoming cycle, specific work output of bottoming cycle increase, due to decrease in work required for compression in bottoming cycle. As a result of this power ratio will decreases with increase in no of intercooling for particular TIT & pressure ratio.

From graph3.5.1

- For each TIT, specific output mirror gas turbine increases with increases in pressure ratio of topping cycle (rp1) and then reaches maximum value at particular pressure ratio (rp1) then decreases with increase in pressure ratio (rp1). This value of pressure ratio (rp1) is called as optimum pressure ratio with respect to work.

- Specific output of mirror gas turbine is higher for higher TIT at particular pressure ratio (rp1).

- Optimum pressure ratio for maximum specific Work output (KJ/Kg) shifts towards

higher-pressure ratio (rp1) with increase in TIT (K).

- With increase in number of intercooler in stages of compression of bottoming cycle, specific work output of mirror gas turbine increases, this is only due to decrease in work of compression in bottoming cycle.

From graph 3.5.2

- Thermal efficiency of mirror gas turbine is higher for higher TIT at particular pressure ratio (rp1).

- For lower TIT i.e.TIT=100K & 1200K Thermal efficiency of mirror gas turbine increases up to maximum value with increase in pressure ratio of topping cycle (rp1)& then decrease in efficiency occur with further rise in pressure ratio (rp1).

- For higher TIT i.e. IT=1600K &1800,thermal Efficiency of mirror gas turbine increases up to maximum value.

- With increase in number of intercooler in stages of compression of bottoming cycle, Thermal efficiency of mirror gas turbine increase, this is only due to decrease in work of compression in bottoming cycle.

From graph 3.5.3

- For lower TIT i.e.TIT=100K & 1200K S.F.C (Kg/K W. hr)of mirror gas turbine decrease up to minimum value with increase in pressure ratio of topping cycle(rp1)& then increase in S.F.C occur with further rise in pressure ratio(rp1).

- For lower TIT i.e.TIT=1000K, S.F.C (Kg/K W. hr) of mirror gas turbine increase very rapidly with increase in pressure ratio (rp1) &at pressure ratio (rp1) 18-20 power ratio reaches maximum value then starts decreasing with increase in pressure ratio (rp1) then starts increasing.

- For higher TIT i.e.TIT=1600K & 1800K,S.F.C of mirror gas turbine decreases up to

minimum value & then flattens with increase in pressure ratio (rp1).

- S.F.C is lower for higher TIT, at particular pressure ratio (rp1).
- S.F.C of mirror gas turbine decreases with intercooling in stages of compressor of bottoming cycle, this is only due to reduced work of compression of mirror gas turbine.

From graph 3.5.4

- For each TIT, specific work output of topping cycle i.e. simple gas turbine cycle first increases with increase in pressure ratio of topping cycle (rp1)& then reaches maximum value at particular pressure ratio then decreases with increase in pressure ratio.
- Specific output of topping cycle i.e. simple gas turbine cycle is higher for higher TIT at particular pressure ratio.
    - Optimum pressure ratio for maximum specific work output of topping cycle (KJ/Kg) shifts towards higher-pressure ratio with increase in TIT.
    - There is no effect of increase in number of intercooling in stages of compression of bottoming cycle on specific work output of topping cycle, i.e. specific work output of topping cycle remains constant even with increase in no. of stages of intercooling.

From graph 3.5.5

- For lower TIT i.e.TIT=100K & 1200K Thermal efficiency of topping cycle increases up to maximum value with increase in pressure ratio of topping cycle (rp1)& then decrease in efficiency occur with further rise in pressure ratio (rp1).
- Thermal Efficiency of topping cycle increases with increase inTIT.
- Thermal Efficiency of topping cycle is higher for higher TIT at particular pressure

ratio (rp1).

- There is no effect of increase in number of intercooling in stages of compression of bottoming cycle on specific output of topping cycle, as a result thermal efficiency of topping cycle remains constant even with increase in no. of stages of intercooling.

From graph 3.5.6

- For each TIT, specific work output of bottoming cycle i.e. inverted gas turbine cycle first decreases with increase in pressure ratio of topping cycle (rp1)& then almost flattens with increase in pressure ratio (rp1).

- Specific work output of bottoming cycle i.e. inverted gas turbine cycle is higher for higher TIT at particular pressure ratio.

- With increase in number of intercooler in stage of compression of bottoming cycle, specific work output of bottoming cycle increases, due to decreases in work required for compression in bottoming cycle. As a result thermal efficiency of bottoming cycle increases with increase in no of intercooler in stage of compression.

From graph 3.5.7

- For each TIT, Thermal efficiency of bottoming cycle i.e. inverted gas turbine cycle first decreases with increase in pressure ratio of topping cycle (rp1)& then almost flattens with increase in pressure ratio (rp1).

- Thermal efficiency of bottoming cycle i.e. inverted gas turbine cycle is higher for higher TIT at particular pressure ratio.

- With increase in number of intercooler in stage of compression of bottoming cycle, specific work output of bottoming cycle increases, due to decreases in work required for compression in bottoming cycle. As a result thermal efficiency of bottoming cycle increases with increase in no of intercooler in stage of compression.

From graph 3.5.8

- For lower TIT i.e.TIT=1000K,power ratio (wtop/wbot) increase very rapidly with increase in pressure ratio (rp1) showing that load on topping cycle increases as compare to bottoming cycle with increase in pressure ratio &at pressure ratio (rp1) 25 power ratio reaches maximum value then starts decreasing with increase in pressure ratio (rp1) then starts increasing.

- For higher TITi.e.TIT1600K&1800K,power ratio (wtop/wbot) increases first with increase in pressure ratio &then almost flattens for higher pressure ratio

- Power ratio of mirror gas turbine is lower for higher TIT.

- With increase in number of intercooler in stage of compression of bottoming cycle, specific work output of bottoming cycle increase, due to decrease in work required for compression in bottoming cycle. As a result of this power ratio will decreases with increase in no of intercooling for particular TIT & pressure ratio.

\From graph3.6.1

- For each TIT, specific output mirror gas turbine increases with increases in pressure ratio of topping cycle (rp1) and then reaches maximum value at particular pressure ratio (rp1) then decreases with increase in pressure ratio(rp1). This value of pressure ratio (rp1) is called as optimum pressure ratio with respect to work.

- Specific output of mirror gas turbine is higher for higher TIT at particular pressure ratio (rp1).

- Optimum pressure ratio for maximum specific Work output (KJ/Kg) shifts towards higher-pressure ratio (rp1) with increase in TIT (K).

- With increase in number of intercooler in stages of compression of bottoming cycle, specific work output of mirror gas turbine increases, this is only due to decrease in work of compression in bottoming cycle.

From graph 3.6.2

- Thermal efficiency of mirror gas turbine is higher for higher TIT at particular pressure ratio (rp1).
- For lower TIT i.e.TIT=100K & 1200K Thermal efficiency of mirror gas turbine increases up to maximum value with increase in pressure ratio of topping cycle(rp1)& then decrease in efficiency occur with further rise in pressure ratio(rp1).
- For higher TIT i.e. IT=1600K &1800,thermal Efficiency of mirror gas turbine increases up to maximum value.
- With increase in number of intercooler in stages of compression of bottoming cycle, Thermal efficiency of mirror gas turbine increase, this is only due to decrease in work of compression in bottoming cycle.

From graph 3.6.3

- For lower TIT i.e.TIT=100K & 1200K, S.F.C(Kg/K W. hr)of mirror gas turbine decrease up to minimum value with increase in pressure ratio of topping cycle(rp1)& then increase in S.F.C occur with further rise in pressure ratio(rp1). Then this phenomenon continues in further rise in pressure ratio.
- For lower TIT i.e.TIT=1000K S.F.C(Kg/K W. hr)of mirror gas turbine increase very rapidly with increase in pressure ratio (rp1) &at pressure ratio (rp1) 18-20 power ratio reaches maximum value then starts decreasing with increase in pressure ratio (rp1) then starts increasing.
- For higher TIT i.e.TIT=1600K & 1800K ,S.F.C of mirror gas turbine decreases up to minimum value & then flattens with increase in pressure ratio(rp1).
- S.F.C is lower for higher TIT, at particular pressure ratio (rp1).
- S.F.C of mirror gas turbine decreases with intercooling in stages of compressor of

bottoming cycle, this is only due to reduced work of compression of mirror gas turbine.

From graph 3.6.4

- For each TIT, specific work output of topping cycle i.e. simple gas turbine cycle first increases with increase in pressure ratio of topping cycle (rp1)& then reaches maximum value at particular pressure ratio then decreases with increase in pressure ratio.

- Specific output of topping cycle i.e. simple gas turbine cycle is higher for higher TIT at particular pressure ratio.

- Optimum pressure ratio for maximum specific work output of topping cycle (KJ/Kg) shifts towards higher-pressure ratio with increase in TIT.

- There is no effect of increase in number of intercooling in stages of compression of bottoming cycle on specific work output of topping cycle, i.e. specific work output of topping cycle remains constant even with increase in no. of stages of intercooling.

From graph 3.6.5

- For lower TIT i.e.TIT=100K & 1200K Thermal efficiency of topping cycle increases up to maximum value with increase in pressure ratio of topping cycle(rp1)& then rapid decrease in efficiency occur with further rise in pressure ratio(rp1).

- Thermal Efficiency of topping cycle increases with increase inTIT.

- Thermal Efficiency of topping cycle is higher for higher TIT at particular pressure ratio (rp1).

- There is no effect of increase in number of intercooling in stages of compression of bottoming cycle on specific output of topping cycle, as a result thermal efficiency of topping cycle remains constant even with increase in no. of stages of intercooling.

From graph 3.6.6

- For each TIT, specific work output of bottoming cycle i.e.inverted gas turbine cycle first decreases with increase in pressure ratio of topping cycle (rp1)& then almost flattens with increase in pressure ratio (rp1).

- Specific work output of bottoming cycle i.e. inverted gas turbine cycle is higher for higher TIT at particular pressure ratio.

- With increase in number of intercooler in stage of compression of bottoming cycle, specific work output of bottoming cycle increases, due to decreases in work required for compression in bottoming cycle. As a result thermal efficiency of bottoming cycle increases with increase in no of intercooler in stage of compression.

From graph 3.6.7

- For each TIT, Thermal efficiency of bottoming cycle i.e. inverted gas turbine cycle first decreases with increase in pressure ratio of topping cycle (rp1)& then almost flattens with increase in pressure ratio (rp1).

- Thermal efficiency of bottoming cycle i.e. inverted gas turbine cycle is higher for higher TIT at particular pressure ratio.

- With increase in number of intercooler in stage of compression of bottoming cycle, specific work output of bottoming cycle increases, due to decreases in work required for compression in bottoming cycle. As a result thermal efficiency of bottoming cycle increases with increase in no of intercooler in stage of compression.

From graph 3.6.8

- For lower TIT i.e.TIT=1000K,power ratio (wtop/wbot) increases with increase in pressure ratio (rp1) showing that load on topping cycle increases as compare to bottoming cycle with increase in pressure ratio &at pressure ratio (rp1) 25 power ratio reaches minimum value then starts increasing with increase in pressure ratio (rp1)

then starts decreasing.

- For higher TITi.e.TIT1600K&1800K,power ratio (wtop/wbot) increases first with increase in pressure ratio &then almost flattens for higher pressure ratio

- Power ratio of mirror gas turbine is lower for higher TIT.

- With increase in number of intercooler in stage of compression of bottoming cycle, specific work output of bottoming cycle increase, due to decrease in work required for compression in bottoming cycle. As a result of this power ratio will decreases with increase in no of intercooling for particular TIT & pressure ratio.

From graph3.7.1

- For each TIT, specific output mirror gas turbine increases with increases in pressure ratio of topping cycle (rp1) and then reaches maximum value at particular pressure ratio (rp1) then decreases with increase in pressure ratio(rp1). This value of pressure ratio (rp1) is called as optimum pressure ratio with respect to work.

- Specific output of mirror gas turbine is higher for higher TIT at particular pressure ratio (rp1).

- Optimum pressure ratio for maximum specific Work output (KJ/Kg) shifts towards higher-pressure ratio (rp1) with increase in TIT (K).

- With increase in number of intercooler in stages of compression of bottoming cycle, specific work output of mirror gas turbine increases, this is only due to decrease in work of compression in bottoming cycle.

From graph 3.7.2

- Thermal efficiency of mirror gas turbine is higher for higher TIT at particular pressure ratio (rp1).

- For lower TIT i.e.TIT=100K & 1200K Thermal efficiency of mirror gas turbine

increases up to maximum value with increase in pressure ratio of topping cycle(rp1)& then decrease in efficiency occur with further rise in pressure ratio(rp1).

- For higher TIT i.e.TIT=1600K &1800,thermal Efficiency of mirror gas turbine increases up to maximum value.

- With increase in number of intercooler in stages of compression of bottoming cycle, Thermal efficiency of mirror gas turbine increase, this is only due to decrease in work of compression in bottoming cycle.

From graph 3.7.3

- For lower TIT i.e.TIT=100K & 1200K,S.F.C(Kg/K W. hr)of mirror gas turbine decrease up to minimum value with increase in pressure ratio of topping cycle(rp1)& then increase in S.F.C occur with further rise in pressure ratio(rp1). Then this phenomena continues in further rise in pressure ratio.

- For lower TIT i.e.TIT=1000K, S.F.C(Kg/K W. hr)of mirror gas turbine increase very rapidly with increase in pressure ratio (rp1) .

- For higher TIT i.e.TIT=1600K & 1800K,S.F.C of mirror gas turbine decreases up to minimum value & then flattens with increase in pressure ratio(rp1).

- S.F.C is lower for higher TIT, at particular pressure ratio (rp1).

- S.F.C of mirror gas turbine decreases with intercooling in stages of compressor of bottoming cycle, this is only due to reduced work of compression of mirror gas turbine.

From graph 3.7.4

- For each TIT, specific work output of topping cycle i.e. simple gas turbine cycle first increases with increase in pressure ratio of topping cycle (rp1)& then reaches maximum value at particular pressure ratio then decreases with increase in pressure

ratio.

- Specific output of topping cycle i.e. simple gas turbine cycle is higher for higher TIT at particular pressure ratio.

- Optimum pressure ratio for maximum specific work output of topping cycle (KJ/Kg) shifts towards higher-pressure ratio with increase in TIT.

- There is no effect of increase in number of intercooling in stages of compression of bottoming cycle on specific work output of topping cycle, i.e. specific work output of topping cycle remains constant even with increase in no. of stages of intercooling.

From graph 3.7.5

- For lower TIT i.e.TIT=100K & 1200K Thermal efficiency of topping cycle increases up to maximum value with increase in pressure ratio of topping cycle (rp1)& then rapid decrease in efficiency occur with further rise in pressure ratio(rp1).

- Thermal Efficiency of topping cycle increases with increase inTIT.

- Thermal Efficiency of topping cycle is higher for higher TIT at particular pressure ratio (rp1).

- There is no effect of increase in number of intercooling in stages of compression of bottoming cycle on specific output of topping cycle, as a result thermal efficiency of topping cycle remains constant even with increase in no. of stages of intercooling.

From graph 3.7.6

- For each TIT, specific work output of bottoming cycle i.e. inverted gas turbine cycle first decreases with increase in pressure ratio of topping cycle (rp1)& then almost flattens with increase in pressure ratio (rp1).

- Specific work output of bottoming cycle i.e. inverted gas turbine cycle is higher for higher TIT at particular pressure ratio.

- With increase in number of intercooler in stage of compression of bottoming cycle, specific work output of bottoming cycle increases, due to decreases in work required for compression in bottoming cycle. As a result thermal efficiency of bottoming cycle increases with increase in no of intercooler in stage of compression.

From graph 3.7.7

- For each TIT, Thermal efficiency of bottoming cycle i.e. inverted gas turbine cycle first decreases with increase in pressure ratio of topping cycle (rp1)& then almost flattens with increase in pressure ratio (rp1).

- Thermal efficiency of bottoming cycle i.e. inverted gas turbine cycle is higher for higher TIT at particular pressure ratio.

- With increase in number of intercooler in stage of compression of bottoming cycle, specific work output of bottoming cycle increases, due to decreases in work required for compression in bottoming cycle. As a result thermal efficiency of bottoming cycle increases with increase in no of intercooler in stage of compression.

From graph 3.7.8

- For lower TIT i.e.TIT=1000K,power ratio (wtop/wbot) increases with increase in pressure ratio (rp1) showing that load on topping cycle increases as compare to bottoming cycle with increase in pressure ratio &at pressure ratio (rp1) 25 power ratio reaches minimum value then starts increasing with increase in pressure ratio (rp1) then starts decreasing.

- For higher TITi.e.TIT1600K&1800K,power ratio (wtop/wbot) increases first with increase in pressure ratio &then almost flattens for higher pressure ratio

- Power ratio of mirror gas turbine is lower for higher TIT.

- With increase in number of intercooler in stage of compression of bottoming cycle, specific work output of bottoming cycle increase, due to decrease in work required

for compression in bottoming cycle. As a result of this power ratio will decreases with increase in no of intercooling for particular TIT & pressure ratio.

From graph3.8.1

- For γ =1.1,1.2,1.3,1.4, specific output mirror gas turbine increases with increases in pressure ratio of topping cycle (rp1) and then reaches maximum value at particular pressure ratio (rp1) then almost flattens with increase in pressure ratio (rp1). This value of pressure ratio (rp1) is called as optimum pressure ratio with respect to work.

- For γ =1.5,1.6,1.66, specific output mirror gas turbine decreases with increase in pressure ratio (rp1).

- Specific output of mirror gas turbine is higher for higher TIT at particular pressure ratio (rp1).

- Optimum pressure ratio for maximum specific Work output (KJ/Kg) shifts towards higher-pressure ratio (rp1) with increase in TIT (K).

- With increase in number of intercooler in stages of compression of bottoming cycle, specific work output of mirror gas turbine increases, this is only due to decrease in work of compression in bottoming cycle.

From graph 3.8.2

- Thermal efficiency of mirror gas turbine is higher for higher TIT at particular pressure ratio (rp1).

- For lower TIT i.e.TIT=100K & 1200K Thermal efficiency of mirror gas turbine increases up to maximum value with increase in pressure ratio of topping cycle (rp1)& then decrease in efficiency occur with further rise in pressure ratio (rp1).

- For higher TIT i.e. TIT=1600K &1800,thermal Efficiency of mirror gas turbine increases up to maximum value.

- With increase in number of intercooler in stages of compression of bottoming cycle, Thermal efficiency of mirror gas turbine increase, this is only due to decrease in work of compression in bottoming cycle.

- For γ =1.1,1.2,1.3,1.4 thermal efficiency of mirror gas turbine increases with increases in pressure ratio of topping cycle (rp1).

- For γ =1.5,1.6,1.66, thermal efficiency of mirror gas turbine decreases with increases in pressure ratio of topping cycle (rp1).

From graph 3.8.3

- For γ =1.1,1.2,1.3,1.4 S.F.C (Kg/K W. hr) of mirror gas turbine increases with increases in pressure ratio of topping cycle (rp1).

- For γ =1.5,1.6,1.66, S.F.C (Kg/K W. hr) of mirror gas turbine increases with increase in pressure ratio initially then decreases with increases in pressure ratio of topping cycle (rp1). After reaching minimum value again it starts increasing with increases in pressure ratio.

- S.F.C of mirror gas turbine decreases with intercooling in stages of compressor of bottoming cycle, this is only due to reduced work of compression of mirror gas turbine.

From graph 3.8.4

- For γ =1.1,1.2,1.3,1.4, specific output topping cycle increases with increases in pressure ratio of topping cycle (rp1) and then reaches maximum value at particular pressure ratio (rp1) then almost flattens with increase in pressure ratio (rp1). This value of pressure ratio (rp1) is called as optimum pressure ratio with respect to work.

- For γ =1.5,1.6,1.66, specific output topping cycle decreases with increase in pressure ratio (rp1).

- Specific output of topping cycle is higher for higher TIT at particular pressure ratio (rp1).

- Optimum pressure ratio for maximum specific Work output (KJ/Kg) shifts towards higher-pressure ratio (rp1) with increase in TIT (K).

- There is no effect of increase in number of intercooling in stages of compression of bottoming cycle on specific work output of topping cycle, i.e. specific work output of topping cycle remains constant even with increase in no. of stages of intercooling.

From graph 3.8.5

- Thermal efficiency of topping cycle is higher for higher TIT at particular pressure ratio (rp1).

- For lower TIT i.e.TIT=100K & 1200K Thermal efficiency of topping cycle increases up to maximum value with increase in pressure ratio of topping cycle (rp1)& then decrease in efficiency occur with further rise in pressure ratio (rp1).

- For γ =1.1,1.2,1.3,1.4 thermal efficiency of topping cycle increases with increases in pressure ratio of topping cycle (rp1).

- For γ =1.5,1.6,1.66, thermal efficiency of topping cycle decreases with increases in pressure ratio of topping cycle (rp1).

- For γ =1.1,1.2,1.3,1.4, Thermal efficiency of topping cycle increases with increase in pressure ratio of topping cycle (rp1) then almost flattens with increase in pressure ratio (rp1).

- For γ =1.5,1.6,1.66, Thermal efficiency of topping cycle increases up to maximum value with increase in pressure ratio of topping cycle(rp1)& then rapid decrease in efficiency occur with further rise in pressure ratio(rp1).

- Thermal Efficiency of topping cycle increases with increase inTIT.

- Thermal Efficiency of topping cycle is higher for higher TIT at particular pressure ratio (rp1).

- There is no effect of increase in number of intercooling in stages of compression of bottoming cycle on specific output of topping cycle, as a result thermal efficiency of topping cycle remains constant even with increase in no. of stages of intercooling.

From graph 3.8.6

- For each **γ**, specific work output of bottoming cycle i.e. inverted gas turbine cycle first decreases with increase in pressure ratio of topping cycle (rp1)& then almost flattens with increase in pressure ratio (rp1).

- Specific work output of bottoming cycle i.e. inverted gas turbine cycle is higher for higher TIT at particular pressure ratio.

- With increase in number of intercooler in stage of compression of bottoming cycle, specific work output of bottoming cycle increases, due to decreases in work required for compression in bottoming cycle. As a result thermal efficiency of bottoming cycle increases with increase in no of intercooler in stage of compression.

From graph 3.8.7

- For each **γ,** Thermal efficiency of bottoming cycle i.e. inverted gas turbine cycle first decreases with increase in pressure ratio of topping cycle (rp1)& then almost flattens with increase in pressure ratio (rp1).

- Thermal efficiency of bottoming cycle i.e. inverted gas turbine cycle is higher for higher TIT at particular pressure ratio.

- With increase in number of intercooler in stage of compression of bottoming cycle, specific work output of bottoming cycle increases, due to decreases in work required for compression in bottoming cycle. As a result thermal efficiency of bottoming cycle increases with increase in no of intercooler in stage of compression.

From graph 3.8.8

- For γ =1.1,1.2,1.3,1.4 power ratio (wtop/wbot) increases with increases in pressure ratio of topping cycle (rp1).

- For γ =1.5,1.6,1.66, power ratio (wtop/wbot) decreases with increases in pressure ratio of topping cycle (rp1).

- For γ =1.1,1.2,1.3,1.4, power ratio (wtop/wbot) increases with increase in pressure ratio of topping cycle(rp1) then increases sharply and decreases with increase in pressure ratio(rp1).

- For γ =1.5,1.6,1.66, power ratio (wtop/wbot) increases up to maximum value with increase in pressure ratio of topping cycle (rp1)& then rapid decrease in efficiency occur with further rise in pressure ratio(rp1).

- For γ =1.1,1.2,1.3,1.4, (n=1,2) power ratio (wtop/wbot) increases with increase in pressure ratio of topping cycle (rp1). For γ =1.5,1.6,1.66, (n=1,2) power ratio (wtop/wbot) decreases with increase in pressure ratio of topping cycle (rp1)

From graph3.9.1

- For γ = 1.1,1.2 specific output mirror gas turbine increases with increases in pressure ratio of topping cycle (rp1) and then reaches maximum value at particular pressure ratio (rp1) then almost flattens with increase in pressure ratio (rp1). This value of pressure ratio (rp1) is called as optimum pressure ratio with respect to work.

- For γ =1.3,1.4,1.5,1.6,1.66, specific output mirror gas turbine increases with increases in pressure ratio of topping cycle (rp1) and then reaches maximum value at particular pressure ratio (rp1) & then decreases with increase in pressure ratio (rp1).

- Specific output of mirror gas turbine is higher for higher TIT at particular pressure ratio (rp1).

- Optimum pressure ratio for maximum specific Work output (KJ/Kg) shifts towards higher-pressure ratio (rp1) with increase in TIT (K).

- With increase in number of intercooler in stages of compression of bottoming cycle, specific work output of mirror gas turbine increases, this is only due to decrease in work of compression in bottoming cycle.

From graph 3.9.2

- For γ = 1.1,1.2, 1.3 Thermal efficiency mirror gas turbine increases with increases in pressure ratio of topping cycle (rp1) and then reaches maximum value at particular pressure ratio (rp1) then almost flattens with increase in pressure ratio (rp1). This value of pressure ratio (rp1) is called as optimum pressure ratio with respect to work.

- For γ =1.4,1.5,1.6,1.66, Thermal efficiency mirror gas turbine increases with increases in pressure ratio of topping cycle (rp1) and then reaches maximum value at particular pressure ratio (rp1) & then decreases with increase in pressure ratio (rp1).

- Thermal efficiency of mirror gas turbine is higher for higher TIT at particular pressure ratio (rp1).

- Optimum pressure ratio for maximum Thermal efficiency shifts towards higher-pressure ratio (rp1) with increase in TIT (K).

- With increase in number of intercooler in stages of compression of bottoming cycle, Thermal efficiency of mirror gas turbine increases, this is only due to decrease in work of compression in bottoming cycle.

From graph 3.9.3

- For γ =1.1,1.2, S.F.C (Kg/K W. hr) of mirror gas turbine decreases with increases in pressure ratio of topping cycle (rp1).

- For γ =1.3,1.4, S.F.C (Kg/K W. hr) of mirror gas turbine decreases with increase in

pressure ratio initially then increases with increases in pressure ratio of topping cycle (rp1).

- For γ =1.5,1.6,1.66, S.F.C (Kg/K W. hr) of mirror gas turbine increases with increase in pressure ratio initially then after reaching maximum value again it starts decreasing with increases in pressure ratio. After reaching minimum value again increases with increases in pressure ratio of topping cycle (rp1).

- S.F.C of mirror gas turbine decreases with intercooling in stages of compressor of bottoming cycle, this is only due to reduced work of compression of mirror gas turbine.

From graph 3.9.4

- For γ =1.1,1.2, specific output topping cycle increases with increases in pressure ratio of topping cycle (rp1) and then reaches maximum value at particular pressure ratio (rp1) then almost flattens with increase in pressure ratio (rp1). This value of pressure ratio (rp1) is called as optimum pressure ratio with respect to work.

- For γ =1.3,1.4, 1.5,1.6,1.66, specific output topping cycle increases with increase in pressure ratio (rp1) then reaches maximum value at particular pressure ratio (rp1) then decreases with increase in pressure ratio (rp1). This value of pressure ratio (rp1) is called as optimum pressure ratio with respect to work.

- Optimum pressure ratio for maximum specific Work output (KJ/Kg) shifts towards higher-pressure ratio (rp1) with increase in TIT (K).

- There is no effect of increase in number of intercooling in stages of compression of bottoming cycle on specific work output of topping cycle, i.e. specific work output of topping cycle remains constant even with increase in no. of stages of intercooling.

From graph 3.9.5

- For γ =1.1,1.2, 1.3, Thermal efficiency topping cycle increases with increases in

pressure ratio of topping cycle (rp1) and then reaches maximum value at particular pressure ratio (rp1) then almost flattens with increase in pressure ratio (rp1). This value of pressure ratio (rp1) is called as optimum pressure ratio with respect to work.

- For γ =1.4, 1.5,1.6,1.66, Thermal efficiency topping cycle increases with increase in pressure ratio (rp1) then reaches maximum value at particular pressure ratio (rp1) then decreases with increase in pressure ratio (rp1). This value of pressure ratio (rp1) is called as optimum pressure ratio with respect to work.

- Optimum pressure ratio for maximum specific Work output (KJ/Kg) shifts towards higher-pressure ratio (rp1) with increase in TIT (K).

- There is no effect of increase in number of intercooling in stages of compression of bottoming cycle on specific output of topping cycle, as a result thermal efficiency of topping cycle remains constant even with increase in no. of stages of intercooling.

From graph 3.9.6

- For each γ, specific work output of bottoming cycle i.e. inverted gas turbine cycle first decreases with increase in pressure ratio of topping cycle (rp1)& then almost flattens with increase in pressure ratio (rp1).

- Specific work output of bottoming cycle i.e. inverted gas turbine cycle is higher for higher TIT at particular pressure ratio.

- With increase in number of intercooler in stage of compression of bottoming cycle, specific work output of bottoming cycle increases, due to decreases in work required for compression in bottoming cycle. As a result thermal efficiency of bottoming cycle increases with increase in no of intercooler in stage of compression.

From graph 3.9.7

- For each γ**,** Thermal efficiency of bottoming cycle i.e. inverted gas turbine cycle first decreases with increase in pressure ratio of topping cycle (rp1).

- Thermal efficiency of bottoming cycle i.e. inverted gas turbine cycle is higher for higher TIT at particular pressure ratio.

- With increase in number of intercooler in stage of compression of bottoming cycle, specific work output of bottoming cycle increases, due to decreases in work required for compression in bottoming cycle. As a result thermal efficiency of bottoming cycle increases with increase in no of intercooler in stage of compression.

From graph 3.9.8

- For γ =1.1,1.2,1.3,1.4 power ratio (wtop/wbot) increases with increases in pressure ratio of topping cycle (rp1) after reaching maximum value again starts decreasing with increasing in pressure ratio of topping cycle (rp1).

- For γ =1.5,1.6,1.66, power ratio (wtop/wbot) decreases with increases in pressure ratio of topping cycle (rp1).

- For γ =1.1,1.2,1.3,1.4, power ratio (wtop/wbot) increases with increase in pressure ratio of topping cycle (rp1) then increases sharply and decreases with increase in pressure ratio (rp1).

- For γ =1.5,1.6,1.66, power ratio (wtop/wbot) increases up to maximum value with increase in pressure ratio of topping cycle (rp1)& then rapid decrease in efficiency occur with further rise in pressure ratio (rp1).

- For γ =1.1,1.2,1.3,1.4, (n=1,2) power ratio (wtop/wbot) increases with increase in pressure ratio of topping cycle (rp1). For γ =1.5,1.6,1.66, (n=1,2) power ratio (wtop/wbot) decreases with increase in pressure ratio of topping cycle (rp1)

CHAPTER - 4

CONCLUSION

Thermal efficiency of mirror gas turbine cycle increases by 3%to 8% by increasing number of intercooling in stages of compression in bottoming cycle up to 2. It is found that there is negligible increase in thermal efficiency if number of intercooling is increases more then 2.

Reheating in stages of expansion in topping cycle of mirror gas turbine cycle is not beneficial, as it reduces thermal efficiency of mirror gas turbine.

For higher components efficiency, mirror gas turbine cycle can give more thermal efficiency then recuperated gas turbine, Hence recuperator may be replaced by inverted Brayton cycle to increase efficiency of cycle by 5% to8%.

Mirror gas turbine cycle may be applied in place of combined Brayton/Rankine cycle with great promise.

It is tentatively concluded that technical difficulties of using a higher pressure & temperature steam turbine with a boiler, condenser,& pump will be removed by successful use of the mirror gas turbine in the future.

Hardware tests for the mirror gas turbine will be the next step to show potentialities of concept & configurations of cycle.

ANNEXURE

ANNEXURE-1 :-

//Programme for Analysis of Mirror Gas Turbine Cycle With or Without Inter Cooling In Stages Of Compression In Bottoming Cycle To Find Net Work Of Topping Cycle, Efficiency Of Topping Cycle, Net Work Of Bottoming Cycle, Efficiency Of Bottoming Cycle, Net Work of Mirror Gas Turbine Cycle, Net Thermal Efficiency of Mirror Gas Turbine Cycle, Specific Fuel Consumption Of Cycle, Power Ratio In Mirror Gas Turbine At Various Pressure Ratio (rp1) for variable specific heat.

```
#include<stdio.h>
#include<math.h>
#include<conio.h>
#include<iostream.h>
#include<string.h>
void main()
{
 double gamma[7]={1.1,1.2,1.3,1.4,1.5,1.6,1.66};
double wctop,wttop,wcbot,wtbot,wttot,wbtot,wtot;
double etot,ecc=0.96,etop,ebot,ec=0.9,et=0.9;
double qtot,qbot,qtop;
double rp1,ma=1,mg,mf,a_f=60,e=0.9,n,ratio,sfc;
double cpg=1.14,cpa=1.005,g=0.2481,a=0.0909;
double t1=297,t2,t3,t4,t5,t6,t7;
char filename[50];
int index;
for(n=0;n<=2;n++)
for(index=0;index<7;index++){
strcpy(filename,"data");
```

```
char number[5];
number[0]='1';
number[1]='.';
number[2]=(int)((gamma[index]*10.0))%10+48;
number[3]=(int)((gamma[index]*100.0))%10+48;
number[4]='\0';
strcat(filename,number);
strcat(filename,"n=");
number[0]=(int)(n)+48;
number[1]='\0';
strcat(filename,number);
strcat(filename,".txt");
a=(gamma[index]-1)/gamma[index];

FILE *p=fopen(filename, "w");
fprintf(p,"\n\tTIT\trp1 \t wtot\t \t wttot \t\t wbtot \t\t etot \t etop \t ebot \t sfc \t
ratio\n\n");
//clrscr();
mf=ma*(1/a_f);
mg=ma+mf;
//for topping cycle
for(t3=1000;t3<=1800;t3=t3+200)
{
 //clrscr();

 cout<<"\n";
 cout<<"TIT="<<t3<<endl;
for(rp1=2;rp1<=30;rp1=rp1+2)
{
cout<<"\n";
```

```
cout<<""<<rp1;
t2=(1/ec)*t1*(pow(rp1,a)-1)+t1;
t4=t3-et*t3*(1-pow(rp1,(-g)));
wctop=ma*cpa*(t2-t1);
wttop=mg*cpg*(t3-t4);
wttot=wttop-wctop;
qtop=(1/ecc)*(mg*cpg*t3-ma*cpa*t2);
etop=wttot/qtop;
//for bottoming cycle
//for n stages of intercooling
{t6=t1-10;
t5=t4-et*t4*(1-pow(4,(-g)));
t7=t6+t6*(1/ec)*(pow(4,g/(n+1))-1);
wtbot=mg*cpg*(t4-t5);
wcbot=(n+1)*mg*cpg*(t7-t6);
wbtot=wtbot-wcbot;
qbot=mg*cpg*t4-ma*cpa*t1;
wtot=wttot+wbtot;
ebot=wbtot/qbot;
qtot=(1/ecc)*(mg*cpg*t3-ma*cpa*t2);
etot=wtot/qtot;
sfc=mf*3600/wtot;
ratio=wttot/wbtot;
cout<<"\n";
printf("\t total work of mirror gas turbine=%.4f",wtot);
cout<<endl;
printf("\t total work of topping cycle=%.2f",wttot);
cout<<endl;
printf("\t total work of bottoming cycle=%.3f",wbtot);
cout<<endl;
```

```
printf("\t thermal efficiency of mirror gas turbine cycle=%.3f",etot);
cout<<endl;
printf("\t thermal efficiency of topping cycle=%.3f" ,etop);
cout<<endl;
printf("\t thermal efficiency of bottoming cycle=%.3f",ebot);
cout<<endl;
printf("\t specific fuel consumption of mirror gas turbine=%.3f",sfc);
cout<<endl;
printf("\t power ratio of mirror gas turbine=%.3f",ratio);
cout<<endl;


fprintf(p,"\n\t%3.0f\t %3.0f \t%.4f \t% .2f \t %.3f \t %.3f \t%.3f \t %.3f\t %.3f\t
%.3f",t3,rp1,wtot,wttot,wbtot,etot,etop,ebot,sfc,ratio);

//getch();
}
//getch();
}
//getch();
}

}
}
```

REFERENCES

[1] Rao A.D.. Yi Y., Samuelsen G.S., 2003, "Gas Turbine Based High Efficiency "Vision 21 "Natural Gas and Coal Central Plants'", *Proceedings of the First International Conference on Industrial Gas Turbine Technologies*

[2] Najjar Y.S.H., 2000. "Gas Turbine Cogeneration Systems: A Review Of Some Novel Cycles", *Applied Thermal Engineering,* 20, 179-197.

[3] Tsujikawa. Y., Kaneko, K, and Fujii. S, 2001 July.Vol.123, "A newly proposed method of exhaust heat recovery", *ASMEjournal of Engineering for Gas turbines and power,* 481-486

[4] Yahya S.M. (2000), 2nd edition, "Turbine Compressor and Fans".

[5] Tsujikawa. Y., Kaneko, K. and Fujii, S., 2000, "Utilization of Cryogenic Energy of LNG by Mirror Gas Turbine" Paper No. OO-GT-0317, *ASME. Turbo Expo. Munich, Germany.*

[6] Korobitsyn M.A., 1998, "New And Advanced Energy Conversion Technologies -analysis of Cogeneration combined and integrated cycles'", *PhD Thesis, University of Twente,*

[7] Heppenstall T., 1998, "Advanced gas turbine cycles for power generation: a critical review". *Applied Thermal Engineering,* 1 8, 837-846.

[8] Bolland, O., Forde. M., and Hande, B. (1996), "Air Bottoming Cycle. Use of Gas Turbine Waste Heal for Power Generation", *ASME* Paper 95-CTP-50. 1995.

[9] Bolland O, (1991). "A Comparative Evaluation of Advance Combined Cycle Alternatives" *ASME Journal of Engineering for Gas Turbine and power,* vol. 1 13,pp-190-197

[10] Wilson, D. G., 1985, The Design of High Efficiency Turbomachinery and Gas Turbine *M.I.T. Press, Cambridge.* MA. nd

[1 l] Holman j. p. 1974, "Thermodynamics" ,2' edition

[12] H. Cohen, GFC Rogers , and IIIII Sarvanmutto, 1972,4" edition, "Gas Turbine Technology",

[13] James Hodge, 1971, " Cycle performance and estimation", 3rd edition. Megraw Hill.

[14] Csandy 1964. "G.T .Theory Of Turbomachines", *Mcgraw Hill.*

[15] www.gas-turbmes.com

[16] www.gepower.com

[17] www.energy.ca.gov

[18] www.ou.edu/spp/turbine/paper.html